MEDICAL UNIVERSITY OF VIENNA

Regenerative potential of the secretome of apoptotic and necroptotic peripheral blood mononuclear cells: from bench to clinical phase I trial in dermal wounds

Doctoral thesis at the Medical University of Vienna

for obtaining the academic degree

Doctor of Philosophy

Submitted by

Dr. med. univ. Elisabeth Simader

Supervisor:

Univ.-Prof. Univ.-Doz. Dr.med.univ. Hendrik Jan Ankersmit, MBA

Department of Thoracic Surgery
Medical University of Vienna
Währinger Gürtel 18-20, 1090 Vienna, Austria

Vienna, March 2024

“Nothing in life is to be feared, it is only to be understood. Now is the time to understand more, so that we may fear less.”

Marie Curie

Table of contents

1 Acknowledgement

The realization of this thesis was only possible, due to the support of Hendrik Jan Ankersmit and Michael Mildner. I am very grateful for the scientific as well as personal support throughout my whole time as PhD-student.

My special thanks go to my colleagues in the Research Laboratory of the Department of Surgery, the Department for Dermatology, Research Division of Biology and Pathobiology of the Skin, the Research Department of Transfusion medicine and the Department of Clinical Pharmacology without your aid these publications would not be possible.

Due to the funding of the Christian Doppler Laboratory for Cardiac and Thoracic Diagnosis and Regeneration, as well as the FFG Research Grant these publications were achieved and I am very grateful for the possibility.

My deep gratitude goes to my parents, my brothers Stefan and Bernhard for their unconditional support and aid on every step of the way.

The results of this thesis were presented at several congresses or have been subject of the following articles:

ÖGDV Jahrestagung 2017 am 30.11-02.12. 2017, Salzburg, Poster presentation
Effect of the secretome of apoptotic peripheral blood mononuclear cells (APOSEC) on tissue regeneration and wound healing

Journal Article: Zellüberstände von apoptotischen, mononukleären Zellen zur Wundheilung - Eine klinische Phase I Untersuchung beim Menschen
Simader E., Mildner M., Ankersmit H.J., Spectrum Dermatologie 4/2017

The paper: Tissue-regenerative potential of the secretome of γ-irradiated peripheral blood mononuclear cells is mediated via TNFRSF1B-induced necroptosis, was awarded the "Theodor Billroth Preis der Ärztekammer für Wien 2020".

2 Declaration

The experiments done to accomplish the following thesis have been conducted at the Department of Thoracic Surgery, at the Medical University of Vienna under the supervision of Hendrik Jan Ankersmit and Michael Mildner. This thesis was realized with the help of the Department for Dermatology, Research Division of Biology and Pathobiology of the Skin (Medical University of Vienna), Department of Clinical Pharmacology (Medical University of Vienna), Clinical Trials Coordinative Centre (Medical University of Vienna), Department of Transfusion Medicine (Medical University of Vienna), Core Facility Flow Cytometry (Medical University of Vienna), Division of Oral and Maxillofacial Surgery (Medical University of Vienna), Synlab Analytics and Services Switzerland AG and the Red Cross Blood Bank in Linz. All animal experiments were completed at the Center for Biomedical Research (Medical University of Vienna). In vitro and ex vivo experiments were performed in cooperation with Michael Mildner, Bahar Golabi, Tanja Wagner, Maria Laggner, Vera Vorstandlechner, Alfred Gugerell, Polina Kalinina, Dragan Copic and Denise Traxler-Weidenauer. Peripheral blood mononuclear cell secretome was produced by the Austrian Red Cross Blood Transfusion Service for Upper Austria, Linz conforming to the good manufacturing process (GMP)-requirement under the lead of Susanne Suessner and Werner Watzinger. Flow Cytometry and Image Stream analysis were performed by Andreas Spittler and Sabine Pietkiewicz. Patient follow-up and clinical controls were realised by the Department of Clinical Pharmacology, Alexandra Geusau and Mahdi Kasiri. Microarray and bio-informatic analysis were implemented at the Genomics Core Facility (Medical University of Vienna) by Markus Jeitler and Lucian Beer. Interpretation of results and the supervision of the writing and experiment design leading to the publications regarding this thesis were accomplished by Michael Mildner and Hendrik Jan Ankersmit.

3 List of figures

4 Abstract

Chronic non-healing ulcers depict a growing concern considering the soaring incidences especially in diabetes. These diabetic wounds are leading to infections and in some cases to amputation and elicit huge costs for the health care system. New treatment methods are needed to promote faster wound closure and avoid complications.

Our working group was able to show in previous studies by Mildner et al. and Hacker et al. that the topical application of supernatant of peripheral blood mononuclear cells (PBMCs) cultured for 24 hours on wound areas lead to accelerated wound healing. We assumed, that this tissue-regenerative effect originates from a plethora of cytokines released by the PBMCs. Thus, we tried to elucidate the role of the secretome of different PBMC subtypes on angiogenesis, which is crucial for successful wound healing. Furthermore, we wanted to investigate the role of apoptosis and necroptosis on the secretion pattern.

In this thesis we could show, that the pro-angiogenic capacity (tested in aortic ring assays) was highest for the secretome of PBMCs cultured together, compared to the secretome of mono-cultures of PBMC subsets (monocytes, T-cells, B-cells and natural killer cells). This implicates possible cell-cell-interactions leading to changes in the supernatant composition.

Moreover, we could reveal that ionizing irradiation of PBMCs prior to cultivation induced not only apoptosis, but also necroptosis. Interestingly tumor necrosis factor-receptor superfamily member 1B acted as main inductor of necroptosis after irradiation. We could further demonstrate that necroptosis boosts the capacity of PBMC secretome to improve tissue regeneration by enhanced angiogenesis.

As a next step towards clinical use, we could demonstrate in a clinical phase I study, that the application of the autologous supernatant of PBMC exposed to ionizing irradiation (produced according to Good Manufacturing Practice (GMP) on dermal wounds is safe and well tolerated. These results may pave the way for future treatment options of chronic wounds and thus alleviate disease burden.

5 Zusammenfassung

Chronische, nicht heilende Wunden stellen ein zunehmendes Problem in der klinischen Praxis dar, insbesondere mit der steigenden Inzidenz von Patienten mit Diabetes. Diabetische Wunden führen oft zu Infektionen und im schwersten Fall bis hin zu Amputationen, was zu hohen Kosten für das Gesundheitssystem führt. Behandlungsmöglichkeiten zur schnelleren Wundheilung fehlen nach wie vor, um diese Belastungen und Komplikationen effektiv zu verringern.

Unsere Arbeitsgruppe konnte zeigen, dass die Applikation des Überstandes von mononukleären Zellen des peripheren Blutes zu einer deutlich schnelleren Wundheilung in murinen und porzinen Modellen führte. Als Ursache für den verbesserten Wundverschluss vermuteten wir den parakrinen Effekt der Vielzahl an ausgeschütteten Zytokinen und Wachstumsfaktoren im Zellüberstand. Der genaue Wirkmechanismus, der verbesserten Angiogenese ist noch zu entschlüsseln und Gegenstand dieser Dissertation. Das Sekretom der T-Zellen, B-Zellen, Natürlichen Killer-Zellen und Monozyten, aus denen sich die PBMC zusammensetzen wurden daher in in-vitro Aorten-Ring Experimenten auf ihr angiogenetisches Potential untersucht.

Überraschenderweise zeigte sich, dass die Kultivierung aller PBMC gemeinsam den deutlichsten, positiven Effekt auf die Angiogenese hatten, während die Monokulturen von Natürlichen Killerzellen, T- und B-Zellen und Monozyten einen deutlich kleineren Effekt im Hinblick auf die Angiogenese zeigten. Dies lässt auf einen mögliche Zell-Zell-Interaktionen, die die Zytokin-Produktion und vor allem Zusammensetzung beeinflussen, schließen.

Zudem konnten wir in bisherigen Studien zeigen, dass die Bestrahlung der PBMC mit ionisierender Strahlung sowohl Apoptose, als auch Nekroptose auslösen kann. In dieser Dissertation fanden wir heraus, dass die Art des Zellniedergangs via Apoptose und Nekroptose die Gefäßaussprossung durch die veränderte Proteinsignatur der ausgeschütteten Zytokine maßgeblich beeinflusst.

Identifiziert wurde neben der Apoptose, vor allem die Nekroptose als wichtiger Faktor der vermehrten Gefäßaussprossung. Durch Rezeptor-Inhibierung des Tumornekrosefaktor-Rezeptor 1B (TNFR1B) konnten wir die Nekroptose-Induktion erfolgreich verhindern. Somit konnten wir auch den verantwortlichen Signalweg der Nekroptose-Entstehung nach bestrahlung identifizieren.

Damit diese Erkenntnisse in Zukunft als mögliches, neues Therapiekonzept Patienten zur Verfügung gestellt werden kann, muss das Sekretom der bestrahlten PBMC (APOSEC)

zunächst auf ihre Sicherheit in der menschlichen Anwendung getestet werden. Hierfür führten wir eine Klinische Phase I Studie durch, welche die sichere Anwendung des modifizierten, GMP-konform hergestellten, autologen APOSEC demonstrierte. Wir hoffen, dass diese Arbeit den Weg für geplante Phase II und III Studien ebnet und in Zukunft eine verbesserte Patientenversorgung ermöglicht.

6 Publications arising from the thesis

Tissue-regenerative potential of the secretome of γ-irradiated peripheral blood mononuclear cells is mediated via TNFRSF1B-induced necroptosis.

Simader E, Beer L, Laggner M, Vorstandlechner V, Gugerell A, Erb M, Kalinina P, Copic D, Moser D, Spittler A, Tschachler E, Jan Ankersmit H[#], Mildner M[#].
Cell Death and Disease 2019 Sep 30;10(10):729. doi: 10.1038/s41419-019-1974-6. PMID: 31570701

Safety and Tolerability of topically administered autologous, apoptotic PBMC secretome (APOSEC) in dermal wounds: a radnomized Phase 1 trial (MARSYAS I).

Simader E*, Traxler D*, Kasiri MM*, Hofbauer H, Wolzt M, Glogner C, Storka A, Mildner M, Gouya G, Geusau A, Fuchs C, Eder C, Graf A, Schaden M, Golabi B, Aretin MB, Suessner S, Gabriel C, Klepetko W, Tschachler E, Ankersmit HJ.
Scientific Reports 2017 Jul 24;7(1):6216. doi: 10.1038/s41598-017-06223-x. PMID 28740204

* These authors contributed equally as first authors

[#] These authors contributed equally as last authors

7 Abbreviations

AMI	Acute myocardial infarction
AP-1	Activator protein
APOSEC	apoptotic PBMC secretome
ATP	Adenosintriphosphat
BAK	Bcl-2 Homologous Antagonist killer
BAX	Bcl-2-associated X protein
BCL-2	B-cell lymphoma-2
BCL-X_L	B-cell lymphoma-extra large
BH3-only	B-cell lymphoma homology 3 -only
BID	BH3 interacting-domain death agonist
CASP	Caspase
CD	Cluster of differentiation
c-IAP1	cellular inhibitor of apoptosis protein
Cyt c	Cytochrom c
DAMP	Damage-associated molecular patterns
DANN	Deoxyribonucleic acid
EGF	Epidermal growth factor
FADD	Fas-associated protein with death domain
FGF	Fibroblast growth factor
FLIP	FLICE-inhibitory protein
HSP	Heat shock protein
IAP	Inhibitor of apoptosis protein
IL	Interleukin
MLKL	Mixed lineage kinase domain like pseudokinase
MOMP	Mitochondrial outer membrane permeabilization
NF-κB	Nuclear factor 'kappa-light-chain-enhancer' of activated B-cells
NK-cell	Natural killer - cell

PBMC	Peripheral blood mononuclear cells
PDGF	Platelet derived growth factor
PUMA	p53 upregulated modulator of apoptosis
RIPK	Receptor interacting protein
RNA	Ribonucleic acid
SMAC	Second mitochondria-derived activator of caspases
TNF	Tumor necrosis factor
TNFR	Tumor necrosis factor receptor
TRADD	Tumor necrosis factor receptor type 1-associated DEATH domain protein
TRAIL	Tumor necrosis factor related apoptosis inducing ligand
VEGF	Vascular endothelial growth factor
XIAP	X-linked inhibitor of apoptosis protein
zVAD	zVAD-fluoromethyl ketone

8 CHAPTER ONE: Introduction

8.1 Structure of the human skin

The skin is the body's largest organ with a surface area of nearly 1,8m^2 (depending on individual size of the human body).[1] The skin can be separated in two main layers, the epidermis and the dermis, which are located on the hypodermis (a subcutaneous fascial layer, connecting the dermis to deeper muscular tissue or periosteum).[2] The structure of the skin displays its complexity.

The epidermis consists of four to five layers of mostly keratinocytes, subdivided in stratum corneum, stratum granulosum, stratum spinosum and stratum basale (stratum lucidum is only present in thicker parts of the skin).[2] The thickness of the epidermis depends on the distinct part of the body and ranges from 1,4mm to 0,8mm (e.g. plantar parts are thicker than palmar skin).[2] Furthermore hair follicles and the corresponding muscles (arrector pili muscles), as well as sebaceous- and sweat glands can be found in the epidermis.[2] Apart from the majority of keratinocytes different cells such as melanocytes, dendritic cells (Langerhans cells) and Merkel cells (especially important for the tactile sensation) are essential parts of the skin.[2] Melanocytes generate melanin and aggregate them in melanosomes, which are presented on dendritic processes and consumed by keratinocytes via phagocytosis and therefore reach the upper layers of skin within the keratinocytes.[2] The phagosomes release the melanin into the cytoplasm, where melanin granules protect the cell from DNA damage via ultraviolet-irradiation.[2] Merkel cells are mechanoreceptors and are specialized on light tactile sensation and are located near afferent, unmyelinated sensory plates.[2] Langerhans cells derive from monocytes of the bone marrow and fulfill the role of macrophages, such as recognition, processing and antigen presentation to naive T-cells.[3] Due to its role of antigen processing Langerhans cells are especially important in autoimmunity, if autoantigens are presented to T-cells and therefore may lead to contact allergic responses.[3]

The dermis connects epidermis to hypodermis and sustains the epidermis with nutrients and is characterized by a strong fibroelastic tissue and extracellular matrix.[2] The dermis consists of a papillary and reticular layer.[2] Recent proteomic analysis showed the composition is a mix of different types of collagens (I, II, III, VI, XII and XIV), defining its flexibility or cohesiveness.[4,5]

The papillary part is an assembly of thin collagen fibers (mostly collagen I), whereas the reticular part displays a stronger and denser collagen composition (primarily collagen type III).[4,5] The avascular epidermis draws its nutrients from looped capillaries in the papillary layer.[2] These capillaries embedded in loose elastic fibers also contribute to temperature regulation of the body.[2] Moreover also here mechanoreceptors called the Meissner corpuscles can be found, which transport tactile stimuli to the nerval system.[2] Beside cells of the connective tissue this layer is populated with a variety of sweat- and sebaceous glands, pressure-recognizing mechanoreceptors known as Pacinian corpuscles, hair follicles and its vascular- and lymphatic-system.[2] Furthermore for stretching sensation Ruffini corpuscles, sensory innervation and muscles (eminently for facial expression) are incorporated.[2] A high amount of arteriovenous shunts in the capillary system and thus vascular tone control of the dermis allows a precise thermoregulation of the skin, necessary to adapt to temperature changes, due to exercise or environmental exposure.[2]

Below the reticular layer of the dermis lies a subcutaneous tissue consisting of loose connective properties which transforms into adipose tissue.[2] This subcutaneous tissue of the hypodermis is highly vascularized with a widespread capillary system, responsible for the excellent absorption of drugs or medication applied via injection.[2] Also the lymphatic system is highly developed in the hypodermis.[2]

These layers form a barrier and protect the human body bidirectionally from fluid or protein loss and on the other hand from intrusion of infections, toxic environmental factors or ultraviolet irradiation.[2]

For a long time the role of skin as barrier to environmental jeopardies, such as a multitude of bacterial and viral infections, was seen as its sole function, yet the skin represents the largest immunological organ of the body.[6] Moreover skin fulfills various essential functions as the regulation of temperature (e.g. by sweating)[5] and is involved in the nervous system regulation for danger signaling and fluid regulation.[5]

8.2 Cutaneous wound healing

Wound healing depicts a myriad of complex processes of different cell types and interactions between the immunologic- and vascular- system, skin and tissue.[7] To accomplish an adequate healing process a variety of cytokines, chemokines, transportation of nutrients to the site of damage with a sufficient blood supply and matrix proteins are necessary.[7-10]

A physiological wound healing starts with hemostasis and activated thrombocytes, which are found at the wounded area to a high amount.[8,11] Due to aggregation of these thrombocytes and haemostasis a stable fibrin clot is formed, stopping the blood loss and closing the endothelial defect.[8] These thrombocytes secrete various different vasoactive and proliferative proteins such as tansforming growth factor β (TGF-β), platelet derived-, fibroblast-, and epidermal growth factor (PDGF, FGF, EGF), prostaglandins, histamine and bradykinin.[8,12] Mast cells and basophils also play an important role in the histamine production, and are enhanced by complement activation, which in turn is activated by platelets.[8,12] The secreted vasoactive proteins lead to initial vasoconstriction in the damaged area, further stopping blood loss.[8,12]

The inflammatory phase starts as soon, as the blood clotting is completed and serves as eradication step of antimicrobial pathogens and foreign objects in the wounded area.[8,13] To fulfill this purpose vasodilation of blood vessels is activated to increase the vascular permeability and transportation of inflammatory cells and peripheral blood mononuclear cells (PBMC) to the damaged area.[8,13] In this regard, especially neutrophils, monocytes and macrophages need to be mentioned as main players in this phase.[8,13] Neutrophils act as first defense line after wounding by eradicating bacteria via secretion (degranulation) of toxic proteases and enzymes and effectively destroying pathogens via phagocytosis and dissolving them in their phagosome.[14] Moreover neutrophils produce free oxygen radicals and lysosomal enzymes to create an acidic, bactericidal environment, to decrease the risk of wound infections.[12,14] Furthermore neutrophils are able to form NETs (Neutrophil extracellular traps) via release of euchromatic DNA, which captures bacteria with its adhesive extracellular structure, spiked with antibacterial proteins.[15] Whereas the NET formation is important for the hindrance of severe infections, it can also lead to hyperergic inflammation (second burn) by chemoattracting further pro-inflammatory immune cells to the site, leading to excess inflammation and furthermore exaggerated NET formation, which leads to serious tissue damage.[15]

Monocytes differentiate into two forms of macrophages: the responsive and the inflammatory macrophage.[12] First pro-inflammatory macrophages (M1) are mostly present in the first stages of wound healing.[16] In later stages of wound repair a shift to anti-inflammatory macrophages (M2) takes place and is associated with more efficient wound closure, especially in subjects with diabetes.[16] Macrophages digest cell debris via phagocytosis, yet a crucial factor of wound healing is their secretion of cytokines and growth factors: e.g. tumor necrosis factors (TNF, especially TNF-α), PDGF, interleukins (IL) and TGF-β.[12] The secretion of numerous pro-inflammatory cytokines such as TNF-α or IL-6 is executed by M1-type macrophages and is

important for first wound cleansing, whereas pro-angiogenic factors as VEGF-α and anti-inflammatory factors (e.g. IL-10) or TGF-β is more associated to M2-type macrophages.[16,17]

In the proliferative phase these growth factors are leading to tissue proliferation, fibroblast collagen production and promotion of endothelial cells to drive angiogenesis in the granulation tissue to form a vascular nutrient supply for better wound healing.[7-10] Fibroblasts are the key players in this phase and appear at around day two or three after injury.[8] Special myofibroblasts lead to constriction of the wounded area and remodeling of the scar tissue.[18]
Another effect of the increased capillary permeability is the transport of proteins from the blood vessels to the wounded tissue and thus fibroblasts to migrate into the damaged tissue area, attracted by chemotactic substances secreted by extracellular matrix (particularly produced by fibronectin and hyaluronate).[12] Fibronectin receptors on fibroblasts act as an scaffold and enable cells to migrate, by binding to actin filaments.[12] The activated fibroblasts synthesize collagen and proteoglycans, which is further enhanced by EGF and TGF-β secreted by macrophages.[12]

Angiogenesis in the destroyed area is necessary for adequate blood supply and starts with the migration of endothelial cells, which form capillary networks under the influence of FGF and TGF-β.[12] If angiogenesis is inhibited, wound healing fails and fibroblasts cannot migrate, which is the pathogenensis of arteriolosclerosis obliterans or other forms of ischemic ulcers.[8] The regulation of angiogenesis also depends on the oxygen level in the surrounding tissue, while hypoxia drives angiogenesis, higher levels of oxygen can stop neo-angiogensis.[8,12]

This reduction of neo-angiogenesis is characteristic for the maturation phase and can be seen macroscopically as a less hyperemic scar.[12] In the maturation phase reorganization of collagen fibres to increase strength and reform the structure of normal skin is the main goal.[8] It should be mentioned, that scar tissue will never demonstrate an exact replica of normal skin with all its complex structures, yet can resemble it, to a certain amount.[8]
In the maturation phase the collagen type III present in new wounds is converted into the more mature collagen type I form, yet the conversion of collagen in wounds can be a process lasting for up to two years.[12,19] The scar formation varies between individuals according to their age, wound location, pathogenesis of the wound and duration of inflammation (especially when it comes to wound infections).[8] Re-epithelialization is an attribute of successful wound healing.[8]

If these delicately orchestrated processes fail, inadequate wound healing with all concomitant negative effects take place.[20] Insufficient wound healing, especially in patients suffering from diabetes, may lead to infections, osteomyelitis and even amputation.[21]

One factor that may prevent physiological wound healing in chronic non-healing ulcers is increased colonization of bacteria and fungi of the skin.[20] This may lead to a constant pro-inflammatory signal, which is important in the first phases of wound healing, yet inhibits the later remodeling phases.[8,13,22]
Another reason for deficient wound healing is an error in angiogenesis, which generates a lack of nutrient transport, necessary cell migration and less oxygen supply in the damaged area.[23] Moreover a dysfunctional immune system or deranged cytokine environment inhibits the shift from the pro-inflammatory to the anti-inflammatory phase, necessary for adequate collagen re-organization and scar-formation.[18] In wound healing neutrophils act as first responders and eradicators of bacteria, due to cytokine stimulation e.g. via IL-8.[18] These neutrophils are phagocytised by macrophages at the transition point to the anti-inflammatory phase.[18] If this phagocytosis never occurs, the ongoing pro-inflammatory process prevents remodelling of the extracellular matrix.[18]

Chronic non-healing wounds are a rising challenge on an individual level, as pain, disability to work and the quality of life is compromised, on the other hand on a socioeconomic level, as around 2,4 to 4,5 million patients in the United States alone are facing this problem.[24-26] The costs for wound treatment products is estimated to reach 25 billion $ annually.[24-27] Seeing these numbers, searching for successful treatment options seems to be an investment into the future and are necessary to accomplish better outcomes to this unmet need.[27]

The role of cytokines and growth factors (paracrine or endocrine) as drivers of fibroblast activation, collagen production and secretion of chemoattractants in wound healing demonstrates its importance for the regenerative research branch with promising results as potential therapeutic targets.[8,12,19,28,29]

8.3 Tissue regeneration concepts using cell therapy

At sites of damage, trauma and cell death, inflammation and healing are essential for the survival of multicellular organisms.[30] To support the body's capacities to overcome these malfunction is the aim of regenerative medicine.

Regenerative medicine, aims to restore damaged or malfunctioning tissue. [30] It has become a globally emerging branch in different research fields in the last century.[30] Despite striking

advances in treatment regimens for organ failure, surgical interventions and solid organ transplantation, regeneration and restoration of injured organs, in particularly the myocardium, kidney, peripheral and central nervous system, lung and skin still remains a tremendous problem.[31]

In this thesis we will focus on the developmental steps of cell-based regenerative medicine and its origin in the research area of myocardial infarction and its adaptation for wound healing as for both the angiogenic potential is of crucial importance.[32-35]

Cell based therapies fulfill various concepts of function, for example as substitute of damaged or destroyed cells.[36]

One of the success-stories of regenerative medicine are solid organ transplantations. Yet the transplant patients have to face constant immunosuppression, as the immune system is recognizing the exogenous tissue.[37] Even under adequate immunosuppressive medication for years the transplanted organs are facing terminal organ failure at some point of its life-span and re-transplantation must be performed, if possible.[37,38]

Yet the dream to transplant single cells, which differentiate into the needed tissue and fully compensate its functions remains. Mesenchymal stem cells (MSCs) appeared to be the ideal substance for regenerative medicine.[39] Due to their ability to differentiate in various other cell types (among others: cardiomyocytes, myocytes, osteoblasts, chrondrocytes and adipocytes).[39-42] MSCs can be obtained by isolation from adipose tissue after plastic surgery, umbilical cord tissue of newborns or aspirated from bone marrow.[41]

The idea of cell-based therapies as surrogate was highly investigated in relation to myocardial infarction, as a source of regeneration of once damaged cells due to hypoxia.[43] The beginning of cell based therapy was set as the finding that certain cells are capable of developing cardiac-like myocytes.[44,45] As an attempt autologous myoblasts from the rat tibialis anterior muscle were transplanted in a rodent model after induction of myocardial infarction.[46] Surprisingly the left ventricular ejection fraction elevated in the group with the transplanted myoblasts.[46] These experiments were implemented in humans via catheter-based injection of myoblasts from the quadriceps muscle.[47] Yet after promising results, the fact was revealed that the transferred muscle cells could not function as cardiac myocytes, lacking the contractile rhythm needed to be a real surrogate.[48] The reason for the mild beneficial outcome of patients remained a secret.

In wound healing the addition of MSCs lead to enhancement of re-epithelialization.[49,50] Felanga et al was able to show, that the addition of MSCs in fibrin spray on dermal wounds lead to accelerated wound closure.[50] Moreover Wu et al. demonstrated, that MSC application in a murine model lead to a faster wound closure by differentiation and ameliorated angiogenesis.[51]

The mode of action behind the increased cutaneous wound closure seems to be explained by neovascularization and angiogenesis growing into the non-vascular fibroblast scaffold built during wound healing.[52] Endothelial progenitor cells derived from bone marrow played an important role in vessel formation in the adult organism.[53,54]

Neovascularization can be induced by two miscellaneous mechanisms: improvement of sprouting of available resident endothelial cells (angiogenesis) or the migration of endothelial progenitor cells (EPCs) derived from bone marrow to build new vessels (vasculogenesis).[55] In diseases with ischemia and inadequate vascularization such as myocardial infarction, peripheral artery disease, stroke and impaired wound repair the positive effect of transplanted EPCs could be revealed.[32-35] Yet the exact mode of action of this effect on ameliorated vascularization remained concealed, as similar to the MSCs also the EPCs could not differentiate into functioning vessels.

Holzinger et al. isolated peripheral blood mononuclear cells (PBMCs) of heparinized blood from patients with non-healing wounds and dripped it on their chronic ulcers.[56] As a result the mean healing time was reduced to 4,6 weeks in the group treated with PBMC, compared to 8,1 weeks in the control group.[56] Holzinger et al. could show this in a try and error concept.[56] Yet the hypothesis behind the successful improvement of the ulcers was not revealed for a long time.

Insufficient wound repair was the consequence of a lack of nutrients and oxygen, as well as the inadequate proliferation of keratinocytes.[8,12,13,56] But even more important is the fact, that without inflammatory cells there is no sufficient wound healing.[8,12,13,56] In patients with chronic ulcers the transport of pro-inflammatory cytokines and nutrients to the wounded area, due to ischemia was the reason for the deranged healing process.[8,12,13,56] The lack of chemo attractant gradients as well as reduced migration of leukocytes was caused by insufficient blood sustenance.[8,12,13,56] Secreted pro-inflammatory factors by leukocytes seemed to make a difference.[8,12,13,56]

Table 2. Mean period of treatment until ulcer closure

	All		CAOD		PTS	
	MNC $n = 33$	Control $n = 30$	MNC $n = 21$	Control $n = 20$	MNC $n = 12$	Control $n = 10$
Weeks until healed (mean)	4.7 ± 1.9	8.1 ± 1.2	5.0 ± 2.0	8.4 ± 2.1	3.9 ± 1.4	7.7 ± 3.5
	$p < 0.01$		$p < 0.01$		$p < 0.01$	
Healed after 75 days	29 (87%)	17 (56%)	18 (85%)	10 (50%)	11 (91%)	7 (70%)

Treatment was discontinued after 75 days if healing had not occurred. Values are mean ± standard deviation. Statistical analysis used the Student's *t*-test.

Eur J Vasc Surg Vol 8, May 1994

Fig. 1. Time of wound healing after treatment with PBMC (mononuclear cells MNC) [56,57] shown in the table is the time needed for wound closure ith and without the use of peripheral blood mononuclear cells (MNC) in all chronic wounds, patients with chronic arterial occlusive disease (CAOD) and post-thrombotic syndrome (PTS).[56,57]

Also, other researchers treated ulcers by addition of immune cells. Danon et al applied macrophages on wounds of elderly patients, to improve the healing capacity.[58] He could depict wound closure in 27% of treated patients compared to 6% in the control group.[58] Danon hypothesized, that the secretory pattern of activated monocytes and macrophages lead to ameliorated angiogenesis, cell migration and collagen production.[59] He even developed a method to further enhance their secretion capacity by hypo-osmotic shock.[59]

8.3.1 From cell based to cell free-therapy

Gnecchi was a pioneer to assume, not only the direct cell-cell interaction being the source for the tissue regeneration, but the secretome, released by the cells acting via paracrine mechanisms.[60]

What is the secretome of cells? The secretome in in vitro experiments is defined as the conditioned medium of stimulated or unstimulated cells.[61] It consists of a complex plethora of lipids, extracellular vesicles, apoptotic bodies, cytokines, chemokines, other proteins, micro ribonucleic acids (miRNAs) and carrier cargo with small non-coding RNAs secreted by the cells into the medium, during cultivation.[61-63]

Over time more and more researchers drew the same deduction:

In the study of Javazon et al. stromal cells from progenitor cells purified from bone marrow improved neovascularization and re-epithelialization in a dermal wound model, compared to bone marrow alone in a murine model. [64] What was rather suprising, that the GFP-marked stromal cells could not be found in the granulation tissue or endothelial cells, allowing the conclusion, that the result was not reached by transdifferentiation.[64]

Another cause for the assumption, was the fact, that only 2% of injected stem cells were reaching the heart in a myocardial infarction model, and therefore could not be solely responsible for the beneficial regenerative effects.[65] Moreover intracoronary stem cell injection in some cases resulted in blood flow reductions, with the pathogenesis of mesenchymal stem cells obstructing small vessels leading to extension of ischemic myocardium.[66]

Manon Desgres et al. tested extracellular vesicles derived from cardiac progenitor cells in doxorubicin induced cardiomyopathy as model for chemotherapy-induced cardiotoxicity. [67] He could reveal that intraperitoneal injection of the extracellular vesicles in a rodent model ameliorates circumferential cardiac strain and preserved systolic and diastolic volumes in rats. [67]

The importance of paracrine effects of bone marrow derived stem cells was further enhanced by the study of Uemura et al., in which preconditioning in culture resulted in less apoptotic cardiomyocytes after myocardial infarction.[68] The regenerative potential of ischemic tissue was not only limited to myocardium, but could be verified for limb ischemia either.[69] In rats the application of conditioned medium of mesenchymal stem cells increased proliferation of smooth muscle cells as well as endothelial cells.[69] These findings were not solely created by the impact of single cytokines, such as the well-known vascular endothelial growth factor (VEGF) or basic fibroblast growth factor (bFGF) found in the conditioned medium, as it was revealed by anti-body blocking experiments.[69] In these experiment the impact of VEGF and bFGF was abolished by antibody binding, yet the results remained the same with enhanced cell proliferation.[69]

Growth factors also seemed to play an important role in dermatological wound healing. In a gangrenous wound of an elderly, diabetic individual, the wound was treated with a mixture of PBMC and added basic fibroblast growth factor.[70] This lead to wound closure within six months without further ulceration in the follow-up controls.[70]

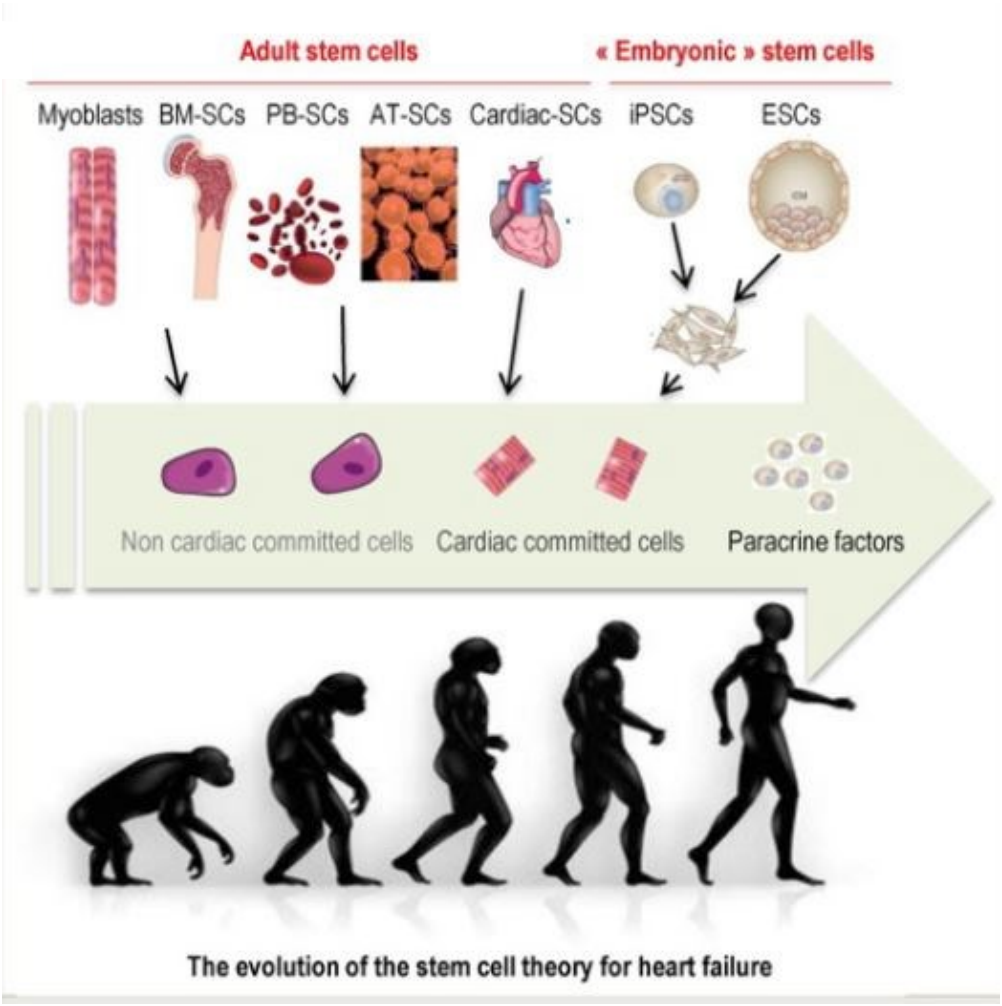

Fig. 2. Developmental stages of stem cell therapy through the example of cardiac insufficiency. Adapted from Silvestre et al. [71] The hope of early studies was a differentiation of bone marrow (BM), adipose tissue (AT) or peripheral blood (PB) derived stem cells (SC) to differentiate into active myocardial muscle cells, via electrical stimulation. The next step was to use cardiac stem cells and finally to culture and trasnplant induced pluripotent stem cells (iPSCs) or embryonic stem cells ESCs.[71] Yet even this approach was abolished as the cells did not reach their goal after intravenous application or failed to proliferate and transform into myocardial muscle.[71] Astonishingly a beneficial effect was detected and even potentiated by administration of the supernatant of the stem cells, leading the studies into a different direction with cytokines and chemokines as the key players in damage repair.[71]

It became more and more clear, that not the applied cells were responsible for the beneficiary wound healing effect, but the growth factors, chemokines or cytokines secreted by the cells. This evolution of cell based to cell-free regenerative medicine was verified by Walter et al.[72] He proved, that the conditioned medium of MSCs derived from bone marrow accelerated dermal wound healing in a scratch assay.[72] In this study keratinocytes and fibroblasts were co-cultured with the supernatant of MSCs and the growth was significantly enhanced.[72] Intriguingly not the proliferation was the predominant mode of action for the wound healing, yet the enhanced cell migration, driven by cytokines as RANTES, MCP-1, IL-8, IL-6 and TGF-β.[72]

It was further speculated that micro vesicles present in the conditioned media were responsible for the regenerative effect after kidney ischemia.[73] To test this hypothesis micro vesicles gathered from mesenchymal stem cell culture media were injected intravenously after ischemia–reperfusion injury and acted cytoprotective (apoptosis prevention) and enhanced proliferation of tubular epithelial cells.[73]

These findings let us hope to find a potential drug that combine cytoprotective and pro-angiogenic effects. Yet the answer which player in the secretome (cytokines or micro-vesicles or the combination) is the most potent remains to be elucidated.

8.3.2 Preconditioning of cell-therapy

To further maximize the positive effect of the cell secretomes and utilizing the cell as bioreactor was the next step in the secretome research field.[74] A common approach to achieve this goal is hypoxia, as dermal wounds often display lower oxygen levels.[74] Zhang et al showed, that mesenchymal stem cells derived from umbilical cords secreted exosomes after exposure to hypoxia.[74] These exosomes enhanced endothelial migration and proliferation.[74] Furthermore apoptosis induction of endothelial cells was diminished compared to stimulation with normoxic secretome of MSC.[74] As probable mode of action the microRNA-125b, which is transported in exosomes could be identified. MicroRNA-125b inhibited apoptosis via reduction of tumor protein p53 inducible nuclear protein 1-expression.[74]

Another study accomplished faster wound healing in a murine wound model by pre-stimulation of MSCs with TNF-α and IFN-γ.[75] This pre-stimulation led to induced angiogenesis in the wounded skin and increased VEGFC levels.[75]

Su et al stimulated melanoma cell lines with IFN-γ to acquire higher amounts of PD-L1 containing exosomes.[76] These exosomes were obtained from the conditioned medium and applied on epidermal cells and fibroblasts and on murine artificial wounds.[76] This stimulation with pre-conditioned exosomes lead to faster re-epithelization, increase in epidermal cell migration via the PD-1 immune checkpoint pathway.[76] The pro-inflammatory cytokine production of $CD8^+$ T-cell was reduced upon stimulation with the PD-L1 enriched extracellular vesicles either.[76]

The next developmental stage of the paracrine effect hypothesis is the fact that dying cells could secrete various different cytokines and chemokines.[77] Thum et al. promulgated the hypothesis that the improvement of cardiac function was induced, due to the immunomodulatory effect of stem cells dying of apoptosis without experimental evidence.[77] Cells of the myocardium that are damaged by the hypoxic conditions of an acute myocardial infarction (AMI) release heat shock proteins, that activated via toll-like receptor protein-4 (TLR-

4) dendritic cells and tissue resident macrophages.[77-79] The macrophages further enhance the tissue damage by secretion of pro-inflammatory cytokines and the dendritic cells leads to the differentiation of effector-T-cells by antigen presentation and migration of these T-cells into the infarct area promoting local inflammation.[77,79] Apoptotic cells on the other hand expressing phosphatidylserine on the outer layer of their cell membrane diminish the activation of dendritic cells and macrophages by interaction with their phosphatidylserine receptors, which results in the secretion of anti-inflammatory cytokines, as interleukin-10 (IL-10) or transforming growth factor- β (TGF-β).[80-82] Moreover the activation of T-cells by antigen presenting dendritic cells is decreased and regulatory T-cells are activated instead.[82,83] The so reduced inflammation of the hypoxic area leads to less scar formation, due to IL-6 down regulation and pro-angiogenesis, due to increased prostaglandin E2 release of apoptotic cells.[77,78,81,84]

The cardiac protection of stem cells could be enhanced by the addition of the supernatant of apoptotic PBMC (APOSEC) in a study by Winkler et al.[85] In this study a porcine myocardial infarction was induced and cardiosphere derived cells with or without APOSEC were injected 15 minutes after reperfusion.[85] After one month a 2-deoxy-2-(18 F)-fluoro-D-glucose-positron emission tomography-magnetic resonance imaging was done, showing less scarred area in the APOSEC treated group, compared to the control group.[85]

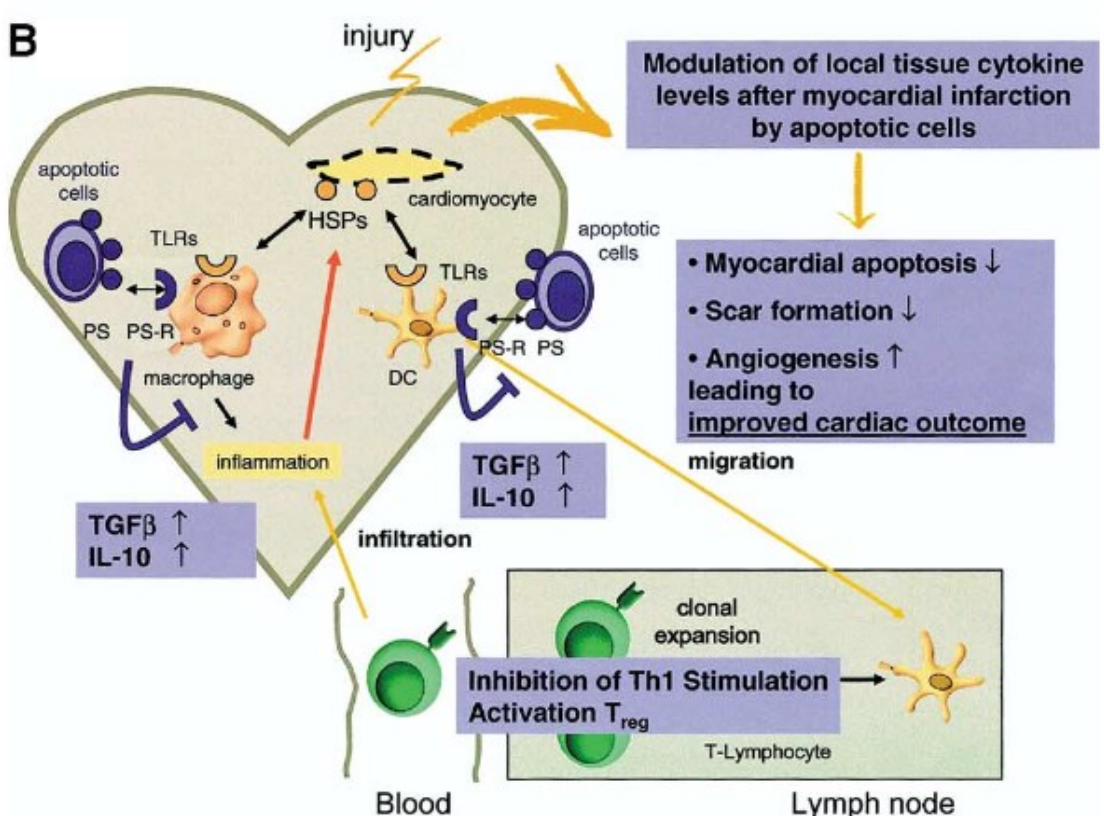

Fig. 3. Theory of the dying stem cell adapted from Thum et al.[77] Depiction of ischemic damage induced by myocardial infarction, leading to Toll-like receptor 4 (TLR-4) expression via heat shock proteins (HSPs) and thus activation of dendritic cells (DC) and tissue resident macrophages, which drive local inflammation.[77] Apoptotic cells (both from application of ex vivo cells or internal production) bind to phosphatidylserine (PS) and phosphatidylserine-receptors (PS-R) on cells of the immune system and lead to secretion of anti-inflammatory proteins, such as TGF-β and IL-10.[77] Additionally they diminish the activation of Th1 cells triggered by dendritic cells. As a result less regulatory T-cells (Treg) drive inflammation at the site of hypoxic damage.[77]

A positive effect of apoptotic cells was not only seen in stem cells, but also in autologous blood cells driven into apoptosis by oxidative stress.[86,87] These apoptotic blood cells were intramuscularly injected in patients suffering from ischemic foot condition due to peripheral arterial occlusive disease.[86,87] After injection the patients developed increased blood flow in the post-ischemic foot.[86,87]

Moreover the application of autologous blood samples in patients with chronic heart failure exposed to oxidative stress lead to promising results with significantly diminished risk of death and hospitalization, compared to the placebo group in acute myocardial infarction.[88]

Our working group could show, that ionizing irradiation induced apoptotic cell death in peripheral blood mononuclear cells (PBMC).[89,90] The conditioned medium of these cells enhanced wound healing and angiogenesis as well as vasodilation in a myocardial infarction model.[89,90]

These studies inspired many researchers to test the effect of the secretome of stressed or dying cells especially in regenerative medicine.[91] Of course these examples make clear, that these preconditioning concepts need to be done outside the human body, as treatment with irradiation, hypoxia or pro-inflammatory cytokines on a systemic level could lead to serious adverse events.

8.4 Secretomes of various cell types in wound healing

A pro-inflammatory state in the first phase of wound healing is important for pathogen clearance, yet in the following phases this excess of inflammation need to be converted into anti-inflammation to path the way for extracellular matrix and collagen repair.[18] Cytokines and chemokines seem to have a crucial role in the initiation of these processes.[18] Suggesting cells for regenerative medicine, which are capable of secreting such factors.

In fact secretomes of various cell types were shown to enhance migration of immune cells to the wounded area and change the cytokine environment of the affected skin. [74-76] In the beginning mostly stem cells were used for production of conditioned medium.[92,93] As positive effects on wound healing were found as a result of addition of various kinds of growth factors, the focus was layed on different cell types.[94] As TGF-β can be produced by keratinocytes, platelets, macrophages or fibroblasts and EGF is secreted by fibroblasts, keratinocytes and macrophages, both essential parts of granulation tissue remodeling and re-epithelialization.[94] the idea to use cells, which are easier to obtain, than stem cells was born.

Thus the conditioned medium of fibroblasts was used and really improved wound healing by pro-angiogenic and anti-inflammatory mechanisms.[95] A positive effect was seen either for the secretome of epithelial cells, but the effect was driven by exosomes (extracellular vesicles).[96]

As the activation of immune cells have a delicate influence on regeneration and wound healing, Laggner et al investigated dendritic cells stimulated with the secretome of PBMC and the resulting differentiation and maturation of this dendritic cells.[97] After the addition of the PBMC secretome the maturation of dendritic cells was diminished and the differentiation was inhibited either.[97] Regarding the pro-inflammatory effects of $CD1a^+$ cells as phagosome development, as well as antigen-presentation the treatment with PBMC secretome lead to drastic decrease in the expression pattern of the necessary genes, which could also lead to a more anti-inflammatory environment.[97]

Furthermore Laggner et al. revealed that treatment with the secretome of apoptotic PBMC could reduce mast cell activation, necessary for allergic reactions.[98] The treatment of in vitro dermal mast cells resulted in secretion of anti-inflammatory signals and diminished the release of inflammation driving α-IgE-induced mediator of these mast cells.[98]

Laggner et al was able to show, that the type of irradiation in a direct comparison of γ-irradiation and electron-irradiation on PBMCs did not show any difference in the production of regenerative paracrine factors.[99] The secretion pattern in concern to the composition of extracellular vesicles, lipids, proteins and on a transcriptome level resembled to a high degree.[99]

The secretome of apoptotic cells seemed to have an effect on microvascular obstruction, as showed in a myocardial infarction model.[90] This beneficial effect, may be evoked by the prevention of aggregation of platelets accompanied by a vasodilating function.[90] This vasodilation is conducted by higher iNOS and p-eNOS activation in coronary arteries, after stimulation with APOSEC.[90]

Another interesting study could show, that the secretome of PBMC decreased neutrophil extracellular trap formation (NET) of neutrophils.[100] These findings could give a hint to the mechanisms of action of cell secretomes on tissue regeneration.[100] NET-formation is necessary for adequate repulsion of pathogens and infection in wounds, however uncontrolled NET activation leads to decreased wound healing, due to reactive oxygen species.[101,102]

Surprisingly also pro-inflammatory factors secreted by macrophages displayed positive effects on wound healing.[103] Also pre-conditioning of mesenchymal stromal cells with pro-inflammatory substances e.g. TNF-α and IFN-γ induces cells to secrete pro-angiogenic factors, which ameliorate wound healing.[75]

The secretome of PBMC may have addiational modes of action to increase wound healing, as Copic et al. could reveal.[104] In a single cell sequencing analysis PBMC stimulated with the supernatant of PBMC (cultured for 24h) showed signitificantly increased expression of genes, that are important modulators of angiogenesis, e.g. VEGFA or SERPINB2.[104] This is furthermore important for successful wound healing, which indicates a role of cell-cell cross-talk in PBMCs, necessary for regeneration.[104] Moreover PAI-2 (plasminogen activator inhibitor type II), which is encoded by SERPINB2 is an important regulator for the endothelial barrier function, which leads to the efflux of immune cells to the wounded area and thus increased inflammation.[104] After stimulation with PBMC secretome the thrombin-mediated leakage of the endothelial barrier function could be inhibited.[104]

It became clear, that not only growth factors are responsible for the improved wound healing, yet a combination of pro-inflammatory, anti-inflammatory, pro-angiogenic proteins and factors affecting matrix-metalloproteinases and different collagens are most efficient. Cells that are capable of secreting all these factors at once, are for instance peripheral blood mononuclear cells. [105,106]

8.5 Peripheral blood mononuclear cells

Peripheral blood mononuclear cells (PBMCs) is a collective term of various different cells, consisting of natural killer cells (NK-cells), T-cells, B-cells, monocytes and dendritic cells.[105,106]

The T-cells can be differentiated into CD4+ and CD8+ cells. Regarding the CD4+ cells further discrimination into Tfh, Treg Th1, Th2, Th9, Th17 and Th22 cells with different functions is possible.[107-111] For instance pro-inflammatory cytokines e.g. INF-γ and TNF are produced by Th1 cells, which play a role in delayed hypersensitivity responses, trigger monocyte-activation and increase cell cytotoxicity, especially upon encounter of intracellular bacteria.[107-111] Regulatory T-cells (Treg) express Forkhead-box-protein P3 (FOXP3) and release anti-imflammatory cytokines as IL-10 and TGF-β.[107-111] Th17 cells secrete IL-17, which acts as driver for autoimmune diseases, e.g. psoriasis or experimental encephalitis.[107-111] Th2 cells produce IL-4 and IL-1β which is crucial for immunoglobulin G1 and E formation and B-cell survival. Tfh cells direct the proliferation and activation of antibody-forming B-cells.[107-111] Th22 secrete IL-22 and Th9 cells IL-9, which is linked to allergies, asthma and other autoimmune diseases.[107-111]

CD8+ T-cells produce IL-12, IFN-γ,TNF-α and act cytotoxic, pro-inflammatory and antigen-specific, yet can also act against cancer growth.[112,113] Moreover they seem to be involved in atherosclerosis.[113]

Follicular B-cells are activated via antigen-presentation of T-cells and react to Toll-like receptors, CD40 and B-cell receptors and may express MHC-II and CD27, resulting in plasma cell or memory B-cell transformation.[114-116] Marginal zone B2 cells play a role in the immune reaction to lipids and act T-cell independent to pathogens.[114-116] The function of B1 B-cells is not yet characterized in humans and still needs to be elucidated.[114-116]

Dendritic cells stimulate T-cells and are characterized by expression of MHC I and II and trigger antigen-specific reactions of the immune system and consist of mDC (derived from monocytoid precursor cells, pDC (plasmacytoid cells) and cDC (classical dendritic cells).[117-122] mDCs are

drivers of inflammation and migrate to inflammation areas and are even used in cancer treatment recently.[117-122] pDC are responsible for antigen-presentation and IFN-I production. cDC are the major antigen-presenting cells especially to CD4+ cells.[117-122]

Monocytes can also be divided in classical (CD14++CD16−, mostly involved in phagocytosis), non-classical (CD14+CD16++, pro-inflammatory and antigen-presenting function), intermediate (CD14++CD16+, having inflammatory functions, as well as phagocytic) and CD40 positive cells. [123-125] The CD40+ monocytes have a strong pro-inflammatory function and are related to chronic kidney disease.[123-125]

Natural killer cells (NK) can be divided in $CD56^{low}CD16^{high}$ cells, which merely act in a cytotoxic manner, or in $CD56^{high}CD16^{high/low}$ cells, which secrete a plethora of pro-inflammatory cytokines.[126]

These different cells of the immune system communicate, inhibit or induce its various functions in a direct or paracrine manner. For example, if mDC are not capable of producing an adequate amount of TGF-β, which is important for wound healing the activation of CD4+ (Th1 and Th17) and CD8+-T-cells will be increased.[126]

A big advantage in using PBMC for research or therapeutical usage is the broad availability as waste product of thrombocyte concentrate production.[127] Here blood samples gathered from healthy donors are divided into their different components, whereas the thrombocytes are obtained and further processed, the PBMC are discarded and may be used for research purposes.[127] This makes them a cost-efficient and easy obtainable resource for future therapeutic applications.

8.6 Types of programmed cell death

At the beginning of the 19th century, Virchow described a specific type of cell death termed necrosis which quickly became the main topic for several research groups worldwide.[128] An austrian researcher (Pischinger et al.) described a so-called "*Leukozytolyse*" [129,130] a death/consumption of leukocytes in blood smears first described in 1957.[129,130]

While necrosis describes an uncontrolled cell death, a regulated form of cell death, so called apoptosis, was later discovered by Lockshin and Williams.[131-134] Today, a plethora of programmed cell death types are known, for example ferroptosis, entotic cell death, autophagy-dependent cell death, immunogenic cell death, lysosome-dependent cell death,

mitochondrial permeability transition (MPT)-dependent necrosis, pyroptosis, parthanatos, NETosis associated cell death (Figure 4). [135,136]

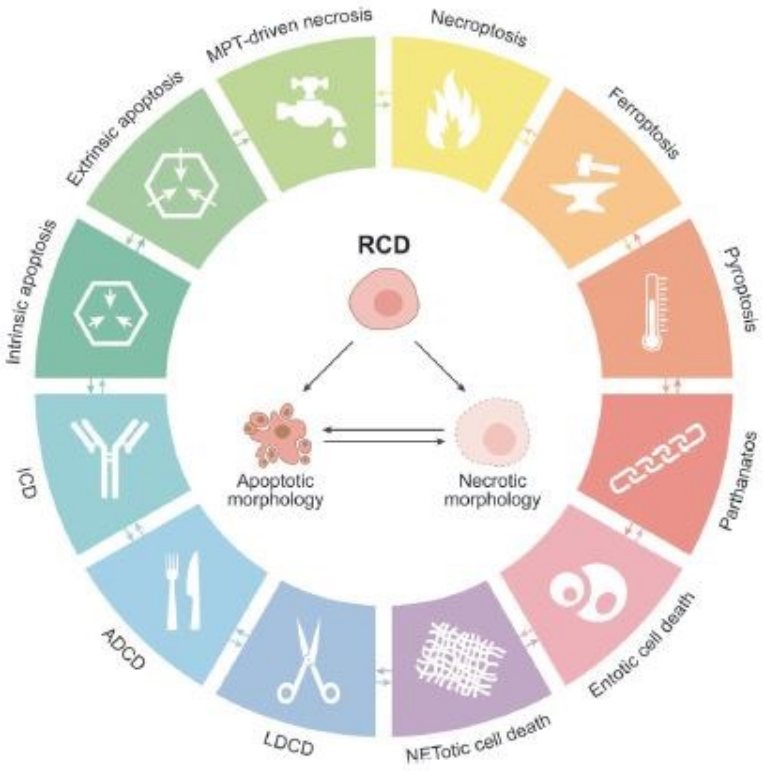

Fig. 4. Molecular mode of actions of cell death: names and distinct types suggested by the Nomenclature Committee on Cell Death published in 2018 and adapted from Lorenzo Galluzzi et al [135]
Shown are the different types of regulated cell death (RCD). Depicted as an example of various morphological characteristics a scheme of an apoptotic and necroptotic cell is depicted in the middle of the figure. Abbreviations: mitochondrial permeability transition (MPT), autophagy-dependent cell death (ADCD), lysosome-dependent cell death (LDCD) and immunogenic cell death (ICD)

Regulated cell death usually occurs upon either of two main triggers including harmful exogenous influence or renewal and development of tissue. While such exogenous damaging stimuli aim for targeted physiological degradation, regulated apoptosis occurs during various physiologic processes as for example hand and finger development during embryonic stage.[135] Furthermore apopotosis is very important for gametogenesis of oocyte and spermatozoid maturation.[137] The signal for apoptosis induction may be DNA damage or unreparable mutations.[137] Apoptosis appears to be of vital importance for a broad range of normal developmental processes since diminished apoptosis in drosophila melanogaster is accompanied with abolished formation of wings, legs and nervous or gastrointestinal system. [138,139] In murine models, downregulation of specific apoptosis triggering genes (e.g. Bax and Bac[140]), lead to limited developmental abnormalities, due to various alternative activation mechanisms of downstream effectors of apoptosis induction, or activation of other non-

apoptotic forms of cell death. [140,141] Furthermore, dysfunctional apoptosis activation implements autoimmune disease, viral infection and cancer. [141]

Apart from the crucial involvement in developmental processes, apoptosis further serves as safety mechanism eliminating potentially harmful cells. Upon exposure to exterior stress signals dying cells secrete paracrine factors , known as damage-associated molecular patterns (DAMPs) or alarmins, to adjacent cells, thereby activating the immune system as first line of defence to bacteria, cancer or trauma to enhance wound healing. [142-144]

Classification of various types of cell death based on morphological characteristics lead to the following three categories: [135]

1) Type I (e.g. apoptosis): pyknosis and nuclear fragmentation, whereas the plasma membrane stays intact and forms blebs, also known as apoptotic bodies, which are engulfed by phagocytosis of immune cells and ultimately degraded in the lysosome of for instance macrophages
2) Type II (e.g. autophagy): vacuolization in the cytoplasm ending by phagocytosis and lysosomal degradation
3) Type III (e.g. necrosis): without blebbing or vacuolization as type I and II, leaving cells with ruptured cell membrane and without phagoytosis

This nomenclature was deficient since it did not consider function, triggers of cell death, secreted factors , impact on surrounding cells or activated signalling pathways. With growing knowledge of mechanisms and function the Nomenclature Committee on Cell Death (NCDD) came up with a new definition in 2005.[135]
The resulting nomenclature is depicted in figure 4 above. Based on this nomenclature the different types of cell death relevant for this thesis will be discussed below.

8.6.1 Apoptosis

Apoptosis is induced via caspase activation leading to a controlled cell death, morphologically characterized by karyorrhexis, pyknosis and most characteristically the blebbing of the plasma membrane.[136] We discriminate two forms of apoptotic cell death: 1) intrinsic and 2) extrinsic apoptosis.[136]

8.6.1.1 Intrinsic Apoptosis

During intrinsic apoptosis the cell membrane remains intact and to some extent even cellular metabolic activity.[145] The final aim of an apoptotic cell is to be phagocytosed by macrophages or other immune cells.[145] Due to the lack of phagocytic cells in vitro, a nearly necrotic form also known as secondary necrosis with degradation of the plasma membrane can be observed in

cell culture. This degradation is associated with pore formation initiated by gasdermin E (DFNA5). [146,147]

Intrinsic apoptosis is initiated by a group of proteins containing domains of B-cell CLL/lymphoma 2 (BCL2) homology (BH), which can be divided in three sub fractions composed of the pro-survival branch (e.g. MCL1, BCL-2 itself and BCL-X_L); the effector protein family that consists of e.g. BCL2 associated X (BAX) and the BCL2 antagonist/killer 1 (BAK); or the pro-apoptotic BH3-only proteins, as for example PUMA (P53 upregulated modulator of apoptosis) and BID (BH3 interacting-domain death agonist). [148,149]

Pro-apoptotic regulation mechanisms

The BH3 proteins act as direct or indirect regulators of the pore forming effectors.[149,150] BAK or BAX induce pore formation in the mitochondrial membrane.[149,150] The mitochondrial outer membrane permeabilization (MOMP) results in apoptosis and is an irreversible process.[149,150,145] These pro-apoptotic BH3-only proteins are upregulated after DNA damage caused by endogenous metabolites, alimentary or environmental carcinogens, or chemotherapy.[149,150] As soon as the pro-apoptotic signalling outweighs the anti-apoptotic players, e.g. MCL1 or BCL-2 that inactivate BH3-only proteins by direct binding, the effector proteins are activated.[149,150] The effectors BAK or BAX can be activated by the BH3-only proteins including BH3 interacting domain death agonist (BID) and BCL2-interacting mediator of cell death (BIM) in a direct manner and result in pore formation in the outer mitochondrial membrane (OMM), leading to the release of cytochrome c (Cyt c) further known as the above mentioned MOMP.[149,151] Cytochrome c acts as trigger in the activation of the caspase cascade resulting in apoptosis.[18] Whereas BAX translocates as inactive monomer between the cytosol and the mitochondria, where it can form active oligomers, BAK stays in the mitochondria as inactive monomeric, membrane protein, often complexed with voltage-dependent anion channel 2 (VDAC2), which inhibits homo-oligomerization of BAK and therefore activation.[152,153]

The activation of BAK and BAX is carried out by BH3-only proteins transcriptionally or post-translationally, which is essential for the regulation of apoptosis.[154-156] Through this strict regulation prevention of autoimmunity by induction of apoptosis of autoreactive T-cells expressing T-cell receptor (TCR)–CD3 complex can be proceeded by the organism.[154-156] The activation of certain BH3-only proteins is induced by transcriptional upregulation, especially in BIM, phorbol-12-myristate-13-acetate induced protein 1 (often referred to as NOXA) and p53-upregulated modulator of apoptosis (PUMA).[154-156]

Whereas the pro-apoptotic function of BID is triggered post-translationally.[157-160] The above mentioned proteins are capable of forming direct interactions with BAK and BAX and as a consequence formation of homo-dimers of mitochondrial BAK via a BH3-in-groove

interface.[161-163] This dimerization in the mitochondrial membrane builds a lipidic pore in the membrane and leads to destabilization.[161-163] BAX is capable of forming arcs and rings after oligomerization leading to MOMP shown by single-molecule localization microscopy after transfection with GFP-Bax.[164 165]

Besides pro-apoptotic activation via BH3-only proteins, auto-activation of BAK and BAX can occur after downregulation of anti-apoptotic proteins such as BCL-2 or MCL1. [157] Furthermore, activation can occur via prolyl isomerase 1 (Pin1), which enhances BAK activation caused by tumor suppressor p53 or diminishing the pro-survival signaling produced by binding of ATR to BID. [166-168 169]

MOMP leads to release of on the one hand cytochrome c and on the other hand second mitochondrial activator of caspases (SMAC) into the cells' cytosol, [170-172] where cytochrome c attaches to apoptotic peptidase activating factor 1 (APAF1), found on the inactive pro-caspase 9 (CASP9).[170-172] Further binding with ATP results in the formation of the crucial apoptosome that initiates the activation of caspase 9.[173] This activation is realized by building homo-dimers of CASP9 or the hetero-dimerization of APAF1 and CASP9 proteins.[174,175] The apoptosome formation catalyses a proteolytic cascade of the executioner caspases 3 and 7 resulting in apoptotic cell death. [176 177] The SMAC protein acts as pro-apoptotic regulator not only by preventing stable binding of X-linked inhibitor of apoptosis (XIAP) to caspases, [171] but also blocking various other inhibitors of apoptosis (IAP)-family members.[172] While the deactivation of XIAP works by direct binding, SMAC proteins (Second mitochondrial activator of caspases) inhibit the function of c-IAP1 and c-IAP2 (cellular inhibitor of apoptosis proteins). c-IAP1 and c-IAP2 are important for the upregulation of anti-apoptotic factors such as caspase 8 or cellular FLICE (FADD-like IL-1β-converting enzyme)-inhibitory protein c-FLIP. [178-180]

The catalytic mechanisms of the executioner caspases results in the degradation of the cell and evokes DNA fragmentation, blebbing of the cell and phosphatidylserine exposure on the outer membrane (which is usually only located on the inner membrane), as the final result of intrinsic apoptosis. [181-183] Phosphatidylserine is a marker often used in flow cytometry to detect apoptotic cells in extracellular stainings. [181-183]

Anti-apoptotic regulation mechanisms

The anti-apoptotic proteins from the BCL-2 family not only inhibit the activation of BH3-only proteins by the above mentioned binding mechanisms. [184 185] Additionally BCL-2 plays an important role in the Ca^{2+} dynamics in the endoplasmic reticulum. [186] The BCL-2 family protein BCL-X_L increases energy metabolism efficiency by binding to the F1FO ATP synthase, thereby enhancing the ATPase activity and diminishing the ion leak, which in turn reduces the conductance of the membrane leak. [187,188] Another anti-apoptotic mechanism of BCL-2,

specifically utilized by cancer cells, is the regulation of cytochrome c oxidase activity and formation of electron transport mechanisms, in consequence of increased energy demands after oxidative stress and thus prevention of reactive oxygen species (ROS) overproduction.[189,190]

The inactivation of BAK (and therefore anti-apoptotic effect) is induced by the binding of its own C-terminal α helix to its activation spot consisting of BH1, BH2 and BH3 domains.[21]

It can be assumed, that X-linked inhibitor of apoptosis proteins (XIAP) acts anti-apoptotic through SMAC degradation in the mitochondria. [191]

Other inhibitor of apoptosis proteins(IAPs)s act by inducing ubiquitination and thus inhibition of caspase activity. [192-194]Furthermore, IAPs can enhance the tumor necrosis factor-α (TNF-α) driven ubiquitination of receptor interacting serine/threonine kinase 1 (RIPK1). [195] The TNF-α-dependent activation of the pro-survival regulator nuclear factor 'kappa-light-chain-enhancer' of activated B-cells (NF-κB) is strongly reduced in the absence of c-IAP1 and c-IAP2. [195]

8.6.1.2 Extrinsic Apoptosis

Extrinsic apoptosis is caused by extracellular stress and initiated predominantly via dependence receptors, which are activated in the absence of its ligands or death receptors, including for exampleTNF receptor superfamily members 1A, 10A, 10B and Fas cell surface death receptor (FAS or CD95) . [196-198] Apoptosis induction through death receptors is initiated by the formation of a death-inducing signalling complex (DISC) upon ligand-stimulation of the FAS receptor or TNF receptor superfamily member 10A and 10B (TRAIL-R1 and TRAIL-R2) at the cytoplasmic tail of the receptor.[199,200] Upon activation and subsequent trimer formation of FAS, TNF receptor superfamily member 1A (TNFR1), TNFR2 or TRAIL2-R1/2, further proteins such as caspase-8 (CASP8) or caspase-10 (CASP10), cFLIP or Fas-associated protein with death domain (FADD) are recruited to the activated receptor. While all trimers eventually lead to apoptosis, their downstream signalling mechanism varies.[199,200] The activated caspases induce apoptosis by either directly cleaving downstream executioner caspases (CASP3, CASP6, CASP7) or initiate the intrinsic apoptosis pathway by cleaving BID.[199,200,201] The TRAIL-receptors build a complex with FADD, caspase-8 and Receptor Interacting Protein (RIP-1) kinase upon activation.[69,201]The TNFR1-trimer can form two pro-apoptotic cytoplasmic complexes, complex IIA, consisting of Tumor necrosis factor receptor type 1-associated DEATH domain (TRADD), FADD and CASP8, and complex IIB, consisting of FADD, RIP-1 and caspase-8. [202,69] Furthermore, the TNFR1-trimer can also form a pro-survival complex composed of the anti-apoptotic c-IAP1/2, TNF receptor-associated factor 2 (TRAF2), TRAF5, TRADD and RIP-1, which activates NF-κB. [69,201] Although only verified for T lymphocytes and glycosylation of FAS, the modification of death receptors affect the sensitivity

for cell death induction of the specific cell type they are attached to.[203] The catalytic function of CASP8 is triggered by the interaction of CASP8 and FADD in the DISC, leading to dimerization of CASP8 molecules. [204,205] Active CASP8 causes the cleavage division of c-FLIP$_L$ and CASP8 heterodimers and give way for the CASP8 homodimerization and activation of cleavage activities. [206]

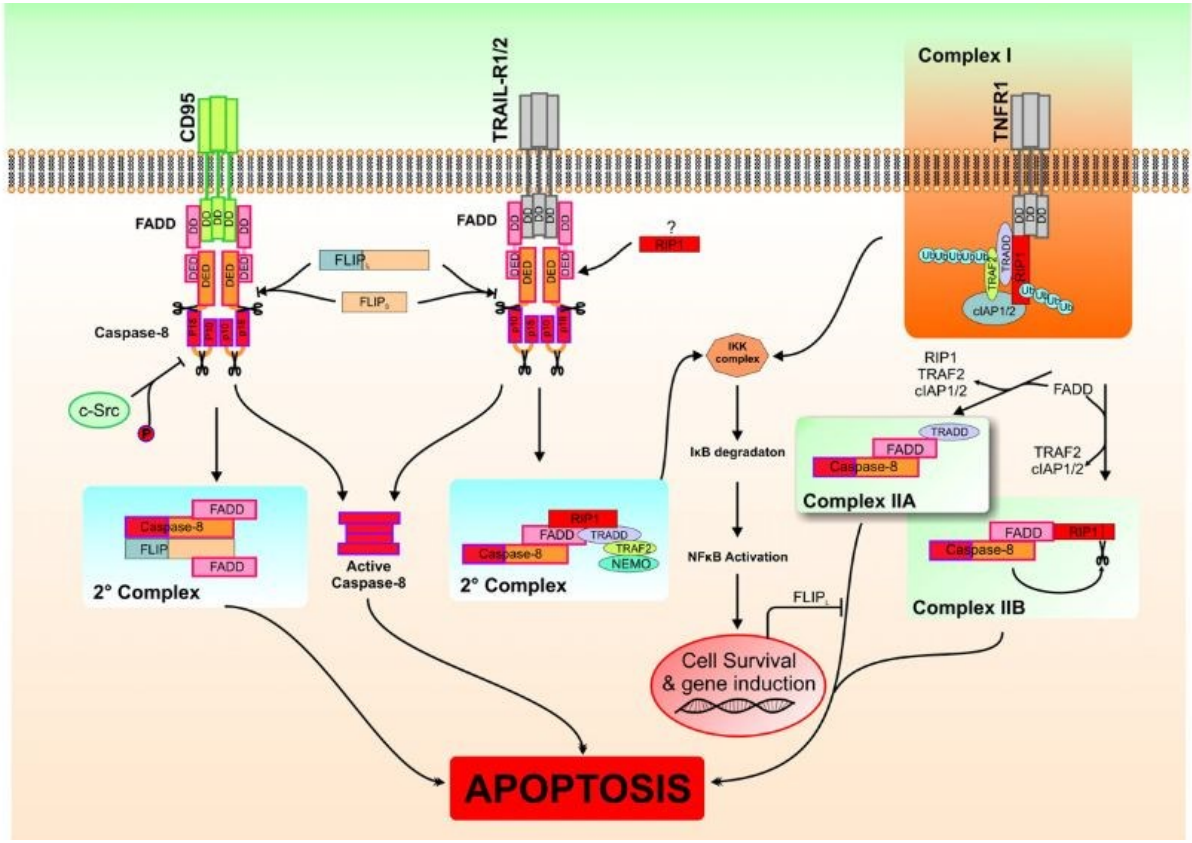

Fig. 5. Extrinsic cell death and its initiation and inhibitory pathways adapted from Dickens et al [200]

In addition to the inhibitory capacity of c-FLIP$_L$, extrinsic apoptosis can further be inhibited by various alternative mechanisms including for example phosphorylation of the tyrosine residue Y380of CASP8.[207] Whereas the phosphorylation of the T273 part of caspase 8 leads to an increase in the pro-apoptotic function. [207-209]

Certain cell types may escape FAS induced extrinsic apoptosis while FAS signalling inevitably results in apoptosis in other cell types.[207-211] In type I cells, such as lymphocytes, activation of CASP3 and CASP7 serves as sufficient trigger for apoptosis and cannot be escaped by anti-apoptotic BCL-2 activity or by depletion of BID.[207-211]

We distinguish between two cell types, where FAS can induce apoptosis: in type I cells such as lymphocytes the activation of caspase-3 and -7 by caspase-8 is a sufficient trigger for

apoptosis and the depletion of BID, nor the anti-apoptotic BCL-2 proteins can prevent this step.[210,211] This serves as crucial mechanism to avoid autoimmunity. Contrarily, type II cells, e.g. hepatocytes, pancreatic β-cells and certain cancer cells, may escape FAS-induced apoptosis by XIAP and the lack of BID. [210,211]

In Type II cells on the other hand, e.g. hepatocytes, β-cells of the pancreas or certain cancer cells the cleavage of caspase-3 and -7 can be averted by XIAP and a lack of BID (which is cleaved by caspase-8) can avoid extrinsic apoptosis.[211-213] Cleaved BID (truncated BID; tBID) acts as a BH3-only protein to activate BAK/BAX in the OMM.[214-216] In addition to these escape mechanisms, CASP10 may also act anti-apoptotic by actively dissociating CASP8 from DISC, whereas the atypical cadherin (FAT1) prevents the association of caspase-8 to the DISC after FAS activation.[217,218]

As shown in figure 5, the activation of TNFR1 is not solely inducing apoptosis, yet after polyubiquitination of RIPK1 by c-IAP1/2 in the complex I or linear ubiquitin assembly complex (LUBAC) a pro-survival signal is sent to the cell.[219-221] RIPK1 can lead to survival by activating (phosphorylation) NF-κB and on the other hand inactivates the inhibitors of NF-κB (IκBα and β) by phosphorylation.[202,222,223] Furthermore the phosphorylation of RIPK1 by IKK, transforming growth factor-β-activated kinase 1 (TAK1) or another kinase known as mitogen-activated protein kinase-activated protein kinase 2 (MAPKAPK2) inhibits its interaction with FADD and caspase-8 resulting in the inhibition of apoptosis.[224-227] On the contrary deubiquitylation of RIPK1 for instance by CYLD (CYLD lysine 63 deubiquitinase) leads to enhanced association of RIPK1 with FADD and capsae-8 to the complex II driving extrinsic apoptosis, in the presence of IAP-inhibitors known as SMAC-mimetics.[228,229] Another mechanism of complex II formation is the ubiquitylation of TRAF2 by HECT domain E3 ligase (HACE1), intriguingly a lack of HACE1 does not impair the TNFR1 induced RIP1/RIP3 assembly important for necroptosis induction.[230]

Extrinsic apoptosis induction is crucial for multicellular organisms, a lack of membrane bound FAS ligand leads to a activation of pro-survival and pro-inflammatory pathways and these mice develop an autoimmune phenotype similar to lupus.[231] Tumor necrosis factor-related apoptosis-inducing ligands (TRAIL) with the help of LUBAC can prepare the ground for both, apoptosis by building the DISC and pro-survival pathways by activation of NF-κB, extracellular signal-regulated kinases (ERK) or p38 among others.[232,233]

The second form of death receptors are the dependence receptor family including 20 different proteins and can be activated by the absence of ligands.[196] Among these receptors we can find Sonic Hedgehog receptors Patched (Ptc), netrin-1 receptors DCC (deleted in colorectal carcinoma), unc-5 netrin receptor A (UNC5A-D), UNC5H1-4, neurotrophin receptor

neurotrophic receptor tyrosine kinase 3 (NTRK3), TRKA and TRKC, nerve growth factor receptor $p75^{NTR}$, insulin receptors and insulin-like growth factor (IGF1r), Neogenin and many more. [234,235] [196] If for example the DCC receptor is cleaved via caspase-3, due to lack of ligands an association of APPL1 (Adaptor protein, phosphotyrosine interacting with PH domain and leucine zipper 1) and caspase-9 is built leading to caspase-cleavage and apoptosis.[236] Patched triggers apoptosis by complex formation of four and a half LIM domains 2 (FHL2 or DRAL), tumor-up-regulated CARD-containing antagonist of caspase nine (TUCAN) and NEDD4 (neural precursor cell expressed, developmentally down-regulated 4, E3 ubiquitin protein ligase), which starts caspase-9 activation.[237,238] UNC5B initiates p53-dependent cell death due to the dephosphorylation of death associated protein kinase 1 (DAPK1) executed via protein phosphatase 2 (PP2A). [239,240] Another unc-5 netrin receptor (UNC5D) after cleavage done by caspase-3 acts as gene expression regulator of pro-apoptotic proteins in the nucleus, whereas Neurotrophic Tyrosine Kinase, Receptor, Type 3 (NTRK3) after being cleaved by caspase-3 relocates into the mitochondria for caspase-9 activation.[241,242] Although the exact molecular mechanism is still to be elucidated TLR3 either is capable of apoptosis induction by activation of caspase-8 involving TIR-domain-containing adapter-inducing interferon-β (TRIF).[243]

8.6.2 Necroptosis

The evolvement and life of multicellular organisms depend on the homeostasis of cell survival and death.[131] Without a programmed and regulated pattern of cell death, embryonic life-forms die during their development.[244-246] The importance of necroptosis for embryonic development is highlighted by the fact that, mice deficient for necroptotic cell death pathways die at an early embryonic stage.[244-246]

Necroptotic cell death is completely independent of caspase activation. Necroptotic cells display morphological properties characterized by translucent cytoplasm, oncosis, permeabilization of both lysosomal and plasma membrane, whereas the nucleus stays intact.[136]

Necroptosis requires the activation of the receptor-interacting protein kinase-1 (RIPK-1) receptor- and interacting protein kinase-3 (RIPK3).[131,247-251] The implications of TNF-α regarding the regulation of molecular pathways and cell death patterns has been investigated since the 1980s, however only the breakthrough discovery of the RIP-kinases enabled the exploration of the necroptosis and its consequences. [131,247-251]

These two momentous findings along with the opportunity to inhibit necroptosis with Necrostatin-1 opened up the possibility for scientists to investigate necroptosis as a formerly

known blank area on the map.[220,252] Programmed cell death is triggered among others by TNF-α which binds to the Tumor necrosis factor -α receptor (TNFR) and induces a polyubiquitination of RIPK1 via the NF-κB pathway.[220,252] Deubiquitination of linear ubiquitin chains of RIPK1 disrupts the RIP-kinases feature to initiate pro-survival signalling.[220,252] Tumor necrosis factor receptor type 1-associated DEATH domain protein (TRADD) and the ligand Fas-Associated protein with Death Domain (FADD) assemble to the pro-caspase-8, yet in deviation to the normal formation of caspase-8 homodimers, FLICE-like inhibitory protein (FLIP) structurally mimics caspase-8 and associates to the protein.[128,245,253-255] Thus a heterodimer lacking protease activity is created, obviating activation of apoptosis.[128,245,253-255] The loss of function of caspase-8 or FLIP leads to an intracellular complex composed by RIPK1 and RIPK3, ending in the formation of the so called “necrosome”.[128,245,253-255] Consequently, mixed lineage kinase domain-like (MLKL) is activated to initiate necroptosis. [128,245,253-255] RIPK3 phosphorylates the MLKL, which can form oligomers and bind to the phosphatidylinositol phosphate species in the cell membrane leading to the flip of the inner membrane to the outside e.g. of phosphatidylserine, which is very important for cell death detection due to its binding capacity to Annexin-V. [245,254,256,257] Heat shock protein-90 (HSP-90) also plays a role in necroptosis as a lack of it inhibited the translocation of activated MLKL to the cell membrane. [258] [259] MLKL can also regulate Ca^{2+} influx after its localization into the cell membrane and thus demonstrates another mechanism of necroptosis induction. [260] Data suggest that MLKL activates a disintegrin and metalloprotease (ADAM), which is a family consisting of various different proteases in the cell membrane, prompting ectodomain shedding of cell adhesion molecules disrupting the cell integrity or leading to cell migration, growth factors or cytokines, which enhance inflammation as soluble fragments.[261] MLKL can pave the way to necroptosis by froming cation channels for Mg^{2+} creating permeability and cell membrane depolarization.[262]

Beside the initiation of necroptosis by TNF many more activators are known, e.g. FAS, TLR3 and TLR4, pathogen recognition receptors (PRRs) and Z-DNA binding protein 1 (ZBP1). [249,263,264] The ligand for TLR3 is double-stranded RNA of viruses in the endosome, whereas TLR4 can be activated by lipopolysaccharides (LPS) in the membrane of gram-negative bacteria or Damage-associated molecular patterns (DAMPs) at the cell surface leading to the RIP homotypic interaction motif (RHIM) and TRIF interaction resulting in RIPK3 activation.[263] ZBP1 detects cytosolic DNA and RNA (also very essential for antiviral immune answer) and acts via interferon type I synthesis induction and NF-κB. [265,266]

As inhibitory player of the necrosome, carboxyl terminus of Hsp70-interacting protein (CHIP) was identified for ubiquitination of RIPK1 and RIPK3 causing lysosomal degradation and A20 for inhibition of the necrosome-complex building by ubiquitination of RIPK3.[267-269] Protein phosphatase Mg2+/Mn2+ dependent 1B (PPM1B) dephosphorylates RIPK3, whereas aurora

kinase A (AURKA) prevent the RIPK1 and RIPK3 interaction by phosphorylation steps and therefore both inhibit the necrosome assembly. [270,271] The RIPK3 activation further depends on the availability of co-stimulatory factors as CDC37 and heat shock protein 90 (HSP-90).[272] One of the most important factors of necropotosis induction is the caspase-8 deficiency or inactivation. [273,274]

Necroptosis may have developed as a cellular opportunity for the defence against intracellular infection. [128,275,276] However, various effects of necroptosis have been shown so far. Necroptosis seems to play a role in atherosclerosis[277], myocardial infarction[278], traumatic brain injury[279] and Salmonella enterica infection. [280]

Despite the increasing number of cellular and clinical research projects, the path of utter understanding of necroptosis is still a long road to go.

8.7 From cell death to cell survival

Our working group around Prof. Ankersmit tried to further develop the conclusion of cell-based regenerative therapies and tried to use the secretome of PBMCs[281] The results were promising with significant reduction of infarct size in a rodent AMI model, after injection of the PBMCsec.[281]

To enhance the regenerative capability of PBMCs, they were driven into apoptosis.[71,282] The apoptosis was triggered by γ-irradiation, as it is commonly used to prepare blood transfusion for patients with immunodeficiency.[281]

As a next step only the secretome of the apoptotic PBMC after 24h of cultivation was used, due to the literature and data gathered from the use of conditioned medium of stem cells in myocardial ischemia.[71,282] The secretome of the irradiated apoptotic PBMC hereinafter referred to as "APOSEC" was able to restore cardiac function after AMI in a rat model, after intravenous infusion.[282] These effects were explained by an increased amount of pro-angiogenic cytokines, for instance IL-8, vascular endothelial growth factor (VEGF) and growth related oncogene-α (GRO-α).[281,282] The inhibition of reperfusion-induced cardiomyocyte death or induction of cytoprotection have been suggested as a potential mechanism of action.[281] Therefore, we have identified several mechanisms that may at least partially elucidate the effects stated above. APOSEC induces cytoprotection, as well as anti-apoptotic, pro-survival mechanisms, in cardiomyocytes in vitro. Incubation of APOSEC augments the phosphorylation of AKT, p42/p44, Erk1/2, p38, MAPK, HSP27, c-Jun, and cAMP response element binding protein

(CREB) in human cardiomyocytes within 60 min, and the observed effects on Hsp27 and CREB phosphorylation are dose-dependent.[281,282] In addition, the expression of anti-apoptotic proteins, such as Bcl-2 and BAG1, was induced. Furthermore, APOSEC prevented cell death in cardiomyocytes in a starvation assay[281] and we showed that the inhibition of select factors (VEGF, IL-8, ENA-78, MMP9) alone or in combination did not attenuate the induction of CREB and Bcl-2 in cardiomyocytes, indicating unknown biological mechanisms.[282]

The regenerative effect was not only shown in stressed cardiomyocytes, but also in a murine wound healing model. Paracrine factors derived from PBMCs induce the activation of cytoprotective proteins in keratinocytes (CREB, Erk1/2, c-Jun, Akt, HSP27), dermal fibroblasts (Erk1/2, c-Jun, Akt, Hsp27), and dermal microvascular endothelial cells (CREB, c-Jun, HSP27).[57]

Furthermore, the PBMC secretome seemed to have vasodilatory effects. [90] Hoetzeneker et al was able to demonstrate that the co-incubation of platelets with APOSEC lead to an enhancement of phosphorylated vasodilator-stimulated phosphoprotein (VASP) and as a consequence inhibiting platelet aggregation.[90] Moreover the treatment of human umbilical vein endothelial cells (HUVEC) with APOSEC lead to an increased release of vasoactive substances such as p-eNOS and iNOS.[90] Not only this indirect regulation was observed, yet also a direct vasodilation in myographical testing on coronary artery rings could be shown.[90] Thus we can suggest a role of APOSEC in vasodilation, which may have an impact on early wound healing. As previously discussed after the initial vaso-contractile period after wounding with thrombocyte clotting to stop the wound from bleeding, vasodilation plays an essential role in the inflammatory phase of wound healing leading to migration of macrophages and nutrient transportation to the wounded site.[7]

In a spinal cord injury (SCI) study in rats, positive effects on the outcome after traumatic stress were revealed.[283] Our working group also demonstrated an up-regulation of Erk1/2 in spinal cord tissue from naive rats exposed to human APOSEC via intraperitoneal injection.[283] Astrocytes and Schwann cells co-incubated with APOSEC exhibit CREB, Erk1/2, c-Jun, Akt, and HSP27 phosphorylation in vitro (the latter only in astrocytes). CREB phosphorylation has also been shown in neurons.[283] Ischaemia is a severe problem in SCI. We showed an increase in pro-angiogenic chemokine (C-X-C motif) ligand 1 (CXCL1) and neuroprotective Brain-Derived Neurotrophic Factor (BDNF) after administration of APOSEC to naïve rats in vivo.[283,284]

The inflammatory response after SCI is mediated by monocytes and macrophages, which resolve inflammation. In a previously published rat model of SCI, Haider et al. demonstrated increased infiltration of CD68+ cells (by immunohistological analysis) to the site of the inflicted injury in the PBMC secretome group.[283] However, the number of iNOS-positive cells (reflecting

microglia activation) was decreased.[283] Haider et al. were also able to show that incubation of CD14+ cells with the MNC secretome up-regulates markers associated with M2 polarization, indicating a shift from pro- to anti-inflammatory immune activation.[283]

Beside the monocytes also the neutrophils, the most numerous subpopulation of leukocytes, play a significant role for wound healing.[100,285] They appear as first responders to a wounded area, to fight infections via phagocytosis and secretion of reactive oxygen species (ROS) and additionally the production of neutrophil extracellular traps (NETs).[100] The NET formation, which is important in the inflammatory phase of wound healing, holds the potential to massively impair tissue regeneration if it is acting excessively.[15] Klas et al. could show, that the stimulation of neutrophils with the secretome of PBMCs reduced the ROS production and diminished the activation of protein arginase deiminase 4 (PAD4), which leads to decreased NET-formation.[100] The exact regulation of NETosis may be an important element in improved wound healing. [63,286]

A synergistic effect of the PBMC secretome could also be verified in further studies of Klas et al.[100] Klas et al could show, that neutrophil extracellular trap (NET)-formation was only diminished after treatment with the supernatant of whole PBMC cultures.[100] Stimulation of neutrophils with lipid or protein subfractions of the PBMCs did not result in the same beneficiary effect.[100]

Bacterial infections also lead to chronic non healing ulcers or prolong adequate healing.[287] Another positive effect on wound healing of APOSEC may be the antimicrobial activity shown by Kasiri et al.[288] He could demonstrate that the growth of Pseudomonas aeruginosa a common gram-negative bacteria was reduced by the application of the PBMC-secretome.[288] Furthermore the growth of Escherichia coli and Staphylococcus aureus were significantly inhibited by the application of APOSEC.[288]

The angiogenic properties of the PBMC secretome have been shown in an aortic ring assay and 3D cultures of spinal cord tissue.[283] In addition, in mesenchymal fibroblasts incubated with APOSEC, our working group demonstrated increased IL-8, MMP9, and mRNA levels of proteins associated with angiogenesis.[91] Moreover, angiogenesis is crucial for wound healing, and the pro-angiogenic capacity of the secretome of PBMC (PBMCsec) has been shown in vitro (increased proliferation of endothelial cells tested via tube formation assay) and in vivo (increased number of CD31+ cells in a mouse model of wound healing).[57]

This pro-angiogenic effect could be verified by Copic et al., as tube formation assays after stimulation with plasma(from whole blood), that was treated with PBMCsec showed increased endothelial activity.[104] This increase in angiogenesis may be induced by the upregulation of genes, such as SERPINB2, VEGFA or CXCL5, as shown in a single cell sequencing analysis

after stimulation of monocytes by PBMCsec.[104] Furthermore upon stimulation of PBMCsec the thrombin-mediated endothial leakage was ameliorated, leading to preserved endothelial barrier function.[104] A retained endothelial barrier function prevents excessive migration of immune cells and thus exaggerated inflammation. [104]

After promising in vitro results for wound healing, our working group sought to explore the effect of PBMCsec in vivo. In the study of Mildner et al after application of the supernatant of PBMC on punch biopsy wounds an increased wound closure could be detected from day 3 and on day seven, the tissue analyzed with histological stainings appeared to have matured to a higher degree, as the control groups treated with medium and sodiumchloride alone.[16] In an scratch assay the migratory capacity of fibroblasts and keratinocytes was ameliorated in vitro after stimulation with the secretome.[57]

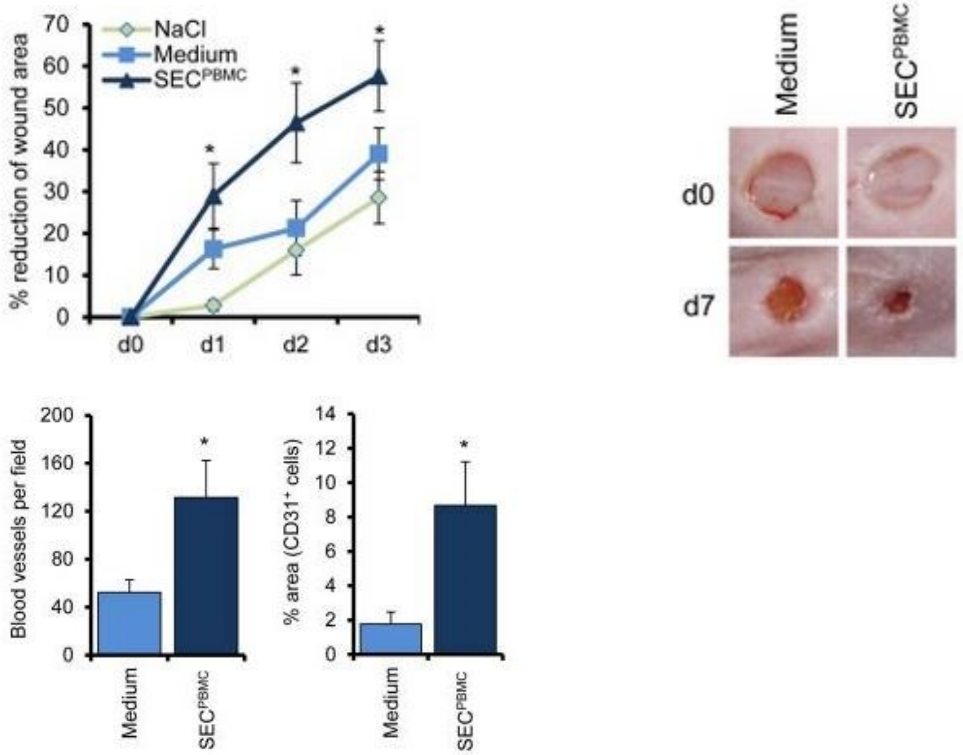

Fig. 6. Effects of PBMC secretome on wound healing in a murine model. Adapted from Mildner et al [57] The time curve displays the wound closure within 3 days in given in percent after daily treatment with PBMC supernatant (SEC_{PBMC}) physiologic sodium chloride-solution (NaCl) or medium alone.[57] The wound closure after seven days is shown on the left and below the neo-angiogenesis was analyzed using histological sections of the wound area.[57]

Wagner et al could reveal a beneficiary effect of the secretome of apoptotic PBMCs (MNCaposec) in a murine diabetic wound model (LepRdb/db mice).[61] After 25 days of wounding the unclosed area was signicantly smaller in the mice treated with APOSEC compared to the vehicle treated control group (showed in the figure below).[61]

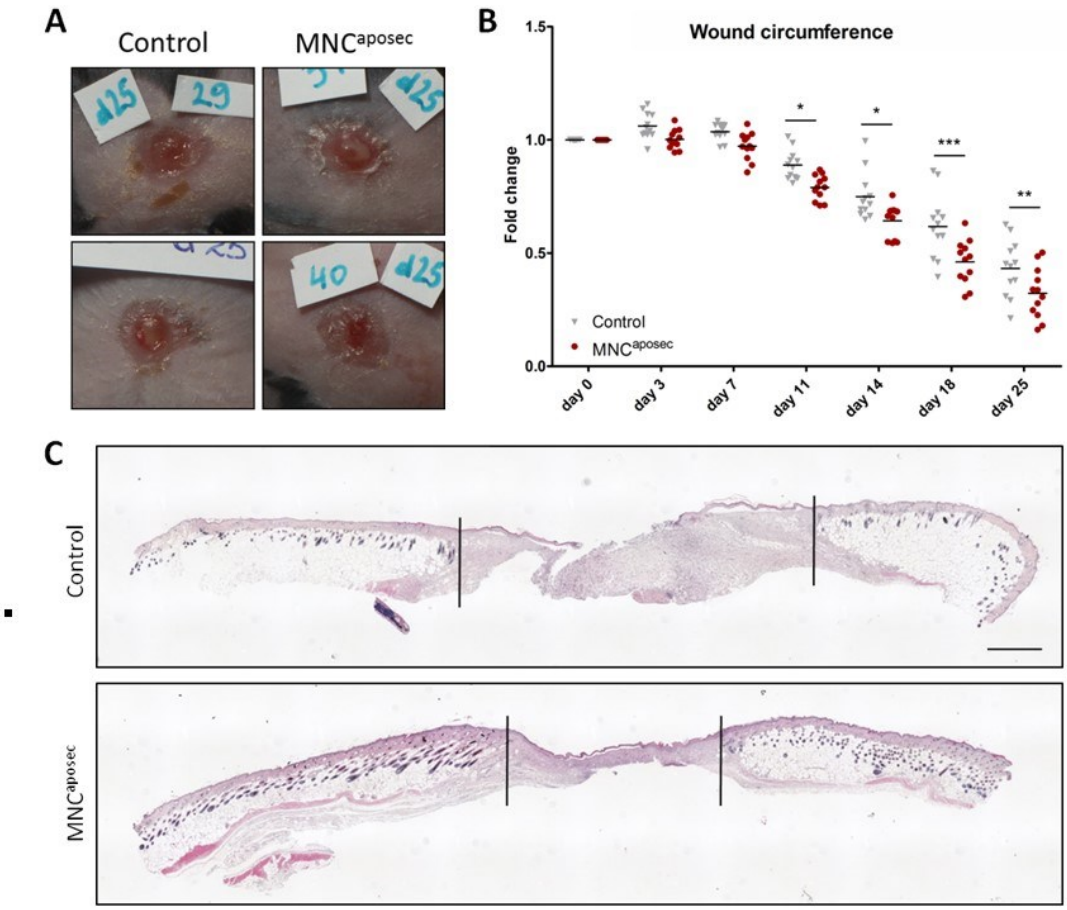

Fig. 7. Effects of the secretome of apoptotic PBMC (MNCaposec) in a murine wound healing model (drug vehicle was used as control)[61] **A** photograph of the wounded area treated with MNCaposec or vehicle. **B** Wound circumference depicted in fold change. **C** Immunohistochemical analysis of the wounded area (representative sections of skin treated with MNCaposec or vehicle.[61]

In immunohistochemical analysis (Hematoxylin and eosin staining) the treatment of wounds with MNCaposec lead to decreased wound area and showed more re-epithelialization compared to the vehicle treated controls.[61]

Furthermore the positive effects of irradiated PBMC on re-epithelialization could be verified in the study of Hacker et al.[89] After a standardized burn injury the skin of pigs treated with the irradiated PBMC secretome depicted an increased epidermal thickness as well as a higher number of CD31+ cells, suggesting a higher angiogenic activity in the damaged tissue.[89] Incubating T cells with the PBMC secretome resulted in the induction of apoptosis, which was blocked by pre-incubation with caspase 3 and caspase 8 inhibitors, indicating the involvement of external pathways.[90]

Moreover, the quality and strength of the newly formed skin was analyzed by quantification of Rete ridges, which act as stabilizers between the epidermis and dermis, leading to better compensation of shear stress.[89] The length of rete ridges was found higher in the area treated with the secretome of PBMC compared to the medium or isotonic sodium chloride solution

(NaCl) treated area. [89] In the histological section of the border zone keratin-10 was stained as marker for epidermal differentiation.[89] As shown in the figure 7 below the increased proliferation of the epidermis in the wounds treated with PBMC secretome could be detected.[89]

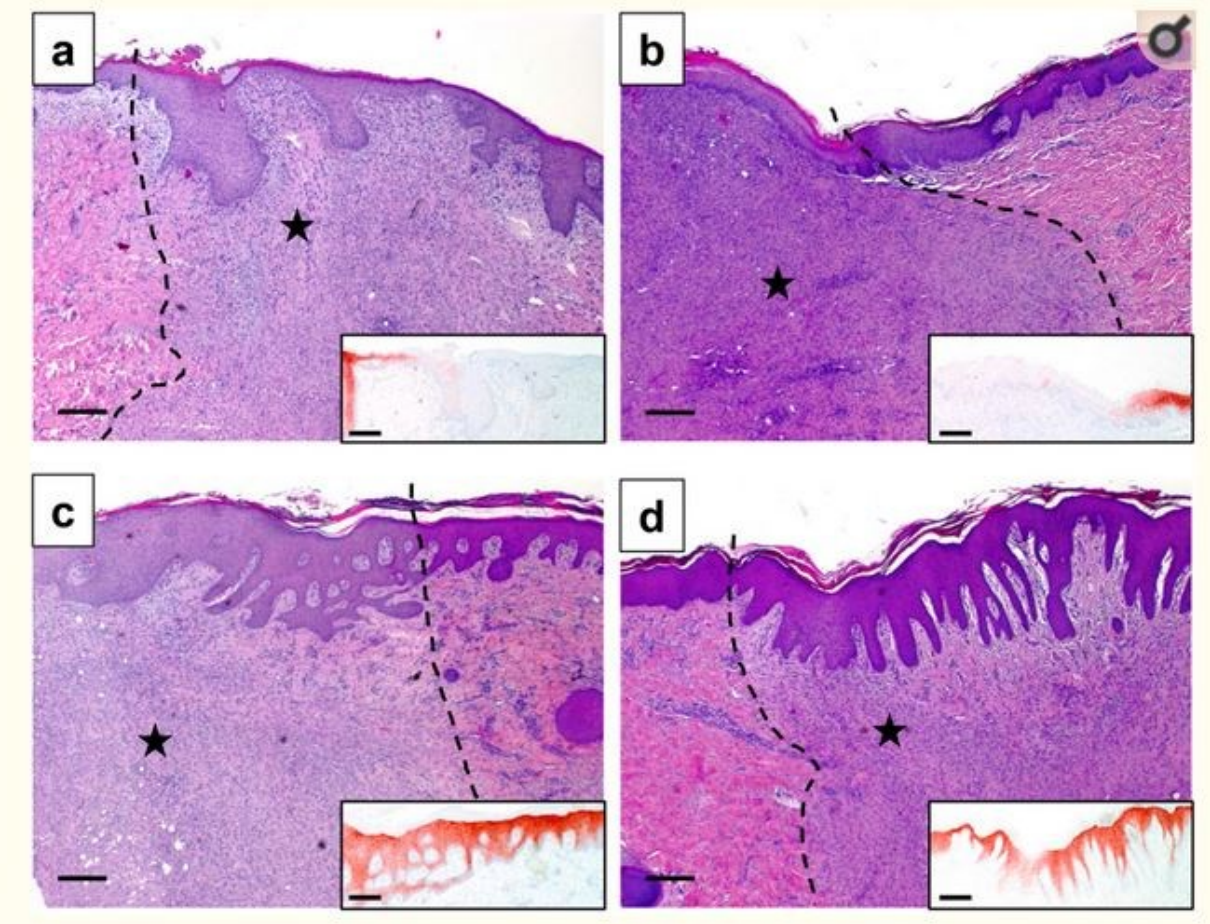

Fig. 8. Keratin 10 staining in porcine wound healing adapted from Hacker et al [89] Increased epidermal proliferation was shown with keratin 10 stainings (red) in a wound treated with a) NaCl b) medium c) the secretome of PBMC or d) the secretome of irradiated PBMC. The asterisk marks the wounded area.

After addition of PBMCsec on rodent skin flap wounds lower necrosis-rates were observed leading to improved wound healing.[289]The wound and flap area were excised after day 7 of PBMCsec application and the number of vessels were evaluated in immunohistochemical sections.[289] The results were astonishing, as the number of vessels was higher in the PBMCsec cohort, whereas the control group undergoing sham surgery clearly showed more von Willebrand factor-positive vessels.[289]

The PBMC secretome seems to have multiple ways to implement its beneficial effects on wound healing. Potential modes of action and the studies referring to the respective range of subjects are summed up in the figure below.

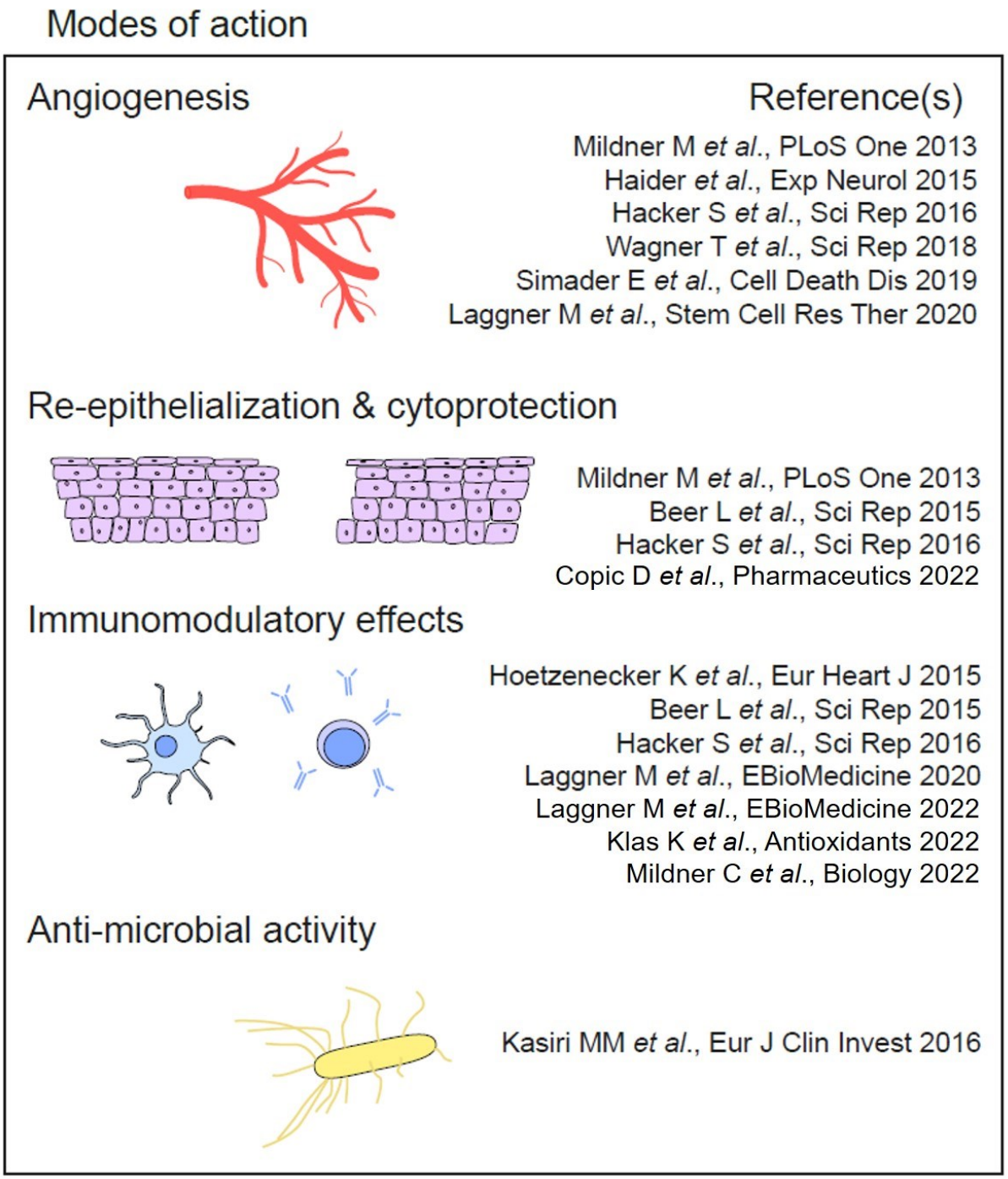

Fig. 9. Possible modes of action of PBMC secretome, regarding pro-angiogenic effects, cytoprotection, and regulation of the immune system.[99] Adapted from Hacker et al. [99]

Beer et al. analyzed the secretome of irradiated and untreated PBMCs regarding their composition of lipids, proteins and microvesicles.[63] He could show, that the supernatants of PBMCs contained higher levels of triglycerides, cholesterol and phospholipids after irradiation.[63] Moreover the amount of oxidized lipids significantly increased in the irradiated group.[63] The number of microvesicles and exosomes was increased in the supernatant of irradiated of PBMCs as well.[63] To investigate the role of proteins, lipids, exosomes and microparticles they were applied on fibroblasts scratch assays.[63] The fibroblasts treated with

exosomes of irradiated PBMCs seemed to display the fastest scratch closure by fibroblast proliferation.[63]

Wagner et al further developed this concept and tried to test the possible angiogenic potential, of the exosomes and lipids and proteins and compared it to the secretome of co-cultured, irradiated PBMC subtypes in an ex vivo aortic ring assay.[286] The results were other than expected, as the formation of new vessels was most prominent after stimulation with the whole secretome, the exosomes, lipids or proteins alone came not even close to this effect.[286] Additionally an AP-1 promoter and HSP-27 phosphorylation assay was done with the subfractions and as a control all isolated exosomes, lipids and proteins were pooled again and used as stimulation.[286] Astonishingly the pooled subfractions could not sum up to the effect the supernatant of whole PBMCs achieved in the activation of AP-1 and HSP-27[286]. These results may indicate a possible synergistic effect.[286] But the main actor of this effect is still not found.

Our working group tried to break the effect of APOSEC down to one effective composite. Wagner and Beer et al. analyzed the impact of proteins, lipids, exosomes and microvesicles, yet without finding a sole actor of the pro-angiogenic effect.[63,286]

To further investigate the source of the angiogenic capacity of the secretome of irradiated (and therefore apoptotic and necroptotic) PBMCs is the aim of this thesis. As elaborated in the following two papers we sought to gain deeper insight in the mechanisms of action of this highly auspicious treatment possibility for enhanced wound healing.

8.8 Aims of this thesis

As previously shown by our working group the secretome of PBMC has the potential to enhance wound healing in a murine and porcine model.[57,89] Thus, the first aim of this thesis was to unravel the cell type of PBMCs, which is responsible for this pro-angiogenic, wound healing capacity. Moreover the cytokine and chemokine composition of T-cells, B-cells, NK-cells and monocytes in that context, were never investigated before.

The changes in the gene signature were further determined via micro-array analysis as well as on protein level via protein assays of the supernatant.

This thesis aims to discover possible differences on the PBMC secretome, according to the initiated cell death.

We sought to analyse the changes in gene and protein expression, resulting from apoptosis and necroptosis in PBMCs and the changes in its paracrine effects.

The last and most important aim of the study is to test, if the application of autologous APOSEC, that was produced under good manufacturing practice (GMP)-guidelines on human skin is safe and does not lead to adverse events. This was observed in a clinical phase I study.

9 CHAPTER TWO: Results

9.1 Prologue

In previous works of our working group known PBMCs showed only low concentration of pro-apoptotic factors, such as TNF-α, soluble CD40 ligand (sCD40L), soluble FAS ligand (sFASL), and sFAS, after irradiation.[90] Blocking them did not result in preventing apoptosis in highly purified CD4+ T-cells.[90] These findings lead to the idea, that not only apoptosis, but another cell death could be triggered in PBMC after irradiation.

In the study of Kasiri et al. we tested different types of cell death induced by irradiation.[290] Due to the help and experience of the guest scientist Pietkiewicz and the new technological possibilities of the Image Stream, we were able to detect necroptosis as a consequence of ionizing irradiation.[291]

We further wanted to observe what happens to the already known angiogenic potential of PBMC secretome, if apoptosis or necroptosis is inhibited. Would this APOSEC or NECROSEC will have similar angiogenic potential?

9.2 Paper 1

Simader et al. *Cell Death and Disease* (2019)10:729
https://doi.org/10.1038/s41419-019-1974-6

Cell Death & Disease

ARTICLE Open Access

Tissue-regenerative potential of the secretome of γ-irradiated peripheral blood mononuclear cells is mediated via TNFRSF1B-induced necroptosis

Elisabeth Simader[1,2,3], Lucian Beer[4,5], Maria Laggner[2,3,6], Vera Vorstandlechner[2,3,6], Alfred Gugerell[2,3,6], Michael Erb[7], Polina Kalinina[8], Dragan Copic[2,3,6], Doris Moser[9], Andreas Spittler[10], Erwin Tschachler[8], Hendrik Jan Ankersmit[2,3,6] and Michael Mildner[8]

Abstract

Peripheral blood mononuclear cells (PBMCs) have been shown to produce and release a plethora of pro-angiogenetic factors in response to γ-irradiation, partially accounting for their tissue-regenerative capacity. Here, we investigated whether a certain cell subtype of PBMCs is responsible for this effect, and whether the type of cell death affects the pro-angiogenic potential of bioactive molecules released by γ-irradiated PBMCs. PBMCs and PBMC subpopulations, including $CD4^+$ and $CD8^+$ T cells, B cells, monocytes, and natural killer cells, were isolated and subjected to high-dose γ-irradiation. Transcriptome analysis revealed subpopulation-specific responses to γ-irradiation with distinct activation of pro-angiogenic pathways, cytokine production, and death receptor signalling. Analysis of the proteins released showed that interactions of the subsets are important for the generation of a pro-angiogenic secretome. This result was confirmed at the functional level by the finding that the secretome of γ-irradiated PBMCs displayed higher pro-angiogenic activity in an aortic ring assay. Scanning electron microscopy and image stream analysis of γ-irradiated PBMCs revealed distinct morphological changes, indicative for apoptotic and necroptotic cell death. While inhibition of apoptosis had no effect on the pro-angiogenic activity of the secretome, inhibiting necroptosis in stressed PBMCs abolished blood vessel sprouting. Mechanistically, we identified tumor necrosis factor (TNF) receptor superfamily member 1B as the main driver of necroptosis in response to γ-irradiation in PBMCs, which was most likely mediated via membrane-bound TNF-α. In conclusion, our study demonstrates that the pro-angiogenic activity of the secretome of γ-irradiated PBMCs requires interplay of different PBMC subpopulations. Furthermore, we show that TNF-dependent necroptosis is an indispensable molecular process for conferring tissue-regenerative activity and for the pro-angiogenic potential of the PBMC secretome. These findings contribute to a better understanding of secretome-based therapies in regenerative medicine.

Introduction

Regenerative medicine, aiming at restoring damaged tissues and organs, has become an emerging branch of translational research in the last century worldwide[1]. However, despite major advances in drug therapies, surgical interventions, and organ transplantation, regeneration of injured organs still remains a major obstacle[2]. A promising new therapeutic avenue may be offered by stem cell-based therapies, on which numerous pre-clinical

Correspondence: Hendrik Ankersmit (hendrik.ankersmit@meduniwien.ac.at) or Michael Mildner (michael.mildner@meduniwien.ac.at)
[1]Department of Internal Medicine III, Division of Rheumatology, Medical University of Vienna, Vienna, Austria
[2]Division of Thoracic Surgery, Medical University of Vienna, Vienna, Austria
Full list of author information is available at the end of the article.
These authors contributed equally: Hendrik Jan Ankersmit and Michael Mildner
Edited by T. Kaufmann

Official journal of the Cell Death Differentiation Association

SPRINGER NATURE CDDpress

studies, investigating their efficacy and mechanisms have been conducted[3–6]. Unfortunately, translation of experimental in vitro studies or animal models to the patient has been shown to be extremely difficult if not impossible[7]. In addition, an increasing number of studies suggests that not stem cells themselves, but rather the factors released from stem cells are important and sufficient to promote tissue regeneration[8,9].

In 2005, Thum et al.[10] speculated that stem cells undergo apoptosis while being processed for clinical applications and thus induce immunomodulatory and tissue-regenerative effects. In addition, the authors doubted the uniqueness of stem cells and suggested that any other nucleated apoptotic cell type would exhibit tissue-regenerative features[10]. The first study providing evidence for tissue repair by stressed peripheral blood mononuclear cells (PBMCs) was performed by Ankersmit et al.[11]. Enhanced regeneration was observed in acute myocardial infarction (AMI) by applying γ-irradiated PBMC suspensions intravenously. In subsequent years, we were able to show that the application of the PBMC secretome alone causes tissue repair in AMI[12–14], stroke[15], spinal cord[16], and skin wounds[17–19], in small and clinically relevant large animals. Although a previous study from our group suggested that γ-irradiation is able to induce apoptosis and necroptosis[20], a contribution of necroptosis to tissue regeneration by the release of paracrine factors has not been investigated so far.

In contrast to necrosis, an uncontrolled form of cell death, apoptosis had already been described as a well-controlled form of programmed cell death decades ago[21]. Later, also a programmed form of necrosis, termed necroptosis[22,23]. The two forms of programmed cell death differ morphologically as well as mechanistically from one another. Morphologically, apoptosis is characterized by karyorrhexis, pyknosis, and blebbing of the plasma membrane[22]. By contrast, necroptotic cells exhibit translucent cytoplasms, oncosis, and permeabilization of the lysosomal and plasma membranes, while nuclei remain intact[22,23]. Instead of caspase activation, necroptosis involves receptor-interacting protein kinase-1 (RIPK1), RIPK3, and mixed lineage kinase domain-like (MLKL) activation[24]. Tumor necrosis factor-α (TNF-α) is one of the best characterized inducers of apoptosis, activating the caspase-8 signalling cascade. However, due to partially overlapping upstream signalling elements, TNF can also activate the necroptotic pathway, which is favored by impaired caspase activity[23]. Whereas the role of necroptosis in several pathological conditions, including atherosclerosis[25], myocardial infarction[26], traumatic brain injury[27], and infections[28] have been investigated so far, the effects of the necroptotic cells on surrounding tissues remains poorly understood.

Although several biological effects of paracrine factors released from stressed PBMCs have already been investigated, the mechanisms by which these factors exert their pro-angiogenic and tissue-regenerative activities have not been fully elucidated so far[17]. In the current study, we therefore addressed two major questions: (1) is the pro-angiogenic potential of the secretome of γ-irradiated PBMC cell type-dependent and (2) does the type of programmed cell death contribute to the pro-angiogenic property of γ-irradiated PBMC secretome (Fig. 1).

Materials and methods

Ethics vote

Heparinized blood samples for PBMC isolation were obtained from healthy volunteers at the Department for Blood Transfusion Medicine of the Medical University of Vienna (ethics committee vote: EK-Nr 1539/2017). All donors provided informed written consent. For ex vivo angiogenesis experiments, mouse experiments were performed according to recent Austrian guidelines for the use and care of laboratory animals and approved by the Animal Research Committee of the Medical University of Vienna (Protocol No. 190097/2015/9).

Isolation of PBMCs and PBMC subsets and production of the secretomes

Cell secretomes were produced as described previously[27]. Briefly, PBMCs were isolated using density gradient centrifugation via Ficoll-Paque PLUS (GE Healthcare Bio-Sciences AB, Sweden). Heparinized blood was diluted with phosphate-buffered saline (PBS, Gibco by Life Technologies, Carlsbad, CA, USA) and layered carefully over Ficoll-Paque PLUS. After centrifugation (800 × *g*, 15 min, room temperature, with slow acceleration and deceleration), buffy coat containing PBMCs was enriched at the interface between Ficoll-Paque PLUS and plasma. For purification of monocytes (CD14), natural killer cells (CD56), $CD4^+$ T cells (CD4), $CD8^+$ T cells (CD8), and B cells (CD19), magnetic microbeads (Miltenyi, Bergisch Gladbach, Germany) against the respective cell surface epitope were used to enrich cells by AutoMacs Pro technology (Miltenyi) according to the manufacturer's protocol. Purity of isolated cells was confirmed by flow cytometry and ranged from 93 to 99% (Supplementary Fig. 1). Whole PBMCs and purified cell subsets were resuspended in CellGro serum-free medium (CellGenix, Freiburg, Germany), irradiated, and cultivated for 24 h at a concentration of 25×10^6 cells/ml in the same medium. γ-Irradiation of isolated PBMCs and purified PBMC subsets with Cesium-137 (60 Gy) was conducted as described previously[29]. To evaluate dose-dependent effects of γ-irradiation, PBMCs were irradiated with 0.9, 1.9, 3.75, 7.5, 15, 30, and 60 Gy. For inhibition of apoptosis and necroptosis, 20 μM zVAD and 100 μM necrostatin-1

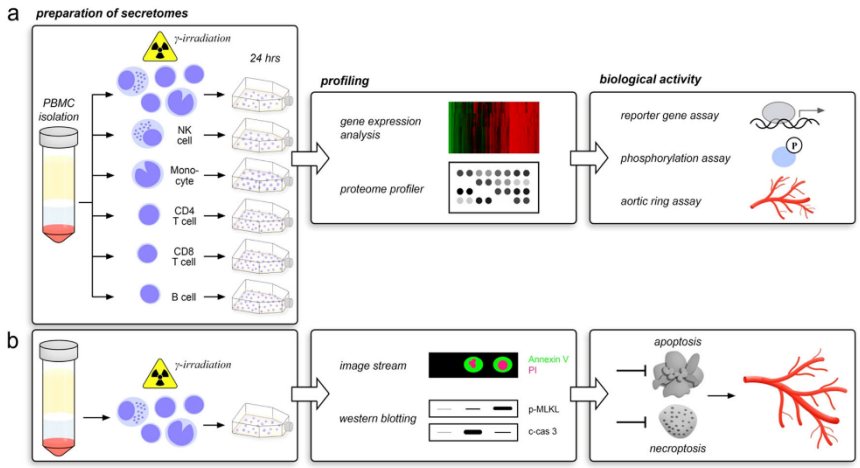

Fig. 1 Schematic illustration of experimental approach. a To determine respective contributions of PBMC subsets to tissue-regenerative properties of secreted factors, secretomes obtained from PBMCs, and subpopulations were compared by gene expression analysis and proteome profiler. Biological activities were analyzed by functional assays using reporter gene constructs, protein phosphorylation, and aortic ring-assisted endothelial cell sprouting. **b** To assess whether the type of programmed cell death affects pro-angiogenic potency of PBMC secretome, dying cells were categorized by image stream and activated intracellular signalling cascades were investigated by Western blotting. Eventually, pro-angiogenic property of apoptotic and necroptotic PBMC secretomes was compared by aortic ring sprouting assay

(both Sellekchem, Munich, Germany) were added immediately after irradiation. After 24 h of incubation, supernatants were collected by centrifugation (400 × *g*, 9 min) and stored at −20 °C. Cells were used for flow cytometric analysis and lysed for protein and messenger RNA (mRNA) analyses as described below.

Imaging flow cytometry analysis

Imaging flow cytometry analysis (Amnis ImageStreamX Mk II, Luminex Corp., Seattle, WA) was performed according to a published protocol using Annexin-V-FLUOS Staining Kit (Roche, Basel, Switzerland) according to the manufacturer's instruction[30].

Scanning electron microscopy

For scanning electron microscopy (SEM), PBMCs were either irradiated with 60 Gy or left untreated, washed twice with PBS, fixed in Karnovsky's fixative (2% paraformaldehyde, 2.5% glutaraldehyde in 0.1 M phosphate buffer (pH 7.4); Morphisto, Frankfurt am Main, Germany), dehydrated, and dried with hexamethyldisilazane (HMDS, Sigma-Aldrich, Taufkirchen, Germany). Samples were fixed to specimen mounts with double-faced adhesive carbon tape, gold sputtered (Sputter Coater, ACE200, Leica Microsystems, Wetzlar, Germany), and examined by a SEM (JSM 6310, Jeol Ltd®, Japan) with an acceleration voltage set to 15 kV.

Western blot analysis

Cells for Western blot analysis were lysed in Lämmli Buffer (Bio-Rad, Hercules, CA, USA) with protease inhibitors (Thermo Fisher, Waltham, MA, USA) and sodium orthovanadate (Sigma Aldrich, St. Louis, MO, USA) according to the manufacturer's protocol. Thirty micrograms of total protein were separated on ExcelGels (GE Healthcare) and transferred onto nitrocellulose membranes (Bio-Rad). After blocking, membranes were incubated with primary antibodies [cleaved caspase-3 antibody (0.5 µg/ml, #MAB835; R&D Systems, Minneapolis, MN, USA), phospho-RIPKs 1 (1:100, #65746; Cell Signalling Technology, Cambridge, UK), phospho-RIPK3 (1:200, #ab209384; Abcam, Cambridge, UK), phospho-MLKL (1:500, #91689; Cell Signalling Technology, Cambridge, UK), or glyceraldehyde 3-phosphate dehydrogenase (1:2000, #2118; Cell Signalling Technology, TNF (1 µg/ml, R&D Systems)] overnight at 4 °C. After further incubation with horseradish-conjugated goat-anti-rabbit antibody (1:10,000, #170-6515; Bio-Rad, Hercules, CA, USA), secondary antibodies were visualized with Supersignal West Dura (Thermo Fisher, Waltham, MA, USA) and signals were detected using ChemiDoc System (Bio-Rad). For blocking of the TNF antibody, 1 µg TNF antibody was pre-incubated with 10 µg recombinant TNF (R&D Systems) for 4 h at 4 °C:

TNF receptor blockade

PBMCs were treated with zVAD and neutralizing antibodies against TNF receptor superfamily member 1A (TNFRSF1A), TNFRSF1B (both 1 µg/ml, R&D Systems), or both were added. Cell lysates were obtained 24 h after irradiation.

Total RNA isolation

Total RNA was isolated from PBMCs and PBMC subsets immediately after cell purification as well as 24 h after irradiation with 60 Gy using Trizol® Reagent (Invitrogen, Carlsbad, CA) according to the manufacturer's instructions. Total RNA was quantified using NanoDrop-1000 spectrophotometer (Peglab, Erlangen, Germany) and RNA quality was assessed by Agilent 2100 Bioanalyzer (Agilent Technologies, Santa Clara, CA, USA). All RNA samples used in further procedures displayed an RNA integrity score between 6.2 and 10.

Microarray analysis

Microarray analysis was carried out at the Genomics Core Facility at the Medical University of Vienna (Vienna, Austria) using Affymetrix Human Transcriptome Array 2.0 (Affymetrix part of Thermo Fisher Scientific Inc.) according to MIAME guidelines[31]. Data were analyzed using GeneSpring Version 15.0 software (Agilent). First, raw data were log 2 transformed, normalized by quintile normalization, and baseline transformed. Thereafter, a filtering step was performed in order to reduce the number of multiple hypotheses and to obtain only genes for which at least 75% of the values in one sample (0 h vs. irradiated) were above the 60th percentile of the average expression value[32]. Moderated paired *t* test was used to identify differentially expressed mRNA with a fold change (FC) ≤ -2 and ≥ 2, respectively. *P* values were corrected for multiplicity by applying Benjamini–Hochberg adjustment with a false discovery rate (FDR) <5%. mRNA clustering was performed with GeneSpring software using Euclidean distance metric and complete average-linkage clustering. Microarray data were published on NCBI Gene expression omnibus at https://www.ncbi.nlm.nih.gov/geo/query/acc.cgi?acc=GSE127982 (GEO Accession number GSE127982). Full access is granted using the password: qnuxcigibxmdfcf.

Gene ontology and pathway analysis

In order to evaluate biological functions of differentially expressed genes in response to irradiation, we categorized them using the WEB-based Gene Stet Analysis Toolkit (WebGestalt)[33]. Gene ontology (GO)-term enrichment analysis was performed to identify biological processes that were enriched (geneontology.org). In addition, pathway analysis was performed using the Kyoto Encyclopedia of Genes and Genomes (KEGG) annotation list[33]. Benjamini–Hochberg method for multiple testing with a significance level of $p \leq 0.05$ and FDR < 5% was applied for both analyses. Activated canonical pathways were identified using Ingenuity Pathway Analysis (Qiagen, Hilden, Germany) with mRNAs displaying an average FC >3 between 60-Gy-irradiated and freshly isolated samples[34,35].

Proteome profiler

Secretomes obtained from PBMCs and PBMC subsets were analyzed using the commercially available Proteome Profiler XL Cytokine Array and Human Apoptosis Array (R&D Systems) according to the manufacturer's instructions. Arrays were analyzed with the ChemiDoc system as described above.

Aortic ring assays

Male C57BL/6 mice were purchased from The Jackson Laboratory (Distributor Charles River, Sulzfeld, Germany) and housed at the Center for Biomedical Research of the Medical University of Vienna (Vienna, Austria). Mice were sacrificed via cervical dislocation and aortas were excised and sliced in 1-mm-thick rings (Supplementary Fig. 2). The aortic ring assay was performed according to a published protocol with minor alterations[16]. Aortic rings were sandwiched in a fibrin matrix composed of fibrinogen (2 mg/ml, Merck Millipore, Burlington, MA, USA), aprotinin (43.3 µg/ml, Sigma-Aldrich, St. Louis, MO, USA), and thrombin (0.6 U/ml, Sigma-Aldrich) as described previousy[29]. Sandwiched aortas were equilibrated with M199 medium, supplemented with 100 µg/ml streptomycin, 4 mM L-glutamine, 100 U penicillin (all from Gibco), 250 ng/ml amphotericin B (Fisher Bioreagents, Fisher Scientific, Waltham, MA, USA), and 10% fetal bovine serum (PAA Laboratories, Pasching, Austria), for 45 min. After equilibration, the medium was removed and supernatants of PBMCs and PBMC subfractions were diluted in M199 medium corresponding to a final concentration of 4×10^6 cells/ml. Aortas were cultured for 3 days. For some sprouting assays, PBMC-derived secretomes generated with the addition of 20 µM zVAD and 100 µM necrostatin-1 directly after irradiation were investigated. Secretomes of PBMCs with zVAD and necrostatin-1 added immediately before starting the sprouting assay were included as controls. Ultimately, calcein dye (Thermo Fisher, Waltham, MA, USA) was added to label viable cells. Sprouts were photographed by Olympus IX83 scanning microscope (Olympus, Tokyo, Japan) and visualized with cellSens Imaging Software (Olympus, Tokyo, Japan). Sprouting areas were calculated using the ImageJ software version 1.48v (Wayne Rasband, National Institutes of Health, Bethesda, MD, USA).

Tube formation assays

Primary human umbilical vein endothelial cells (HUVECs) were cultivated in endothelial cell growth medium (EGM-2, Lonza, Basel, Switzerland). Before starting the tube formation experiment, cells were subsequently starved with basal medium (EBM-2, Lonza, without growth factors) supplemented with 2% FBS (Gibco) for 12 h and without serum for 3 h. µ-Slide angiogenesis tissue culture slides (Ibidi USA Inc., Fitchburg, WI, USA) were filled with growth factor reduced Matrigel matrix (Corning, Corning, NY, USA), according to manufacturer's protocol. A total of 1×10^4 cells/well were seeded and treated with PBMC-derived secretome corresponding to a final concentration of 4×10^6 cells/ml or medium alone. PBMC secretomes generated with the addition of 20 µM zVAD and 100 mM necrostatin-1 directly after irradiation were also investigated. Secretomes of PBMCs with zVAD and necrostatin-1 added immediately before starting the tube formation assay were included as controls. After 3 h of stimulation, microphotographs were taken and the number of nodes, junctions, and branches were analyzed via Angiogenesis Analyzer ImageJ plugin using default settings (Wayne Rasband, National Institutes of Health, USA).

Reporter gene assays and potency assays

Reporter gene assays for activator protein-1 (AP-1), nuclear factor 'kappa-light-chain-enhancer' of activated B cells (NF-κB), and heat-shock protein 27 (HSP-27) developed at Synlab Pharma Institute AG (Bern, Switzerland) were used to compare the potential of the different secretomes to activate these pathways. Human neuroblastoma SH-SY5Y cells were cultured in Ham's F12/MEM (50:50) Glutamax (Gibco) supplemented with 1 µg/ml puromycin, 2 mM L-glutamine, and non-essential amino acid solution (all from Sigma-Aldrich, St. Louis, MO, USA), 15% fetal bovine serum and SH-SY5Y cells were stably transfected with a firefly luciferase transcriptionally regulated by AP-1 promoter. Cells were seeded in 96-well plates at a concentration of 20,000 cells per well and stimulated with secretomes of γ-irradiated monocyte supernatant and PBMCs, both pooled from four donors. To evaluate reporter activity, SteadyGlo (Promega, Fitchburg, WI, USA) was added and luminescence was measured via luminescence reader (EnVision, Perkin-Elmer or Centro LB960, Berthold). To quantify phosphorylation of HSP-27 at Ser82, adenocarcinomic human alveolar basal epithelial cells (A549) were treated with supernatants for 30 min, fixed, and permeabilized. After sequential addition of antibodies directed against the phosphorylated form of HSP-27 and peroxidase-conjugated antibody, chemiluminescent signals were measured with the luminescence reader (EnVision, Perkin-Elmer or Centro LB960, Berthold) and relative potency was calculated with the PLA software (Stegmann Systems GmbH, Rodgau, Germany).

Enzyme-linked immunosorbent assay

TNF-α (R&D Systems) and lymphotoxin A (LTA; R&D Systems) were quantified by enzyme-linked immunosorbent assay according to the manufacturer's instructions.

Graphical overview

The methodological approach was designed using the InDesign CS software (version 7.0, Adobe Systems Inc., San Jose, CA, USA) and is shown in Fig. 1.

Statistical analysis

Data were analyzed using GraphPad Prism 6 software (GraphPad Software Inc., La Jolla, CA, USA) and IBM SPSS Statistics version 23 (SPSS Inc., Chicago, IL, USA). Two-tailed Student's *t* test was used to compare parametric variables and stated as arithmetic mean ± standard deviation (SD). One-way analysis of variance with Bonferroni post hoc test or Kruskal–Wallis with Dunn's post hoc test was used according to data distribution. Aberrations were excluded according to the Gibbs outlier test. *P* values below 0.05 were considered statistically significant and are marked with asterisks.

Results

γ-Irradiation differentially affects transcriptional profiles of PBMCs and purified cell subsets

To assess the impact of γ-irradiation on transcriptional networks of PBMCs and PBMC subsets, we conducted mRNA microarray analysis four different healthy volunteers with and without γ-irradiation. In total, 756 annotated genes were differentially expressed in PBMCs and PBMC subsets (Supplementary Table 1). Global gene expression analysis showed significant differences between stressed PBMCs and stressed purified cell types (Fig. 2a, b). Principal component analysis of global gene expression patterns showed a clear distinction between the different cell types except for natural killer (NK) and $CD4^+$ T cells, which clustered together, suggesting high transcriptional similarity (Fig. 2b). Monocytes, B cells, and PBMCs displayed markedly distinct global gene expression patterns. Canonical pathway analysis of genes upregulated by γ-irradiation in PBMCs suggested activation of death receptors, upregulation of TNF receptor 2 (TNFRSF1B) signalling, and induction of apoptosis. Moreover, we identified activation of cytokine and cell signalling pathways, including NF-κB and the stress-activated protein kinase c-Jun-N-terminal kinase, both of which are linked to tissue-regenerative and angiogenic processes (Fig. 2c)[36–38].

To gain more detailed biological information on the pathways identified, we investigated expression profiles of

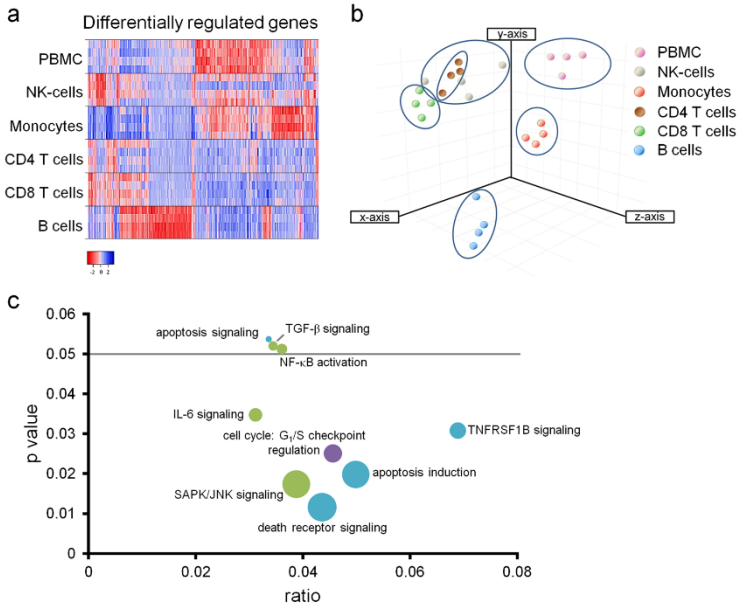

Fig. 2 γ-Radiation differentially affects gene expression of PBMCs and purified cell subsets. a Heat map showing expression values of 910 transcripts differentially expressed between non-irradiated cells and cells 24 h after irradiation. Fold expression ranged from −2.7 (red, downregulation) to 2.7 (blue, upregulation). Each cell subset exhibited a unique expression pattern. **b** Principal component analysis (PCA) of global gene expression pattern clearly showed clustering of cell subsets, indicating a strong homogeneity within each cell fraction and different donors, but heterogeneity between all cell fractions. **c** Visualization of overrepresented GO terms in irradiated PBMCs is shown. Each node represents a biological process-specific term. Node size indicates *p* value, node color was selected to group terms according to their function (blue, apoptosis; green, pro-inflammatory signalling; purple, cell cycle). Ratios indicate relative amounts of activated genes per pathway. Among the most enriched terms were "TNFRSF1B signaling," "apoptosis induction," and "death receptor signalling." $n = 4$ donors per group

key signalling molecules of these pathways in the different cell subsets. Selected genes involved in the processes of cytokine production (Fig. 3a and Supplementary Table 2), angiogenesis (Fig. 3b and Supplementary Table 3), and wound healing (Fig. 3c and Supplementary Table 4) displayed notable differences in their expression pattern in PBMCs compared to PBMC subsets. GO-term and KEGG-pathway analyses of genes induced by γ-irradiation (Fig. 3d–i) reflected the differences observed on transcriptional level also in a functional context. All selected biological functions, including cytokine production (Fig. 3d), response to hypoxia (Fig. 3e), and cell cycle (Fig. 3f), as well as the tumor growth factor-β (TGF-β) pathway (Fig. 3g), mitogen-activated protein kinase (MAPK) pathway (Fig. 3h), and p53 pathway (Fig. 3i) varied significantly between the different cell groups. While genes encoding cytokines were strongly enriched in PBMCs and NK cells (Fig. 3d), genes constituting the TGF-β signalling pathway were found mainly activated in PBMCs, CD14 monocytes, and $CD8^+$ T cells (Fig. 3g). Genes associated with stress response (response to hypoxia) were exclusively enriched in irradiated PBMCs (Fig. 3e), while the MAPK pathway was most upregulated in monocytes (Fig. 3h). Cell cycle genes were enriched after irradiation in PBMCs as well as in B cells and $CD8^+$ T cells (Fig. 3f), whereas genes involved in the p53 signalling were significantly enriched in all samples evaluated, showing strongest activation in PBMCs (Fig. 3i). In conclusion, results presented here indicate that various signalling pathways and biological processes are differentially regulated after γ-irradiation in the respective cellular subsets constituting PBMCs. Moreover, cell populations are in reciprocal relationships which, although mutually, differentially influence cellular signalling events in PBMCs.

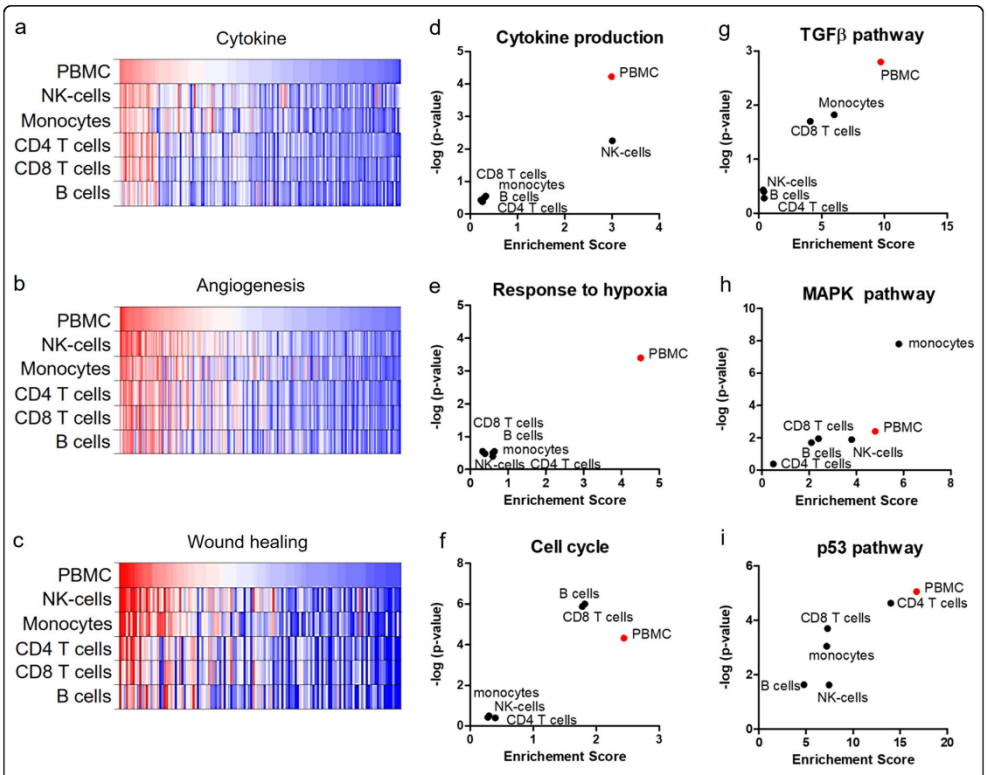

Fig. 3 Tissue-regenerative potential varies between PBMCs and purified cell subsets. Genes associated with the biological process of **a** cytokine production (742 genes), **b** angiogenesis (509 genes), and **c** wound healing (361 genes) (mean values of four samples) revealed transcriptional heterogeneity between the different purified cells subsets and PBMCs. Expression values ranged from log(2) = 1 (red, low expression) to log(2) = 9 (blue, strong expression). GO-term enrichment analysis for **d** "cytokine production," **e** "response to hypoxia," and **f** "cell cycle" as well as KEGG-pathway enrichment analysis for **g** "TGF-β", **h** "MAPK", and **i** "p53 pathway" are shown. Irradiated PBMCs (highlighted in red) uniformly enriched genes associated with these biological processes and pathways, while individual cell subsets showed a more heterogeneous pattern. The analysis was performed using *Webgestalt* platform. *P* values are represented as the minus base 10 log. $n = 4$ per group

γ-Irradiated PBMC subpopulations synergistically induce blood vessel sprouting

As we have previously described a strong tissue-regenerative and pro-angiogenic activity of the secretome derived from γ-irradiated PBMCs[29,39], and since our bioinformatics analysis revealed differential transcriptional signatures, we now asked whether a specific cell subtype of PBMCs would account for the observed effects. We therefore performed aortic ring assays with supernatants from γ-irradiated PBMCs, NK cells, monocytes, $CD4^+$ T cells, $CD8^+$ T cells, and B cells. As shown in Fig. 4a, b, strongest pro-angiogenic activity was observed in aortic rings cultured with the secretome of whole PBMCs. Intriguingly, monocytes displayed vessel sprouting-inducing capacity, which was higher compared to medium, yet compromised compared to that of the PBMC-derived secretome. Stimulation of aortic rings with secretomes derived from NK cells, $CD4^+$ and $CD8^+$ T cells, and B cells showed no increased pro-angiogenic effects compared to control medium (not shown) in our assay system (Fig. 4a, b). We furthermore sought to profile the specific protein signatures obtained from PBMCs and subsets. Analysis of cytokines revealed that certain cytokines, including matrix metallopeptidase-9, interleukin-18Bpa (IL-18Bpa), osteopontin, epithelial derived neutrophil attractant-78, IL-8, RANTES (regulated on activation, normal T cell expressed and secreted), angiogenin, and IL-1ra were exclusively detected in the

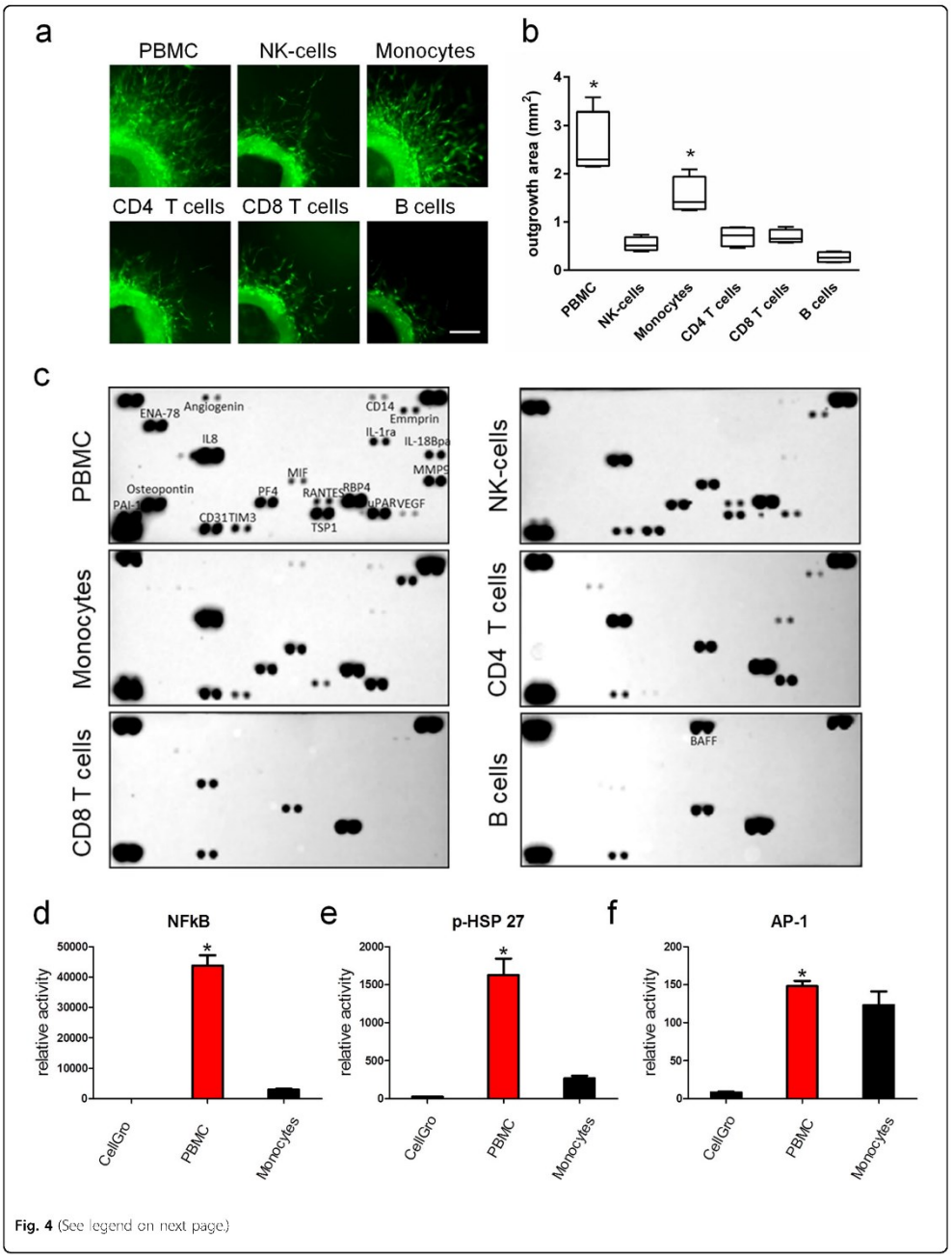

Fig. 4 (See legend on next page.)

(see figure on previous page)

Fig. 4 Blood vessel sprouting is synergistically induced by γ-irradiated PBMC subpopulations. a Representative images of calcein-labelled mouse aortic rings on day three of cultivation are shown. Scale bar, 250 µm. **b** Box plots of averaged outgrowth areas are shown. Whiskers indicate minimal and maximal values. Quantitative analysis showed a significant induction of sprouting blood vessels when adding the supernatant of PBMCs as well as the supernatant of purified monocytes. *P values <0.05 compared to CellGro. **c** Analysis of cytokines present in the different secretomes revealed that certain cytokines, including MMP-9, IL-18Bpa, osteopontin, ENA78, IL-8, RANTES, angiogenin, and IL-1ra, were exclusively detected in the supernatant of γ-irradiated PBMC. **d**–**f** Tissue-regenerative capacity of secretomes of γ-irradiated PBMCs and monocytes was further assessed using standardized reporter gene assays. NF-κB promoter activity and HSP-27 phosphorylation were strongly induced by PBMC supernatant, whereas AP-1 promotor was induced by PBMC and monocyte secretome. *P values <0.05 compared to CellGro. $n = 4$

supernatant of γ-irradiated PBMC (Fig. 4c, Supplementary Fig. 4). Since pro-angiogenic activity was unique to secretomes of PBMC and monocytes, we next compared the capability of these secretomes to activate signalling pathways known to be involved in tissue-regenerative and pro-angiogenic processes. Interestingly, NF-κB promoter activity (Fig. 4d) and HSP-27 phosphorylation (Fig. 4e) were strongly induced by PBMC-derived secretome, while being only moderately activated by the secretome obtained from irradiated monocytes. In contrast, both secretomes comparably activated the AP-1 promotor (Fig. 4f). Together, our data suggest that secretomes of PBMC subsets exhibit differential pro-angiogenic capacities and that a synergistic action of γ-irradiated PBMC subpopulations is necessary for efficient release of pro-angiogenic mediators.

High-dose γ-irradiation induces apoptosis and necroptosis in PBMCs

Since our bioinformatics analysis suggested an activation of death receptors and an involvement of TNF receptor signalling, we were interested which type of cell death is induced in PBMCs and PBMC subsets after γ-irradiation. We therefore assessed cellular morphology, indicative of the manner by which cells die, by SEM. Intriguingly, we found comparable number of cells showing morphological signs of either apoptosis or necroptosis in irradiated PBMCs (Fig. 5a). Interestingly, the levels of cells displaying either apoptotic or necroptotic features varied significantly between different populations (Fig. 5b). As already observed by electron microscopy, quantification of apoptotic and necroptotic cells in γ-irradiated PBMCs confirmed an almost equal abundance (22% apoptotic vs. 28% necroptotic) of both forms of controlled cell death. In contrast, most of NK cells were necroptotic (3% apoptotic vs. 94% necroptotic). Although around half of $CD4^+$ and $CD8^+$ T cells underwent necroptosis, the highest number of apoptotic cells were also detected in these populations ($CD8^+$ T cells: 21% apoptotic vs. 54% necroptotic; $CD4^+$ T cells: 37% apoptotic vs. 45% necroptotic). By contrast, B cells and monocytes displayed low amounts of apoptotic cells (B cells: 8% apoptotic vs. 68% necroptotic; monocytes: 5% apoptotic vs. 59% necroptotic). These data were further corroborated by an apoptosis protein array, showing that the induction of proteins involved in the apoptotic process was strongly induced in cell types that were mainly driven into apoptotic cell death (Supplementary Fig. 5). These results highlight the different susceptibilities of PBMC subsets to preferentially undergo apoptosis or necroptosis after high-dose γ-irradiation.

To assess kinetics and dose dependency of apoptosis and necroptosis induction after γ-irradiation on the molecular level, we evaluated cleavage of caspase-3 (c-cas 3) and phosphorylation of RIPK3 and MLKL, respectively (Fig. 5c, d). MLKL phosphorylation, indicative of induction of necroptosis, occurred in a dose-dependent manner, reaching its maximum at an irradiation dose of 15 Gy (Fig. 5d). Comparably, caspase-3 cleavage was induced by γ-irradiation starting from 30 Gy. For further characterization of the irradiation-induced programmed cell death, phosphorylation of RIPK3, MLKL, and c-cas 3 was assessed at different time points. While sustained phosphorylation of RIPK3 was detected starting from 2 h post irradiation, phosphorylation of MLKL and caspase-3 cleavage displayed highest levels 24 h post irradiation (Fig. 5c). Interestingly, we detected two smaller bands of 35 and 25 kDa in the phosphorylated (p)-RIPK3 Western blot. In contrast to γ-irradiation, induction of RIPK3 and MLKL phosphorylation by TNF-α and zVAD peaked as soon as 2 h after stimulation (Supplementary Fig. 6) and did not induce cleavage of p-RIPK3. Since MLKL phosphorylation occurs rapidly after induction of necroptosis, our finding that MLKL phosphorylation peaked 24 h after γ-irradiation suggests an indirect induction of necroptosis in PBMCs after exposure to γ-radiation.

Pro-angiogenic capacity of PBMC secretome requires irradiation-induced necroptosis

Next, we determined whether the type of cell death affects the pro-angiogenic potential of PBMC secretome. Therefore, irradiated PBMCs were cultivated in the presence of zVAD, a pan-caspase inhibitor, or necrostatin-1, an inhibitor of necroptosis, and the angiogenic capacity of the resulting secretome was assessed in murine aortic ring sprouting assays (Fig. 6b, c) and tube formation assays with HUVECs (Fig. 6d, e). Irradiation-induced c-cas 3 and phosphorylation of MLKL were efficiently abrogated by

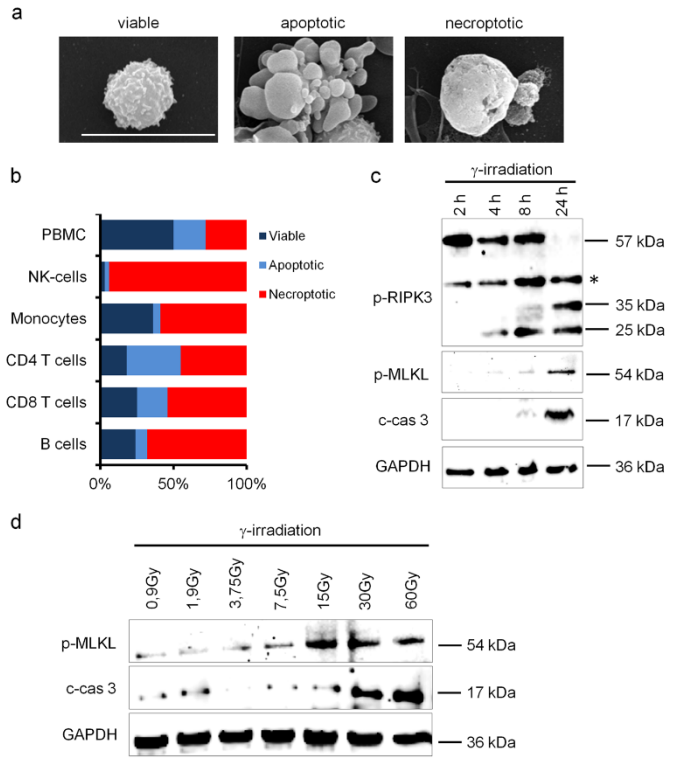

Fig. 5 γ-irradiation differentially induces apoptosis and necroptosis in PBMC and purified cell subsets. a Representative scanning electron microscopy images of viable, apoptotic, and necroptotic cells 24 h after irradiation. Scale bar, 10 µm. **b** Relative amounts of viable, apoptotic, and necroptotic cells in PBMC and PBMC subpopulations. **c** Immunoblot analysis of receptor-interacting protein kinase-3 (p-RIPK3), pseudokinase mixed lineage kinase domain-like phosphorylation (p-MLKL), and cleaved caspase (c-cas 3) in PBMC shows a time-dependent induction 24 h after γ-irradiation. The position of an unidentified, most likely unspecific, band on the p-RIPK3 Western blot is indicated by an asterisk. **d** γ-Irradiation dose-dependently induces phosphorylation of MLKL and caspase-3 cleavage. $n = 3$

zVAD and necrostatin-1, respectively (Fig. 6a), indicating that γ-irradiated PBMCs treated with zVAD and necrostatin-1 preferentially undergo apoptosis or necroptosis. In both assay systems, blood vessel sprouting was strongly induced by the secretome of irradiated PBMCs (Fig. 6b–e), as described above, and was comparably high with blocked caspase-dependent apoptosis (zVAD, Fig. 6b–e). Intriguingly, the pro-angiogenic capacity of the secretome was remarkably compromised when necroptosis was inhibited by necrostatin-1 (Fig. 6b–e). Freshly added zVAD and necrostatin-1 to the secretome of γ-irradiated PBMC during the assay had no effect on vessel sprouting (Supplementary Fig. 7a). Our data indicate that necroptosis represents an indispensable prerequisite for the pro-angiogenic action of secretomes derived from γ-irradiated PBMCs.

Necroptotic cell death in γ-irradiated PBMCs is induced via paracrine activation of the TNFRSF1B

We next sought to elucidate the mechanism by which γ-irradiation induces necroptosis in PBMCs. Since previous studies identified the TNF-α pathway as one of the main drivers of necroptosis, and our bioinformatics analysis suggested an activation of the TNFRSF1B signalling pathway in response to irradiation, we analyzed the expression of *TNF* and its receptors (*TNFRSF1A* and *TNFRSF1B*). Low *TNF* expression was detectable in PBMCs and all subfractions, with highest mRNA levels in

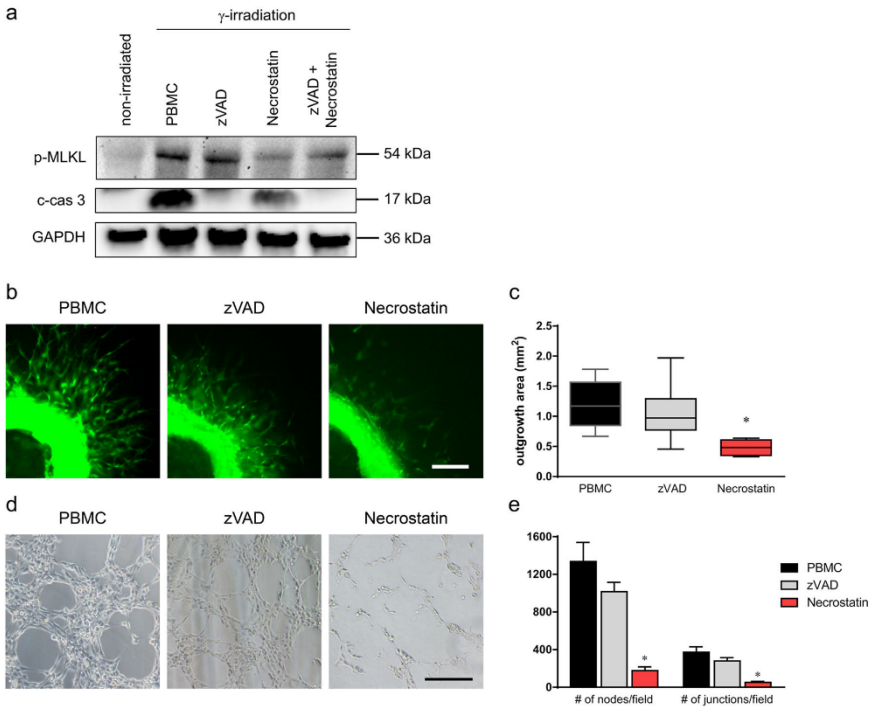

Fig. 6 Induction of necroptosis is necessary for the pro-angiogenic capacity of the PBMC secretome. a Immunoblot analysis of phosphorylated MLKL and cleaved caspase (c-cas) 3 in non-irradiated and γ-irradiated PBMCs is shown. Irradiated PBMCs were cultivated with either zVAD, necrostatin-1, or both. **b** Representative images of murine aortic rings after 3 days of cultivation with conditioned medium from γ-irradiated PBMC treated with zVAD, necrostatin-1, or both. Viable cells were visualized with calcein (green). Scale bar, 200 µm. **c** Box plot diagrams of vessel areas are shown. Whiskers indicate minimal and maximal values. Necrostatin-1 added to irradiated PBMC significantly reduced sprout-inducing ability of the PBMC secretome, while addition of zVAD did not compromise pro-angiogenic potential. **d** Endothelial cells were incubated with the secretome of γ-irradiated PBMCs alone or treated with zVAD or necrostatin for 3 h after overnight starvation. The PBMC secretome treated with necrostatin-1 lead to significantly reduced tube formation. **e** Bar graph depicting a significant decrease in the number of nodes and junction after treatment with necrostatin-1. Scale bar, 200 µm. *P values below 0.05 compared to PBMC. $n = 3$

monocytes (Fig. 7a). Whereas *TNFRSF1A* showed little expression values in PBMCs and PBMC subsets (Fig. 7b), *TNFRSF1B* was strongly expressed in PBMCs and to a minor degree in all subsets (Fig. 7c). Interestingly, we neither detected soluble TNF-α nor LTA, a TNF homologous ligand of TNFRSF1A and TNFRSF1B, in the PBMC secretome (not shown). However, Western blot analysis showed a significant induction of membrane-bound TNF (mTNF) in PBMC after γ-irradiation (Fig. 7d). To further investigate the necroptosis signalling cascade, we specifically blocked both TNF receptors of γ-irradiated PBMCs with monoclonal blocking antibodies and assessed MLKL phosphorylation. As shown in Fig. 7e, induction of necroptosis was only effectively abolished by neutralizing antibody directed against TNFRSF1B, but not by TNFRSF1A. Our data thus indicate that γ-irradiation-induced necroptosis of PBMCs occurs via an mTNF-TNFRSF1B signalling cascade.

Discussion

In the past, stem cell therapies had been praised as a promising therapeutic option for tissue regeneration of a variety of damaged organs[40–43]. Yet, most of the high expectations from in vitro and animal experiments were disappointed when stem cells employed in human clinical trials showed only minor tissue-regenerative potential[44]. We have reported previously that the release of regenerative factors is not an exclusive feature of stem cells,

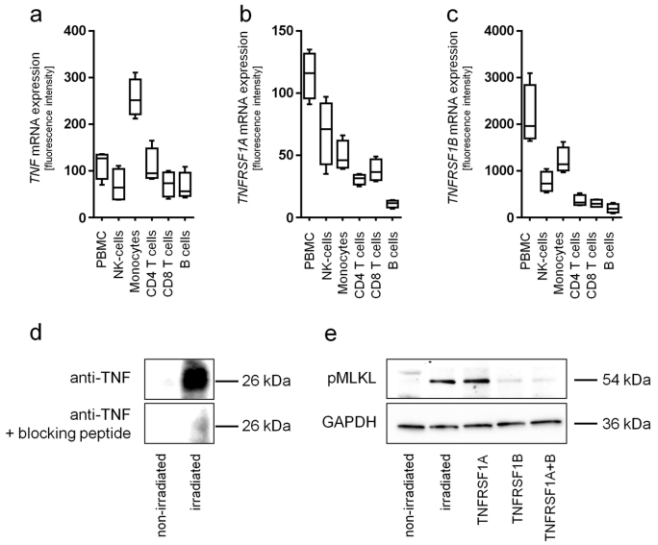

Fig. 7 TNFRSF1B mediates radiation-induced necroptosis via a paracrine mechanism. Expressions of *TNF* (**a**), *TNFRSF1A* (**b**), and *TNFRSF1B* (**c**) assessed by microarray analysis are shown. *TNF* is expressed in PBMCs and in all subfractions. While expression of *TNFRSF1A* is low, *TNFRSF1B* is highly expressed in PBMCs and cell subsets. **d** Western blot analysis shows induction of membrane-bound TNF (mTNF) in PBMCs after γ-irradiation (upper panel). The specificity of the antibody was confirmed by pre-absorption of the antibody with recombinant TNF (lower blot). **e** Immunoblot analysis of phosphorylated MLKL in γ-irradiated PBMC treated with blocking antibodies against TNFRSF1A, TNFRSF1B, or a combination of both is shown. Blocking TNFRSF1B, but not TNFRSF1A, reduced necroptosis induction as shown by reduced MLKL phosphorylation. Diagrams show means of four independent experiments. Western blots show one representative experiment of 5

since secretomes derived from γ-irradiated PBMCs also displayed high tissue-regenerative activity in various experimental models. These regenerative effects were mainly attributed to the secretomes' pro-angiogenic and cytoprotective properties[12,13,16,18]. These results raised the question whether all cell types are potentially capable of producing and releasing sufficient factors with tissue-regenerative properties after stress-induced cell death. Our analyses revealed pronounced differences in gene expression and released proteins between the respective cell types and total PBMCs in response to γ-irradiation. Importantly, certain cytokines were exclusively released when irradiated PBMCs were cultured together, but were not present in the secretomes derived from purified cell populations. In addition, using murine aortic rings for blood vessel sprouting assays, high pro-angiogenic activity was only detected in secretomes from total PBMCs. Both analyses suggest that a crosstalk of PBMC subpopulations is required for the release of angiogenesis-promoting factors. Therefore, our study argues against the initial hypothesis that the secretome of any stressed cell type exhibits tissue-regenerative characteristics and suggests that paracrine communication between different cell types is fundamental for the release of a unique composition of tissue-regenerating mediators. Thus, future clinical studies on damaged tissue will elucidate the full tissue-regenerative efficacy of the PBMC-derived secretome. Since toxicological studies and studies on the viral safety of an allogeneic secretome from γ-irradiated PBMC produced under Good Manufacturing Practice (GMP) conditions have already been successfully conducted, our study paves the way for a first clinical trial in the indication of diabetic foot ulcer[45,46].

Here, we also investigated the impact of the type of cell death on the tissue-regenerative capacity of the secretome. Although γ-radiation is a known inducer for both apoptosis and necroptosis[20,47–51], it is unknown whether γ-radiation-induced necroptosis has tissue-regenerative effects or further aggravates tissue damage. While Castle et al.[49] showed that mice lacking RIP3, a critical molecule in the necroptosis pathway, were not rescued from acute radiation syndrome, a protective activity of necrostatin-1 administration in mice after lethal full body irradiation has been reported in several studies[47,52]. Although the underlying mechanisms are still not known, the aforementioned data by Huang et al.[47] and Steinman et al.[52]

suggest that inhibition of necroptosis by necrostatin-1 is indeed favorable in a lethal setting, due to the prevention of massive cell death and organ destruction. To the best of our knowledge, our study is the first to describe that necroptosis of PBMCs exerts pro-angiogenetic effects, thereby potentially contributing to tissue regeneration in chronically damaged tissues. As shown by aortic ring assays, addition of necrostatin-1 to PBMCs before irradiation abolishes its pro-angiogenic activity, indicating that necroptosis is important for the release of factors involved in blood vessel formation. However, since PBMCs used in this study were ex vivo γ-irradiated and then applied to the tissue, we do not currently know whether similar processes are also present in stressed tissue in vivo, or in tissues under physiological conditions. Our study builds a basis for further studies, which would address these questions in more sophisticated experiments. Another interesting finding was the detection of low molecular forms of phosphorylated RIPK3 after γ-irradiation. Whether these forms are still active or only non-functional degradation products occurring during massive cell death after γ-irradiation remains to be determined.

Here we identified the TNF/TNFRSF1B signalling cascade as an inducer of necroptosis after γ-irradiation. In line with our observations, recent guidelines of the American College of Rheumatology instruct doctors to stop medication with anti-TNF therapy before surgery to avoid wound healing problems, highlighting the importance of TNF for proper wound healing, presumably due to its necroptosis-inducing action[53]. Interestingly, release of soluble TNF was not detectable in our secretomes. However, Western blot analysis revealed a significant increase in membrane-bound TNF. When analyzing TNF receptors, we found strong expression of TNFRSF1B. This is in line with previous studies, suggesting that mTNF preferentially signals through TNFRSF1B[54,55]. Currently, the mechanism of γ-radiation-induced necroptosis is still not fully understood. While activation of necroptosis by TNF requires additional inhibition of apoptosis (Supplementary Fig. 7b), γ-irradiation simultaneously induced necroptosis and apoptosis in PBMC[22,56,57]. Since high-dose ionizing radiation leads to DNA damage, activation of cytosolic DNA sensors could account for this phenomenon. Indeed, the cytosolic DNA sensor DNA-dependent activator of interferon regulatory factors has been shown to directly induce necroptosis via RIPK3 after virus infection[58]. Further studies are needed to investigate whether similar mechanisms also account for the induction of necroptosis in our experimental setting.

In conclusion, we could demonstrate that secretomes of PBMCs and PBMC subsets show different tissue-regenerative capacities, refuting the paradigm that any cell type is able to release paracrine factors with regenerative potential. Furthermore, we identified the TNF/TNFRSF1B signalling pathway as the mechanism underlying the γ-irradiation-induced release of pro-angiogenic factors. Based on these findings we believe that necroptosis, although seemingly paradox, is indeed an essential prerequisite for tissue regeneration and that forced induction of necroptosis might facilitate the development of novel therapeutic approaches in the near future.

Acknowledgements
This research project was financed in part by the Austrian Research Promotion Agency (FFG) Grant "APOSEC" (852748; 2015–2019), the Wiener Wirtschaftsagentur "APOSEC to clinic (2343727), the Vienna Business Agency, and the Aposcience AG under group leader H.J.A. We thank Hans Peter Haselsteiner for his belief in this private-public partnership to augment patients' health. We thank Ms. Heidemarie. Rossiter for critical reading of the manuscript. For technical support regarding the image stream analysis, we thank Sabine Pietkiewicz. We want to thank Prof. Dr. Ulrike Baranyi and Prof. Dr. Barbara Messner for their kind support in cell culture experiments. The authors acknowledge the Core Facilities of the Medical University of Vienna, a member of VLSI.

Author details
[1]Department of Internal Medicine III, Division of Rheumatology, Medical University of Vienna, Vienna, Austria. [2]Division of Thoracic Surgery, Medical University of Vienna, Vienna, Austria. [3]FFG Project 852748 "APOSEC", Medical University of Vienna, Vienna, Austria. [4]Department of Biomedical Imaging and Image-guided Therapy, Medical University of Vienna, Vienna, Austria. [5]Department of Radiology and Cancer Research UK Cambridge Center, Cambridge CB2 0QQ, UK. [6]Vienna Business Agency Project 2343727 "APOSEC to clinic", Medical University Vienna, Vienna, Austria. [7]Synlab Analytics and Services Switzerland AG, Birsfelden, Switzerland. [8]Research Division of Biology and Pathobiology of the SkinDepartment of Dermatology, Research Division of Biology and Pathobiology of the Skin, Medical University of Vienna, Vienna, Austria. [9]Division of Oral and Maxillofacial Surgery, Medical University of Vienna, Vienna, Austria. [10]Research Laboratories, Core Facility Flow Cytometry, Medical University of Vienna, Vienna, Austria

Authors' contributions
E.S., H.J.A. and M.M. designed and analyzed the results, and wrote the paper. E.S. and L.B. performed bioinformatics analyses. A.S. performed flow cytometric characterization and data evaluation. E.S., M.L., and V.V. performed cell culture experiments. D.M. performed SEM. D.C., A.G., M.E., P.K. and E.T. contributed to experimental design and data interpretation. All authors analyzed the results and approved the final version of the manuscript.

Conflict of interest
Financial interest is claimed by the Medical University of Vienna and the Aposcience AG, which holds two patents related to this work (EP20080450198 and EP20080450199). H.J.A. is a shareholder of Aposcience AG. The other authors declare that they have no conflict of interest.

Supplementary Information accompanies this paper at (https://doi.org/10.1038/s41419-019-1974-6).

Received: 10 June 2019 Revised: 5 September 2019 Accepted: 9 September 2019
Published online: 30 September 2019

References

1. Ptaszek, L. M., Mansour, M., Ruskin, J. N. & Chien, K. R. Towards regenerative therapy for cardiac disease. *Lancet* **379**, 933–942 (2012).
2. Gurtner, G. C., Werner, S., Barrandon, Y. & Longaker, M. T. Wound repair and regeneration. *Nature* **453**, 314–321 (2008).
3. Miyahara, Y. et al. Monolayered mesenchymal stem cells repair scarred myocardium after myocardial infarction. *Nat. Med.* **12**, 459–465, https://doi.org/10.1038/nm1391 (2006).
4. Gnecchi, M., Zhang, Z., Ni, A. & Dzau, V. J. Paracrine mechanisms in adult stem cell signaling and therapy. *Circ. Res.* **103**, 1204–1219 (2008).
5. Mirotsou, M., Jayawardena, T. M., Schmeckpeper, J., Gnecchi, M. & Dzau, V. J. Paracrine mechanisms of stem cell reparative and regenerative actions in the heart. *J. Mol. Cell. Cardiol.* **50**, 280–289 (2011).
6. Saas, P., Bonnefoy, F., Kury-Paulin, S., Kleinclauss, F. & Perruche, S. Mediators involved in the immunomodulatory effects of apoptotic cells. *Transplantation* **84**, S31–S34 (2007).
7. Gyongyosi, M. et al. Meta-Analysis of Cell-based CaRdiac stUdiEs (ACCRUE) in patients with acute myocardial infarction based on individual patient data. *Circ. Res.* **116**, 1346–1360 (2015).
8. Dai, W. et al. Allogeneic mesenchymal stem cell transplantation in post-infarcted rat myocardium: short- and long-term effects. *Circulation* **112**, 214–223, (2005).
9. Gnecchi, M., Danieli, P., Malpasso, G. & Ciuffreda, M. C. Paracrine mechanisms of mesenchymal stem cells in tissue repair. *Methods Mol. Biol.* **1416**, 123–146 (2016).
10. Thum, T., Bauersachs, J., Poole-Wilson, P. A., Volk, H. D. & Anker, S. D. The dying stem cell hypothesis: immune modulation as a novel mechanism for progenitor cell therapy in cardiac muscle. *J. Am. Coll. Cardiol.* **46**, 1799–1802 (2005).
11. Ankersmit, H. J. et al. Irradiated cultured apoptotic peripheral blood mononuclear cells regenerate infarcted myocardium. *Eur. J. Clin. Invest.* **39**, 445–456 (2009).
12. Lichtenauer, M. et al. Secretome of apoptotic peripheral blood cells (APOSEC) confers cytoprotection to cardiomyocytes and inhibits tissue remodelling after acute myocardial infarction: a preclinical study. *Basic Res. Cardiol.* **106**, 1283–1297 (2011).
13. Lichtenauer, M. et al. Intravenous and intramyocardial injection of apoptotic white blood cell suspensions prevents ventricular remodelling by increasing elastin expression in cardiac scar tissue after myocardial infarction. *Basic Res. Cardiol.* **106**, 645–655 (2011).
14. Pavo, N. et al. Long-acting beneficial effect of percutaneously intramyocardially delivered secretome of apoptotic peripheral blood cells on porcine chronic ischemic left ventricular dysfunction. *Biomaterials* **35**, 3541–3550 (2014).
15. Altmann, P. et al. Secretomes of apoptotic mononuclear cells ameliorate neurological damage in rats with focal ischemia. *F1000Res.* **3**, 131, https://doi.org/10.12688/f1000research.4219.2 (2014).
16. Haider, T. et al. The secretome of apoptotic human peripheral blood mononuclear cells attenuates secondary damage following spinal cord injury in rats. *Exp. Neurol.* **267**, 230–242 (2015).
17. Beer, L., Mildner, M., Gyongyosi, M. & Ankersmit, H. J. Peripheral blood mononuclear cell secretome for tissue repair. *Apoptosis* **21**, 1336–1353 (2016).
18. Hacker, S. et al. Paracrine factors from irradiated peripheral blood mononuclear cells improve skin regeneration and angiogenesis in a porcine burn model. *Sci. Rep.* **6**, 25168 (2016).
19. Beer, L. et al. Analysis of the secretome of apoptotic peripheral blood mononuclear cells: impact of released proteins and exosomes for tissue regeneration. *Sci. Rep.* **5**, 16662 (2015).
20. Kasiri, M. M. et al. Dying blood mononuclear cell secretome exerts antimicrobial activity. *Eur. J. Clin. Invest.* https://doi.org/10.1111/eci.12667 (2016).
21. Kerr, J. F., Wyllie, A. H. & Currie, A. R. Apoptosis: a basic biological phenomenon with wide-ranging implications in tissue kinetics. *Br. J. Cancer* **26**, 239–257 (1972).
22. Pasparakis, M. & Vandenabeele, P. Necroptosis and its role in inflammation. *Nature* **517**, 311–320 (2015).
23. Linkermann, A. & Green, D. R. Necroptosis. *N. Engl. J. Med.* **370**, 455–465 (2014).
24. Chen, S. et al. RIPK1/RIPK3/MLKL-mediated necroptosis contributes to compression-induced rat nucleus pulposus cells death. *Apoptosis* **22**, 626–638 (2017).
25. Lin, J. et al. A role of RIP3-mediated macrophage necrosis in atherosclerosis development. *Cell Rep.* **3**, 200–210 (2013).
26. Lim, S. Y., Davidson, S. M., Mocanu, M. M., Yellon, D. M. & Smith, C. C. The cardioprotective effect of necrostatin requires the cyclophilin-D component of the mitochondrial permeability transition pore. *Cardiovasc. Drugs Ther.* **21**, 467–469 (2007).
27. You, Z. et al. Necrostatin-1 reduces histopathology and improves functional outcome after controlled cortical impact in mice. *J. Cereb. Blood Flow Metab.* **28**, 1564–1573 (2008).
28. Robinson, N. et al. Type I interferon induces necroptosis in macrophages during infection with *Salmonella enterica* serovar Typhimurium. *Nat. Immunol.* **13**, 954–962 (2012).
29. Wagner, T. et al. Different pro-angiogenic potential of gamma-irradiated PBMC-derived secretome and its subfractions. *Sci. Rep.* **8**, 18016 (2018).
30. Pietkiewicz, S., Schmidt, J. H. & Lavrik, I. N. Quantification of apoptosis and necroptosis at the single cell level by a combination of Imaging Flow Cytometry with classical Annexin V/propidium iodide staining. *J. Immunol. Methods* **423**, 99–103 (2015).
31. Brazma, A. et al. Minimum information about a microarray experiment (MIAME)-toward standards for microarray data. *Nat. Genet.* **29**, 365–371 (2001).
32. Beer, L. et al. High dose ionizing radiation regulates micro RNA and gene expression changes in human peripheral blood mononuclear cells. *BMC Genomics* **15**, 814 (2014).
33. Wang, J., Duncan, D., Shi, Z. & Zhang, B. WEB-based GEne SeT AnaLysis Toolkit (WebGestalt): update 2013. *Nucleic Acids Res.* **41**, W77–W83 (2013).
34. Song, X. et al. Autophagy deficient keratinocytes display increased DNA damage, senescence and aberrant lipid composition after oxidative stress in vitro and in vivo. *Redox Biol.* **11**, 219–230 (2017).
35. Narzt, M. S. et al. A novel role for NUPR1 in the keratinocyte stress response to UV oxidized phospholipids. *Redox Biol.* **20**, 467–482 (2019).
36. Ferrer, I., Friguls, B., Dalfo, E. & Planas, A. M. Early modifications in the expression of mitogen-activated protein kinase (MAPK/ERK), stress-activated kinases SAPK/JNK and p38, and their phosphorylated substrates following focal cerebral ischemia. *Acta Neuropathol.* **105**, 425–437 (2003).
37. Nagata, D., Mogi, M. & Walsh, K. AMP-activated protein kinase (AMPK) signaling in endothelial cells is essential for angiogenesis in response to hypoxic stress. *J. Biol. Chem.* **278**, 31000–31006 (2003).
38. Ebelt, N. D., Cantrell, M. A. & Van Den Berg, C. L. c-Jun N-terminal kinases mediate a wide range of targets in the metastatic cascade. *Genes Cancer* **4**, 378–387 (2013).
39. Mildner, M. et al. Secretome of peripheral blood mononuclear cells enhances wound healing. *PLoS ONE* **8**, e60103 (2013).
40. Yu, C. et al. The application of neural stem/progenitor cells for regenerative therapy of spinal cord injury. *Curr. Stem Cell Res. Ther.* https://doi.org/10.2174/1574888x14666190329095638 (2019).
41. Kosaric, N., Kiwanuka, H. & Gurtner, G. C. Stem cell therapies for wound healing. *Expert Opin. Biol. Ther.* https://doi.org/10.1080/14712598.2019.1596257, 1–11 (2019).
42. Segers, V. F. & Lee, R. T. Stem-cell therapy for cardiac disease. *Nature* **451**, 937–942 (2008).
43. Abbas, O. L. et al. Bone marrow mesenchymal stem cell transplantation enhances nerve regeneration in a rat model of hindlimb replantation. *Plast. Reconstr. Surg.* **143**, 758e–768e (2019).
44. Gyongyosi, M., Haller, P. M., Blake, D. J. & Martin Rendon, E. Meta-analysis of cell therapy studies in heart failure and acute myocardial infarction. *Circ. Res.* **123**, 301–308 (2018).
45. Wuschko, S. et al. Toxicological testing of allogeneic secretome derived from peripheral mononuclear cells (APOSEC): a novel cell-free therapeutic agent in skin disease. *Sci. Rep.* **9**, 5598 (2019).
46. Gugerell, A. et al. Viral safety of APOSEC(): a novel peripheral blood mononuclear cell derived-biological for regenerative medicine. *Blood Transfus.* https://doi.org/10.2450/2019.0249-18 (2019).
47. Huang, Z. et al. Necrostatin-1 rescues mice from lethal irradiation. *Biochim. Biophys. Acta* **1862**, 850–856 (2016).
48. Kuwahara, Y. et al. Association between radiation-induced cell death and clinically relevant radioresistance. *Histochem. Cell Biol.* **150**, 649–659, (2018).
49. Castle, K. D. et al. Mice lacking RIP3 kinase are not protected from acute radiation syndrome. *Radiat. Res.* **189**, 627–633, https://doi.org/10.1667/rr15001.1 (2018).
50. Wang, H. H. et al. Ablative hypofractionated radiation therapy enhances non-small cell lung cancer cell killing via preferential stimulation of necroptosis in vitro and in vivo. *Int. J. Radiat. Oncol. Biol. Phys.* **101**, 49–62 (2018).

51. Wu, X. et al. TNF-alpha sensitizes chemotherapy and radiotherapy against breast cancer cells. *Cancer Cell Int.* **17**, 13 (2017).
52. Steinman, J. et al. Improved total-body irradiation survival by delivery of two radiation mitigators that target distinct cell death pathways. *Radiat. Res.* **189**, 68–83 (2018).
53. Goodman, S. M. et al. 2017 American College of Rheumatology/American Association of Hip and Knee Surgeons Guideline for the Perioperative Management of Antirheumatic Medication in Patients With Rheumatic Diseases Undergoing Elective Total Hip or Total Knee Arthroplasty. *Arthritis Rheumatol.* **69**, 1538–1551 (2017).
54. Grell, M. Tumor necrosis factor (TNF) receptors in cellular signaling of soluble and membrane-expressed TNF. *J. Inflamm.* **47**, 8–17 (1995).
55. Grell, M. et al. The transmembrane form of tumor necrosis factor is the prime activating ligand of the 80 kDa tumor necrosis factor receptor. *Cell* **83**, 793–802 (1995).
56. Hannes, S., Abhari, B. A. & Fulda, S. Smac mimetic triggers necroptosis in pancreatic carcinoma cells when caspase activation is blocked. *Cancer Lett.* **380**, 31–38 (2016).
57. Wu, Y. T. et al. zVAD-induced necroptosis in L929 cells depends on autocrine production of TNFalpha mediated by the PKC-MAPKs-AP-1 pathway. *Cell Death Differ.* **18**, 26–37 (2011).
58. Upton, J. W., Kaiser, W. J. & Mocarski, E. S. DAI/ZBP1/DLM-1 complexes with RIP3 to mediate virus-induced programmed necrosis that is targeted by murine cytomegalovirus vIRA. *Cell Host Microbe.* **11**, 290–297 (2012).

Supplementary Figure 1

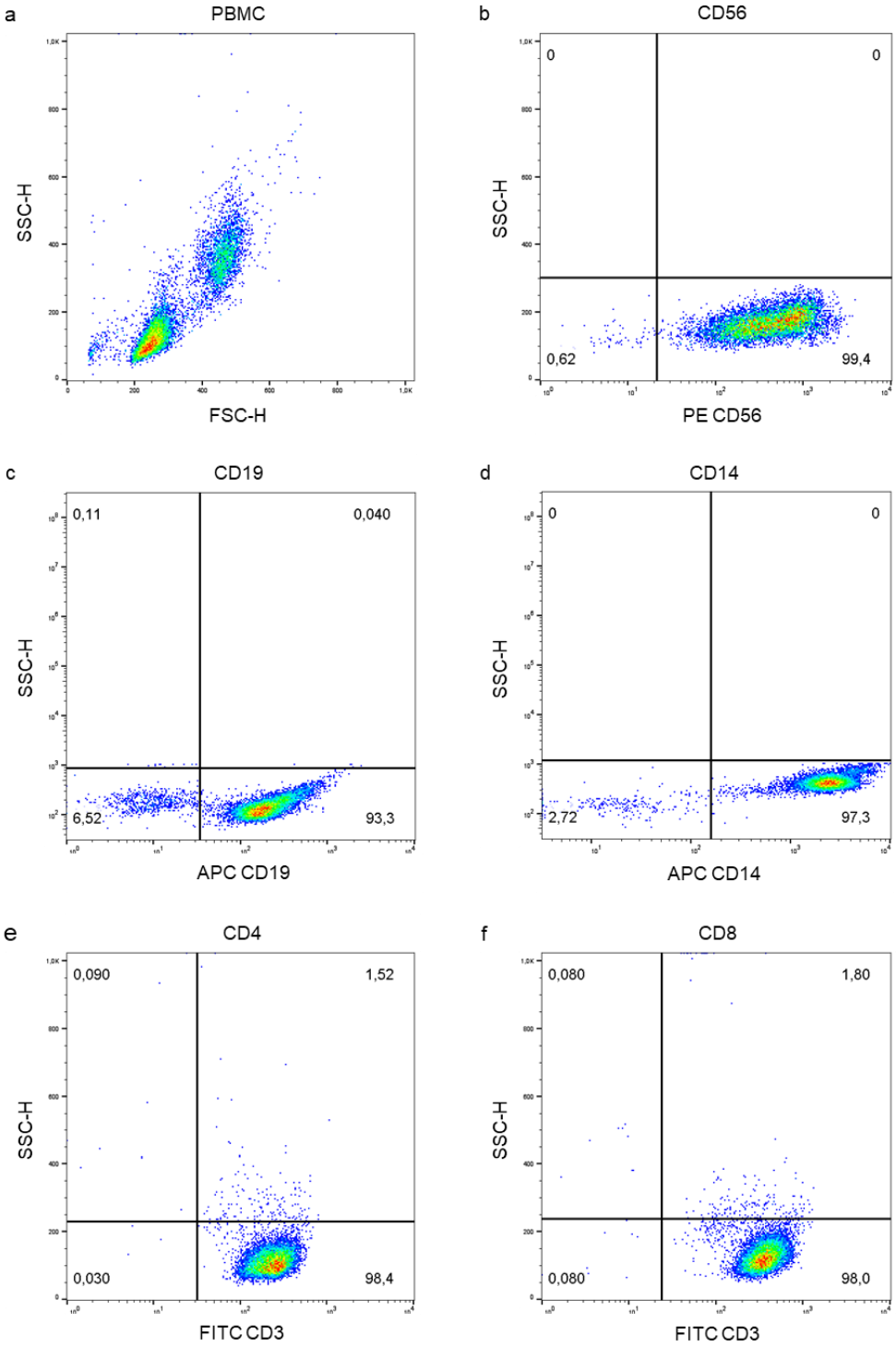

Supplementary Figure 1. Purity of isolated PBMC subsets. Polychromatic flow cytometric analysis for purified PBMC subsets. a) Forward-sidescatter dot plot of PBMCs. b) Purified natural killer cells expressing CD56 (99.4% cell purity). c) Purified B-cells expressing CD19 (93.3% cell purity). d) Purified monocytes expressing CD14 (97.3 cell purity). e) Purified CD4 T-cells expressing CD3 (95.4%). f) Purified CD8 T-cells expressing CD3 (98% cell purity). One experiment out of three is shown.

Supplementary Figure 2

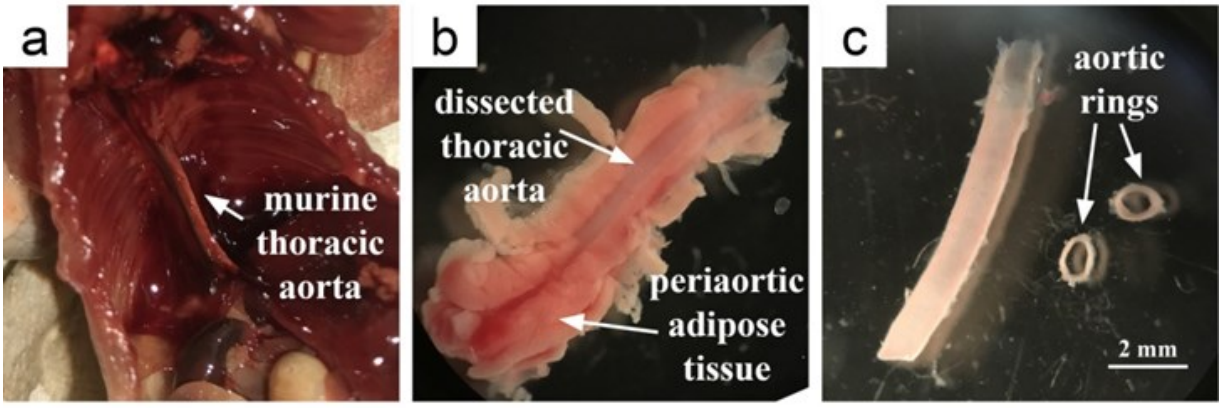

Supplementary Figure 2. Preparation of aortic rings. a) Mice were sacrificed via cervical dislocation, the rib cage was opened, heart and lungs were removed. c) Thoracic aorta including periaortic adipose tissue was carefully dissected from vertebrae. c) Adipose tissue was surgically removed and the aorta was cut in 1 mm-thick rings.

Supplementary Figure 3

a

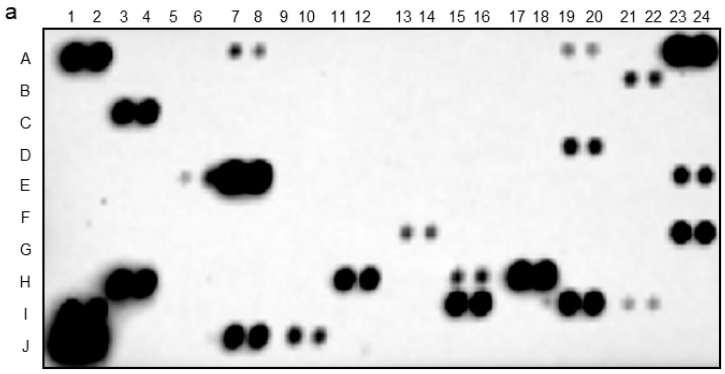

b

A1, A2	B3, B4	C3, C4	D1, D2	E1, E2	F1, F2	G1, G2	H1, H2	I1, I2	J1, J2
Reference Spots			GROα	IL-4	IL-19	Leptin	Myeloperoxidase	Serpin E1	Reference Spots
Adiponectin	CD40 ligand	ENA-78	Growth Hormone	IL-5	IL-22	LIF	Osteopontin	SHBG	
A5, A6	B5, B6	C5, C6	D5, D6	E5, E6	F5, F6	G5, G6	H5, H6	I5, I6	J5, J6
Apolipoprotein A-I	Chitinase 3-like 1	Endoglin	HGF	IL-6	IL-23	Lipocalin-2	PDGF-AA	ST2	Vitamin D BP
A7, A8	B7, B8	C7, C8	D7, D8	E7, E8	F7, F8	G7, G8	H7, H8	I7, I8	J7, J8
Angiogenin	Complement Factor D	Fas Ligand	ICAM-1	IL-8	IL-24	MCP-1	PDGF-AB/BB	TARC	CD31
A9, A10	B9, B10	C9, C10	D9, D10	E9, E10	F9, F10	G9, G10	H9, H10	I9, I10	J9, J10
Angiopoietin-1	C-Reactive Protein	FGF basic	IFN-γ	IL-10	IL-27	MCP-3	Pentraxin 3	TFF3	TIM-3
A11, A12	B11, B12	C11, C12	D11, D12	E11, E12	F11, F12	G11, G12	H11, H12	I11, I12	J11, J12
Angiopoietin-2	Cripto-1	FGF-7	IGFBP-2	IL-11	IL-31	M-CSF	PF4	TfR	VCAM-1
A13, A14	B13, B14	C13, C14	D13, D14	E13, E14	F13, F14	G13, G14	H13, H14	I13, I14	
BAFF	Cystatin C	FGF-19	IGFBP-3	IL-12 p70	IL-32	MIF	RAGE	TGF-α	
A15, A16	B15, B16	C15, C16	D15, D16	E15, E16	F15, F16	G15, G16	H15, H16	I15, I16	
BDNF	Dkk-1	Flt-3 Ligan	IL-1α	IL-13	IL-33	MIG	RANTES	Thrombospondin-1	
A17, A18	B17, B18	C17, C18	D17, D18	E17, E18	F17, F18	G17, G18	H17, H18	I17, I18	
Complement C5/a	DPPIV	G-CSF	IL-1β	IL-15	IL-34	MIP-1α/MIP-1β	RBP-4	TNF-α	
A19, A20	B19, B20	C19, C20	D19, D20	E19, E20	F19, F20	G19, G20	H19, H20	I19, I20	
CD14	EGF	GDF-15	IL-1ra	IL-16	IP-10	MIP-3α	Relaxin-2	uPAR	
A21, A22	B21, B22	C21, C22	D21, D22	E21, E22	F21, F22	G21, G22	H21, H22	I21, I22	
CD30	Emmprin	GM-CSF	IL-2	IL-17A	I-TAC	MIP-3β	Resistin	VEGF	
A23, A24			D23, D24	E23, E24	F23, F24	G23, G24	H23, H24		J23, J24
Reference Spots			IL-3	IL-18Bpa	Kallikrein 3	MMP-9	SDF-1α		Negative Controls

Supplementary Figure 3. Cytokine protein array of γ-irradiated PBMCs. a) Membrane arrays detecting 102 cytokines and cytokine-related proteins were incubated with supernatant from 25x10^6 γ-irradiated PBMCs 24 hours after incubation. b) Legend for spotted antibodies.

Supplementary Figure 4

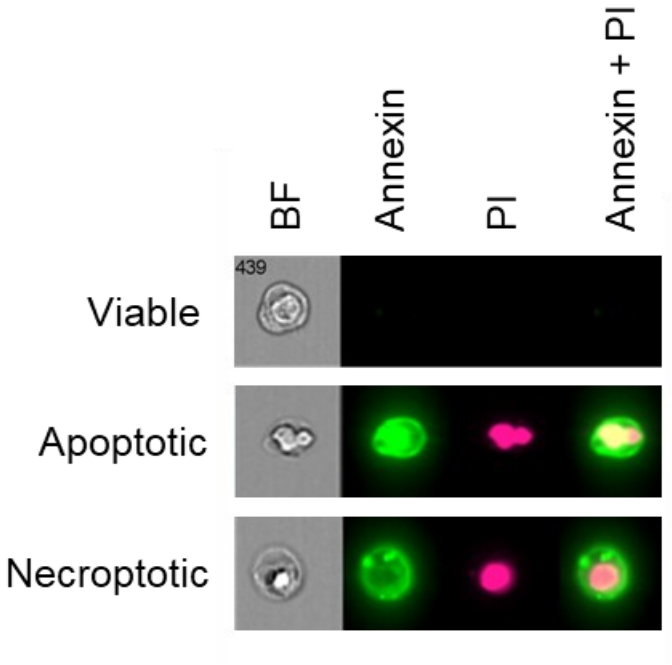

Supplementary Figure 4. Representative image stream micrographs of viable, apoptotic, and necroptotic cells. Viable cells were morphologically characterised by their intact cell shape in the bright field (BF) channel and by the lack of annexin and propidium iodide (PI). Apoptotic cells showed decreased cell volume, exposed Annexin on the surface, and displayed nuclear fragmentation (PI positive). Cells undergoing necroptosis were enlarged, indicating cytoplasmic swelling and the nucleus remained non-fragmented.

Supplementary Figure 5

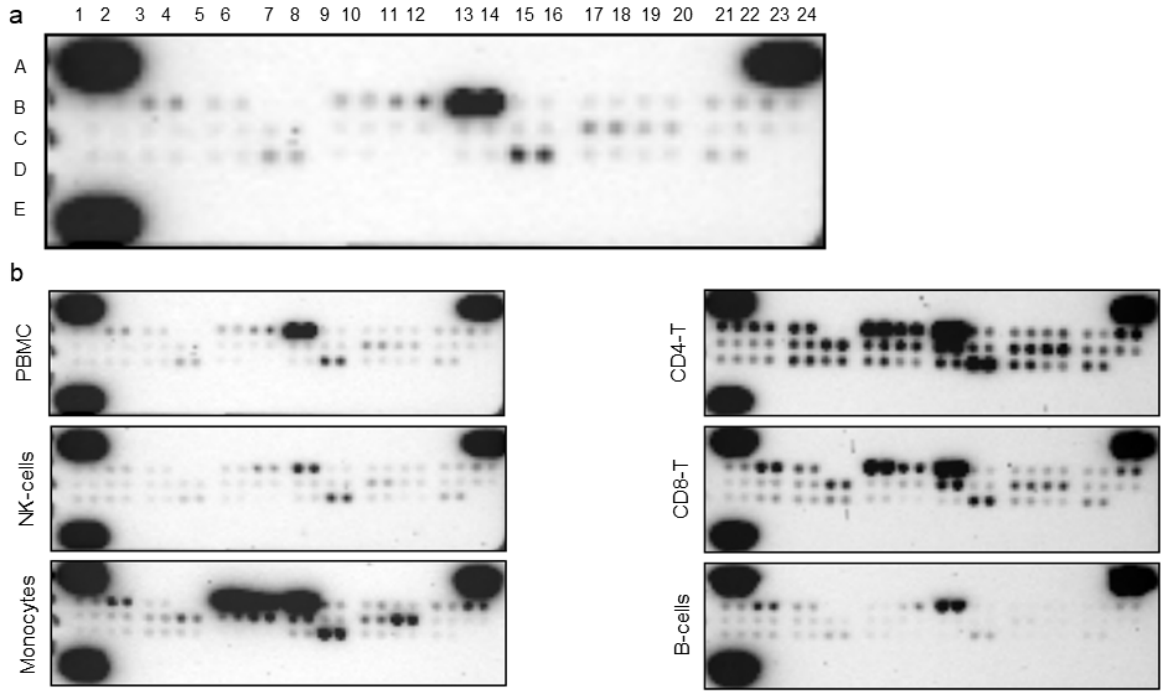

A1	A2	Reference	C13	C14	HO-2/HMOX2
A23	A24	Reference	C15	C16	HSP27
B1	B2	Bad	C17	C18	HSP60
B3	B4	Bax	C19	C20	HSP70
B5	B6	Bcl-2	C21	C22	HTRA2/Omi
B7	B8	Bcl-x	C23	C24	Livin
B9	B10	Pro-Caspase-3	D1	D2	PON2
B11	B12	Cleaved Caspase-3	D3	D4	p21/CIP1/CDKN1A
B13	B14	Catalase	D5	D6	p27/Kip1
B15	B16	cIAP-1	D7	D8	Phospho-p53
B17	B18	cIAP-2	D9	D10	Phospho-p53
B19	B20	Claspin	D11	D12	Phospho-p53
B21	B22	Clusterin	D13	D14	Phospho-Rad17
B23	B24	Cytochrome c	D15	D16	SMAC/Diablo
C1	C2	TRAIL R1/DR4	D17	D18	Survivin
C3	C4	TRAIL R2/DR5	D19	D20	TNF
C5	C6	FADD	D21	D22	XIAP
C7	C8	Fas/TNFRSF6/CD95	D23	D24	negative control
C9	C10	HIF-1α	E1	E2	Reference
C11	C12	HO-1/HMOX1/HSP32			

Supplementary Figure 5. Array of apoptosis-related proteins secreted by γ-irradiated PBMCs. a) Membrane arrays detecting 35 apoptosis-related proteins were incubated with cell lysates from $25x10^6$ γ-irradiated PBMCs 24 hours after exposure. b) Plots of PBMCs, NK-cells, monocytes, CD4 T-cells, CD8 T-cells, and B-cells are shown. Table lists the proteins analysed.

Supplementary Figure 6

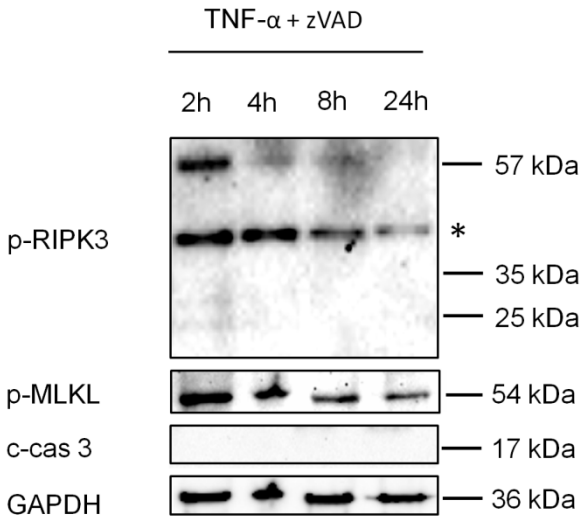

Supplementary Figure 6. TNFα and zVAD induce necroptosis in PBMCs. PBMCs were stimulated with a combination of TNFα and zVAD and cultivated for up to 24 hours. Co-incubation of PBMCs with TNFα and zVAD abrogated caspase-3 cleavage and lead to phosphorylation of RIPK3 and MLKL. After stimulation with TNF and zVAD phosphorylated RIPK3 was shown with 57 kDA displayed its peak after 2h, whereas the cleavage product seen after irradiation (Fig. 5) at 35kDA and 25kDA could not be detected, n=3.

Supplementary Figure 7

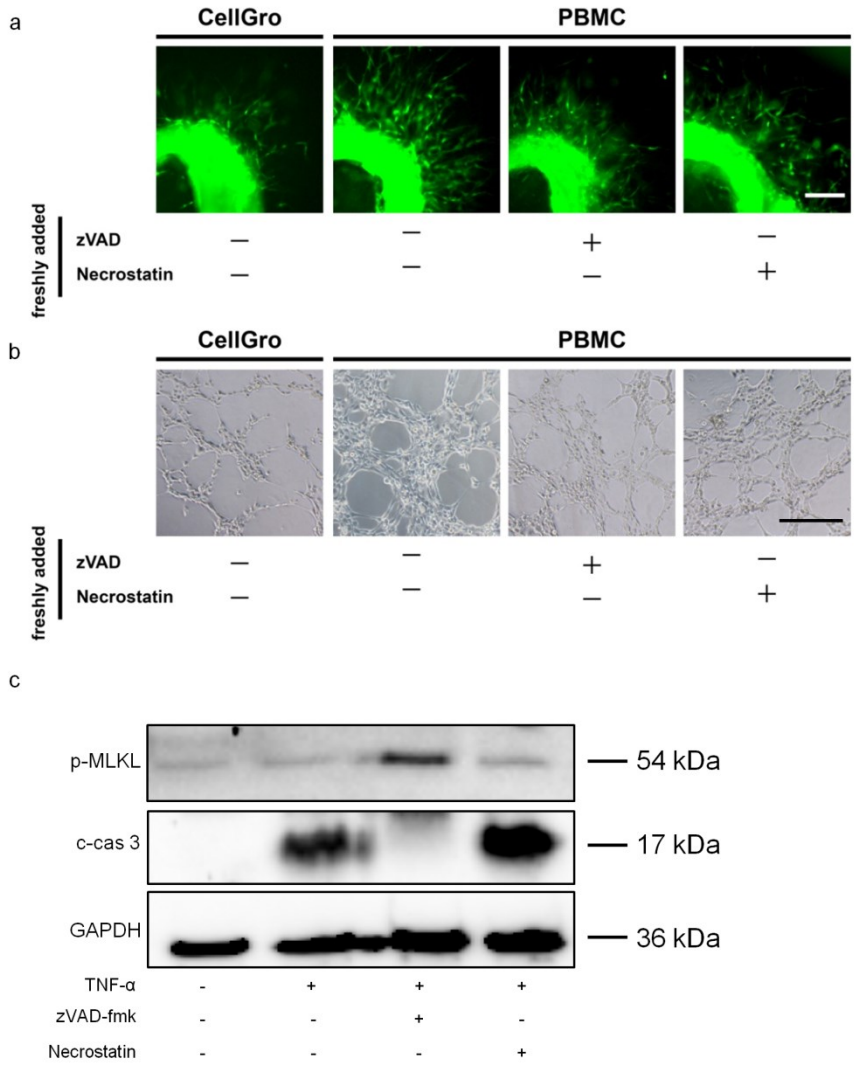

Supplementary Figure 7. TNFα induces apoptosis and necroptosis in PBMCs which were inhibited by zVAD and necrostatin, respectively. a) Aortic rings were incubated with the secretome of γ-irradiated PBMCs together with freshly added zVAD, necrostatin or a combination of both for 3 days. Thereafter calcein (green dye) was added to label viable cells. Neither zVAD nor necrostatin significantly inhibited blood vessel sprouting in the aortic ring assay. Scale bar, 200 µm. n=3. b) Endothelial cells were incubated with the secretome of γ-irradiated PBMCs together with freshly added zVAD and necrostatin for 3 hours after starvation overnight. Cell Gro medium was used as negative control. The tube formation was diminished in the medium control, yet the fresh addition of zVAD and necrostatin had no effect on endothelial outgrowth compared to the PBMC secretome. Scale bar, 200 µm. c) PBMCs were stimulated with combinations of TNFα, zVAD and necrostatin and were cultivated for 24 hours. Stimulation with TNFα resulted in cleavage of caspase-3 (c-cas 3). Co-incubation of PBMCs with TNFα and zVAD abrogated caspase-3 cleavage and lead to phosphorylation MLKL while co incubation with necrostatin favored caspase-3 cleavage. n=3

9.3 Interlude

An increasing number of chronic wound healing deficiencies are counted in the US (estimated 6,5 million patients) due to the rising numbers of diabetes.[7,292] These chronic non-healing ulcers lead to increasing economic burden, as the treatment of one diabetic ulcer costs nearly 50.000$.[7,292,293] These great expenses illustrate an unmet need in patient care.

For an adequate tissue repair and wound healing many factors such as growth factors, inflammatory cells, oxygen and blood perfusion to deliver these factors to the required area are needed.[294,295] In diabetic patients the vasculature is often impaired and further aggravating the dysfunctional healing process.[294,296] As we have showed previously, the secretome of irradiated PBMC could provide enhanced angiogenesis and growth factors/cytokines necessary to improve wound healing.[57,89,281,282,297]

Yet for every promising therapeutic compound various stages to proof safety and tolerability have to be fulfilled. Therefore, the safe application of autologous APOSEC (which was produced according to current GMP guidelines) was tested in a clinical phase I study.

9.4 Paper 2

www.nature.com/scientificreports

OPEN

Safety and tolerability of topically administered autologous, apoptotic PBMC secretome (APOSEC) in dermal wounds: a randomized Phase 1 trial (MARSYAS I)

Received: 28 February 2017
Accepted: 20 June 2017
Published online: 24 July 2017

Elisabeth Simader[1,2,9,10], Denise Traxler[1,2], Mohammad Mahdi Kasiri[1,2], Helmut Hofbauer[1,2,9,10], Michael Wolzt[3], Christoph Glogner[1,2], Angela Storka[3,11,12], Michael Mildner[4,9], Ghazaleh Gouya[3], Alexandra Geusau[5], Carola Fuchs[3], Claudia Eder[3], Alexandra Graf[6], Michaela Schaden[7], Bahar Golabi[4], Marie-Bernadette Aretin[11], Susanne Suessner[8], Christian Gabriel[13], Walter Klepetko[1], Erwin Tschachler[4] & Hendrik Jan Ankersmit[1,2,9,10]

Developing effective therapies against chronic wound healing deficiencies is a global priority. Thus we evaluated the safety of two different doses of topically administered autologous APOSEC, the secretome of apoptotic peripheral blood mononuclear cells (PBMCs), in healthy male volunteers with artificial dermal wounds. Ten healthy men were enrolled in a single-center, randomized, double-blinded, placebo-controlled phase 1 trial. Two artificial wounds at the upper arm were generated using a 4-mm punch biopsy. Each participant was treated with both topically applied APOSEC and placebo in NuGel for 7 consecutive days. The volunteers were randomized into two groups: a low-dose group (A) receiving the supernatant of 12.5×10^6 PBMCs and a high-dose group (B) receiving an equivalent of 25×10^6 PBMCs resuspended in NuGel Hydrogel. Irradiated medium served as placebo. The primary outcome was the tolerability of the topical application of APOSEC. All adverse events were recorded until 17 days after the biopsy. Local tolerability assessment was measured on a 4-point scale. Secondary outcomes were wound closure and epithelization at day 7. No therapy-related serious adverse events occurred in any of the participants, and both low- and high-dose treatments were well tolerated. Wound closure was not affected by APOSEC therapy.

[1]Division of Thoracic Surgery, Medical University of Vienna, Vienna, Austria. [2]Christian Doppler Laboratory for Cardiac and Thoracic Diagnosis and Regeneration, Medical University of Vienna, Vienna, Austria. [3]Department of Clinical Pharmacology, Medical University of Vienna, Vienna, Austria. [4]Research Division of Biology and Pathobiology of the Skin, Department of Dermatology, Medical University of Vienna, Vienna, Austria. [5]Division of Immunology, Allergy, and Infectious Diseases, Department of Dermatology, Medical University of Vienna, Vienna, Austria. [6]Section of Medical Statistics, Centre for Medical Statistics, Informatics and Intelligent Systems, Medical University of Vienna, Vienna, Austria. [7]Clinical Trials Coordinative Centre, Medical University of Vienna, Vienna, Austria. [8]Austrian Red Cross Blood Transfusion Service for Upper Austria, Linz, Austria. [9]FFG Project 852748 "APOSEC", Medical University of Vienna, Vienna, Austria. [10]Aposcience AG, Company No.: 308089, Vienna, Austria. [11]AKH Vienna pharmacy, Medical University of Vienna, Vienna, Austria. [12]Danubian Hospital, Social and medical center of eastern Vienna, Vienna, Austria. [13]Ludwig Boltzmann Institute for experimental and clinical traumatology, Vienna, Austria. Elisabeth Simader, Denise Traxler and Mohammad Mahdi Kasiri contributed equally to this work. Correspondence and requests for materials should be addressed to H.J.A. (email: hendrik.ankersmit@meduniwien.ac.at)

The global incidence of non-healing wounds is soaring due to increasing prevalence of diabetes and obesity. These wounds are a major cause of morbidity, have a negative impact on quality of life, and result in enormous costs for the health care system[1]. Although several highly expensive products are on the market, the process of wound healing takes a long time and is often incomplete, entailing amputation in severe cases[2].

Many approaches to new therapies have been investigated over the last decades, but no sufficient therapeutic option yet exists. Wound healing involves a complex interplay of various cell types as well as cellular and biochemical events. This process depends on a supply of oxygen, nutrients, and growth factors. Diabetic patients have an impaired vasculature, which results in reduced blood perfusion to the wound area, leading to decreased migration of inflammatory cells[3,4]. However, inflammatory cells are an essential part of chronic wound healing, acting in both beneficial and harmful ways[5–7]. The application of stem cells, genetically modified cells, or paracrine factors on chronic wound areas has led to encouraging results, regarding wound healing[8–10]. A paper by Holzinger *et al.* showed that topical application of activated, autologous peripheral blood mononuclear cells (PBMCs) effectively initiated epithelialization of ulcerated, dermal wounds and that wound closure was present in 92% of patients after 60 days, compared to standard therapy[11]. In particular, paracrine factors are being considered as a promising option because they provide pro-angiogenic and anti-apoptotic mediators for cell proliferation and migration[12]. To advance Holzinger's "activated PBMC-based therapy," we applied the cell-free secretome of apoptotic PBMCs, the APOptotic PBMC SECretome (APOSEC), produced according to good manufacturing practice (GMP) guidelines. APOSEC contains a myriad of cytokines, lipids, proteins, exosomes, and vasoactive substances[13]. To increase the secretory output of PBMCs, we induced apoptosis via ionizing radiation[13–17].

In a recent publication, we reported positive effects of APOSEC on angiogenesis and skin regeneration in a mouse wound-healing model and in a clinically more relevant porcine third-degree burn model[10,14]. Further approaches in preclinical models revealed that the secretome of PBMCs attenuates hypoxic injury in acute and latent myocardial infarction[15,18–20], spinal cord injury, and stroke[21,22]. Additionally, APOSEC augments de novo secretion of antimicrobial peptides[23] and attenuates experimental myocarditis by inducing caspase 8–dependent CD4 T cell apoptosis[19]. These promising preclinical data encouraged us to initiate the production of APOSEC for human application under the auspices of the Austrian Agency for Food and Drug Safety (AGES) (AGES-Nr. INS-480102-0013-007). APOSEC as a drug substance has been classified as "biological" and can be applied in a personalized manner (autologous) or in an allogeneic approach (pooled product). This first clinical trial using autologous APOSEC was approved by the certified authority (AGES) to explore its safety and tolerability in artificial skin wounds in healthy, male participants.

Materials and Methods

Trial design and study population. This study was a prospective, single-center, randomized, double-blinded, placebo-controlled, dose-finding phase 1 trial to assess the safety and tolerability of two different doses of autologous APOSEC in artificial dermal wounds. A secondary potential objective was to investigate the effect on wound closure. The study population consisted of 10 healthy male volunteers. Five participants were assigned to each group: a low-dose group (GMP APOSEC from 12.5×10^6 irradiated, lyophilized PBMC/ml) and a high-dose group (GMP APOSEC from 25×10^6 irradiated lyophilized PBMC/ml). (Supplementary Table S1 in the Supplement). Medium served as placebo. Both APOSEC and placebo were applied on two artificial dermal wounds (proximal and distal) on the upper non-dominant arm of the participant to reduce intra-individual reactions to a minimum (Fig. 1). (Exclusion criteria can be accessed at ClinicalTrials.gov Identifier: NCT02284360; https://clinicaltrials.gov/ct2/show/NCT02284360).

Trial registration. EudraCT-Number: 2013-000756-17, NCT 02284360, AGES INS-480102-0013-007 https://clinicaltrials.gov/ct2/show/NCT02284360?term=02284360&rank=1, ClinicalTrials.gov Identifier: NCT02284360 (First received: October 30, 2014; Last updated: September 25, 2015; Last verified: September 2015).

Screening/run-in phase. After eligible study volunteers gave written informed consent, clinical and laboratory testing was performed to verify inclusion and exclusion criteria. Physical examination and vital signs were obtained and a standard 12-lead ECG was performed. Blood samples for hematology, serum chemistry, virology and urine samples for urine analysis were obtained. Demographic and medical history data as well as concomitant medication were assessed. Before initiation of the treatment phase, 450 ml blood was collected at the GMP facility at the Austrian Red Cross Blood Transfusion Service of Upper Austria (Linz, Austria) (AGES INS-480102-0013-007), and autologous APOSEC, was produced according to GMP guidelines (Fig. 2). Afterwards, APOSEC was transferred to the Pharmacy of the Medical University of Vienna by Med Log courier.

Randomization/treatment phase. Randomization and blinding were performed by the AKH Vienna pharmacy (Vienna, Austria). To reduce potential adverse events resulting from the investigative medicinal product (IMP) or wound dressing (Tegaderm Film 10 × 12 cm, 3M, Maplewood, MN, US), a blinded test treatment with APOSEC and placebo on intact skin of the inner upper dominant arm was performed 24 h before initiation of the treatment phase. Any study participants who developed adverse events were excluded from the treatment phase. If adverse events were not considered to be IMP related, these volunteers were replaced. (Supplementary Table S2 in the Supplement).

Lyophilized APOSEC or the culture medium CellGro was resuspended in 200 µl 0.9% NaCl until complete dissolution, followed by mixing with 800 µl NuGel Hydrogel (Systagenix, Gatwick, West Sussex, UK) for topical administration only. The so produced verum or placebo was supplied in single-use tubes as a sterile preserved white gel.

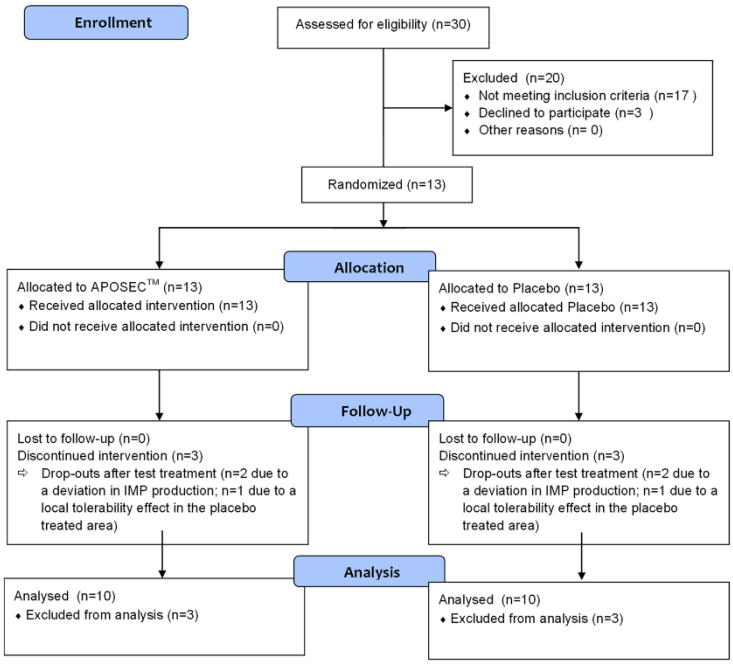

Figure 1. CONSORT Study Design of MARSYAS. The screening and design of the study were developed and conducted by the Department of Clinical Pharmacology of the Medical University of Vienna. Ten participants were included after giving written informed consent. Allocation to the low-dose group A and high-dose group B was completed after an interim analysis. To avoid inter-individual differences, every study participant received both verum and placebo on different positions on the same arm. The randomization of verum and placebo to the proximal or distal artificial arm wound was performed in a 1:1 ratio.

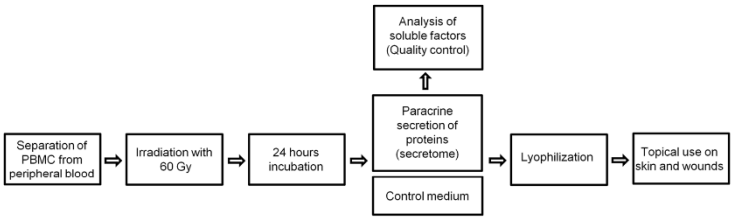

Figure 2. APOSEC production. Preparation process of APOSEC according to good manufacturing practice (GMP) in the facility of the Austrian Red Cross Blood Transfusion Service of Upper Austria (Linz, Austria), with the following steps. The first step was separating the PBMCs from the whole blood samples, inducing apoptosis via ionizing irradiation, and incubating for 24 h. During this 24 h, the PBMCs secrete a multitude of cytokines and chemokines. The quantity of cytokines is measured using ELISA and immunoassay (Luminex®100IS) for quality control. After the lyophilization, APOSEC is ready for topical use on skin and wounds.

Artificial wounds were generated by two 4-mm punch biopsies (distal and proximal, respectively) on the inner upper side of the non-dominant arm under local anesthesia. The distance between both biopsies was at least 8 cm. After being cleaned with 0.9% NaCl, one wound was treated with approximately 1 ml of APOSEC and the second with approximately 1 ml of placebo according to previous randomization. Wound dressing was applied covering the whole wound area. On the following 6 days, APOSEC and placebo were re-applied daily. At day 7, treatment was terminated, wound closure and scar formation were evaluated, and wounds were closed with a

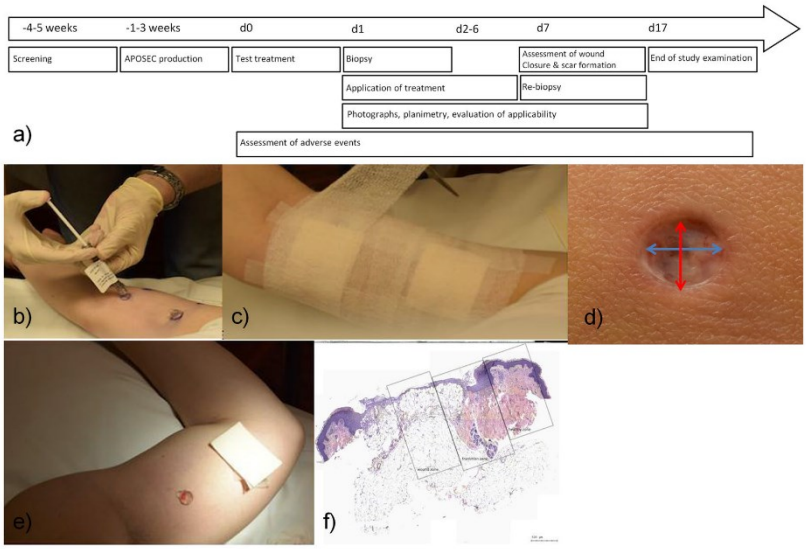

Figure 3. Study timeline and application of APOSEC/placebo. Study timeline (**a**). Application of APOSEC/placebo on intact skin (test treatment) (**b**). Bandaging of study site (**c**). Maximal (blue line) and minimal (red line) diameter of biopsy wound (**d**). Applied IMP/placebo on artificial wound (**e**). Tissue sample from day 7, boxes show wound, transition, and healthy zones in which measurements were performed (**f**).

suture. During the whole treatment period, wounds were assessed for the appearance of adverse events, and photographs for planimetric assessment were taken (Fig. 3). For standardization of the planimetric measurements, a pacer (CASTEL-COP-DIGI, CASTEL-L, Novoflex, Germany), ensuring the exact same distance for every picture was used (Supplementary Figure S1).

Follow-up phase. Each study participant was asked to return to the clinic to allow evaluation of whether or not adverse events emerged during the whole study period. At 17 days after treatment initiation, study participants returned for a follow-up visit. Sutures were removed, a physical examination was performed, vital signs and adverse events were assessed, and blood samples were taken. (Supplementary Table S3 in the Supplement).

Authorization and ethics statement. The study was approved by the ethics committee of the Medical University of Vienna, Austria (EK Nr. 1285/2013) and conducted according to the Declaration of Helsinki. This trial was registered in the EU clinical trial register (EudraCT-Number: 2013-000756-17; NCT02284360; AGES INS-480102-0013-007).

Production of APOSEC and placebo. Blood obtained from each study volunteer at the Austrian Red Cross Blood Transfusion Service of Upper Austria was used to produce autologous APOSEC according to current GMP guidelines. PBMCs were separated from whole blood samples of the participants by density centrifugation using LSM 1077 (Lymphocyte Separation Medium, Lonza, Switzerland). Removal of LSM was achieved by two washing steps using Dulbecco's phosphate-buffered saline (Lonza, Switzerland). PBMCs were resuspended in phenol red–free CellGro GMP DC medium (CellGenix, Freiburg, Germany) containing no xenogeneic proteins. A sample was drawn for complete blood count to adjust white blood cells to a concentration of 25×10^6 cells/ml. Irradiation with 60 Gy induced apoptosis of PBMCs. By cultivation of apoptotic PBMCs in CellGro GMP DC medium, release of the secretome was achieved. After incubation for $24\,h \pm 2\,h$, cells were removed by centrifugation. The supernatant containing the secretome was sterile filtered at a pore size of 0.22 µm. The adequate production of APOSEC was defined by appropriate secretion of the following important cytokines: interleukin (IL)-8 (0–5214 pg/ml), epidermal growth factor (EGF; 25–226 pg/ml), and transforming growth factor-β (TGF-3; 2575–21732 pg/ml).

Lyophilized culture medium not containing any cells (CellGro, CellGenix, Freiburg, Germany) served as placebo.

Quality and stability. The raw material, i.e., separated PBMCs, was irradiated with 60 Gy and cultured for 24 h. The supernatant of the cells was obtained and subjected to quality assurance protocols. Quality control of the product was realized in several steps. First, sterility testing of the final product was performed. Second, induction

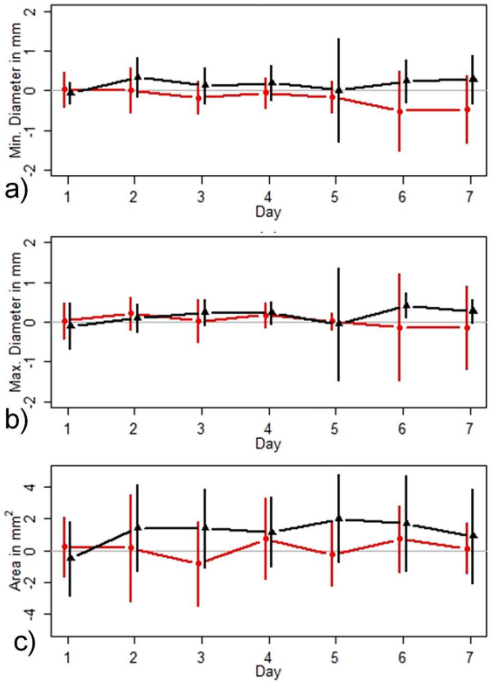

Figure 4. Effect of APOSEC on wound healing. Mean progression as well as the standard deviation (vertical lines) of minimal (**a**) and maximal (**b**) diameters and area (**c**) of the artificial wound during 7 days, represented as the difference of APOSEC – placebo. (red, group A = low-dose group; black, group B = high-dose group).

of apoptosis was determined before irradiation and after cultivation of the cells by fluorescence-activated cell sorting analysis using the FITC Annexin V Apoptosis Detection Kit (BD Biosciences, Franklin Lakes, NJ, US). Third, concentrations of IL-8/C × CL8 (C × C-motive-chemokine 8), EGF, and TGF-β were determined with enzyme-linked immunosorbent assay (ELISA) to verify successful production of APOSEC according to GMP definitions. The fourth part of quality control was endotoxin, mycoplasma and sterility testing of the final product. Cell culture supernatant samples were additionally screened for herpes contamination via polymerase chain reaction. AGES approved APOSEC as a test product according to current guidelines of the Austrian Drug Registration and Administration Act (AGES INS-480102-0013-007).

Evaluation of adverse events. Adverse events were documented if reported by study participants or observed by physicians. Skin alterations were graded using a local tolerability assessment scale (0 = no visible reaction; 1 = faint, minimal erythema; 2 = erythema; 3 = erythema with induration or vesicles; and 4 = severe erythema with induration, vesicles, or bullae or pustules and/or erosion/ulceration). A detailed description of all adverse events can be found in the supplementary (Table S2).

Evaluation of wound healing progression. Progression of wound healing was evaluated by planimetric measurement of photographs, expressed as minimum diameter, maximum diameter, and area measured from day 1 to day 7. (Fig. 4) Measurements were performed using ImageJ version 1.48 v (Wayne Rasband, National Institutes of Health, USA). (Supplementary Tables S4, S5, and S6) Moreover, wound healing and condition were assessed in comparison to prior day (stable, improving, impaired) according to the following criteria: presence or absence of inflammation, presence or absence of exsudate on the dressing, presence or absence of re-epithelialization and presence or absence of undermining and tunneling. Local tolerability was evaluated using the following criteria: (0 = no visible reaction; 1 = faint, minimal erythema; 2 = erythema; 3 = erythema with induration or vesicles; and 4 = severe erythema with induration, vesicles, or bullae or pustules and/or erosion/ulceration).

Immunohistochemical staining. For microscopic examination, tissue specimens were collected on day 1 and day 7.

Immunohistochemical staining was performed for CD45, keratin 10, factor VIII, and podoplanin. A detailed description of the staining and results can be found in the supplementary material.

Statistical analysis. Data obtained were evaluated statistically using R version 3.2.1., IBM SPSS Statistics version 23 (SPSS Inc., Chicago, USA), and GraphPad Prism 6 software (GraphPad Software Inc., La Jolla, CA, USA). The analyses were performed for the "as treated" population using descriptive statistics. For the continuous parameters of wound and scar assessment, means, standard deviations as well as medians, quartiles, minima and maxima were calculated separately for the two APOSEC groups and the placebo group as well as for the difference between APOSEC and placebo for all investigated days.

Data Availability. The datasets generated during and/or analysed during the current study are available from the corresponding author on reasonable request.

Results

Study population. In February 2015, fourteen volunteers were assessed for study eligibility, received a case report form (CRF) number, and gave their written informed consent. One was preliminarily excluded before receiving any test treatment, due to a screening failure. Two study participants dropped out due to a deviation in production of APOSEC, and one was excluded because of erythema at the site of placebo application on intact skin at day 0. The proband (CRF 9), excluded before test treatment was included in the 17 screened subjects not meeting inclusion criteria in Fig. 1. The 3 participants excluded due to production deviation and erythema at the placebo treated areal were declined to participate (Fig. 1). The "as treated" population consisted of 10 healthy male study participants.

Supplementary Table S1 describes participant characteristics at the beginning and end of study. At the baseline and end of study visit, study subjects assigned to groups A and B did not show any relevant differences.

Topical application of APOSEC is safe and well tolerated. The main objective was to monitor for and identify adverse events after topical application of APOSEC. All adverse events were reported by participants or observed by study researchers (from the Department of Clinical Pharmacology of the Medical University of Vienna, Austria) and are shown in (Supplementary Table S2 in the Supplement). All identified events were characterized as mild.

Wound closure and APOSEC. Due to the short intervention time, we could not demonstrate a further increase in wound closure progression in wounds treated with APOSEC GMP compared to wounds treated with placebo. No wound closure in the artificial wounds was assessed. Figure 3 shows mean time course for maximum wound diameter (A), minimum wound diameter (B), and wound area (C) for the relative difference between verum and placebo measurements separately for group A (red line: 12.5×10^6 PBMC/ml) and B (black line: 25.0×10^6 PBMC/ml). A value below 0 indicates improved wound closure in the APOSEC group as compared to placebo.

Discussion

In this first clinical prospective phase 1 study utilizing the autologous secretome of PBMCs in humans, we showed that the application of APOSEC is safe and well tolerated in human intact skin, as well as on the open wound area. The secondary endpoint of wound closure was not achieved, which is attributable to the short duration of the study.

This study was performed as a "prerequisite" for the further development of the allogeneic APOSEC product, derived from healthy blood donors in order to treat patients with non-healing wounds. This disease causes in our society an ever increasing financial and psychological burden - for both, patients and the health care system[1].

In particular, cell-based therapies are a rapidly expanding sector in wound closure treatments. For example, the application of cellular 3D fibroblast constructs (Dermagraft) (Shire Regenerative Medicine, San Diego, CA) received market authorization in multiple countries after Phase 3 trials[24–29]. Another approach has been the use of allogeneic gamma-irradiated cord blood mononuclear cells in a patient with critical limb ischemia, which led to improved wound closure and vascularity[30].

A similar method was chosen for a clinical trial financed by Macrocure Ltd. In two US Food and Drug Administration (FDA)-approved studies, hypo-osmotic shock-exposed allogeneic PBMCs were injected subcutaneously for the treatment of diabetic and venous foot ulcers[31, 32] (https://clinicaltrials.gov/ct2/show/NCT01421966).

Both investigations were prematurely terminated because of futility (http://investor.macrocure.com/releasedetail.cfm?ReleaseID=928245).

In contrast to these cell-based therapies, we have concentrated on the biological effects of paracrine factors derived from stressed white blood cells. The supernatant provides a potent cell-free alternative, displaying a possible diminished immunogenicity as compared to cell-based therapy. APOSEC stimulates migration of fibroblasts, keratinocytes, and endothelial cells *in vitro*[10, 13], which are crucial elements in the physiology of wound healing. Moreover, APOSEC contains significant amounts of antimicrobial peptides that possess antimicrobial activity against opportunistic skin pathogens, especially *Escherichia coli* and *Pseudomonas aeruginosa*[23]. With regard to the cataclysmic consequences of bacterial infection for wound regeneration and healing, in severe cases involving non-remediable tissue impairment necessitating amputation, this particular attribute emphasizes the clinical potential of APOSEC [2].

Results from a murine wound-healing model, as well as a porcine third-degree burn model have already indicated the effectiveness of topical application of PBMC-derived paracrine factors[10, 14]. Mildner *et al.* showed in this first investigation that the PBMC secretome increases angiogenesis and wound closure in mice[10, 14]. All

of these features are most desirable for wound healing, but it is a fact that the PBMC secretome is a mixture of paracrine factors containing multiple pro-angiogenic proteins, lipids, and exosomes[13]. From our point of view, the observed effects are not attributable to a single factor but to the combination of different components of APOSEC. This hypothesis has already been corroborated by Lichtenauer *et al.*, who selectively blocked different factors, including matrix metalloproteinase-9 (MMP-9), vascular endothelial growth factor (VEGF), and IL-8, and failed to attenuate the biological activity in selected potency assays[18]. Thus, the identification of a single mechanism of action (MOA) remains challenging because on the one hand, we deal with a complex composition of paracrine factors, and on the other hand, we deal with a plethora of biological effects. Based on our long lasting research in the effect of PBMC secretome (APOSEC) we feel that the search for "the target" or "the MOA" in skin regeneration is not feasible[33].

Before the "off the shelf" drug substance of allogeneic APOSEC enters regulatory approval, multiple requirements must be met by a drug developer. These are stability studies, development of validated potency assays, and the completion of incremental and repeated dose toxicology studies in two animal species.

All of these manufacturing and regulatory hurdles must be accomplished before a transition into the clinic will become reality. In addition to a positive verdict of the internal reviewer board (IRB), trial registration and approval of national and super national regulatory agencies are mandatory.

Only a proof of concept phase II study will show whether scientific insights generated at our surgical research laboratory will find its translation in the treatment of non-healing wounds.

References

1. Sen, C. K. *et al.* Human skin wounds: a major and snowballing threat to public health and the economy. *Wound Repair Regen* **17**, 763–771, doi:10.1111/j.1524-475X.2009.00543.x (2009).
2. Dos Santos, V. P., da Silveira, D. R. & Caffaro, R. A. Risk factors for primary major amputation in diabetic patients. *Sao Paulo Med J* **124**, 66–70 (2006).
3. Falanga, V. Wound healing and its impairment in the diabetic foot. *Lancet* **366**, 1736–1743, doi:10.1016/s0140-6736(05)67700-8 (2005).
4. Gurtner, G. C., Werner, S., Barrandon, Y. & Longaker, M. T. Wound repair and regeneration. *Nature* **453**, 314–321, doi:10.1038/nature07039 (2008).
5. Badiavas, E. V. & Falanga, V. Treatment of chronic wounds with bone marrow-derived cells. *Arch Dermatol* **139**, 510–516, doi:10.1001/archderm.139.4.510 (2003).
6. Martin, P. & Nunan, R. Cellular and molecular mechanisms of repair in acute and chronic wound healing. *Br J Dermatol* **173**, 370–378, doi:10.1111/bjd.13954 (2015).
7. Demidova-Rice, T. N., Durham, J. T. & Herman, I. M. Wound Healing Angiogenesis: Innovations and Challenges in Acute and Chronic Wound Healing. *Adv Wound Care (New Rochelle)* **1**, 17–22, doi:10.1089/wound.2011.0308 (2012).
8. Chen, J. S., Wong, V. W. & Gurtner, G. C. Therapeutic potential of bone marrow-derived mesenchymal stem cells for cutaneous wound healing. *Front Immunol* **3**, 192, doi:10.3389/fimmu.2012.00192 (2012).
9. Koyama, T. *et al.* A new technique of *ex vivo* gene delivery of VEGF to wounds using genetically modified skin particles promotes wound angiogenesis. *J Am Coll Surg* **212**, 340–348, doi:10.1016/j.jamcollsurg.2010.10.017 (2011).
10. Mildner, M. *et al.* Secretome of peripheral blood mononuclear cells enhances wound healing. *PLoS One* **8**, e60103, doi:10.1371/journal.pone.0060103 (2013).
11. Holzinger, C. *et al.* Treatment of non-healing skin ulcers with autologous activated mononuclear cells. *Eur J Vasc Surg* **8**, 351–356 (1994).
12. Rehman, J. *et al.* Secretion of angiogenic and antiapoptotic factors by human adipose stromal cells. *Circulation* **109**, 1292–1298, doi:10.1161/01.CIR.0000121425.42966.F1 (2004).
13. Beer, L. *et al.* Analysis of the Secretome of Apoptotic Peripheral Blood Mononuclear Cells: Impact of Released Proteins and Exosomes for Tissue Regeneration. *Scientific reports* **5**, 16662, doi:10.1038/srep16662 (2015).
14. Hacker, S. *et al.* Paracrine Factors from Irradiated Peripheral Blood Mononuclear Cells Improve Skin Regeneration and Angiogenesis in a Porcine Burn Model. *Sci Rep* **6**, 25168, doi:10.1038/srep25168 (2016).
15. Ankersmit, H. J. *et al.* Irradiated cultured apoptotic peripheral blood mononuclear cells regenerate infarcted myocardium. *Eur J Clin Invest* **39**, 445–456, doi:10.1111/j.1365-2362.2009.02111.x (2009).
16. Beer, L. *et al.* High dose ionizing radiation regulates micro RNA and gene expression changes in human peripheral blood mononuclear cells. *BMC Genomics* **15**, 814, doi:10.1186/1471-2164-15-814 (2014).
17. Beer, L., Mildner, M., Gyongyosi, M. & Ankersmit, H. J. Peripheral blood mononuclear cell secretome for tissue repair. *Apoptosis* **21**, 1336–1353, doi:10.1007/s10495-016-1292-8 (2016).
18. Lichtenauer, M. *et al.* Secretome of apoptotic peripheral blood cells (APOSEC) confers cytoprotection to cardiomyocytes and inhibits tissue remodelling after acute myocardial infarction: a preclinical study. *Basic research in cardiology* **106**, 1283–1297, doi:10.1007/s00395-011-0224-6 (2011).
19. Hoetzenecker, K. *et al.* Mononuclear cell secretome protects from experimental autoimmune myocarditis. *Eur Heart J* **36**, 676–685, doi:10.1093/eurheartj/ehs459 (2015).
20. Pavo, N. *et al.* Long-acting beneficial effect of percutaneously intramyocardially delivered secretome of apoptotic peripheral blood cells on porcine chronic ischemic left ventricular dysfunction. *Biomaterials* **35**, 3541–3550, doi:10.1016/j.biomaterials.2013.12.071 (2014).
21. Haider, T. *et al.* The secretome of apoptotic human peripheral blood mononuclear cells attenuates secondary damage following spinal cord injury in rats. *Exp Neurol* **267**, 230–242, doi:10.1016/j.expneurol.2015.03.013 (2015).
22. Altmann, P. *et al.* Secretomes of apoptotic mononuclear cells ameliorate neurological damage in rats with focal ischemia. *F1000Res* **3**, 131, doi:10.12688/f1000research.4219.2 (2014).
23. Kasiri, M. M. *et al.* Dying Blood Mononuclear Cell Secretome Exerts Antimicrobial Activity. *Eur J Clin Invest*, doi:10.1111/eci.12667 (2016).
24. Marston, W. A., Hanft, J., Norwood, P. & Pollak, R. The efficacy and safety of Dermagraft in improving the healing of chronic diabetic foot ulcers: results of a prospective randomized trial. *Diabetes Care* **26**, 1701–1705 (2003).
25. Harding, K., Sumner, M. & Cardinal, M. A prospective, multicentre, randomised controlled study of human fibroblast-derived dermal substitute (Dermagraft) in patients with venous leg ulcers. *Int Wound J* **10**, 132–137, doi:10.1111/iwj.12053 (2013).
26. Loots, M. A. *et al.* Differences in cellular infiltrate and extracellular matrix of chronic diabetic and venous ulcers versus acute wounds. *J Invest Dermatol* **111**, 850–857, doi:10.1046/j.1523-1747.1998.00381.x (1998).
27. Margolis, D. J., Kantor, J. & Berlin, J. A. Healing of diabetic neuropathic foot ulcers receiving standard treatment. A meta-analysis. *Diabetes Care* **22**, 692–695 (1999).

28. Brem, H., Sheehan, P., Rosenberg, H. J., Schneider, J. S. & Boulton, A. J. Evidence-based protocol for diabetic foot ulcers. *Plast Reconstr Surg* **117**, 193S-209S; discussion 210S-211S, doi:10.1097/01.prs.0000225459.93750.29 (2006).
29. Gentzkow, G. D. *et al.* Use of dermagraft, a cultured human dermis, to treat diabetic foot ulcers. *Diabetes Care* **19**, 350–354 (1996).
30. Perotti, C. *et al.* Allogeneic lethally irradiated cord blood mononuclear cells in no-option critical limb ischemia: a "box of rain". *Stem Cells Dev* **22**, 2806–2812, doi:10.1089/scd.2013.0172 (2013).
31. Orenstein, A. *et al.* Treatment of deep sternal wound infections post-open heart surgery by application of activated macrophage suspension. *Wound Repair Regen* **13**, 237–242, doi:10.1111/j.1067-1927.2005.130304.x (2005).
32. Zuloff-Shani, A. *et al.* Macrophage suspensions prepared from a blood unit for treatment of refractory human ulcers. *Transfus Apher Sci* **30**, 163–167, doi:10.1016/j.transci.2003.11.007 (2004).
33. Beer, L., Mildner, M. & Ankersmit, H. J. Cell secretome based drug substances in regenerative medicine: when regulatory affairs meet basic science. *Ann Transl Med* **5**, 170, doi:10.21037/atm.2017.03.50 (2017).

Acknowledgements

We thank the APOSCIENCE AG, the Christian Doppler Laboratory for Diagnosis & Regeneration in Thoracic Diseases (2009-2015) and the FFG-Grant "APOSEC" (#852748; 2015-2018) for their financial support. We are indebted to Michael Gnant, Walter Klepetko, and Michael Wolzt for their support in realizing this study. We thank all scientific colleagues involved in the clinical trial for their valuable input. Credit has to be given to the angel Investors HPH, MB, IP, HJA, KF for supporting this public private partnership including the Medical University of Vienna.

Author Contributions

Dr. Hendrik Jan Ankersmit had full access to all of the data in the study and takes responsibility for the integrity of the data and the accuracy of the data analysis. *Study concept and design*: G.G., A.S., M.S., A.G., M.M., H.H., E.T., M.W. *Acquisition, analysis, and interpretation of data*: C.F., C.E., M.K., C.G., B.G., M.A., C.G., S.S., E.S., D.T. *Drafting of the manuscript*: E.S., D.T., H.A. *Critical revision of the manuscript for important intellectual content*: H.A. *Statistical analysis*: A.G. *Obtained funding*: H.A. *Administrative, technical, or material support*: C.F., C.E., M.W., A.S., M.A., W.K. *Study supervision*: C.F., C.E., M.W.

Additional Information

Supplementary information accompanies this paper at doi:10.1038/s41598-017-06223-x

Competing Interests: Financial interest is claimed by the Medical University of Vienna, the Aposcience AG, which holds two patents related to this work (EP20080450198 and EP20080450199), and Hendrik Jan Ankersmit in the capacity of a shareholder of Aposcience AG. The remaining authors have no conflict of interest to declare.

Publisher's note: Springer Nature remains neutral with regard to jurisdictional claims in published maps and institutional affiliations.

Supplementary

Safety and tolerability of topically administered autologous, apoptotic PBMC secretome (APOSEC™) in dermal wounds: a randomized phase 1 trial (MARSYAS I)

Elisabeth Simader MD[1,2,9,10#], Denise Traxler[1,2#], Mohammad Mahdi Kasiri MD[1,2#], Helmut Hofbauer DPhil[1,2,9,10], Michael Wolzt MD[3], Christoph Glogner[1,2], Angela Storka[12], MD[3,11], Michael Mildner PhD,[4,9], Ghazaleh Gouya MD[3], Alexandra Geusau MD[5], Carola Fuchs RN[3], Claudia Eder RN[3], Alexandra Graf PhD[6], Michaela Schaden MSc[7], Bahar Golabi[4], Marie-Bernadette Aretin DP[11], Susanne Suessner MSc[8], Christian Gabriel MD[13], Walter Klepetko MD[1], Erwin Tschachler MD[4],Hendrik Jan Ankersmit MD*[1,2,9,10]

[#] the authors contributed equally to the study

[1] Division of Thoracic Surgery, Medical University of Vienna, Austria
[2] Christian Doppler Laboratory for Cardiac and Thoracic Diagnosis and Regeneration, Medical University of Vienna, Austria
[3] Department of Clinical Pharmacology, Medical University of Vienna, Austria
[4] Research Division of Biology and Pathobiology of the Skin, Department of Dermatology, Medical University of Vienna, Vienna, Austria.
[5] Division of Immunology, Allergy, and Infectious Diseases, Department of Dermatology, Medical University of Vienna
[6] Section of Medical Statistics, Centre for Medical Statistics, Informatics and Intelligent Systems, Medical University of Vienna, Austria.
[7] Clinical Trials Coordinative Centre, Medical University of Vienna, Austria
[8] Austrian Red Cross Blood Transfusion Service for Upper Austria, Linz, Austria
[9] FFG Project 852748 “APOSEC“, Medical University of Vienna, Austria
[10] Aposcience AG, Company No.: 308089, Vienna, Austria
[11] AKH Vienna pharmacy, Medical University of Vienna, Austria
[12] Danubian Hospital, Social and medical center of eastern Vienna, Austria
[13] Ludwig Boltzmann Institute for experimental and clinical traumatology, Austria

***Corresponding Author:**
Hendrik Jan Ankersmit, MD
Division of Thoracic Surgery
Medical University of Vienna
Waehringer Guertel 18-20
1090 Vienna, Austria
Tel: +43-1-4040069770
E-Mail: hendrik.ankersmit@meduniwien.ac.at

Supplementary

Adverse event screening

Participants were examined using laboratory tests, ECG and physical examination.

The **physical examination** included an examination of the abdomen, head, ears, eyes, nose, throat, neck, neurological and psychiatric status, as well as pulmonary, cardiovascular, skeletal, muscular, urogenitary tract; measurement of height and weight, BMI. The vital signs measurement included the assessment of the systolic and diastolic pressure, as well as the pulse rate.
Regarding the general physical examinations, no abnormalities were found at any of the screened subjects.

The **standard 12-lead ECG** (25mm/s and 0.1mV/mm) was recorded after at least 5 minutes rest at screening visit via Siemens Megacart or GE MAC 1200ST. For 5 subjects ECG abnormalities were detected at the screening, but none was regarded as clinical significant by the investigator team.

Hematology **parameters included the determination of erythrocytes, leukocytes, hemoglobin, hematocrit, thrombocytes, MCV, MCH, MCHC, PTT and aPTT. The levels were obtained at screening and the follow-up for CRF Nr. 01,02,03,04,05,06,07,08,10,11,12,13,14). No abnormalities were detected at any of the subjects.**

Serum chemistry **included the determination of sodium, potassium, total protein, albumin, chloride, BUN, creatinine, glucose, ASAT, ALAT, AP and gamma GT. The levels were obtained at screening and the follow-up for CRF Nr. 01, 02, 03, 04, 05, 06, 07, 08, 10, 11, 12, 13, 14). No abnormalities were detected at any of the subjects.**

Virology included the determination of HBs Ag, HCV Ab and HIV-1/2 Ab levels. No latent or active infection was detected in any of the screened subjects.

Urine analysis included the determination of pH, leukocytes, nitrite, protein, glucose and blood. No abnormalities were detected at any of the screened subjects regarding the pH Analysis, moreover all revealed negative results with respect to the parameters measured at the screening.

Supplementary Tables

Supplementary Table S1. Disposition of subjects according to dose group

CRF Nr.	Dose group	Treatment proximal	Treatment distal	Randomization code	Status	Drop-out	Reason
1	A (12.5×10^6 PBMC/ml)	Placebo	Verum	DR2	Drop-out	Day 1	Primary reason for discontinuation is deviation in IMP production (Sponsor decision) Evaluation of test treatment on day 1: Area proximal: 01: faint, minimal erythema. area distal: 03: erythema with induration or vesicles, hives, no itching, no pain, no burning
2	A (12.5×10^6 PBMC/ml)	Verum	Placebo	DR1	Drop-out	Day 1	Primary reason for discontinuation is deviation in IMP production (Sponsor decision) Evaluation of test treatment on day 1: Area proximal: 0: hives without itching, no erythema. Area distal: 0: no visible reaction
3	A (12.5×10^6 PBMC/ml)	Verum*	Placebo*	DR2*	Completed	n.a.	n.a.
4	A (12.5×10^6 PBMC/ml)	Placebo*	Verum*	DR1*	Completed	n.a.	n.a.
5	A (12.5×10^6 PBMC/ml)	Verum	Placebo	DR1	Completed	n.a.	n.a.
6	A (12.5×10^6 PBMC/ml)	Verum	Placebo	DR1	Completed	n.a.	n.a.
7	A (12.5×10^6 PBMC/ml)	Placebo	Verum	DR2	Drop-out	Day 1	Evaluation of test treatment on day 1: Area proximal: 01 faint, minimal erythema
8	A (12.5×10^6 PBMC/ml)	Verum	Placebo	DR1	Completed	n.a.	n.a.
9	B (25.0×10^6 PBMC/ml)	n.a.	n.a.	n.a.	Not included	Preliminary exclusion	Due to a screening failure, the patient was preliminarily excluded before test treatment
10	B (25.0×10^6 PBMC/ml)	Placebo	Verum	DR2	Completed	n.a.	n.a.
11	B (25.0×10^6 PBMC/ml)	Placebo	Verum	DR2	Completed	n.a.	n.a.
12	B (25.0×10^6 PBMC/ml)	Verum	Placebo	DR1	Completed	n.a.	n.a.

Supplementary Table S1. Disposition of subjects according to dose group (continued)

13	B (25.0×10^6 PBMC/ml)	Verum	Placebo	DR1	Completed	n.a.	n.a.
14	B (25.0×10^6 PBMC/ml)	Verum	Placebo	DR1	Completed	n.a.	n.a.

Supplementary Table S1

Summary of all study subjects and their treatment randomization. Dose group A represents the low-dose group. Dose group B was the high-dose group. Verum was applied on the proximal artificial wound and placebo on the distal wound when coded with DR1. DR2 coded participants had an application of verum to the distal wound and placebo to the proximal wound. The double-blinded study randomization was performed by the AKH pharmacy.

*Subjects CRF Nrs. 3 and 4 were treated vice versa from the assigned randomization code; this alteration occurred throughout the study. The outcome of the randomizer web application revealed code DR1 for treatment at distal and code DR2 for treatment at proximal. The AKH pharmacy determined to administer placebo to the randomized location.

Supplementary Table S2. Index of adverse events

			MedDRA Coding											
CRF#	**Description**	**Applied IMP**	**LLT** **MedDRA Coding**	**LLT**	**SOC**	**SOC**	**Comment/** **Query**	**Outcome**	**Severity**	**Unexpected**	**Serious**	**Drug treatment**	**Action**	**Relation**
1	Faint, minimal erythema area proximal	Placebo Dose group A	Application site erythema	10003041	Skin and subcutaneous tissue disorders	10040785	Comment: graded as local tolerability 1	No follow-up	Not assessed due to grading as local tolerability via score			No	Premature study discontinuation[1]	Not assessed due to grading as local tolerability via score
1	Erythema with induration or vesicles, hives no itching, no pain, no burning area distal	Verum Dose group A	Application site erythema	10003041	Skin and subcutaneous tissue disorders	10040785	Comment: graded as local tolerability 3	No follow-up	Not assessed due to grading as local tolerability via score			No	Premature study discontinuation[1]	Not assessed due to grading as local tolerability via score
2	Hives without itching, no erythema area proximal	Verum Dose group A	Hives	10020197	Skin and subcutaneous tissue disorders	10040785	Comment: graded as local tolerability 0	No follow-up	Not assessed due to grading as local tolerability via score			No	Premature study discontinuation[1]	Not assessed due to grading as local tolerability via score
4	Redness right upper arm at the patch area	Not assignable to verum or placebo Dose group A	Application site redness	10003058	Skin and subcutaneous tissue disorders	10040785	Comment: upper right arm	Resolved	Mild	Yes	No	No	No action	Unlikely
7	Sore throat	Not assignable to verum or placebo Dose group A	Sore throat	10041367	Respiratory, thoracic, and mediastinal disorders	10038738	Comment: Not applicable	Resolved	Mild	Yes	No	No	No action	Unrelated

Supplementary Table S2. Index of adverse events (continued)

7	Erythema in area proximal	Placebo Dose group A	Application site erythema	10003041	Skin and subcutaneous tissue disorders	10040785	Comment: proximal; Graded as local tolerability grade 1	Resolved	Mild	Yes	No	No	Premature study discontinuation, no further action	Probably (documented as both adverse events and local tolerability effect).
8	Distal wound opened and bleeding	Placebo Dose group A	Wound bleeding	10051386	Injury, poisoning, and procedural complications	10022117	Comment: distal	Resolved	Mild	Yes	No	No	01.05.2015: Cleaning and application of dressing 04.05.2015: Photo documentation Assessment: slough dry and application of dressing	Unrelated
8	Two hematomas left upper arm around the puncture site of the local anesthetic	Not assignable to verum or placebo Dose group A	Injection site hematoma	10055371	General disorders and administration site conditions	10018065	Comment: left upper arm	Resolved	Mild	Yes	No	No	No action	Unrelated
11	Sensitivity of skin by Steri Strips in the dressing area proximal	Placebo Dose group B	Adhesive plaster sensitivity	10001290	Skin and subcutaneous tissue disorders	10040785	Comment: proximal	Resolved	Mild	Yes	No	No	No action	Unrelated
14	Muscle tension left arm	Not assignable to verum or placebo Dose group B	Muscle tension	10070541	Musculoskeletal and connective tissue disorders	10028395	Comment: left arm	Resolved	Mild	Yes	No	Transfer to neurologist	No action	Unrelated
14	Itching distal wound	Placebo Dose group B	Wound itching	10062873	Injury, poisoning, and procedural complications	10022117	Comment: distal	Resolved	Mild	Yes	No	No	No action	Probably

14	Itching proximal wound	VerumDose group B	Wound itching	10062873	Injury, poisoning, and procedural complications	10022117	Comment: proximal	Resolved	Mild	Yes	No	No	No action	Probably

Supplementary Table S2

Summary of all adverse events and attribution to verum and placebo. CRF#: ID of the study participants. In the dose group A, the low dose was applied, and in dose group B, the high dose of APOSEC™ was applied. Tolerability was quantified using a 4-point local tolerability assessment scale (0=no visible reaction; 1=faint, minimal erythema; 2=erythema; 3=erythema with induration or vesicles; 4=severe erythema with induration, vesicles, or bullae or pustules and/or erosion/ulceration).

Supplementary Table S3. Demographic characteristics of the study participants

eCRF Nr.	Visit date	ICF signed	ICF date	Screening Nr.	Birth year	Gender	Ethnicity	Alcohol consumption	Alcohol units [units/week]*	Smoking	Smoking quantity [cigarettes/day]
1	13 Feb 2015	Yes	13 Feb 2015	17	1986	Male	Caucasian	Yes	1	Non-smoker	0
2	09 Feb 2015	Yes	09 Feb 2015	16	1984	Male	Caucasian	No	0	Non-smoker	0
3	26 Feb 2015	Yes	26 Feb 2015	21	1988	Male	Caucasian	Yes	1	Non-smoker	0
4	20 Feb 2015	Yes	20 Feb 2015	18	1989	Male	Caucasian	No	0	Non-smoker	0
5	23 Feb 2015	Yes	23 Feb 2015	19	1994	Male	Caucasian	No	0	Non-smoker	0
6	24 Feb 2015	Yes	24 Feb 2015	20	1989	Male	Caucasian	Yes	n.a.	Non-smoker	0
7	02 Mar 2015	Yes	02 Mar 2015	22	1987	Male	Caucasian	Yes	2	Smoker	20
8	06 Mar 2015	Yes	06 Mar 2015	25	1990	Male	Caucasian	Yes	3	Non-smoker	0
10	02 Mar 2015	Yes	02 Mar 2015	23	1985	Male	Caucasian	No	0	Ex-smoker	20
11	25 Mar 2015	Yes	25 Mar 2015	27	1989	Male	Caucasian	Yes	1	Smoker	4
12	27 Mar 2015	Yes	27 Mar 2015	28	1983	Male	Caucasian	No	0	Non-smoker	0
13	09 Apr 2015	Yes	09 Apr 2015	30	1987	Male	Caucasian	No	0	Smoker	7
14	09 Apr 2015	Yes	09 Apr 2015	29	1988	Male	Caucasian	No	0	Smoker	10

Supplementary Table S3

Summary of all volunteers, depicting anonymization ID during the study (eCRF Nr.), date of signing the informed written consent (ICF), screening number, age, gender, ethnicity, alcohol consumption, and smoking characteristics.
*1 unit equals half a liter of beer, 200 mL wine, or 50 mL of spirits.

Supplementary Table S4. Time course of the maximum wound diameter for both dose groups

Day	Group	Statistic	Verum	Placebo	Difference
Day 1	Group A	Mean (SD)	5.14 (0.45)	5.11 (0.28)	0.03 (0.46)
		Median (Q1 to Q3)	4.94 (4.93 to 4.98)	5.07 (4.92 to 5.24)	0.02 (-0.09 to 0.09)
		Min to Max	4.91 to 5.94	4.82 to 5.52	-0.59 to 0.7
	Group B	Mean (SD)	5.21 (0.31)	5.31 (0.37)	-0.09 (0.58)
		Median (Q1 to Q3)	5.09 (5.07 to 5.19)	5.08 (5.08 to 5.49)	-0.11 (-0.4 to 0.11)
		Min to Max	4.97 to 5.75	5.01 to 5.88	-0.81 to 0.74
Day 2	Group A	Mean (SD)	5.24 (0.5)	5.03 (0.19)	0.21 (0.42)
		Median (Q1 to Q3)	5.13 (4.95 to 5.66)	5.03 (5.01 to 5.14)	0.4 (-0.08 to 0.52)
		Min to Max	4.64 to 5.84	4.73 to 5.24	-0.37 to 0.6
	Group B	Mean (SD)	5.08 (0.07)	4.97 (0.37)	0.11 (0.36)
		Median (Q1 to Q3)	5.07 (5.05 to 5.07)	5 (4.86 to 5.24)	0.14 (-0.17 to 0.2)
		Min to Max	5 to 5.2	4.41 to 5.35	-0.28 to 0.64
Day 3	Group A	Mean (SD)	4.9 (0.51)	4.88 (0.15)	0.03 (0.53)
		Median (Q1 to Q3)	5.09 (4.45 to 5.16)	4.85 (4.79 to 4.99)	0.03 (-0.25 to 0.37)
		Min to Max	4.3 to 5.52	4.7 to 5.06	-0.69 to 0.67
	Group B	Mean (SD)	5.06 (0.11)	4.81 (0.31)	0.25 (0.32)
		Median (Q1 to Q3)	5.04 (5.01 to 5.05)	4.83 (4.66 to 4.93)	0.32 (0.14 to 0.39)
		Min to Max	4.97 to 5.25	4.4 to 5.24	-0.23 to 0.64
Day 4	Group A	Mean (SD)	4.94 (0.35)	4.76 (0.18)	0.17 (0.3)
		Median (Q1 to Q3)	4.94 (4.8 to 5.22)	4.78 (4.62 to 4.89)	0.25 (-0.09 to 0.39)
		Min to Max	4.43 to 5.29	4.55 to 4.97	-0.19 to 0.51
	Group B	Mean (SD)	4.86 (0.06)	4.64 (0.27)	0.23 (0.29)
		Median (Q1 to Q3)	4.85 (4.84 to 4.86)	4.58 (4.43 to 4.79)	0.38 (0.02 to 0.43)
		Min to Max	4.81 to 4.96	4.37 to 5.02	-0.18 to 0.48
Day 5	Group A	Mean (SD)	4.66 (0.33)	4.65 (0.21)	0.02 (0.22)
		Median (Q1 to Q3)	4.59 (4.44 to 4.87)	4.6 (4.47 to 4.77)	-0.07 (-0.16 to 0.12)
		Min to Max	4.29 to 5.12	4.45 to 4.94	-0.16 to 0.35
	Group B	Mean (SD)	4.39 (1.06)	4.44 (0.44)	-0.05 (1.42)
		Median (Q1 to Q3)	4.87 (4.76 to 4.89)	4.56 (4.08 to 4.57)	0.37 (0.32 to 0.68)
		Min to Max	2.49 to 4.93	3.95 to 5.05	-2.56 to 0.92
Day 6	Group A	Mean (SD)	4.48 (1.3)	4.61 (0.15)	-0.14 (1.35)
		Median (Q1 to Q3)	4.86 (4.66 to 5.32)	4.57 (4.54 to 4.73)	0.44 (0.12 to 0.52)
		Min to Max	2.21 to 5.33	4.42 to 4.8	-2.52 to 0.76
	Group B	Mean (SD)	4.82 (0.13)	4.41 (0.31)	0.42 (0.31)
		Median (Q1 to Q3)	4.77 (4.72 to 4.9)	4.33 (4.16 to 4.63)	0.56 (0.08 to 0.68)
		Min to Max	4.71 to 5.01	4.09 to 4.82	0.08 to 0.68
Day 7	Group A	Mean (SD)	4.31 (1.19)	4.45 (0.3)	-0.15 (1.04)
		Median (Q1 to Q3)	4.8 (4.36 to 4.98)	4.45 (4.21 to 4.49)	0.22 (-0.13 to 0.53)
		Min to Max	2.24 to 5.15	4.18 to 4.93	-1.94 to 0.59
	Group B	Mean (SD)	4.61 (0.12)	4.33 (0.24)	0.28 (0.29)
		Median (Q1 to Q3)	4.66 (4.48 to 4.71)	4.41 (4.13 to 4.46)	0.3 (0.2 to 0.35)
		Min to Max	4.48 to 4.72	4.05 to 4.62	-0.14 to 0.67

Supplementary Table S4

Descriptive statistics of the maximum diameter. Mean diameter and standard deviation (SD) as well as median, quantiles, minima and maxima in mm for application days 1–7, separated for dose group A (low-dose group) and group B (high-dose group).

Supplementary Table S5. Time course of the minimum wound diameter for both dose groups

Day	Group	Statistic	Verum	Placebo	Difference
Day 1	Group A	Mean (SD)	4.31 (0.3)	4.28 (0.41)	0.03 (0.43)
		Median (Q1 to Q3)	4.26 (4.25 to 4.5)	4.47 (4.13 to 4.51)	-0.01 (-0.01 to 0.12)
		Min to Max	3.88 to 4.66	3.63 to 4.67	-0.59 to 0.63
	Group B	Mean (SD)	4.6 (0.11)	4.67 (0.24)	-0.07 (0.27)
		Median (Q1 to Q3)	4.56 (4.55 to 4.69)	4.69 (4.54 to 4.78)	0 (-0.04 to 0.01)
		Min to Max	4.47 to 4.74	4.36 to 4.99	-0.52 to 0.2
Day 2	Group A	Mean (SD)	4.29 (0.62)	4.28 (0.09)	0.01 (0.57)
		Median (Q1 to Q3)	4.07 (3.82 to 4.66)	4.33 (4.27 to 4.33)	-0.2 (-0.41 to 0.31)
		Min to Max	3.72 to 5.19	4.13 to 4.35	-0.51 to 0.86
	Group B	Mean (SD)	4.38 (0.16)	4.04 (0.4)	0.34 (0.49)
		Median (Q1 to Q3)	4.48 (4.25 to 4.49)	4.01 (3.77 to 4.25)	0.48 (0.27 to 0.48)
		Min to Max	4.18 to 4.52	3.58 to 4.61	-0.43 to 0.9
Day 3	Group A	Mean (SD)	4.04 (0.56)	4.21 (0.22)	-0.18 (0.4)
		Median (Q1 to Q3)	3.86 (3.54 to 4.62)	4.32 (4.13 to 4.37)	-0.32 (-0.46 to 0.23)
		Min to Max	3.53 to 4.64	3.86 to 4.39	-0.6 to 0.27
	Group B	Mean (SD)	4.21 (0.22)	4.08 (0.39)	0.13 (0.45)
		Median (Q1 to Q3)	4.24 (4.2 to 4.31)	3.82 (3.79 to 4.33)	0.02 (-0.09 to 0.52)
		Min to Max	3.84 to 4.44	3.79 to 4.65	-0.45 to 0.65
Day 4	Group A	Mean (SD)	4.03 (0.59)	4.09 (0.29)	-0.06 (0.38)
		Median (Q1 to Q3)	3.88 (3.82 to 4.59)	4.15 (3.83 to 4.19)	0.05 (-0.33 to 0.14)
		Min to Max	3.22 to 4.63	3.78 to 4.49	-0.56 to 0.4
	Group B	Mean (SD)	4.17 (0.3)	3.98 (0.34)	0.19 (0.45)
		Median (Q1 to Q3)	4.2 (4.11 to 4.34)	3.8 (3.8 to 4)	0.4 (-0.1 to 0.48)
		Min to Max	3.7 to 4.48	3.72 to 4.56	-0.45 to 0.62
Day 5	Group A	Mean (SD)	3.85 (0.42)	4.01 (0.25)	-0.16 (0.39)
		Median (Q1 to Q3)	3.6 (3.57 to 4.27)	3.86 (3.86 to 4.1)	-0.27 (-0.4 to -0.14)
		Min to Max	3.46 to 4.35	3.84 to 4.41	-0.5 to 0.49
	Group B	Mean (SD)	3.69 (0.93)	3.69 (0.38)	0 (1.31)
		Median (Q1 to Q3)	3.99 (3.66 to 4.34)	3.6 (3.47 to 3.66)	0.33 (0.06 to 0.89)
		Min to Max	2.1 to 4.36	3.37 to 4.33	-2.23 to 0.97
Day 6	Group A	Mean (SD)	3.44 (1.02)	3.95 (0.16)	-0.52 (1.01)
		Median (Q1 to Q3)	3.4 (3.35 to 4.14)	4.03 (3.91 to 4.04)	-0.35 (-0.51 to 0.05)
		Min to Max	1.82 to 4.47	3.7 to 4.09	-2.21 to 0.43
	Group B	Mean (SD)	3.93 (0.24)	3.69 (0.42)	0.24 (0.53)
		Median (Q1 to Q3)	3.99 (3.81 to 4.07)	3.66 (3.34 to 3.71)	0.15 (-0.13 to 0.73)
		Min to Max	3.58 to 4.18	3.34 to 4.38	-0.39 to 0.84
Day 7	Group A	Mean (SD)	3.41 (1.06)	3.89 (0.42)	-0.47 (0.84)
		Median (Q1 to Q3)	3.62 (3.3 to 3.96)	3.95 (3.65 to 3.96)	-0.07 (-0.33 to 0)
		Min to Max	1.69 to 4.5	3.37 to 4.5	-1.96 to 0
	Group B	Mean (SD)	3.91 (0.34)	3.62 (0.35)	0.29 (0.61)
		Median (Q1 to Q3)	3.94 (3.65 to 4.2)	3.52 (3.48 to 3.61)	0.33 (-0.03 to 0.72)
		Min to Max	3.49 to 4.27	3.29 to 4.22	-0.57 to 0.98

Supplementary Table S5

Descriptive statistics of the minimum diameter. Mean diameter and standard deviation (SD) as well as median, quantiles, minima and maxima in mm for application days 1–7, separated for dose group A (low-dose group) and group B (high-dose group).

.

Supplementary Table S6. Time course of the wound area for both dose groups

Day	Group	Statistic	Verum	Placebo	Difference
Day 1	Group A	Mean (SD)	16.88 (2.15)	16.64 (1.09)	0.25 (1.87)
		Median (Q1 to Q3)	16.32 (16.19 to 17.69)	16.8 (16.16 to 17.6)	0.09 (0.03 to 1.31)
		Min to Max	14.2 to 20.02	15.01 to 17.62	-2.6 to 2.4
	Group B	Mean (SD)	18.5 (1.11)	19.01 (1.78)	-0.51 (2.36)
		Median (Q1 to Q3)	18.55 (17.61 to 18.56)	18 (17.89 to 20.93)	0.32 (-2.38 to 0.56)
		Min to Max	17.52 to 20.28	17.29 to 20.96	-3.44 to 2.39
Day 2	Group A	Mean (SD)	16.51 (3.8)	16.36 (1)	0.15 (3.34)
		Median (Q1 to Q3)	14.32 (13.84 to 18.93)	16.44 (16.27 to 16.72)	-0.49 (-2.6 to 2.66)
		Min to Max	13.45 to 22.03	14.81 to 17.56	-3.27 to 4.47
	Group B	Mean (SD)	16.48 (0.94)	15.05 (2.48)	1.43 (2.71)
		Median (Q1 to Q3)	15.89 (15.79 to 17.48)	14.04 (13.62 to 16.07)	1.85 (1.41 to 3.07)
		Min to Max	15.71 to 17.53	12.64 to 18.88	-3.09 to 3.91
Day 3	Group A	Mean (SD)	14.71 (3.13)	15.54 (0.93)	-0.83 (2.65)
		Median (Q1 to Q3)	13.71 (12.52 to 17.97)	15.53 (14.85 to 16.04)	-1.14 (-3.17 to 1.16)
		Min to Max	11.32 to 18.05	14.49 to 16.81	-3.52 to 2.52
	Group B	Mean (SD)	15.74 (1.32)	14.33 (2.15)	1.41 (2.47)
		Median (Q1 to Q3)	16.19 (15.82 to 16.59)	13.58 (13.53 to 14.56)	2.03 (-0.13 to 3.1)
		Min to Max	13.45 to 16.63	12.13 to 17.84	-2.02 to 4.06
Day 4	Group A	Mean (SD)	15.14 (3.11)	14.41 (1.67)	0.73 (2.54)
		Median (Q1 to Q3)	13.09 (13.06 to 18.22)	13.88 (13.82 to 14.3)	-0.31 (-0.79 to 0.98)
		Min to Max	12.5 to 18.85	12.81 to 17.24	-1.24 to 5.03
	Group B	Mean (SD)	15.1 (0.98)	13.95 (2)	1.15 (2.2)
		Median (Q1 to Q3)	15.4 (15.02 to 15.47)	13.13 (12.78 to 13.61)	1.79 (0.75 to 2.69)
		Min to Max	13.5 to 16.11	12.75 to 17.48	-2.46 to 2.98
Day 5	Group A	Mean (SD)	13.51 (2.55)	13.76 (1.45)	-0.25 (2)
		Median (Q1 to Q3)	12.19 (11.95 to 15.54)	13.23 (13.04 to 13.76)	-0.69 (-1.28 to -0.35)
		Min to Max	10.97 to 16.88	12.54 to 16.23	-2.07 to 3.12
	Group B	Mean (SD)	14.69 (1.5)	12.68 (2.61)	2.01 (2.77)
		Median (Q1 to Q3)	15.04 (14.26 to 15.92)	11.99 (11.51 to 12.63)	2.75 (-0.32 to 3.05)
		Min to Max	12.31 to 15.92	10.2 to 17.06	-1.14 to 5.72
Day 6	Group A	Mean (SD)	13.95 (2.89)	13.21 (1.19)	0.74 (2.09)
		Median (Q1 to Q3)	12.22 (11.85 to 16.67)	13.1 (12.87 to 13.35)	0.13 (-0.65 to 2.48)
		Min to Max	11.5 to 17.5	11.72 to 15.02	-1.6 to 3.32
	Group B	Mean (SD)	14.05 (1.5)	12.33 (2.33)	1.72 (3.02)
		Median (Q1 to Q3)	14.12 (13.29 to 14.18)	11.9 (11.2 to 12)	2.09 (0.29 to 2.22)
		Min to Max	12.29 to 16.36	10.25 to 16.3	-2.12 to 6.11
Day 7	Group A	Mean (SD)	13.12 (2.8)	12.98 (2.5)	0.14 (1.58)
		Median (Q1 to Q3)	12.11 (11.97 to 14.28)	12.96 (11.82 to 13.03)	0.37 (-0.99 to 1.25)
		Min to Max	9.94 to 17.3	10.15 to 16.93	-1.88 to 1.96
	Group B	Mean (SD)	12.94 (1.62)	12.02 (1.66)	0.92 (2.98)
		Median (Q1 to Q3)	12.58 (12.1 to 13.97)	11.55 (11.08 to 12.51)	1.5 (-1.57 to 2.42)
		Min to Max	10.94 to 15.1	10.32 to 14.63	-2.53 to 4.78

Supplementary Table S6

Descriptive statistics of the wound area in mm^2. Mean area and standard deviation (SD) as well as median, quantiles, minima and maxima in mm^2 for application days 1–7, separated for dose group A (low-dose group) and group B (high-dose group).

Supplementary Methods

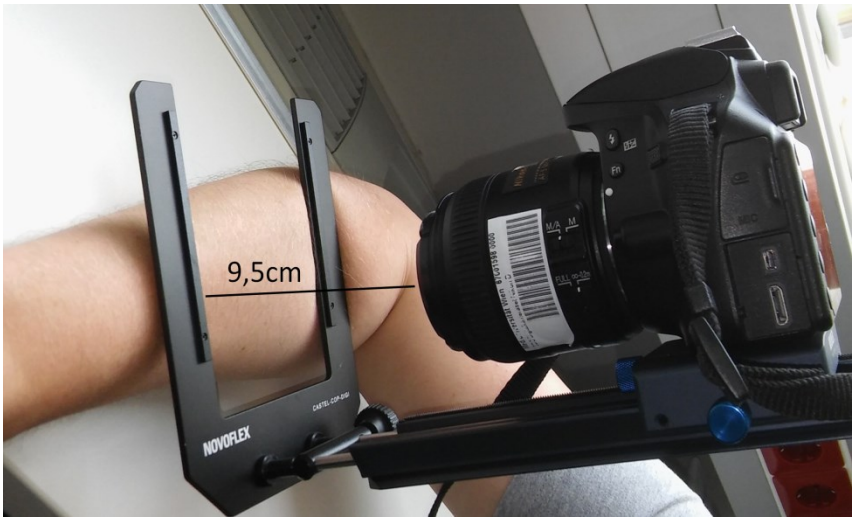

Supplementary Fig. S1

Depiction of the pacer (CASTEL-COP-DIGI, CASTEL-L, Novoflex, Germany) with the camera, in a re-enactment. The distance between the camera lens and the skin amounts to a constant 9,5cm.

Immunohistochemical staining

The specimen taken at day 1 before initiation of therapy depicts a baseline value. A punch biopsy was performed on day 1 (4mm) and day 7 (6mm).The tissue specimens were gathered, by the same surgeon. The depth of the biopsy was defined by the depth of the metal blade (7mm), as the granulation tissue has formed a depth of 7mm was enough to acquire the wound in its entirety on day 7. The tissue specimens were cut in half and one part was prepared for cryosection and the second part for paraffin-embedding. The samples were put into a sterile plastic tube and immediately frozen (for cryosection) or kept in formaldehyde 7.5% for 24 hours. After 24h, sections were prepared for paraffin embedding, by standardized protocols of the Department of Dermatology (Medical University of Vienna). Immunohistochemical staining was performed according to the manufacturer's protocol using the Avidin Biotin Peroxidase complex technique. CD45 (ab10558, Abcam, Cambridge, UK; dilution: 1:100) was stained on frozen sections and keratin 10 (PRB-159P, Covance Research Products Inc., Denver, PA, USA; dilution: 1:1000), factor VIII (A0082, DAKO, Santa Clara, CA, USA; dilution: 1:1000), and podoplanin (clone: D2-40; 322M-15; Cell Marque Corporation, Rocklin, CA, USA; dilution: 1:50) were stained on formalin-fixed, paraffin-embedded sections. In brief, frozen tissue was embedded in OCT prior to sectioning and stored at -80°C. Tissue specimens were cut into sections 6–8 µm thick and fixed using 4% paraformaldehyde. Formalin-fixed, paraffin-embedded tissue specimens were cut into sections 4–6 µm thick and deparaffinized. The following steps were conducted on frozen as well as formalin-fixed, paraffin-embedded sections. Briefly, heat-mediated antigen retrieval was performed using citrate buffer, pH 6.0. Endogenous peroxidase activity was quenched with 0.3% hydrogen peroxide. Sections were incubated with the appropriate primary antibody overnight at 4°C, followed by incubation with either anti-IgG mouse or anti-IgG rabbit secondary antibody (RPN1001V, Chalfont St. Giles, GB; BA-1000, Vector Laboratories, Burlingame, CA, USA) diluted in 10% sheep or goat

normal serum (sc-2488, Santa Cruz Biotechnology Inc., Dallas, TX, USA; X0907, DAKO, Santa Clara, CA, USA) for 30 min at room temperature. Slides were then incubated with ABC reagent (PK 4000, Vector Laboratories, Burlingame, CA, USA) for 30 min at room temperature. The reaction was visualized with AEC substrate (K3469, DAKO, Santa Clara, CA, USA) under the microscope and counterstained with hematoxylin (1.09253.500, Merck, Darmstadt, Germany). As negative controls, the primary antibody was omitted. Additionally, on formalin-fixed, paraffin-embedded sections, hematoxylin–eosin staining was performed according to a standard protocol.

Digital scanning of tissue sections was performed using an automated scanning microscope, TissueFAXs (TissueGnostics, Vienna, Austria). Tissue sections were rated by a blinded observer. Tissue sections from day 7 were divided into transition, wound, and healthy zones. The number of factor VIII–positive or podoplanin-positive vessels per cm^2 (MVD) was counted at a magnification level of 20x. The effect of MVD by APOSEC low dose, APOSEC high dose, or placebo was evaluated at day 7 in wound area (as fold increase to day 1). The number of $CD45^+$ cells per high power field was counted at a magnification level of 20× in wound area (as fold increase to day 1) and the percentage of $CD45^+$ cells was calculated.

Factor VIII APOSEC low dose vs. placebo (median fold increase [range]) (0.67 [0.20; 0.93] vs. 1.24 [0.09; 3.33], p=0.44), Factor VIII APOSEC high dose vs. placebo (median [range]) (1.01 [0.33; 1.48] vs. 0.84 [0.17; 1.49, p=0.63). No podoplanin vessels were found in the tissue specimens. No K10 positive epidermal layer in the wound area was found in any patient at day 7.CD45 APOSEC low dose vs. placebo (median fold increase [range]) (4.03 [1.15; 8.92] vs. 2.09 [0.77; 3.87], p=0.38), CD45 APOSEC high dose vs. placebo (median [range]) (1.58 [0.44; 2.72] vs. 1.48 [0.21; 2.00, p=0.48)

10 CHAPTER THREE: Discussion

Chronic non healing ulcers depict a field of unmet need, as these complex mechanisms are a multitude of processes concerning a successful wound healing.[7] To gain an insight on the effect of irradiated PBMC secretome on wound healing, a lot of mechanisms of wound healing must be taken into consideration.

This thesis aimed to elucidate 1) the role of regulated cell death on wound healing. 2) the role of various cell types of the immune system on wound healing and angiogenesis and 3) if the application of the irradiated PBMC-secretome is safe in human application. To conclude our findings and compare them to the known literature is the goal of this discussion.

Apoptosis is known as orchestrated cell suicide, with the least destructive effect on surrounding cells, due to the blebbing of cell fragments without the rupture of the cell membrane and efflux of possible harmful cell compartments.[298] To fully understand the importance of controlled cell death, one should have a look on the processes of uncontrolled cell migration and activation:

If we take a deeper look on the inflammatory processes in wound healing, starting for example with neutrophils, that invade the wound area first. We will observe, that they produce pro-inflammatory cytokines such as TNF-α and IL-1, which lead to enhanced activation of the immune system.[298,299] If this process is out of control, the release of this cytokines result in a stress response, which is characterized by increased catecholamines and corticosteroids as in severe infections.[298] This stress response is believed to play a role in e.g. acute respiratory distress syndrome/Sepsis, as activated neutrophils emigrate in the blood stream, reach the lungs and damage endothelial cells of the lung tissue and consequently the alveoli either.[298] Apoptosis on the other hand is necessary to regulate and break the circle of more and more activated and harmful neutrophils, which then are often eliminated by phagocytosis of macrophages.[298,299]

In later stages of wound healing the amount of collagen is crucial to gain physiological wound healing, if collagen production is exaggerated, due to an imbalance of fibroblast apoptosis, hypertrophic scars and keloid formation are the results.[298,300]

When we have a look on a second important cell death: necroptosis, only a few studies are found to address this subject in wound healing.

Necroptosis seems to be profusely present in chronic wounds.[301] Surprisingly the literature depicts contradictory effects of necroptosis on wound healing. When it comes to wound healing, one question remains unanswered: programmed cell death friend or foe?

One study observed, that necroptosis inflicted more oxidative stress on wounds via Silencing information regulator 2 related enzyme 3 (SIRT3) and even prolonged wound healing in diabetic mice.[302,303]

As increased RIPK3 was found in excised hypertrophic murine and human scar tissue, Izumov et al believed, that fibroblasts were responsible for the higher RIPK3 levels.[304] After stimulation of wound fibroblasts with Lipopolysaccharide (LPS) and TGF-β higher fluorescence was seen in an RIPK3-antibody fluorescence staining, compared to non-stimulated control fibroblasts.[304] Yet when isolating the cells and analyzing the gene expression level of RIPK3 via rtPCR, no difference between the control fibroblasts and wound fibroblasts could be detected.[304] He speculated, that an epithelial-mesenchymal crosstalk between cells is necessary for fibroblasts to upregulate the expression of RIPK3.[304] He also considered, that RIPK3 may not have a role in hypertrophic scar formation and that RIPK3 may have another function in wound repair.[304]

Injarabian et al found interesting results regarding the role of necroptosis in wound healing. She observed, that the number of monocytes and macrophages decreased, when the wound matured from the inflammatory phase into the proliferatory phase.[305] Especially $Ly6C^{high}$ drive inflammation and angiogenesis, both processes necessary for successful wound healing, but hyperergic and long lasting monocyte and macrophage acitivity may hinder wound closure in later phases.[305] She suspected that the regulation to lower numbers of monocytes/macrophages was done with the induction of apoptosis and necroptosis.[305] To test this hypothesis the authors created a $Ripk3^{-/-}$ mouse, which also lacks FADD, but only in monocytes and macrophages ($Fadd^{fl/fl}Ripk3^{-/-}Cx3cr1^{Cre/wt}$).[305] In this model monocytes and macrophages were not capable to undergo extrinsic apoptosis and necroptosis.[305] Excisional wounds were applied on these mice and controls, leading to higher numbers of monocytes and macrophages in the later phases of wound healing, proving that necroptosis is a major regulator of monocyte numbers.[305] Furthermore the wound closure was significantly delayed without necroptosis and apoptosis in monocytes.[305] The granulation tissue was less on day 7 either, indicating decreased tissue remodeling in the presence of more monocytes and macrophages.[305] Moreover excessive levels of TNF were found in the wound area of the double mutant mice.[305] As the group suspected the TNF pathway responsible for this effect, they used a TNFR2-Inhibitor (Etanercept), which lead to normalization of wound healing.[305]

Leading to the conclusion, that a dysfunctional TNF receptor signaling leads to the decreased wound healing.[305] Pure Ripk3$^{-/-}$ knock-out mice showed a similar wound healing, as the control mice.[305]

This study shows, that different cell death mechanisms are important for regulating the adequate regeneration process. In this thesis we investigated, which cells are prone to necroptosis and apoptosis, after stimulation with γ-irradiation.[297] PBMC as co-culture were least sensitive to the irradiation, displaying the highest number of living cells, compared to the natural killer cells, mostly showing necroptotic cell death.[297] In monocytes we could find the most balanced proportion of apoptosis and necroptosis.[297] These findings hint different pathways activated and the possibility of various individual receptors involved.

Moreover we were able to show, that necroptosis is mediated via the TNFRSF1B receptor after irradiation.[297] Whereas in wound healing an abundant amount of TNF-α activates TNF-receptor 1, which which leads to activation of NF-κB, after recruiting TRADD, TRAF2/5 and among others RIPK1. [306] The TNF pathway is especially interesting regarding its role in wound healing. As a computational analysis done by Luthfiana et al. revealed a possible role in diabetic wound healing of Dolastatin 16 mediated via the TNF/ NF-κB pathway.[306] As upon activation of NF-κB the production of MMP-9 is upregulated, disturbing the reorganization of tissue architecture, whereas Dolastatin 16 could act as inhibitor of MMP-9.

What surprised us, was that in our reporter gene assays the promoter activity of NF-κB was highest after application of irradiated PBMC supernatant.[297] The stimulation with the apotptotic and necroptotic monocyte supernatant could not reach the same impact.[297] This implicates cellular cross-talk between different cell populations, necessary to fully activate the NF-κB pathway.[297] The consequence of this finding for wound healing needs to be addressed in further studies.[297] Could this also play a role in the increased angiogenesis in the sprouting assays, which was highest after treatment with the PBMC supernatant, compared to those of pure monocyte cultures.[297]

Furthermore the type of cell death mattered for the angiogenesis.[297] As we have showed by blocking necroptosis and apoptosis by addition of necrostatin-1 and zVAD.[297] After irradiation, the cells were cultured with the blocking agents for 24 hours and then the supernatant was used for stimulation of endothelial cells and aortic rings.[297] Only the addition of necrostatin-1, which blocks necroptosis induction, significantly decreased the sprouting ability and the tube formation of endothelial cells.[297] Intriguingly the fresh addition of necrostatin-1 into the sprouting assays and endotheial cell cultures, did not show differences on their angiogenic potential.[297] Maybe the positive effects on angiogenesis are not the cells undergoing

programmed cell death, but the factors, that are secreted by them. So, the key to understand the effects of cell death may lie in the secreted factors of necroptotic cell death.

The role of apoptosis in wound healing seemed to be limited to the eradication of damaged cells in the wounded area, to prevent exaggerated inflammation.[298,307] Yet more and more studies find a paracrine effect of dying cells on the surrounding tissue.

As dermal wound areas usually consist of a certain amount of dying cells, researchers are becoming more and more aware of this neglected, yet important cells and their paracrine effect.[308,309] The secreted factors of dying, apototic cells affecting surrounding cells were labeled ‘‘metabolite secretome’’ by Medina et al.[309] A further look on the impact of apoptotic cells took Li et al.[310] He used irradiated mouse embryonic fibroblasts (MEF) to simulate dying cells from wounded dermal tissue and observed their proliferative effect on firefly luciferase labeled neighboring cells.[310] He then elucidated growth-promoting and proliferative effects on MSCs, epidermal keratinocyte progenitor cells and even neural stem cells.[310] He assumed caspase 3 and caspase 7 as possible inducers of this positive effects and tested his hypothesis with single and double caspase deficient mice.[310] He irradiated the caspase deficient MEFs and co-cultured them with wildtype fibroblasts, resulting in less cell proliferation, which was aggravated in the caspase 3 and 7 double deficient co-cultures.[310] As a further step in vivo angiogenesis assays were proceeded in caspase 3 knock-out mice and wildtype mice and astonishingly vascular growth in the knock out mice did not differ from the negative control and therefore displayed poor angiogenic potential.[310] Furthermore wound closure was finished by day 9 in wild type mice, whereas in caspase 3 knock-out mice required nearly 14 days.[310]

It may be possible, that apoptosis and we speculate also necroptosis is necessary in chronic non healing wounds, to improve angiogenesis.[297] In dysfunctional tissue repair a lack of vascularization is a main problem.[295]

A myriad of cytokines and growth factors have a major effect on the accomplishment of wound healing.[7] These cytokines are responsible for wound cleansing and chemoattracting and are secreted not only by inflammatory cells, but also fibroblasts.[7] Fibroblasts also produce growth factors, which gained attention in the scientific field to enhance wound healing.[7] Many single growth factors were used as therapeutic options to ameliorate wound closure.[7]

Moreover chronic non healing wounds lack various different proteins, among them: EGF, TGF-β, FGF, PDGF, VEGF, IL-1 and -6, and TNF-α.[28] This fact in mind leads us to the idea that in

such a deranged and deregulated system, the substitution of only one factor may never be enough.

Compromised angiogenesis is a crucial pathomechanism in diabetic non healing ulcers.[8,311] One key player in neovascularization is the family of vascular endothelial growth factors (VEGFs).[103] Secretomes of mesenchymal stem cells and gingival fibroblasts had higher levels of VEGF and applied on wounds led to accelerated wound healing.[95,103] So one could argue, that it would be enough to substitute VEGF to a nonhealing wound. However, Li et al could show, that application of mesenchymal stem cell secretome on a damaged dermal defect, could boost the target cells' own VEGF production, which may account to the regenerative potential.[312]

Pro-angiogenic signals are not only determined by cytokines, also intracellular pathways are essential regulatory factors.[313,314] The phosphatidylinositol 3-kinase(PI3K)/AKT/ mammalian target of rapamycin (mTOR) pathway can increase VEGF secretion after activation.[313] VEGF itself can again activate intracellular PI3K pathway in endothelial cells regulating cell migration.[313]

When analyzing the protein signature of the secretome of irradiated PBMC, we could find the only significant amount of VEGF in the supernatant of irradiated PBMC.[297] Lower levels of secreted VEGF could be seen in the mono-cultures of monocytes, but in all other PBMC subsets we could not detect relevant amounts of VEGF in the used proteome profiler.[297]

Multiple studies of our working group could measure upregulation of not only pro-angiogenic factors such as VEGF type A, CXCL1 and CXCL8, but also PDGF, FGF, MMP-9 and TIMP in the secretome of irradiated PBMCs. [57,62,63,315] These factors are important for collagen and extracellular matrix remodeling and wound healing.[57,62,63,315] So maybe the secretome could improve collagen reconstruction by keratinocytes and fibroblasts activation in wounds.[57,62,63,315]

Regarding the protein secretion pattern of the different PBMC subsets, one protein was especially interesting, as it was present in the supernatant of all subsets: IL-8.[297] We noticed the highest amounts produced by PBMC and monocytes, and the least in B-cells.[297] This may also contribute to the pro-angiogenic effects we monitored.[297]

As previously mentioned concerning angiogenesis in aortic ring assays, as well as VEGF production, our work made it more and more clear, that monocytes are a very important cell subset.[297] But when compared to the PBMC secretome the angiogenic potential, as well as the secretion of pro-angiogenic potential succeeded the combination of all mono-cultures.[297] Which may indicate a cross-talk between the different types of immune cells and delicate regulation, concerning the wound environment.[297]

It can also be speculated that the activation of the immune system has a major influence on the orchestration of wound healing as already described by Polly Matzinger.[316] The immune system is not only in charge of self-defense against foreign bacteria or viruses.[316] As previously discussed every wound needs an inflammatory phase, with pro-inflammatory and pro-angiogenic cytokines, yet the sole addition of growth factors and other cytokines secreted by immune cells, did not show any beneficiary effect.[8,12,19,28,29] This gives us a hint, that cytokine production in PBMC is a much more complex process and can be affected especially by the presence and secretion pattern of other cell-subsets of PBMC.[8,12,19,28,29] These cell-cell interaction may lead to the necessary reprogramming of cells and therefore different secretion pattern necessary for a functioning wound healing. It may be argued, that these so far not further elucidated interactions may also be responsible for the effect we have seen in our ex-vivo angiogenesis assays.[297] The observed sprouting of new vessels was mostly increased upon stimulation with the secretome of a co-culture of all PBMC-subsets, compared to mono-cultures of its cell subtypes.[297]

As PBMCs are a composition of different cell subsets, it is necessary to have a closer look on the various subpopulations of the immune system and their effect on wound healing.

Laggner et al was able to demonstrate that treatment of dendritic cells with PBMC secretome can suppress a hyperergic immune reaction of dendritic cells in a contact hypersensitivity animal model.[97] This effect is caused by induction of immuno suppressive pathways and downregulation of antigen-presenting function of CD1a and $CD11c^{+}$ cells.[97] Intriguingly the lipid fraction of PBMC secretome was especially effective in restraining the MoDC effect. [97]

Copic et al. could show, that monocytes treated with PBMC secretome had higher upregulation of Interleukin-1 beta, vascular endothelial growth factor A and C–X–C motif chemokine ligand 1,3 and 5 (CXCL-1, -3, -5) as well as SERPINB2 (which inhibits endopeptidase activity) in a single cell analysis.[104] This upregulated expression was confirmed on protein level.[104] As a next step the regenerative potential on endothelial cells was tested in vitro with the plasma gathered from PBMC treated whole blood.[104] The pretreated plasma lead to higher neo-angiogenesis in a tube formation assay. [104] Therefore the upregulation of pro-angiogenic genes, really is of biological importance and has an appropriate stimulatory effect on endothelial cells. [104]

Mast cells are known for their essential role in allergic diseases, however more and more knowledge is gathered concerning their role in angiogenesis, vasodilation, skin barrier homeostasis, influence on the adaptive and innate immune system, fibrosis, diabetes and wound healing.[317-319] Mast cells can be found in nearly every tissue and in proximity to fibroblasts, epithelial cells, vessels of the vascular or lymphatic system and nerves.[320]

Activation of mast cells is induced by Immunoglobulin E (IgE), which leads to degranulation and emission of histamine, tryptase, chymase, also neuroactive serotonin.[320] Furthermore mast cells are also a source of cytokine and chemokine secretion e.g. TNF, VEGF, IL-6, IL-8, TGF-β,PDGF, CCL1-5 and CCL7-9, CCL11, -17 and -22 as well as IL-4.[319] Especially IL-4 is interesting, as IL-4 and IL-13 usually produced by TH2 T-cells in turn are detrimental for the B-cell class switch and IgE production.[319,320] Moreover the secretion of pro-angiogenic factors, especially VEGF is of interest for wound healing and regenerative medicine.

Bot et al hypothesized, that in an ischemic environment increases activation of mast cells and consequently neovascularization.[321] So they induced hind limb ischemia in mice and measured a higher amount of activated mast cells in inguinal lymph nodes.[321] The collateral diameter and number of $CD31^+$ cells in capillaries was higher in mice with activated mast cells, compared to the controls.[321] As hypoxic conditions are also found in dermal wounds, that may be an interesting field for future studies.[74]

In obese patients with a low-grade chronic inflammation higher tryptase levels (commonly found in mast cell granules) were found in the serum, giving a hint to increased degranulation and activation in this patient cohort.[322]

Egozi et al observed wound healing in a mast cell deficient mouse strain WBB6F1/J-KitW/KitW–v and recognized less neutrophil infiltration in the wounded area in the pro-inflammatory phase.[323] While T-cell and macrophage migration remained similar compared to wildtype mice.[323] The cytokine levels of TNF-α and macrophage inflammatory protein-2, a common chemoattractant for neutrophils, resembled those of WT mice.[323] A change in the wound healing in the proliferative phase could not be detected in this study, emphasizing the importance of mast cells in the very first inflammatory phase.[323]

Weller et al used the same mast cell deficient mouse strain, but added mast cells in the first six days after wounding and could reveal, that wound closure and the neutrophil recruitment were normalized.[324] He could also demonstrate that H1-receptor antagonists or the absence of TNF-α abates wound closure, an effect not seen under the influence of a H2-receptor antagonist.[324]

The chymase released by activated mast cells also regulates proliferation of human skin fibroblasts. [325] After addition of chymase, proliferation of fibroblasts was increased (measured with MTT test) and higher expression levels of TGF-β1 were measured after six hours of stimulation.[325]

Of all PBMC subsets addressed in this thesis, the monocytes seemed to have the most important role on angiogenesis, as the sprouting area of newly formed vessels from aortic ring

assays was the widest.[297] Furthermore monocytes were capable of activating NF-κB in a promotor assays.[297] Interestingly in the literature not the monocytes, but the macrophages are mostly studied, regarding wound healing.

Macrophages derive from monocytes and develop into classical ($CD14^{++}16^{-}$, M1 macrophages), intermediate- or non-calssical ($CD14^{++}16^{++}$, M2) macrophages according to their exposure to cytokines and microenvironment.[22] The M1 subtypes are considered pro-inflammatory as [326] they differentiate under lipopolysaccharide (LPS) and TNF-a stimulation and secrete pro-inflammatory cytokines such as IL-12 and IL-23 and produce reactive oxygen species (ROS).[22,326] On the other hand the non-classical M2 macrophages show anti-inflammatory and pro-healing effects on their environment by secretion growth factors such as IGF (insulin-like growth factor) and TGF-β.[22] M2 macrophages develop upon stimulation with anti-inflammatory of IL-4 and IL-10 cytokines.[22] Whereas in normal wound healing the M1 cells are predominant within the first three days and are replaced with M2 until day seven, in diabetic wounds this transition from M1 to M2 never takes place.[326] In diabetic mice the prevailing M1 dominance in the wound area leads to inadequate collagen formation, impaired wound closure and compromised angiogenesis.[22,327] Thus the idea to promote the M2 macrophage polarization in chronic wounds seems to be a promising target. [22] A hyperglycemic environment as seen in diabetic mice and humans assists macrophage M1 polarization, by increased expression of pro-inflammatory cytokines.[328] An interesting study could observe, that these M1 macrophages lead to more TNF-α expression, which impaired keratinocyte migration to the wounded area.[328] Furthermore matrix-metalloproteinase 1 (MMP-1) expression levels were decreased, another factor, that dampens keratinocyte migration.[328]

The hyperglycemic environment not only leads to higher differentiation of monocytes to M1 macrophages, but also initiates their activation by IL-6, TNF-α and IL-1β, one of 13 pro-inflammatory cytokines found especially in settings with high glucose levels.[329] In turn activated M1 macrophages themselves lead to further secretion of these three cytokines, enhancing a vicious cycle.[329]

IL-17 appears to have a major influence in the M1 macrophage polarization, as a IL-17 knock-out in a murine model lead to shifting into M2 subpopoulation.[330] Moreover diabetic mice treated with anti-IL-23- or anti-IL-17 antibodies were found to have faster wound closure.[330] This accelerated wound healing 14 days after wound implication, correlated with the higher amount of M2 macrophages.[330] So maybe IL-17 blockade may be useful in diabetic foot ulcers, especially as already approved drugs are used in psoriasis arthritis. Yet further studies must be proceeded in humans, especially as the systemic immunosuppressive effect of IL-17 inhibitors to bacteria and fungi exposed or even infected diabetic wounds may be counterproductive.

Wound infections and thus LPS exposure drive the M1 shift in diabetic wounds.[331] A study stimulated mesenchymal stem cells with LPS and added the exosomes of the supernatant to a diabetic wound in mice.[332] Surprisingly this resulted in increased M2 polarization and accelerated wound healing.[332] A finding that may suggest, that pro-inflammatory stimulation of cells, leads to a change in their secretion pattern, towards anti-inflammatory regulation. The above-mentioned study revealed, that the miRNA let-7b in exosomes may play a crucial role in the M1-M2 shift via the TLR-4/ NF-κB/ STAT3/ AKT pathways.[332]

These data depict the importance of the immune system for physiological wound healing and strengthen that our findings are a promising area for future research projects.[310] Yet we have to consider the destructive power of a mis leaded immune system on wound healing either.[310,332]

Wu coined the idea that apoptosis of immune cells mark the turning point in wound healing from the inflammatory phase into the proliferative phase.[308] Without the factors secreted by these dying cells the damaged wound area would remain trapped in an ongoing inflammatory phase.[308] We may add the importance of necroptosis to that idea.

Last but not least, we were able to test the irradiated PBMC secretome (APOSEC) for safety on human skin.[333] As it is crucial and necessary for all drugs to undergo strict controls to prove, that they do not inflict any harm on humans, phase I studies are of utmost importance.[333]

First step is to prove a drugs' safe use are done with toxicological assays.[334] Wuschko and Gugerell et al. described this preclinical testing.[334] Acute neuropharmacological adverse events and toxicity was tested intravenously in a murine model, with negative results.[334] In the repeated intravenous toxicity tests over four weeks, no harm or death could be assessed in the tested rodents.[334] As the drug is planned to be used topically on wounds, also the subcutaneous application was necessary to test, to verify safe use with direct contact to the subcutaneous fat.[334] To verify non-toxicity in a non-rodent species, mini pigs were selected for s.c. application.[334] To observe topical effects, the local lymph node assay was chosen.[334] All animals were examined once a day for clinical signs of illness or changes in behaviour.[334] Laboratory parameters, urine analysis and ophthalmological or auditory abnormalities were checked and at the end of the intervention period histopathological examination was performed. [334] No animal died after i.v. or s.c injections, proving non-toxicity of the tested doses (max 500 U/kg).[334] In the local lymph node test, no signs of intolerance were detected.[334] These results are building the foundation for all subsequent safety tests.[334]

Furthermore, stability assays need to prove the safe storage and maintenance of efficacy of future drug compounds.[335] Lyophilization does the trick, to stabilize this biological agent and makes it possible to store them in temperatures other, than -80°C, which would restrict the broad use in a clinical setting.[334,335] To test this steady quality, potency assays for batch controls need to be designed.[61] The potency assays developed for APOSEC are described in the first paper of this thesis and are aiming NFκB, HSP-27 and AP-1.[297] Before verification of the safe and stable quality, no clinical testing would be possible, especially in "biological" therapies.[335] With the use of different immune cells, which can show interindividual differences, comparable quality and function is a major concern.[334] To minimize this effect, several secretomes from different donors are pooled.[61,333] The pooled product was tested with the potency assays and depicted comparable results between batches.[61] This was another milestone before the use in humans was reasonable.

To conduct a Phase I or II clinical study a lot of safety concerns need to be addressed in advance.[333] Viral transfection of blood products is a concern, that needs to be addressed.[336] Gugerell et al. tested upfront different methods to diminish viral viability and titers with lyophilization, treatment of methylene blue (activated with visible light) or the irradiation with 25kGy of ionizing irradiation of lyophilized APOSEC.[336] For this the effects on the human immunodeficiency virus (HIV-1), Hepatitis A virus (HAV), pseudorabies virus (PRV) or porcine parvovirus (PPV) were observed.[336] Methylene blue treatment served as standard of care for viral inactivation, according to the world health organization (WHO).[337] The supernatant of PBMC was spiked with the mentioned viruses and treated with methylene blue (MB) and light, lyophilization or γ-irradiation with 25kGy after lyophilization.[336] After addition of MB the enveloped viruses (HIV, PRV) and the bovine viral diarrhoea (BVD)-virus showed infectivity in APOSEC as a result of successful viral inactivation.[337] But the non-enveloped species such as HAV and PPV displayed infectivity after MB treatment.[337] Lyophilization resulted in significantly reduced virus titers of BVDV and considerably less decrease in HAV and PRV.[337] In all other viruses no difference in number or activity could be detected after lyophilization.[337] In a combined approach of lyophilization and consecutive gamma irradiation, both the enveloped viruses (PRV, HIV and BVDV), as well as the non-enveloped ones (HAV) were inactivated.[337] Only the PPV could not be inactivated by the combined procedure.[337]

To further optimize the already very safe approach for viral infections, the testing of healthy donors for viral infections should be implemented prior to blood donations.[333] To accomplish this goal the working group around Prof. Ankersmit started a cooperation with the Austrian Red Cross Blood Transfusion Service for Upper Austria, Linz.[333] The PBMC were isolated from tested and healthy blood donors fulfilling GMP criteria.[333]

The secretome of PBMC can be manufactured in two manners. Either autologous, which means, that the probands' or patients' own blood is obtained for PBMC isolation, or allogeneic using PBMCs of blood donations.[333] The use of the patients own blood seems may decrease the risk of having allergic reactions, yet we do know little about dysfunctional secretion patterns, that may lead to decreased wound healing.[333]

An allogeneic approach may hold the probability to elicit immunological reactions.[99] Thus, we processed the PBMCs the same way as blood donations for immune compromised patients are treated, with ionizing irradiation.[99] Due to the irradiation possible graft versus host diseases are very unlikely and the proliferation of T-cells inhibited.[99] On the other hand, to this date it is not fully elucidated, if the malfunctioning of autologous immune cells is one reason for inadequate wound healing, therefore allogeneic PBMC secretome, may be necessary for improving the body's regenerative capacity.[99,297]

Furthermore, possible alternatives have been considered for γ-irradiation.[99] Laggner et al tested the effect on the secretome after electron-irradiation of PBMC, which showed similar protein expression patterns, as well as comparable angiogenic capacity on tube formation assays.[99] As γ-irradiation is available throughout the country as a standard procedure in blood donations, the phase I study was designed to prove its safety.[99] But it is a matter of special importance to have the possibility to use other non-radioactive, biologically equivalent manufacturing methods.[99]

We tested the safety of autologous APOSEC on intact human skin in healthy probands in a double-blinded, randomized clinical phase I study.[333] The primary aim of the study was the tolerability and safety on human skin and furthermore on a wounded area.[333]

According to the standard of care two doses of APOSEC were tested to identify dose dependent adverse events or effects on the wound area.[333] The healthy probands were randomized to the two dose groups or placebo and were observed in a double-blinded manner.[333]

The probands had regular clinical check-ups, before and after treatment consisting of physical examination, laboratory parameters were checked with an emphasis on blood count, kidney and liver parameters, as well as inflammatory parameters (C reactive protein).[333] Due to the autologous approach, participants donated 450ml blood at the Red Cross Blood Transfusion Service Center in Linz, where the processing was completed according to GMP guidelines.[333] The autologous, irradiated PBMC secretome or Placebo were applied on intact skin first, to monitor allergic reactions or irritation of the skin.[333] If no signs of allergic reactions could be observed, we proceeded to test APOSEC on an artificial wound.[333] After a punch biopsy was done to generate a wound with the same dimension for every group, the treatment was

applied.[333] No severe adverse events were seen, only mild reactions could be detected.[333] No clinically significant changes in the laboratory results were found in the healthy probands and also in the follow-up visits no delayed reactions could be documented.[333] Participants were asked for symptoms at every study visit.[333] The applicability was tested either and showed satisfactory results.[333]

This study was of great importance for the development of future study medications, as the safe use is the corner stone for clinical use in patients.[333] Furthermore if the autologous PBMC secretome would have not been tolerated, no proceeding to the allogeneic product would have been possible.[333]

Outlook

All these preliminary data pave the way for the clinical phase II study of allogeneic APOSEC in the treatment for chronic wound healing deficiency.[333] We hope that irradiated PBMC secretome will lead to enhanced wound healing and help people to regain a higher quality of life and reduce severe consequences of wound healing, such as loss of function or even amputation.[25,333,338,339]

Moreover, PBMC are a waste product of blood donations usually discarded and therefore easily to obtain, in contrast to stem cells.[333] As PBMCs are obtained from healthy blood donors, the risk of deregulated or deranged immune reaction is minimized.[333] The irradiation of PBMC is normally conducted to diminish immunological reactions in blood donations for immune deficient patients (e.g., after transplantation), thus the irradiation of PBMC is an already tested and safe procedure for cell products.[99,333,336] Another safety step is the controlled production, according to good manufacturing principles (GMP) standards.[333]

If the regenerative capacity of wound healing observed in the above-mentioned studies can be shown in human chronic wounds, the origin of a possible new treatment option for patients with unmet need would be created.[57,89,289,297] Planned is the topical application on chronic, diabetic foot ulcers with standardized digital measurement software and the comparison of the effect in a placebo and treatment group.[340] The test period will be several weeks to have the opportunity to depict epithelialization.[340] Positive results may open the doors to the realm of new treatment options for patients with chronic disease.[340]

The clinical phase II study (ClinicalTrials.gov Identifier: NCT04277598) "*A Study to Evaluate Safety and Efficacy of APO-2 at Three Different Doses in Patients with Diabetic Foot Ulcer*"[340] is the first trial to test allogeneic PBMC secretome of healthy donors on wound healing.[340] The

allogeneic approach is more practical, than the isolation and processing of patient's own blood samples.[340] Thus, it could be used as an off the shelf product in clinical practice.[340] The longer a skin barrier is open, the more infections may occur and therefore quick closure is also a matter of systemic health.[7,26,27,31,341] Wound infections and sepsis are often a reason for hospitalization and additional costs for the health system and in some cases a life-threatening condition for the patient.[7,26,27,31,341] Another important factor is the development of antibiotic resistance, which is increasing in the western world.[342-344] All these aspects lead to the conclusion, that the most important reason for wound closure is the fast restoration of our largest protector against infections: the skin.[7,26,27,31,341]

11 CHAPTER FOUR: Methods

11.1 Ethical and legal aspects

These two studied were conducted according to the current principles of the Ethics Committee of the Medical University of Vienna as well as the Declaration of Helsinki and Good Clinical Practice. The experiments and trials were approved by the Ethics Committee of the Medical University of Vienna (EK Nr. 1285/2013 and EK-Nr 1539/2017) and the animal research Animal Research Committee (Medical University of Vienna) (Protocol No. 190097/2015/9). Furthermore the clinical study was notified at the EU clinical trial register (EudraCT-Number: 2013-000756-17; NCT02284360; AGES INS-480102-0013-007).

11.2 PBMC preparation and secretome production

The isolation of PBMC was conducted from heparinized whole-blood samples or from leukocyte chambers after blood donation from healthy donors at the Department of Transfusion Medicine or the Red Cross Blood Transfusion Service of Upper Austria. The samples were diluted with Hanks` balanced salt solution and max. 35ml layered over 15ml of Ficoll-Paque PLUS (GE Healthcare Bio-Sciences AB, Sweden). By density gradient centrifugation (800g, 15min without brake) the PBMC were separated at the Buffy Coat between the plasma and the Ficoll, segregated from erythrocytes and granulocytes at the bottom of the vessel. PBMC were washed with phosphate-buffered saline (PBS-/-, Gibco by Life Technologies, Carlsbad, CA, USA) and γ-irradiated with 60 Gy for apoptosis and necroptosis induction and cultured at a concentration of 25 Mio cells per ml in Cell Gro medium (Cellgenix, Freiburg, Germany) at 37°C for 24h. For dose dependent effects samples were irradiated with 0.9, 1.9, 3.75, 7.5, 15, 30, and 60 Gy. The inhibtors of apoptosis and necroptosis zVAD (20 µM) and Necrostatin-1 (100 µM) both from Sellekchem, Munich, Germany) or neutralizing antibodies against TNF receptor superfamily 1A and 1B (both (R&D Systems, Minneapolis, MN, USA) at a concentration of 1 µg/ml, were added immediately after irradiation and left in the wells for the whole culture period. After the culture period the samples were centrifuged (400 × g, 9 min) the pellet was used for protein analysis e.g. westerblotting and Lämmli buffer (Bio-Rad, Hercules, CA, USA) phosphatase and proteinase inhibitors (Thermo Fisher, Waltham, MA, USA) were added or lyzed in Trizol (Invitrogen, Carlsbad, CA) for RNA isolation and frozen at -80°C. The supernatant was used for stimulation and protein analysis and preserved at -20°C.

For further separation of the different cell subsets of the PBMC positive isolation with magnetic microbeads (Miltenyi, Bergisch Gladbach, Germany) was used. For purification to a purity of

93 to 99% microbeads against the epiptopes of CD14 (monocytes), CD19 (B cells), CD4 (CD4 T cells), CD8 (CD8 T cells) and CD56 (natural killer cells) were used. The incubation and separation was conducted according to the manufacturer' s instruction. After isolation the cells were treated as mentioned above, irradiated and all cultured in the same Cell Gro medium for 24h.

For production of PBMC secretome according to current GMP principles the laboratory of the Austrian Red Cross Blood Transfusion Service for Upper Austria, Linz was gained as a partner for the clinical phase 1 study.

11.3 Westernblot

The samples obtained from the PBMC separation were further analyzed by protein blottings. For this purpose 30µg of protein of the cell lysate in Lämmli buffer (Bio-Rad, Hercules, CA, USA) with the above-mentioned proteinase and phosphatase inhibitors were pipetted on ExcelGels (GE Healthcare). After protein separation according to their specific kDa transfer onto nitrocellulose membranes (Bio-Rad) was done according to manufacturer' s protocol and blocked. After incubation with one of the following antibodies for necroptosis detection phospho-RIPK 1 at a concentration of 1:100 (Cell Signalling Technology, Cambridge, UK), phospho-RIPK3 at a concentration of 1:200 (Abcam, Cambridge, UK) and phospho-MLKL at a concentration of 1:500 (Cell Signalling Technology, Cambridge, UK) according to the manufacturer' s protocol overnight under motion at an environment with 4°C. For apoptosis a cleaved-caspase 3 antibody was used at a concentration of 0.5 µg/ml (R&D Systems, Minneapolis, MN, USA). Furthermore glyceraldehyde 3-phosphate dehydrogenase antibody at a concentration of 1:2000 (Cell Signalling Technology, Cambridge, UK) and TNF antibody at a concentration of 1 µg/ml (R&D Systems, Minneapolis, MN, USA). For the blockade of the TNF-antibody it was incubated for 4 hours ata concentration of 1µg vs 10 µg of recombinant TNF ((R&D Systems, Minneapolis, MN, USA). After several washing steps the membrane was incubated with a second step antibody at a concentration of 1:10,000 Bio-Rad, Hercules, CA, USA) and afterwards with Supersignal West Dura (Thermo Fisher, Waltham, MA, USA). The detection of the bands was achieved with the ChemiDoc System (Bio-Rad, Hercules, CA, USA).

11.4 Scanning electron microscopy

Irradiated or untreated PBMC after 24h of culture were washed with PBS and fixated with a Karnovsky' s fixative (Morphisto, Frankfurt am Main, Germany) consisting of glutaraldehyde (2,5%), and paraformaldehyde (2%) in phosphate Buffer iwth a pH of 7,4. Afterwards the cells were dried with hexamethyldisilazane (Sigma-Aldrich, Taufkirchen, Germany) and fixed via gold sputter (ACE200, Leica Microsystems, Wetzlar, Germany). The evaluation and

photography was done with a scanning electron microscop (JSM 6310, Jeol Ltd®, Japan) at an acceleration voltage of 15kV.

11.5 Flow cytometry

The Annexin-V/PI staining for necroptosis and apoptosis imaging was accomplished with the Annexin-V-FLUOS Staining Kit according to the manufacturer' s protocol (Roche, Basel, Switzerland) and visualized via the Amnis Image Stream X Mk II (Luminex Corp., Seattle, WA) at the Core Facility of the Medical University of Vienna.

11.6 Protein assays

The supernatant obtained after cell culture were frozen at -20°C until further processing. The protein concentrations of TNF-α and lymphotoxin-A (both R&D Systems, Minneapolis, MN, USA) in the supernatant were determined with enzyme-linked immunosorbent assay (ELISA) following the distributor's instructions. In short, the capture antibody was coatet on a 96-well plate and incubated overnight. After washing and reduction of unspecific bindings with blocking buffer the samples were added. Thereafter another washing step was conducted and the detection antibody was pipetted into the wells. For identification horse radish peroxidase was applied and after further washing steps the colouring reaction was started with 3,3′,5,5′-Tetramethylbenzidine (TMB) and stopped with 2% sulphuric acid and measured with a photometric analyzer at a wavelength of 450nm (PerkinElmer, Boston, Massachusetts, USA).

For the protein detection of the secretome of the different PBMC subsets, apoptotic and necroptotic (with or without inhibitors) after irradiation or untreated the samples were analyzed with the Proteome Profiler XL Cytokine Array (R&D Systems, Minneapolis, MN, USA) strictly applying to the manufacturer' s instructions. The detection of pro- and anti-apoptotic proteins was measured with the Human Apoptosis Array (R&D Systems, Minneapolis, MN, USA) also according to the manual, but in advance the cells itself were lyzed in the specific buffers. The measurement and analysis was done with the ChemiDoc System (Bio-Rad, Hercules, CA, USA).

11.7 Potency assays

The reporter gene assays as well as the potency assays were developed and realized by the Synlab Pharma Institute AG (Bern, Switzerland), to determine the capability of the cell secretome with regard to activation of HSP-27, NF-κB and the activator protein-1 (AP-1). Therefore, human neuroblastoma SH-SY5Y cells were transfected with firefly luciferase, that is activated by a promoter of AP-1in a mixture of Glutamax-Medium and Ham's F12/MEM (Gibco, Thermo Fisher, Waltham, MA, USA) with 15% fetal bovine serum (FBS) and puromycin (1 µg/ml) and L-glutamine (2 mM) (Sigma-Aldrich, St. Louis, MO, USA). 20.000 cells were

exposed to the pooled secretome of four donors of monocytes, PBMCs or medium control and the fluorescence signal after the addition of SteadyGlo (Promega, Fitchburg, WI, USA) was analyzed. For the detection of the luminisience the signal was quantified with the EnVision reader (Perkin-Elmer or Centro LB960, Berthold). A different procedure was used for the activation of HSP-27 and NF-κB pathways. For that reason, the cells were incubated with the secretome for 30 minutes and permeabilized. The permeabilized cells were exposed to antibodies detecting phosphorylated HSP-27 and NF-κB and for luminescence reaction peroxidase-conjugated antibodies similar to an ELISA. This luminescence reaction was envisioned with the same reader mentioned above. The quantification was done with the PLA software (Stegmann Systems GmbH, Rodgau, Germany).

11.8 Aortic ring assays

For testing of the pro-angiogenic effect of the PBMC supernatant ex-vivo aortic ring assays were conducted. The aorta of male C57BL/6 mice was obtained after cervical dislocation and sliced into 1mm thick rings. The protocol was slightly adapted from a previously published [283] experiment. The rings were embedded between two layers of fibrin, composed of 43.3 µg/ml aprotinin, 0.6 U/ml thrombin (both from Sigma-Aldrich, St. Louis, MO, USA) and fibrinogen at a concentration of 2 mg/ml (Merck Millipore, Burlington, MA, USA). After hardening the layers and aortic rings were equilibrated in M199 medium supplemented with 4 mM L-glutamine, 10% FBS and antibiotics and anti-mycotic substances (100 µg/ml streptomycin, 100 U penicillin and 250 ng/ml amphotericin B (all from Gibco, Thermo Fisher, Waltham, MA, USA except the FBS (PAA Laboratories, Pasching, Austria)) for 45 minutes and spare medium was removed. M199 medium was diluted with the supernatant of apoptotic and necroptotic PBMC or their freshly addded respective inhibitors (20 µM zVAD and 100 µM necrostatin-1) as controls as well as with the secretome of the different irradiated PBMC subsets as previously described and cultivated for 3 days. To evaluate the living sproutings after these 3 days of cultivation calcein dye (Thermo Fisher, Waltham, MA, USA) was added according to the manufacturer's description and photographed with the Olympus IX83 scanning microscope (Olympus, Tokyo, Japan). The quantification was conducted using the ImageJ software version 1.48v (Wayne Rasband, National Institutes of Health, Bethesda, MD, USA).

11.9 Tube formation assays

For the in vitro evaluation of angiogenesis, a tube formation assay was performed with primary human umbilical vein endothelial cells (HUVECs). For starvation purposes the cells were incubated overnight (for 12h) at basal EBM-2 medium without growth factors (Lonza, Basel, Switzerland) and 2% FBS followed by 3h basal EBM-2 without FBS. The tissue culture plates provided by the tube formation kit from ibidi were layered with a matrigel matrix with decreased

growth factors (Ibidi USA Inc., Fitchburg, WI, USA) following the manuals instructions. 1×10^4 cells of the HUVECs were placed in each well and stimulated with the secretome of apoptotic and necroptotic PBMCs at a final concentration of 4×10^6 cells/ml (same dilution as in the aortic ring assays), medium and freshly added inhibitors served as control. After 3 hours of stimulation period the results were photographed with the Olympus IX83 scanning microscope (Olympus, Tokyo, Japan) and length and inteconnections of the tubes was calculated with the Angiogenesis Analyzer ImageJ plugin (Wayne Rasband, National Institutes of Health, Bethesda, MD, USA).

11.10 Immunohistochemistry

After saoking in formaldehyde for 6 to 24h, according to the organ tissue, the samples were embedded in paraffin by the Department of Dermatology. The staining process was conducted apllying to the Avidin Biotin Peroxidase complex protocol.[345] The antibodies used for detection are the following: podoplanin 1:50 (clone: D2-40; 322M-15; Cell Marque Corporation, Rocklin, CA, USA), keratin 10 1:1000 (PRB-159P, Covance Research Products Inc., Denver, PA, USA) and factor VIII 1:1000 (A0082, DAKO, Santa Clara, CA, USA). The tissue samples were cut into 4–6 µm thick sections and pretreated to remove the paraffin. The specimens were treated with citrate buffer (pH 0,6) and hydrogen peroxide (0,3%) and afterwards incubated with the pimary antibodies overnight at 4°C. Washing steps were applied and the secondary antibody added on the sections and incubated for 30 minutes, depending on the primary antibody either rabbit or mouse (RPN1001V, Chalfont St. Giles, GB; BA-1000, Vector Laboratories, Burlingame, CA, USA). To avoid unspecific binding the antibodies were diluted in sheep or goat serum (10%, sc-2488, Santa Cruz Biotechnology Inc., Dallas, TX, USA; X0907, DAKO, Santa Clara, CA, USA). After another washing step the previously mentioned ABC reagent (PK 4000, Vector Laboratories, Burlingame, CA, USA) was kept on the samples for another 30 minutes. The colour reaction was implemented with AEC substrate (K3469, DAKO, Santa Clara, CA, USA) and the tissue specimen stained with haematoxylin-eosin (1.09253.500, Merck, Darmstadt, Germany).

Frozen sections were kept in OCT at -80°C and stained with CD45 1:100 (ab10558, Abcam, Cambridge, UK). The stained slices were photographed by an automated microscope TissueFAXs (TissueGnostics, Vienna, Austria) situated at the Core Facility (medical University of Vienna).

11.11 RNA purification

The cell pellets of the irradiation or untreated PBMC and the PBMC subsets after 24h of cultivation were lyzed in 500µl Trizol (Invitrogen, Carlsbad, CA) and preserved at -80°C. For purification of the RNA 200µl chloroform was added to an adequate amount of lyzed sample

and kept on ice for 5 minutes followed by centrifugation to separate the organic phase. The aqueous phase containing the RNA was mixed with the same amount of propanol and centrifuged followed by washing steps with 75% and 100% ethanol. The RNA containing pellet was dried and resuspended in RNA-free H_2O and the quality measured by the Agilent 2100 Bioanalyzer (Agilent Technologies, Santa Clara, CA, USA), whereas the quantity was analyzed via NanoDrop-1000 spectrophotometer (Peglab, Erlangen, Germany).

11.12 Microarray

The samples were analyzed with the Affymetrix Human Transcriptome Array 2.0 (Affymetrix, Thermo Fisher Scientific Inc. Waltham, MA, USA) after RNA purification at the Genomics Core Facility of the Medical University of Vienna applying to the MIAME[346] principles. The data from the microarray testing were analyzed using the Gene GeneSpring Version 15.0 software (Agilent) after log2 transformation and quintile normalization. According to previously published techniques the data was filtered to minimize the multiple hypotheses and to work mostly with genes, with an expression level above the 60% percentile.[62] To find statistically significant differences in mRNA expression a moderated paired t-test was calculated with a Benjamini-Hochberg post-hoc test (FDR <5%) for genes with a fold-change ≤ −2 and ≥2. Clustering of mRNA expression was analyzed with Euclidean distance metric as well as average-linkage clustering. According to current guidelines the results were published with the GEO Accession number GSE127982 at the ncbi website (the password can be found in the publication) https://www.ncbi.nlm.nih.gov/geo/query/acc.cgi?acc=GSE127982.

11.13 Pathway analysis

For evaluation of the differences in the expression of biologically relevant genes three methods were used: 1) for pathway analysis the Kyoto Encyclopedia of Genes and Genomes (KEGG), 2) for biological enrichment of processes Gene ontology-enrichment was calculated and 3) categorization of the different genes according to biological function via WEB-based Gene Set Analysis Toolkit (WebGestalt)[347].[348,349] Post-hoc corrections were applied as described above in the section microarray. Additionally activated canonical pathways were searched with the help of Ingenuity Pathway Analysis (Qiagen, Hilden, Germany) for mRNA depicting a fold change of >3 comparing freshly lyzed cells vs irradiated PBMC.

11.14 Statistical methods

Data obtained during these studies were analyzed via GraphPad Prism 5 (GraphPad Software Inc., California, USA), R version 3.2.1 or SPSS (SPSS Inc., Chicago, USA). The values were stated as mean ± standard deviation (SD), minima and maxima if not stated otherwise. Depending on the data distribution (Gaussian distribution) one-way analysis of variance or

Kruskal-wallis test was used with its respective post-hoc analysis (Bonferroni or Dunn's), as well as two-tailed student's t test. The Gibbs outlier test was utilized to truncate discordant values. P-values below 0.05 were considered statistically significant.

References

1 Chambers, E. S. & Vukmanovic-Stejic, M. Skin barrier immunity and ageing. *Immunology* **160**, 116-125, doi:10.1111/imm.13152 (2020).

2 Arda, O., Göksügür, N. & Tüzün, Y. Basic histological structure and functions of facial skin. *Clin Dermatol* **32**, 3-13, doi:10.1016/j.clindermatol.2013.05.021 (2014).

3 Romani, N. *et al.* Cultured human Langerhans cells resemble lymphoid dendritic cells in phenotype and function. *J Invest Dermatol* **93**, 600-609, doi:10.1111/1523-1747.ep12319727 (1989).

4 Mikesh, L. M. *et al.* Proteomic anatomy of human skin. *J Proteomics* **84**, 190-200, doi:10.1016/j.jprot.2013.03.019 (2013).

5 Dąbrowska, A. K. *et al.* The relationship between skin function, barrier properties, and body-dependent factors. *Skin Res Technol* **24**, 165-174, doi:10.1111/srt.12424 (2018).

6 Wong, R., Geyer, S., Weninger, W., Guimberteau, J. C. & Wong, J. K. The dynamic anatomy and patterning of skin. *Exp Dermatol* **25**, 92-98, doi:10.1111/exd.12832 (2016).

7 Han, G. & Ceilley, R. Chronic Wound Healing: A Review of Current Management and Treatments. *Adv Ther* **34**, 599-610, doi:10.1007/s12325-017-0478-y (2017).

8 Stadelmann, W. K., Digenis, A. G. & Tobin, G. R. Physiology and healing dynamics of chronic cutaneous wounds. *Am J Surg* **176**, 26S-38S, doi:10.1016/s0002-9610(98)00183-4 (1998).

9 Zhang, S., Young Phelps, S., Brent Hill, M. & Ruiz, R. Tensile Strength of Surgical Skin Adhesives: A Novel Wound Closure Test. *Wounds* **31**, 166-172 (2019).

10 HOWES, E. L., SOOY, J. W. & HARVEY, S. C. THE HEALING OF WOUNDS AS DETERMINED BY THEIR TENSILE STRENGTH. *Journal of the American Medical Association* **92**, 42-45, doi:10.1001/jama.1929.02700270046011 (1929).

11 Raziyeva, K. *et al.* Immunology of Acute and Chronic Wound Healing. *Biomolecules* **11**, doi:10.3390/biom11050700 (2021).

12 Steed, D. L. The role of growth factors in wound healing. *Surg Clin North Am* **77**, 575-586, doi:10.1016/s0039-6109(05)70569-7 (1997).

13 Wynn, T. A. & Barron, L. Macrophages: master regulators of inflammation and fibrosis. *Semin Liver Dis* **30**, 245-257, doi:10.1055/s-0030-1255354 (2010).

14 Fine, N., Tasevski, N., McCulloch, C. A., Tenenbaum, H. C. & Glogauer, M. The Neutrophil: Constant Defender and First Responder. *Front Immunol* **11**, 571085, doi:10.3389/fimmu.2020.571085 (2020).

15 Fadini, G. P. *et al.* NETosis Delays Diabetic Wound Healing in Mice and Humans. *Diabetes* **65**, 1061-1071, doi:10.2337/db15-0863 (2016).

16 Fu, J., Huang, J., Lin, M., Xie, T. & You, T. Quercetin Promotes Diabetic Wound Healing via Switching Macrophages From M1 to M2 Polarization. *J Surg Res* **246**, 213-223, doi:10.1016/j.jss.2019.09.011 (2020).

17 Shapouri-Moghaddam, A. *et al.* Macrophage plasticity, polarization, and function in health and disease. *J Cell Physiol* **233**, 6425-6440, doi:10.1002/jcp.26429 (2018).

18 Ellis, S., Lin, E. J. & Tartar, D. Immunology of Wound Healing. *Curr Dermatol Rep* **7**, 350-358, doi:10.1007/s13671-018-0234-9 (2018).

19 Haukipuro, K., Melkko, J., Risteli, L., Kairaluoma, M. & Risteli, J. Synthesis of type I collagen in healing wounds in humans. *Ann Surg* **213**, 75-80, doi:10.1097/00000658-199101000-00013 (1991).

20 Bjarnsholt, T. *et al.* Why chronic wounds will not heal: a novel hypothesis. *Wound Repair Regen* **16**, 2-10, doi:10.1111/j.1524-475X.2007.00283.x (2008).

21 Apelqvist, J. Diagnostics and treatment of the diabetic foot. *Endocrine* **41**, 384-397, doi:10.1007/s12020-012-9619-x (2012).
22 Louiselle, A. E., Niemiec, S. M., Zgheib, C. & Liechty, K. W. Macrophage polarization and diabetic wound healing. *Transl Res* **236**, 109-116, doi:10.1016/j.trsl.2021.05.006 (2021).
23 DiPietro, L. A. Angiogenesis and wound repair: when enough is enough. *J Leukoc Biol* **100**, 979-984, doi:10.1189/jlb.4MR0316-102R (2016).
24 Frykberg, R. G. & Banks, J. Challenges in the Treatment of Chronic Wounds. *Adv Wound Care (New Rochelle)* **4**, 560-582, doi:10.1089/wound.2015.0635 (2015).
25 Brownrigg, J. R., Apelqvist, J., Bakker, K., Schaper, N. C. & Hinchliffe, R. J. Evidence-based management of PAD & the diabetic foot. *Eur J Vasc Endovasc Surg* **45**, 673-681, doi:10.1016/j.ejvs.2013.02.014 (2013).
26 Richmond, N. A., Maderal, A. D. & Vivas, A. C. Evidence-based management of common chronic lower extremity ulcers. *Dermatol Ther* **26**, 187-196, doi:10.1111/dth.12051 (2013).
27 Sen, C. K. *et al.* Human skin wounds: a major and snowballing threat to public health and the economy. *Wound Repair Regen* **17**, 763-771, doi:10.1111/j.1524-475X.2009.00543.x (2009).
28 Bennett, N. T. & Schultz, G. S. Growth factors and wound healing: biochemical properties of growth factors and their receptors. *Am J Surg* **165**, 728-737, doi:10.1016/s0002-9610(05)80797-4 (1993).
29 Rothe, M. J. & Falanga, V. Growth factors and wound healing. *Clin Dermatol* **9**, 553-559, doi:10.1016/0738-081x(91)90084-x (1991).
30 Ptaszek, L. M., Mansour, M., Ruskin, J. N. & Chien, K. R. Towards regenerative therapy for cardiac disease. *Lancet* **379**, 933-942, doi:10.1016/S0140-6736(12)60075-0

S0140-6736(12)60075-0 [pii] (2012).
31 Gurtner, G. C., Werner, S., Barrandon, Y. & Longaker, M. T. Wound repair and regeneration. *Nature* **453**, 314-321, doi:10.1038/nature07039 (2008).
32 Asahara, T. *et al.* Bone marrow origin of endothelial progenitor cells responsible for postnatal vasculogenesis in physiological and pathological neovascularization. *Circ Res* **85**, 221-228, doi:10.1161/01.res.85.3.221 (1999).
33 Edelberg, J. M., Tang, L., Hattori, K., Lyden, D. & Rafii, S. Young adult bone marrow-derived endothelial precursor cells restore aging-impaired cardiac angiogenic function. *Circ Res* **90**, E89-93, doi:10.1161/01.res.0000020861.20064.7e (2002).
34 Hess, D. C. *et al.* Bone marrow as a source of endothelial cells and NeuN-expressing cells After stroke. *Stroke* **33**, 1362-1368, doi:10.1161/01.str.0000014925.09415.c3 (2002).
35 Crosby, J. R. *et al.* Endothelial cells of hematopoietic origin make a significant contribution to adult blood vessel formation. *Circ Res* **87**, 728-730, doi:10.1161/01.res.87.9.728 (2000).
36 Gage, F. H. Cell therapy. *Nature* **392**, 18-24 (1998).
37 Lam, N. N. *et al.* Mortality and Morbidity in Kidney Transplant Recipients With a Failing Graft: A Matched Cohort Study. *Can J Kidney Health Dis* **7**, 2054358120908677, doi:10.1177/2054358120908677 (2020).
38 Agrawal, N. & Pavlakis, M. Caring for the patient with a failing allograft: challenges and opportunities. *Curr Opin Organ Transplant* **24**, 416-423, doi:10.1097/mot.0000000000000655 (2019).
39 Lee, D. E., Ayoub, N. & Agrawal, D. K. Mesenchymal stem cells and cutaneous wound healing: novel methods to increase cell delivery and therapeutic efficacy. *Stem Cell Res Ther* **7**, 37, doi:10.1186/s13287-016-0303-6 (2016).

40 Ojeh, N., Pastar, I., Tomic-Canic, M. & Stojadinovic, O. Stem Cells in Skin Regeneration, Wound Healing, and Their Clinical Applications. *Int J Mol Sci* **16**, 25476-25501, doi:10.3390/ijms161025476 (2015).
41 Ding, D. C., Shyu, W. C. & Lin, S. Z. Mesenchymal stem cells. *Cell Transplant* **20**, 5-14, doi:10.3727/096368910x (2011).
42 Toma, C., Pittenger, M. F., Cahill, K. S., Byrne, B. J. & Kessler, P. D. Human mesenchymal stem cells differentiate to a cardiomyocyte phenotype in the adult murine heart. *Circulation* **105**, 93-98, doi:10.1161/hc0102.101442 (2002).
43 Dargie, H. Heart failure post-myocardial infarction: a review of the issues. *Heart* **91 Suppl 2**, ii3-6; discussion ii31, ii43-38, doi:10.1136/hrt.2005.062018 (2005).
44 Chiu, R. C., Zibaitis, A. & Kao, R. L. Cellular cardiomyoplasty: myocardial regeneration with satellite cell implantation. *Ann Thorac Surg* **60**, 12-18 (1995).
45 Bergmann, O. *et al.* Evidence for cardiomyocyte renewal in humans. *Science* **324**, 98-102, doi:10.1126/science.1164680 (2009).
46 Pouzet, B. *et al.* Intramyocardial transplantation of autologous myoblasts: can tissue processing be optimized? *Circulation* **102**, III210-215, doi:10.1161/01.cir.102.suppl_3.iii-210 (2000).
47 Smits, P. C. *et al.* Catheter-based intramyocardial injection of autologous skeletal myoblasts as a primary treatment of ischemic heart failure: clinical experience with six-month follow-up. *J Am Coll Cardiol* **42**, 2063-2069, doi:10.1016/j.jacc.2003.06.017 (2003).
48 Menasche, P. Stem cell therapy for heart failure: are arrhythmias a real safety concern? *Circulation* **119**, 2735-2740, doi:10.1161/circulationaha.108.812693 (2009).
49 Smith, A. N. *et al.* Mesenchymal stem cells induce dermal fibroblast responses to injury. *Exp Cell Res* **316**, 48-54, doi:10.1016/j.yexcr.2009.08.001 (2010).
50 Falanga, V. *et al.* Autologous bone marrow-derived cultured mesenchymal stem cells delivered in a fibrin spray accelerate healing in murine and human cutaneous wounds. *Tissue Eng* **13**, 1299-1312, doi:10.1089/ten.2006.0278 (2007).
51 Wu, Y., Chen, L., Scott, P. G. & Tredget, E. E. Mesenchymal stem cells enhance wound healing through differentiation and angiogenesis. *Stem Cells* **25**, 2648-2659, doi:10.1634/stemcells.2007-0226 (2007).
52 Velazquez, O. C. Angiogenesis and vasculogenesis: inducing the growth of new blood vessels and wound healing by stimulation of bone marrow-derived progenitor cell mobilization and homing. *J Vasc Surg* **45 Suppl A**, A39-47, doi:10.1016/j.jvs.2007.02.068 (2007).
53 Asahara, T. *et al.* VEGF contributes to postnatal neovascularization by mobilizing bone marrow-derived endothelial progenitor cells. *EMBO J* **18**, 3964-3972, doi:10.1093/emboj/18.14.3964 (1999).
54 Tepper, O. M. *et al.* Adult vasculogenesis occurs through in situ recruitment, proliferation, and tubulization of circulating bone marrow-derived cells. *Blood* **105**, 1068-1077, doi:10.1182/blood-2004-03-1051 (2005).
55 Isner, J. M. & Asahara, T. Angiogenesis and vasculogenesis as therapeutic strategies for postnatal neovascularization. *J Clin Invest* **103**, 1231-1236, doi:10.1172/jci6889 (1999).
56 Holzinger, C. *et al.* Treatment of non-healing skin ulcers with autologous activated mononuclear cells. *Eur J Vasc Surg* **8**, 351-356 (1994).
57 Mildner, M. *et al.* Secretome of peripheral blood mononuclear cells enhances wound healing. *PLoS One* **8**, e60103, doi:10.1371/journal.pone.0060103 (2013).
58 Danon, D. *et al.* Treatment of human ulcers by application of macrophages prepared from a blood unit. *Exp Gerontol* **32**, 633-641, doi:10.1016/s0531-5565(97)00094-6 (1997).

59 Frenkel, O. *et al.* Activated macrophages for treating skin ulceration: gene expression in human monocytes after hypo-osmotic shock. *Clin Exp Immunol* **128**, 59-66, doi:10.1046/j.1365-2249.2002.01630.x (2002).
60 Gnecchi, M., Zhang, Z., Ni, A. & Dzau, V. J. Paracrine mechanisms in adult stem cell signaling and therapy. *Circ Res* **103**, 1204-1219, doi:10.1161/circresaha.108.176826 (2008).
61 Wagner, T. *et al.* Different pro-angiogenic potential of γ-irradiated PBMC-derived secretome and its subfractions. *Sci Rep* **8**, 18016, doi:10.1038/s41598-018-36928-6 (2018).
62 Beer, L. *et al.* High dose ionizing radiation regulates micro RNA and gene expression changes in human peripheral blood mononuclear cells. *BMC Genomics* **15**, 814, doi:10.1186/1471-2164-15-814 (2014).
63 Beer, L. *et al.* Analysis of the Secretome of Apoptotic Peripheral Blood Mononuclear Cells: Impact of Released Proteins and Exosomes for Tissue Regeneration. *Sci Rep* **5**, 16662, doi:10.1038/srep16662 (2015).
64 Javazon, E. H. *et al.* Enhanced epithelial gap closure and increased angiogenesis in wounds of diabetic mice treated with adult murine bone marrow stromal progenitor cells. *Wound Repair Regen* **15**, 350-359, doi:10.1111/j.1524-475X.2007.00237.x (2007).
65 Leiker, M., Suzuki, G., Iyer, V. S., Canty, J. M., Jr. & Lee, T. Assessment of a nuclear affinity labeling method for tracking implanted mesenchymal stem cells. *Cell Transplant* **17**, 911-922, doi:10.3727/096368908786576444 (2008).
66 Gyongyosi, M. *et al.* Delayed recovery of myocardial blood flow after intracoronary stem cell administration. *Stem Cell Rev Rep* **7**, 616-623, doi:10.1007/s12015-010-9213-7 (2011).
67 Desgres, M. *et al.* Therapeutic potential of extracellular vesicles derived from cardiac progenitor cells in rodent models of chemotherapy-induced cardiomyopathy. *Front Cardiovasc Med* **10**, 1206279, doi:10.3389/fcvm.2023.1206279 (2023).
68 Uemura, R., Xu, M., Ahmad, N. & Ashraf, M. Bone marrow stem cells prevent left ventricular remodeling of ischemic heart through paracrine signaling. *Circ Res* **98**, 1414-1421, doi:10.1161/01.res.0000225952.61196.39 (2006).
69 Kinnaird, T. *et al.* Local delivery of marrow-derived stromal cells augments collateral perfusion through paracrine mechanisms. *Circulation* **109**, 1543-1549, doi:10.1161/01.cir.0000124062.31102.57 (2004).
70 Asai, J. *et al.* Successful treatment of diabetic gangrene with topical application of a mixture of peripheral blood mononuclear cells and basic fibroblast growth factor. *J Dermatol* **33**, 349-352, doi:10.1111/j.1346-8138.2006.00081.x (2006).
71 Silvestre, J. S. & Menasché, P. The Evolution of the Stem Cell Theory for Heart Failure. *EBioMedicine* **2**, 1871-1879, doi:10.1016/j.ebiom.2015.11.010 (2015).
72 Walter, M. N., Wright, K. T., Fuller, H. R., MacNeil, S. & Johnson, W. E. Mesenchymal stem cell-conditioned medium accelerates skin wound healing: an in vitro study of fibroblast and keratinocyte scratch assays. *Exp Cell Res* **316**, 1271-1281, doi:10.1016/j.yexcr.2010.02.026 (2010).
73 Gatti, S. *et al.* Microvesicles derived from human adult mesenchymal stem cells protect against ischaemia-reperfusion-induced acute and chronic kidney injury. *Nephrol Dial Transplant* **26**, 1474-1483, doi:10.1093/ndt/gfr015 (2011).
74 Zhang, X. F. *et al.* Hypoxic ucMSC-secreted exosomal miR-125b promotes endothelial cell survival and migration during wound healing by targeting TP53INP1. *Mol Ther Nucleic Acids* **26**, 347-359, doi:10.1016/j.omtn.2021.07.014 (2021).

75 Zhu, M. *et al.* Mesenchymal stromal cells pretreated with pro-inflammatory cytokines promote skin wound healing through VEGFC-mediated angiogenesis. *Stem Cells Transl Med* **9**, 1218-1232, doi:10.1002/sctm.19-0241 (2020).
76 Su, D. *et al.* Exosomal PD-L1 functions as an immunosuppressant to promote wound healing. *J Extracell Vesicles* **9**, 1709262, doi:10.1080/20013078.2019.1709262 (2019).
77 Thum, T., Bauersachs, J., Poole-Wilson, P. A., Volk, H. D. & Anker, S. D. The dying stem cell hypothesis: immune modulation as a novel mechanism for progenitor cell therapy in cardiac muscle. *J Am Coll Cardiol* **46**, 1799-1802, doi:10.1016/j.jacc.2005.07.053 (2005).
78 Frantz, S., Vincent, K. A., Feron, O. & Kelly, R. A. Innate immunity and angiogenesis. *Circ Res* **96**, 15-26, doi:10.1161/01.RES.0000153188.68898.ac (2005).
79 Gallucci, S., Lolkema, M. & Matzinger, P. Natural adjuvants: endogenous activators of dendritic cells. *Nat Med* **5**, 1249-1255, doi:10.1038/15200 (1999).
80 Voll, R. E. *et al.* Immunosuppressive effects of apoptotic cells. *Nature* **390**, 350-351, doi:10.1038/37022 (1997).
81 Fadok, V. A. *et al.* Macrophages that have ingested apoptotic cells in vitro inhibit proinflammatory cytokine production through autocrine/paracrine mechanisms involving TGF-beta, PGE2, and PAF. *J Clin Invest* **101**, 890-898, doi:10.1172/jci1112 (1998).
82 Jonuleit, H., Schmitt, E., Schuler, G., Knop, J. & Enk, A. H. Induction of interleukin 10-producing, nonproliferating CD4(+) T cells with regulatory properties by repetitive stimulation with allogeneic immature human dendritic cells. *J Exp Med* **192**, 1213-1222, doi:10.1084/jem.192.9.1213 (2000).
83 Read, S. & Powrie, F. CD4(+) regulatory T cells. *Curr Opin Immunol* **13**, 644-649, doi:10.1016/s0952-7915(01)00273-4 (2001).
84 Frangogiannis, N. G., Smith, C. W. & Entman, M. L. The inflammatory response in myocardial infarction. *Cardiovasc Res* **53**, 31-47, doi:10.1016/s0008-6363(01)00434-5 (2002).
85 Winkler, J. *et al.* Quantitative Hybrid Cardiac [(18)F]FDG-PET-MRI Images for Assessment of Cardiac Repair by Preconditioned Cardiosphere-Derived Cells. *Mol Ther Methods Clin Dev* **18**, 354-366, doi:10.1016/j.omtm.2020.06.008 (2020).
86 Edvinsson, L. I., Edvinsson, M. L. & Angus Deveber, G. Vasogen's immune modulation therapy (IMT) improves postischemic foot skin blood flow and transcutaneous pO(2) recovery rates in patients with advanced peripheral arterial occlusive disease. *Int Angiol* **22**, 141-147 (2003).
87 Babaei, S., Stewart, D. J., Picard, P. & Monge, J. C. Effects of VasoCare therapy on the initiation and progression of atherosclerosis. *Atherosclerosis* **162**, 45-53, doi:10.1016/s0021-9150(01)00680-3 (2002).
88 Torre-Amione, G., Sestier, F., Radovancevic, B. & Young, J. Effects of a novel immune modulation therapy in patients with advanced chronic heart failure: results of a randomized, controlled, phase II trial. *J Am Coll Cardiol* **44**, 1181-1186, doi:10.1016/j.jacc.2004.06.047 (2004).
89 Hacker, S. *et al.* Paracrine Factors from Irradiated Peripheral Blood Mononuclear Cells Improve Skin Regeneration and Angiogenesis in a Porcine Burn Model. *Sci Rep* **6**, 25168, doi:10.1038/srep25168 (2016).
90 Hoetzenecker, K. *et al.* Secretome of apoptotic peripheral blood cells (APOSEC) attenuates microvascular obstruction in a porcine closed chest reperfused acute myocardial infarction model: role of platelet aggregation and vasodilation. *Basic Res Cardiol* **107**, 292, doi:10.1007/s00395-012-0292-2 (2012).

91 Ankersmit, H. J. *et al.* Irradiated cultured apoptotic peripheral blood mononuclear cells regenerate infarcted myocardium. *Eur J Clin Invest* **39**, 445-456, doi:10.1111/j.1365-2362.2009.02111.x (2009).
92 Baraniak, P. R. & McDevitt, T. C. Stem cell paracrine actions and tissue regeneration. *Regen Med* **5**, 121-143, doi:10.2217/rme.09.74 (2010).
93 An, Y. H. *et al.* High-Efficient Production of Adipose-Derived Stem Cell (ADSC) Secretome Through Maturation Process and Its Non-scarring Wound Healing Applications. *Front Bioeng Biotechnol* **9**, 681501, doi:10.3389/fbioe.2021.681501 (2021).
94 Md Fadilah, N. I. *et al.* Cell secretomes for wound healing and tissue regeneration: Next generation acellular based tissue engineered products. *J Tissue Eng* **13**, 20417314221114273, doi:10.1177/20417314221114273 (2022).
95 Ahangar, P., Mills, S. J., Smith, L. E., Gronthos, S. & Cowin, A. J. Human gingival fibroblast secretome accelerates wound healing through anti-inflammatory and pro-angiogenic mechanisms. *NPJ Regen Med* **5**, 24, doi:10.1038/s41536-020-00109-9 (2020).
96 Sjöqvist, S. *et al.* Exosomes derived from clinical-grade oral mucosal epithelial cell sheets promote wound healing. *J Extracell Vesicles* **8**, 1565264, doi:10.1080/20013078.2019.1565264 (2019).
97 Laggner, M. *et al.* Therapeutic potential of lipids obtained from γ-irradiated PBMCs in dendritic cell-mediated skin inflammation. *EBioMedicine* **55**, 102774, doi:10.1016/j.ebiom.2020.102774 (2020).
98 Laggner, M. *et al.* The secretome of irradiated peripheral blood mononuclear cells attenuates activation of mast cells and basophils. *EBioMedicine* **81**, 104093, doi:10.1016/j.ebiom.2022.104093 (2022).
99 Laggner, M. *et al.* Comparing the efficacy of γ- and electron-irradiation of PBMCs to promote secretion of paracrine, regenerative factors. *Mol Ther Methods Clin Dev* **21**, 14-27, doi:10.1016/j.omtm.2021.02.016 (2021).
100 Klas, K. *et al.* The Effect of Paracrine Factors Released by Irradiated Peripheral Blood Mononuclear Cells on Neutrophil Extracellular Trap Formation. *Antioxidants (Basel)* **11**, doi:10.3390/antiox11081559 (2022).
101 Brinkmann, V. *et al.* Neutrophil extracellular traps kill bacteria. *Science* **303**, 1532-1535, doi:10.1126/science.1092385 (2004).
102 Sollberger, G., Tilley, D. O. & Zychlinsky, A. Neutrophil Extracellular Traps: The Biology of Chromatin Externalization. *Dev Cell* **44**, 542-553, doi:10.1016/j.devcel.2018.01.019 (2018).
103 Ahangar, P., Mills, S. J. & Cowin, A. J. Mesenchymal Stem Cell Secretome as an Emerging Cell-Free Alternative for Improving Wound Repair. *Int J Mol Sci* **21**, doi:10.3390/ijms21197038 (2020).
104 Copic, D. *et al.* Paracrine Factors of Stressed Peripheral Blood Mononuclear Cells Activate Proangiogenic and Anti-Proteolytic Processes in Whole Blood Cells and Protect the Endothelial Barrier. *Pharmaceutics* **14**, doi:10.3390/pharmaceutics14081600 (2022).
105 Mallone, R. *et al.* Isolation and preservation of peripheral blood mononuclear cells for analysis of islet antigen-reactive T cell responses: position statement of the T-Cell Workshop Committee of the Immunology of Diabetes Society. *Clin Exp Immunol* **163**, 33-49, doi:10.1111/j.1365-2249.2010.04272.x (2011).
106 Fang, P. *et al.* Immune cell subset differentiation and tissue inflammation. *J Hematol Oncol* **11**, 97, doi:10.1186/s13045-018-0637-x (2018).

107 Shan, Y. *et al.* Increased frequency of peripheral blood follicular helper T cells and elevated serum IL-21 levels in patients with knee osteoarthritis. *Mol Med Rep* **15**, 1095-1102, doi:10.3892/mmr.2017.6132 (2017).
108 Morita, R. *et al.* Human blood CXCR5(+)CD4(+) T cells are counterparts of T follicular cells and contain specific subsets that differentially support antibody secretion. *Immunity* **34**, 108-121, doi:10.1016/j.immuni.2010.12.012 (2011).
109 Duhen, T., Geiger, R., Jarrossay, D., Lanzavecchia, A. & Sallusto, F. Production of interleukin 22 but not interleukin 17 by a subset of human skin-homing memory T cells. *Nat Immunol* **10**, 857-863, doi:10.1038/ni.1767 (2009).
110 Sallusto, F., Zielinski, C. E. & Lanzavecchia, A. Human Th17 subsets. *Eur J Immunol* **42**, 2215-2220, doi:10.1002/eji.201242741 (2012).
111 Dardalhon, V. *et al.* IL-4 inhibits TGF-beta-induced Foxp3+ T cells and, together with TGF-beta, generates IL-9+ IL-10+ Foxp3(-) effector T cells. *Nat Immunol* **9**, 1347-1355, doi:10.1038/ni.1677 (2008).
112 Liu, X., Kwon, H., Li, Z. & Fu, Y. X. Is CD47 an innate immune checkpoint for tumor evasion? *J Hematol Oncol* **10**, 12, doi:10.1186/s13045-016-0381-z (2017).
113 Cochain, C. *et al.* CD8+ T Cells Regulate Monopoiesis and Circulating Ly6C-high Monocyte Levels in Atherosclerosis in Mice. *Circ Res* **117**, 244-253, doi:10.1161/circresaha.117.304611 (2015).
114 Allman, D. & Pillai, S. Peripheral B cell subsets. *Curr Opin Immunol* **20**, 149-157, doi:10.1016/j.coi.2008.03.014 (2008).
115 Möller, B. *et al.* Class-switched B cells display response to therapeutic B-cell depletion in rheumatoid arthritis. *Arthritis Res Ther* **11**, R62, doi:10.1186/ar2686 (2009).
116 Genestier, L. *et al.* TLR agonists selectively promote terminal plasma cell differentiation of B cell subsets specialized in thymus-independent responses. *J Immunol* **178**, 7779-7786, doi:10.4049/jimmunol.178.12.7779 (2007).
117 Merad, M., Sathe, P., Helft, J., Miller, J. & Mortha, A. The dendritic cell lineage: ontogeny and function of dendritic cells and their subsets in the steady state and the inflamed setting. *Annu Rev Immunol* **31**, 563-604, doi:10.1146/annurev-immunol-020711-074950 (2013).
118 Nussenzweig, M. C., Steinman, R. M., Gutchinov, B. & Cohn, Z. A. Dendritic cells are accessory cells for the development of anti-trinitrophenyl cytotoxic T lymphocytes. *J Exp Med* **152**, 1070-1084, doi:10.1084/jem.152.4.1070 (1980).
119 Wakim, L. M., Waithman, J., van Rooijen, N., Heath, W. R. & Carbone, F. R. Dendritic cell-induced memory T cell activation in nonlymphoid tissues. *Science* **319**, 198-202, doi:10.1126/science.1151869 (2008).
120 Gardner, A. & Ruffell, B. moDCs, Less Problems. *Immunity* **48**, 6-8, doi:10.1016/j.immuni.2017.12.017 (2018).
121 Reizis, B., Bunin, A., Ghosh, H. S., Lewis, K. L. & Sisirak, V. Plasmacytoid dendritic cells: recent progress and open questions. *Annu Rev Immunol* **29**, 163-183, doi:10.1146/annurev-immunol-031210-101345 (2011).
122 Macal, M. *et al.* Self-Renewal and Toll-like Receptor Signaling Sustain Exhausted Plasmacytoid Dendritic Cells during Chronic Viral Infection. *Immunity* **48**, 730-744 e735, doi:10.1016/j.immuni.2018.03.020 (2018).
123 Cros, J. *et al.* Human CD14dim monocytes patrol and sense nucleic acids and viruses via TLR7 and TLR8 receptors. *Immunity* **33**, 375-386, doi:10.1016/j.immuni.2010.08.012 (2010).
124 Yang, J. *et al.* Chronic Kidney Disease Induces Inflammatory CD40+ Monocyte Differentiation via Homocysteine Elevation and DNA Hypomethylation. *Circ Res* **119**, 1226-1241, doi:10.1161/circresaha.116.308750 (2016).

125 Mukherjee, R. *et al.* Non-Classical monocytes display inflammatory features: Validation in Sepsis and Systemic Lupus Erythematous. *Sci Rep* **5**, 13886, doi:10.1038/srep13886 (2015).
126 Lievens, D. *et al.* Abrogated transforming growth factor beta receptor II (TGFβRII) signalling in dendritic cells promotes immune reactivity of T cells resulting in enhanced atherosclerosis. *Eur Heart J* **34**, 3717-3727, doi:10.1093/eurheartj/ehs106 (2013).
127 Cognasse, F. *et al.* Assessment of the soluble proteins HMGB1, CD40L and CD62P during various platelet preparation processes and the storage of platelet concentrates: The BEST collaborative study. *Transfusion* **63**, 217-228, doi:10.1111/trf.17200 (2023).
128 Linkermann, A. & Green, D. R. Necroptosis. *N Engl J Med* **370**, 455-465, doi:10.1056/NEJMra1310050 (2014).
129 Pischinger, A. [The system of basic regulation]. *Zahnarztl Mitt* **67**, 1255-1256 (1977).
130 Pischinger, A. *Das System der Grundregulation.*, 106-119 (Haug, 1975).
131 Vanden Berghe, T., Linkermann, A., Jouan-Lanhouet, S., Walczak, H. & Vandenabeele, P. Regulated necrosis: the expanding network of non-apoptotic cell death pathways. *Nat Rev Mol Cell Biol* **15**, 135-147, doi:10.1038/nrm3737 (2014).
132 Lockshin, R. A. Programmed cell death 50 (and beyond). *Cell Death Differ* **23**, 10-17, doi:10.1038/cdd.2015.126 (2016).
133 Lockshin, R. A. & Williams, C. M. PROGRAMMED CELL DEATH--I. CYTOLOGY OF DEGENERATION IN THE INTERSEGMENTAL MUSCLES OF THE PERNYI SILKMOTH. *J Insect Physiol* **11**, 123-133, doi:10.1016/0022-1910(65)90099-5 (1965).
134 Lockshin, R. A. & William, C. M. PROGRAMMED CELL DEATH. 3. NEURAL CONTROL OF THE BREAKDOWN OF THE INTERSEGMENTAL MUSCLES OF SILKMOTHS. *J Insect Physiol* **11**, 601-610, doi:10.1016/0022-1910(65)90142-3 (1965).
135 Galluzzi, L. *et al.* Molecular mechanisms of cell death: recommendations of the Nomenclature Committee on Cell Death 2018. *Cell Death Differ* **25**, 486-541, doi:10.1038/s41418-017-0012-4 (2018).
136 Pasparakis, M. & Vandenabeele, P. Necroptosis and its role in inflammation. *Nature* **517**, 311-320, doi:10.1038/nature14191 (2015).
137 Brill, A., Torchinsky, A., Carp, H. & Toder, V. The role of apoptosis in normal and abnormal embryonic development. *J Assist Reprod Genet* **16**, 512-519, doi:10.1023/a:1020541019347 (1999).
138 Fuchs, Y. & Steller, H. Programmed cell death in animal development and disease. *Cell* **147**, 742-758, doi:10.1016/j.cell.2011.10.033 (2011).
139 Ryoo, H. D. & Baehrecke, E. H. Distinct death mechanisms in Drosophila development. *Curr Opin Cell Biol* **22**, 889-895, doi:10.1016/j.ceb.2010.08.022 (2010).
140 Lindsten, T. & Thompson, C. B. Cell death in the absence of Bax and Bak. *Cell Death Differ* **13**, 1272-1276, doi:10.1038/sj.cdd.4401953 (2006).
141 Thompson, C. B. Apoptosis in the pathogenesis and treatment of disease. *Science* **267**, 1456-1462, doi:10.1126/science.7878464 (1995).
142 Krysko, D. V. *et al.* Immunogenic cell death and DAMPs in cancer therapy. *Nat Rev Cancer* **12**, 860-875, doi:10.1038/nrc3380 (2012).
143 McDonald, B. *et al.* Intravascular danger signals guide neutrophils to sites of sterile inflammation. *Science* **330**, 362-366, doi:10.1126/science.1195491 (2010).
144 Galluzzi, L., Kepp, O. & Kroemer, G. Mitochondria: master regulators of danger signalling. *Nat Rev Mol Cell Biol* **13**, 780-788, doi:10.1038/nrm3479 (2012).
145 Green, D. R., Oguin, T. H. & Martinez, J. The clearance of dying cells: table for two. *Cell Death Differ* **23**, 915-926, doi:10.1038/cdd.2015.172 (2016).

146 Vanden Berghe, T. *et al.* Necroptosis, necrosis and secondary necrosis converge on similar cellular disintegration features. *Cell Death Differ* **17**, 922-930, doi:10.1038/cdd.2009.184 (2010).
147 Rogers, C. *et al.* Cleavage of DFNA5 by caspase-3 during apoptosis mediates progression to secondary necrotic/pyroptotic cell death. *Nat Commun* **8**, 14128, doi:10.1038/ncomms14128 (2017).
148 Czabotar, P. E., Lessene, G., Strasser, A. & Adams, J. M. Control of apoptosis by the BCL-2 protein family: implications for physiology and therapy. *Nat Rev Mol Cell Biol* **15**, 49-63, doi:10.1038/nrm3722 (2014).
149 Moldoveanu, T., Follis, A. V., Kriwacki, R. W. & Green, D. R. Many players in BCL-2 family affairs. *Trends Biochem Sci* **39**, 101-111, doi:10.1016/j.tibs.2013.12.006 (2014).
150 Shamas-Din, A., Kale, J., Leber, B. & Andrews, D. W. Mechanisms of action of Bcl-2 family proteins. *Cold Spring Harb Perspect Biol* **5**, a008714, doi:10.1101/cshperspect.a008714 (2013).
151 Roos, W. P., Thomas, A. D. & Kaina, B. DNA damage and the balance between survival and death in cancer biology. *Nat Rev Cancer* **16**, 20-33, doi:10.1038/nrc.2015.2 (2016).
152 Edlich, F. *et al.* Bcl-x(L) retrotranslocates Bax from the mitochondria into the cytosol. *Cell* **145**, 104-116, doi:10.1016/j.cell.2011.02.034 (2011).
153 Cheng, E. H., Sheiko, T. V., Fisher, J. K., Craigen, W. J. & Korsmeyer, S. J. VDAC2 inhibits BAK activation and mitochondrial apoptosis. *Science* **301**, 513-517, doi:10.1126/science.1083995 (2003).
154 Bouillet, P. *et al.* Proapoptotic Bcl-2 relative Bim required for certain apoptotic responses, leukocyte homeostasis, and to preclude autoimmunity. *Science* **286**, 1735-1738, doi:10.1126/science.286.5445.1735 (1999).
155 Bouillet, P. *et al.* BH3-only Bcl-2 family member Bim is required for apoptosis of autoreactive thymocytes. *Nature* **415**, 922-926, doi:10.1038/415922a (2002).
156 Villunger, A. *et al.* p53- and drug-induced apoptotic responses mediated by BH3-only proteins puma and noxa. *Science* **302**, 1036-1038, doi:10.1126/science.1090072 (2003).
157 Chen, H. C. *et al.* An interconnected hierarchical model of cell death regulation by the BCL-2 family. *Nat Cell Biol* **17**, 1270-1281, doi:10.1038/ncb3236 (2015).
158 Ren, D. *et al.* BID, BIM, and PUMA are essential for activation of the BAX- and BAK-dependent cell death program. *Science* **330**, 1390-1393, doi:10.1126/science.1190217 (2010).
159 Dai, H. *et al.* Transient binding of an activator BH3 domain to the Bak BH3-binding groove initiates Bak oligomerization. *J Cell Biol* **194**, 39-48, doi:10.1083/jcb.201102027 (2011).
160 Luo, X., Budihardjo, I., Zou, H., Slaughter, C. & Wang, X. Bid, a Bcl2 interacting protein, mediates cytochrome c release from mitochondria in response to activation of cell surface death receptors. *Cell* **94**, 481-490, doi:10.1016/s0092-8674(00)81589-5 (1998).
161 Bleicken, S. *et al.* Structural model of active Bax at the membrane. *Mol Cell* **56**, 496-505, doi:10.1016/j.molcel.2014.09.022 (2014).
162 Zhang, Z. *et al.* BH3-in-groove dimerization initiates and helix 9 dimerization expands Bax pore assembly in membranes. *EMBO J* **35**, 208-236, doi:10.15252/embj.201591552 (2016).
163 Dewson, G. *et al.* Bax dimerizes via a symmetric BH3:groove interface during apoptosis. *Cell Death Differ* **19**, 661-670, doi:10.1038/cdd.2011.138 (2012).
164 Salvador-Gallego, R. *et al.* Bax assembly into rings and arcs in apoptotic mitochondria is linked to membrane pores. *EMBO J* **35**, 389-401, doi:10.15252/embj.201593384 (2016).

165 Grosse, L. *et al.* Bax assembles into large ring-like structures remodeling the mitochondrial outer membrane in apoptosis. *EMBO J* **35**, 402-413, doi:10.15252/embj.201592789 (2016).
166 Chipuk, J. E. *et al.* Direct activation of Bax by p53 mediates mitochondrial membrane permeabilization and apoptosis. *Science* **303**, 1010-1014, doi:10.1126/science.1092734 (2004).
167 Follis, A. V. *et al.* Pin1-Induced Proline Isomerization in Cytosolic p53 Mediates BAX Activation and Apoptosis. *Mol Cell* **59**, 677-684, doi:10.1016/j.molcel.2015.06.029 (2015).
168 Hilton, B. A. *et al.* ATR Plays a Direct Antiapoptotic Role at Mitochondria, which Is Regulated by Prolyl Isomerase Pin1. *Mol Cell* **60**, 35-46, doi:10.1016/j.molcel.2015.08.008 (2015).
169 Iyer, S. *et al.* Identification of an activation site in Bak and mitochondrial Bax triggered by antibodies. *Nat Commun* **7**, 11734, doi:10.1038/ncomms11734 (2016).
170 Scorrano, L. *et al.* A distinct pathway remodels mitochondrial cristae and mobilizes cytochrome c during apoptosis. *Dev Cell* **2**, 55-67, doi:10.1016/s1534-5807(01)00116-2 (2002).
171 Du, C., Fang, M., Li, Y., Li, L. & Wang, X. Smac, a mitochondrial protein that promotes cytochrome c-dependent caspase activation by eliminating IAP inhibition. *Cell* **102**, 33-42, doi:10.1016/s0092-8674(00)00008-8 (2000).
172 Verhagen, A. M. *et al.* Identification of DIABLO, a mammalian protein that promotes apoptosis by binding to and antagonizing IAP proteins. *Cell* **102**, 43-53, doi:10.1016/s0092-8674(00)00009-x (2000).
173 Li, P. *et al.* Cytochrome c and dATP-dependent formation of Apaf-1/caspase-9 complex initiates an apoptotic protease cascade. *Cell* **91**, 479-489, doi:10.1016/s0092-8674(00)80434-1 (1997).
174 Hu, Q. *et al.* Molecular determinants of caspase-9 activation by the Apaf-1 apoptosome. *Proc Natl Acad Sci U S A* **111**, 16254-16261, doi:10.1073/pnas.1418000111 (2014).
175 Wu, C. C. *et al.* The Apaf-1 apoptosome induces formation of caspase-9 homo- and heterodimers with distinct activities. *Nat Commun* **7**, 13565, doi:10.1038/ncomms13565 (2016).
176 Shalini, S., Dorstyn, L., Dawar, S. & Kumar, S. Old, new and emerging functions of caspases. *Cell Death Differ* **22**, 526-539, doi:10.1038/cdd.2014.216 (2015).
177 Julien, O. & Wells, J. A. Caspases and their substrates. *Cell Death Differ* **24**, 1380-1389, doi:10.1038/cdd.2017.44 (2017).
178 Eckelman, B. P., Salvesen, G. S. & Scott, F. L. Human inhibitor of apoptosis proteins: why XIAP is the black sheep of the family. *EMBO Rep* **7**, 988-994, doi:10.1038/sj.embor.7400795 (2006).
179 Silke, J. & Meier, P. Inhibitor of apoptosis (IAP) proteins-modulators of cell death and inflammation. *Cold Spring Harb Perspect Biol* **5**, doi:10.1101/cshperspect.a008730 (2013).
180 Eckelman, B. P. & Salvesen, G. S. The human anti-apoptotic proteins cIAP1 and cIAP2 bind but do not inhibit caspases. *J Biol Chem* **281**, 3254-3260, doi:10.1074/jbc.M510863200 (2006).
181 Nagata, S. DNA degradation in development and programmed cell death. *Annu Rev Immunol* **23**, 853-875, doi:10.1146/annurev.immunol.23.021704.115811 (2005).
182 Naito, M., Nagashima, K., Mashima, T. & Tsuruo, T. Phosphatidylserine externalization is a downstream event of interleukin-1 beta-converting enzyme family protease activation during apoptosis. *Blood* **89**, 2060-2066 (1997).

183 Sebbagh, M. *et al.* Caspase-3-mediated cleavage of ROCK I induces MLC phosphorylation and apoptotic membrane blebbing. *Nat Cell Biol* **3**, 346-352, doi:10.1038/35070019 (2001).
184 Barclay, L. A. *et al.* Inhibition of Pro-apoptotic BAX by a noncanonical interaction mechanism. *Mol Cell* **57**, 873-886, doi:10.1016/j.molcel.2015.01.014 (2015).
185 Antonsson, B. *et al.* Inhibition of Bax channel-forming activity by Bcl-2. *Science* **277**, 370-372, doi:10.1126/science.277.5324.370 (1997).
186 Scorrano, L. *et al.* BAX and BAK regulation of endoplasmic reticulum Ca2+: a control point for apoptosis. *Science* **300**, 135-139, doi:10.1126/science.1081208 (2003).
187 Alavian, K. N. *et al.* Bcl-xL regulates metabolic efficiency of neurons through interaction with the mitochondrial F1FO ATP synthase. *Nat Cell Biol* **13**, 1224-1233, doi:10.1038/ncb2330 (2011).
188 Bonora, M. *et al.* Molecular mechanisms of cell death: central implication of ATP synthase in mitochondrial permeability transition. *Oncogene* **34**, 1475-1486, doi:10.1038/onc.2014.96 (2015).
189 Chen, Z. X. & Pervaiz, S. Bcl-2 induces pro-oxidant state by engaging mitochondrial respiration in tumor cells. *Cell Death Differ* **14**, 1617-1627, doi:10.1038/sj.cdd.4402165 (2007).
190 Chen, Z. X. & Pervaiz, S. Involvement of cytochrome c oxidase subunits Va and Vb in the regulation of cancer cell metabolism by Bcl-2. *Cell Death Differ* **17**, 408-420, doi:10.1038/cdd.2009.132 (2010).
191 Hamacher-Brady, A. & Brady, N. R. Bax/Bak-dependent, Drp1-independent Targeting of X-linked Inhibitor of Apoptosis Protein (XIAP) into Inner Mitochondrial Compartments Counteracts Smac/DIABLO-dependent Effector Caspase Activation. *J Biol Chem* **290**, 22005-22018, doi:10.1074/jbc.M115.643064 (2015).
192 Ditzel, M. *et al.* Inactivation of effector caspases through nondegradative polyubiquitylation. *Mol Cell* **32**, 540-553, doi:10.1016/j.molcel.2008.09.025 (2008).
193 Lee, T. V. *et al.* Drosophila IAP1-mediated ubiquitylation controls activation of the initiator caspase DRONC independent of protein degradation. *PLoS Genet* **7**, e1002261, doi:10.1371/journal.pgen.1002261 (2011).
194 Lisi, S., Mazzon, I. & White, K. Diverse domains of THREAD/DIAP1 are required to inhibit apoptosis induced by REAPER and HID in Drosophila. *Genetics* **154**, 669-678 (2000).
195 Varfolomeev, E. *et al.* c-IAP1 and c-IAP2 are critical mediators of tumor necrosis factor alpha (TNFalpha)-induced NF-kappaB activation. *J Biol Chem* **283**, 24295-24299, doi:10.1074/jbc.C800128200 (2008).
196 Gibert, B. & Mehlen, P. Dependence Receptors and Cancer: Addiction to Trophic Ligands. *Cancer Res* **75**, 5171-5175, doi:10.1158/0008-5472.can-14-3652 (2015).
197 Strasser, A., Jost, P. J. & Nagata, S. The many roles of FAS receptor signaling in the immune system. *Immunity* **30**, 180-192, doi:10.1016/j.immuni.2009.01.001 (2009).
198 Aggarwal, B. B., Gupta, S. C. & Kim, J. H. Historical perspectives on tumor necrosis factor and its superfamily: 25 years later, a golden journey. *Blood* **119**, 651-665, doi:10.1182/blood-2011-04-325225 (2012).
199 Boldin, M. P., Goncharov, T. M., Goltsev, Y. V. & Wallach, D. Involvement of MACH, a novel MORT1/FADD-interacting protease, in Fas/APO-1- and TNF receptor-induced cell death. *Cell* **85**, 803-815, doi:10.1016/s0092-8674(00)81265-9 (1996).
200 Dickens, L. S., Powley, I. R., Hughes, M. A. & MacFarlane, M. The 'complexities' of life and death: death receptor signalling platforms. *Exp Cell Res* **318**, 1269-1277, doi:10.1016/j.yexcr.2012.04.005 (2012).

201 Micheau, O. & Tschopp, J. Induction of TNF receptor I-mediated apoptosis via two sequential signaling complexes. *Cell* **114**, 181-190, doi:10.1016/s0092-8674(03)00521-x (2003).
202 Brenner, D., Blaser, H. & Mak, T. W. Regulation of tumour necrosis factor signalling: live or let die. *Nat Rev Immunol* **15**, 362-374, doi:10.1038/nri3834 (2015).
203 Toscano, M. A. *et al.* Differential glycosylation of TH1, TH2 and TH-17 effector cells selectively regulates susceptibility to cell death. *Nat Immunol* **8**, 825-834, doi:10.1038/ni1482 (2007).
204 Fu, T. M. *et al.* Cryo-EM Structure of Caspase-8 Tandem DED Filament Reveals Assembly and Regulation Mechanisms of the Death-Inducing Signaling Complex. *Mol Cell* **64**, 236-250, doi:10.1016/j.molcel.2016.09.009 (2016).
205 Dickens, L. S. *et al.* A death effector domain chain DISC model reveals a crucial role for caspase-8 chain assembly in mediating apoptotic cell death. *Mol Cell* **47**, 291-305, doi:10.1016/j.molcel.2012.05.004 (2012).
206 Hughes, M. A. *et al.* Co-operative and Hierarchical Binding of c-FLIP and Caspase-8: A Unified Model Defines How c-FLIP Isoforms Differentially Control Cell Fate. *Mol Cell* **61**, 834-849, doi:10.1016/j.molcel.2016.02.023 (2016).
207 Powley, I. R., Hughes, M. A., Cain, K. & MacFarlane, M. Caspase-8 tyrosine-380 phosphorylation inhibits CD95 DISC function by preventing procaspase-8 maturation and cycling within the complex. *Oncogene* **35**, 5629-5640, doi:10.1038/onc.2016.99 (2016).
208 Helmke, C. *et al.* Ligand stimulation of CD95 induces activation of Plk3 followed by phosphorylation of caspase-8. *Cell Res* **26**, 914-934, doi:10.1038/cr.2016.78 (2016).
209 Koenig, A. *et al.* The c-FLIPL cleavage product p43FLIP promotes activation of extracellular signal-regulated kinase (ERK), nuclear factor kappaB (NF-kappaB), and caspase-8 and T cell survival. *J Biol Chem* **289**, 1183-1191, doi:10.1074/jbc.M113.506428 (2014).
210 Strasser, A., Harris, A. W., Huang, D. C., Krammer, P. H. & Cory, S. Bcl-2 and Fas/APO-1 regulate distinct pathways to lymphocyte apoptosis. *EMBO J* **14**, 6136-6147 (1995).
211 Jost, P. J. *et al.* XIAP discriminates between type I and type II FAS-induced apoptosis. *Nature* **460**, 1035-1039, doi:10.1038/nature08229 (2009).
212 Yin, X. M. *et al.* Bid-deficient mice are resistant to Fas-induced hepatocellular apoptosis. *Nature* **400**, 886-891, doi:10.1038/23730 (1999).
213 Li, H., Zhu, H., Xu, C. J. & Yuan, J. Cleavage of BID by caspase 8 mediates the mitochondrial damage in the Fas pathway of apoptosis. *Cell* **94**, 491-501, doi:10.1016/s0092-8674(00)81590-1 (1998).
214 Gross, A. *et al.* Caspase cleaved BID targets mitochondria and is required for cytochrome c release, while BCL-XL prevents this release but not tumor necrosis factor-R1/Fas death. *J Biol Chem* **274**, 1156-1163, doi:10.1074/jbc.274.2.1156 (1999).
215 Huang, K. *et al.* Cleavage by Caspase 8 and Mitochondrial Membrane Association Activate the BH3-only Protein Bid during TRAIL-induced Apoptosis. *J Biol Chem* **291**, 11843-11851, doi:10.1074/jbc.M115.711051 (2016).
216 Tan, C. T. *et al.* MOAP-1 Mediates Fas-Induced Apoptosis in Liver by Facilitating tBid Recruitment to Mitochondria. *Cell Rep* **16**, 174-185, doi:10.1016/j.celrep.2016.05.068 (2016).
217 Horn, S. *et al.* Caspase-10 Negatively Regulates Caspase-8-Mediated Cell Death, Switching the Response to CD95L in Favor of NF-kappaB Activation and Cell Survival. *Cell Rep* **19**, 785-797, doi:10.1016/j.celrep.2017.04.010 (2017).

218 Kranz, D. & Boutros, M. A synthetic lethal screen identifies FAT1 as an antagonist of caspase-8 in extrinsic apoptosis. *EMBO J* **33**, 181-197, doi:10.1002/embj.201385686 (2014).
219 Li, H., Kobayashi, M., Blonska, M., You, Y. & Lin, X. Ubiquitination of RIP is required for tumor necrosis factor alpha-induced NF-kappaB activation. *J Biol Chem* **281**, 13636-13643, doi:10.1074/jbc.M600620200 (2006).
220 Gerlach, B. *et al.* Linear ubiquitination prevents inflammation and regulates immune signalling. *Nature* **471**, 591-596, doi:10.1038/nature09816 (2011).
221 Bertrand, M. J. *et al.* cIAP1 and cIAP2 facilitate cancer cell survival by functioning as E3 ligases that promote RIP1 ubiquitination. *Mol Cell* **30**, 689-700, doi:10.1016/j.molcel.2008.05.014 (2008).
222 DiDonato, J. A., Hayakawa, M., Rothwarf, D. M., Zandi, E. & Karin, M. A cytokine-responsive IkappaB kinase that activates the transcription factor NF-kappaB. *Nature* **388**, 548-554, doi:10.1038/41493 (1997).
223 Liu, Z. G., Hsu, H., Goeddel, D. V. & Karin, M. Dissection of TNF receptor 1 effector functions: JNK activation is not linked to apoptosis while NF-kappaB activation prevents cell death. *Cell* **87**, 565-576, doi:10.1016/s0092-8674(00)81375-6 (1996).
224 Ting, A. T. & Bertrand, M. J. M. More to Life than NF-kappaB in TNFR1 Signaling. *Trends Immunol* **37**, 535-545, doi:10.1016/j.it.2016.06.002 (2016).
225 Geng, J. *et al.* Regulation of RIPK1 activation by TAK1-mediated phosphorylation dictates apoptosis and necroptosis. *Nat Commun* **8**, 359, doi:10.1038/s41467-017-00406-w (2017).
226 Dondelinger, Y. *et al.* NF-kappaB-Independent Role of IKKalpha/IKKbeta in Preventing RIPK1 Kinase-Dependent Apoptotic and Necroptotic Cell Death during TNF Signaling. *Mol Cell* **60**, 63-76, doi:10.1016/j.molcel.2015.07.032 (2015).
227 Jaco, I. *et al.* MK2 Phosphorylates RIPK1 to Prevent TNF-Induced Cell Death. *Mol Cell* **66**, 698-710 e695, doi:10.1016/j.molcel.2017.05.003 (2017).
228 Fulda, S. & Vucic, D. Targeting IAP proteins for therapeutic intervention in cancer. *Nat Rev Drug Discov* **11**, 109-124, doi:10.1038/nrd3627 (2012).
229 Hitomi, J. *et al.* Identification of a molecular signaling network that regulates a cellular necrotic cell death pathway. *Cell* **135**, 1311-1323, doi:10.1016/j.cell.2008.10.044 (2008).
230 Tortola, L. *et al.* The Tumor Suppressor Hace1 Is a Critical Regulator of TNFR1-Mediated Cell Fate. *Cell Rep* **15**, 1481-1492, doi:10.1016/j.celrep.2016.04.032 (2016).
231 LA, O. R. *et al.* Membrane-bound Fas ligand only is essential for Fas-induced apoptosis. *Nature* **461**, 659-663, doi:10.1038/nature08402 (2009).
232 von Karstedt, S., Montinaro, A. & Walczak, H. Exploring the TRAILs less travelled: TRAIL in cancer biology and therapy. *Nat Rev Cancer* **17**, 352-366, doi:10.1038/nrc.2017.28 (2017).
233 Lafont, E. *et al.* The linear ubiquitin chain assembly complex regulates TRAIL-induced gene activation and cell death. *EMBO J* **36**, 1147-1166, doi:10.15252/embj.201695699 (2017).
234 Goldschneider, D. & Mehlen, P. Dependence receptors: a new paradigm in cell signaling and cancer therapy. *Oncogene* **29**, 1865-1882, doi:10.1038/onc.2010.13 (2010).
235 Mehlen, P. & Tauszig-Delamasure, S. Dependence receptors and colorectal cancer. *Gut* **63**, 1821-1829, doi:10.1136/gutjnl-2013-306704 (2014).
236 Liu, J. *et al.* Mediation of the DCC apoptotic signal by DIP13 alpha. *J Biol Chem* **277**, 26281-26285, doi:10.1074/jbc.M204679200 (2002).

237 Joubert, O. *et al.* Functional studies of membrane-bound and purified human Hedgehog receptor Patched expressed in yeast. *Biochim Biophys Acta* **1788**, 1813-1821, doi:10.1016/j.bbamem.2009.05.009 (2009).
238 Fombonne, J. *et al.* Patched dependence receptor triggers apoptosis through ubiquitination of caspase-9. *Proc Natl Acad Sci U S A* **109**, 10510-10515, doi:10.1073/pnas.1200094109 (2012).
239 Llambi, F. *et al.* The dependence receptor UNC5H2 mediates apoptosis through DAP-kinase. *EMBO J* **24**, 1192-1201, doi:10.1038/sj.emboj.7600584 (2005).
240 Guenebeaud, C. *et al.* The dependence receptor UNC5H2/B triggers apoptosis via PP2A-mediated dephosphorylation of DAP kinase. *Mol Cell* **40**, 863-876, doi:10.1016/j.molcel.2010.11.021 (2010).
241 Zhu, Y. *et al.* Dependence receptor UNC5D mediates nerve growth factor depletion-induced neuroblastoma regression. *J Clin Invest* **123**, 2935-2947, doi:10.1172/jci65988 (2013).
242 Ichim, G. *et al.* The dependence receptor TrkC triggers mitochondria-dependent apoptosis upon Cobra-1 recruitment. *Mol Cell* **51**, 632-646, doi:10.1016/j.molcel.2013.08.021 (2013).
243 Ruckdeschel, K. *et al.* Signaling of apoptosis through TLRs critically involves toll/IL-1 receptor domain-containing adapter inducing IFN-beta, but not MyD88, in bacteria-infected murine macrophages. *J Immunol* **173**, 3320-3328, doi:10.4049/jimmunol.173.5.3320 (2004).
244 Mori, C. *et al.* Programmed cell death in the interdigital tissue of the fetal mouse limb is apoptosis with DNA fragmentation. *Anat Rec* **242**, 103-110, doi:10.1002/ar.1092420114 (1995).
245 Sun, L. *et al.* Mixed lineage kinase domain-like protein mediates necrosis signaling downstream of RIP3 kinase. *Cell* **148**, 213-227, doi:10.1016/j.cell.2011.11.031 (2012).
246 Dillon, C. P. *et al.* Survival function of the FADD-CASPASE-8-cFLIP(L) complex. *Cell Rep* **1**, 401-407, doi:10.1016/j.celrep.2012.03.010 (2012).
247 Laster, S. M., Wood, J. G. & Gooding, L. R. Tumor necrosis factor can induce both apoptic and necrotic forms of cell lysis. *J Immunol* **141**, 2629-2634 (1988).
248 Grooten, J., Goossens, V., Vanhaesebroeck, B. & Fiers, W. Cell membrane permeabilization and cellular collapse, followed by loss of dehydrogenase activity: early events in tumour necrosis factor-induced cytotoxicity. *Cytokine* **5**, 546-555 (1993).
249 Degterev, A. *et al.* Identification of RIP1 kinase as a specific cellular target of necrostatins. *Nat Chem Biol* **4**, 313-321, doi:10.1038/nchembio.83 (2008).
250 He, S. *et al.* Receptor interacting protein kinase-3 determines cellular necrotic response to TNF-alpha. *Cell* **137**, 1100-1111, doi:10.1016/j.cell.2009.05.021 (2009).
251 Cho, Y. S. *et al.* Phosphorylation-driven assembly of the RIP1-RIP3 complex regulates programmed necrosis and virus-induced inflammation. *Cell* **137**, 1112-1123, doi:10.1016/j.cell.2009.05.037 (2009).
252 Mevissen, T. E. *et al.* OTU deubiquitinases reveal mechanisms of linkage specificity and enable ubiquitin chain restriction analysis. *Cell* **154**, 169-184, doi:10.1016/j.cell.2013.05.046 (2013).
253 Wu, J. *et al.* Mlkl knockout mice demonstrate the indispensable role of Mlkl in necroptosis. *Cell Res* **23**, 994-1006, doi:10.1038/cr.2013.91 (2013).
254 Zhao, J. *et al.* Mixed lineage kinase domain-like is a key receptor interacting protein 3 downstream component of TNF-induced necrosis. *Proc Natl Acad Sci U S A* **109**, 5322-5327, doi:10.1073/pnas.1200012109 (2012).
255 Li, J. *et al.* The RIP1/RIP3 necrosome forms a functional amyloid signaling complex required for programmed necrosis. *Cell* **150**, 339-350, doi:10.1016/j.cell.2012.06.019 (2012).

256 Rodriguez, D. A. *et al.* Characterization of RIPK3-mediated phosphorylation of the activation loop of MLKL during necroptosis. *Cell Death Differ* **23**, 76-88, doi:10.1038/cdd.2015.70 (2016).
257 Gong, Y. N. *et al.* ESCRT-III Acts Downstream of MLKL to Regulate Necroptotic Cell Death and Its Consequences. *Cell* **169**, 286-300 e216, doi:10.1016/j.cell.2017.03.020 (2017).
258 Jacobsen, A. V. *et al.* HSP90 activity is required for MLKL oligomerisation and membrane translocation and the induction of necroptotic cell death. *Cell Death Dis* **7**, e2051, doi:10.1038/cddis.2015.386 (2016).
259 Zhao, X. M. *et al.* Hsp90 modulates the stability of MLKL and is required for TNF-induced necroptosis. *Cell Death Dis* **7**, e2089, doi:10.1038/cddis.2015.390 (2016).
260 Cai, Z. *et al.* Plasma membrane translocation of trimerized MLKL protein is required for TNF-induced necroptosis. *Nat Cell Biol* **16**, 55-65, doi:10.1038/ncb2883 (2014).
261 Cai, Z. *et al.* Activation of cell-surface proteases promotes necroptosis, inflammation and cell migration. *Cell Res* **26**, 886-900, doi:10.1038/cr.2016.87 (2016).
262 Xia, B. *et al.* MLKL forms cation channels. *Cell Res* **26**, 517-528, doi:10.1038/cr.2016.26 (2016).
263 Kaiser, W. J. *et al.* Toll-like receptor 3-mediated necrosis via TRIF, RIP3, and MLKL. *J Biol Chem* **288**, 31268-31279, doi:10.1074/jbc.M113.462341 (2013).
264 Upton, J. W., Kaiser, W. J. & Mocarski, E. S. DAI/ZBP1/DLM-1 complexes with RIP3 to mediate virus-induced programmed necrosis that is targeted by murine cytomegalovirus vIRA. *Cell Host Microbe* **11**, 290-297, doi:10.1016/j.chom.2012.01.016 (2012).
265 Maelfait, J. *et al.* Sensing of viral and endogenous RNA by ZBP1/DAI induces necroptosis. *EMBO J* **36**, 2529-2543, doi:10.15252/embj.201796476 (2017).
266 Lin, J. *et al.* RIPK1 counteracts ZBP1-mediated necroptosis to inhibit inflammation. *Nature* **540**, 124-128, doi:10.1038/nature20558 (2016).
267 Seo, J. *et al.* CHIP controls necroptosis through ubiquitylation- and lysosome-dependent degradation of RIPK3. *Nat Cell Biol* **18**, 291-302, doi:10.1038/ncb3314 (2016).
268 Gyrd-Hansen, M. All roads lead to ubiquitin. *Cell Death Differ* **24**, 1135-1136, doi:10.1038/cdd.2017.93 (2017).
269 Onizawa, M. *et al.* The ubiquitin-modifying enzyme A20 restricts ubiquitination of the kinase RIPK3 and protects cells from necroptosis. *Nat Immunol* **16**, 618-627, doi:10.1038/ni.3172 (2015).
270 Chen, W. *et al.* Ppm1b negatively regulates necroptosis through dephosphorylating Rip3. *Nat Cell Biol* **17**, 434-444, doi:10.1038/ncb3120 (2015).
271 Xie, Y. *et al.* Inhibition of Aurora Kinase A Induces Necroptosis in Pancreatic Carcinoma. *Gastroenterology* **153**, 1429-1443 e1425, doi:10.1053/j.gastro.2017.07.036 (2017).
272 Li, D. *et al.* A cytosolic heat shock protein 90 and cochaperone CDC37 complex is required for RIP3 activation during necroptosis. *Proc Natl Acad Sci U S A* **112**, 5017-5022, doi:10.1073/pnas.1505244112 (2015).
273 Kaiser, W. J. *et al.* RIP3 mediates the embryonic lethality of caspase-8-deficient mice. *Nature* **471**, 368-372, doi:10.1038/nature09857 (2011).
274 Oberst, A. *et al.* Catalytic activity of the caspase-8-FLIP(L) complex inhibits RIPK3-dependent necrosis. *Nature* **471**, 363-367, doi:10.1038/nature09852 (2011).
275 Cho, Y., McQuade, T., Zhang, H., Zhang, J. & Chan, F. K. RIP1-dependent and independent effects of necrostatin-1 in necrosis and T cell activation. *PLoS One* **6**, e23209, doi:10.1371/journal.pone.0023209 (2011).
276 Kaiser, W. J., Upton, J. W. & Mocarski, E. S. Viral modulation of programmed necrosis. *Curr Opin Virol* **3**, 296-306, doi:10.1016/j.coviro.2013.05.019 (2013).

277 Lin, J. *et al.* A role of RIP3-mediated macrophage necrosis in atherosclerosis development. *Cell Rep* **3**, 200-210, doi:10.1016/j.celrep.2012.12.012 (2013).
278 Lim, S. Y., Davidson, S. M., Mocanu, M. M., Yellon, D. M. & Smith, C. C. The cardioprotective effect of necrostatin requires the cyclophilin-D component of the mitochondrial permeability transition pore. *Cardiovasc Drugs Ther* **21**, 467-469, doi:10.1007/s10557-007-6067-6 (2007).
279 You, Z. *et al.* Necrostatin-1 reduces histopathology and improves functional outcome after controlled cortical impact in mice. *J Cereb Blood Flow Metab* **28**, 1564-1573, doi:10.1038/jcbfm.2008.44 (2008).
280 Robinson, N. *et al.* Type I interferon induces necroptosis in macrophages during infection with Salmonella enterica serovar Typhimurium. *Nat Immunol* **13**, 954-962, doi:10.1038/ni.2397 (2012).
281 Lichtenauer, M. *et al.* Intravenous and intramyocardial injection of apoptotic white blood cell suspensions prevents ventricular remodelling by increasing elastin expression in cardiac scar tissue after myocardial infarction. *Basic Res Cardiol* **106**, 645-655, doi:10.1007/s00395-011-0173-0 (2011).
282 Lichtenauer, M. *et al.* Secretome of apoptotic peripheral blood cells (APOSEC) confers cytoprotection to cardiomyocytes and inhibits tissue remodelling after acute myocardial infarction: a preclinical study. *Basic Res Cardiol* **106**, 1283-1297, doi:10.1007/s00395-011-0224-6 (2011).
283 Haider, T. *et al.* The secretome of apoptotic human peripheral blood mononuclear cells attenuates secondary damage following spinal cord injury in rats. *Exp Neurol* **267**, 230-242, doi:10.1016/j.expneurol.2015.03.013 (2015).
284 Altmann, P. *et al.* Secretomes of apoptotic mononuclear cells ameliorate neurological damage in rats with focal ischemia. *F1000Res* **3**, 131, doi:10.12688/f1000research.4219.2 (2014).
285 Rosales, C. Neutrophil: A Cell with Many Roles in Inflammation or Several Cell Types? *Front Physiol* **9**, 113, doi:10.3389/fphys.2018.00113 (2018).
286 Wagner, T. *et al.* Different pro-angiogenic potential of gamma-irradiated PBMC-derived secretome and its subfractions. *Sci Rep* **8**, 18016, doi:10.1038/s41598-018-36928-6 (2018).
287 Trengove, N. J., Stacey, M. C., McGechie, D. F. & Mata, S. Qualitative bacteriology and leg ulcer healing. *J Wound Care* **5**, 277-280, doi:10.12968/jowc.1996.5.6.277 (1996).
288 Kasiri, M. M. *et al.* Dying Blood Mononuclear Cell Secretome Exerts Antimicrobial Activity. *Eur J Clin Invest*, doi:10.1111/eci.12667 (2016).
289 Hacker, S. *et al.* The secretome of stressed peripheral blood mononuclear cells increases tissue survival in a rodent epigastric flap model. *Bioeng Transl Med* **6**, e10186, doi:10.1002/btm2.10186 (2021).
290 Kasiri, M. M. *et al.* Dying Blood Mononuclear Cell Secretome Exerts Antimicrobial Activity. *European Journal of Clinical Investigation* (2016).
291 Pietkiewicz, S., Schmidt, J. H. & Lavrik, I. N. Quantification of apoptosis and necroptosis at the single cell level by a combination of Imaging Flow Cytometry with classical Annexin V/propidium iodide staining. *J Immunol Methods* **423**, 99-103, doi:10.1016/j.jim.2015.04.025 (2015).
292 Paquette, D. & Falanga, V. Leg ulcers. *Clin Geriatr Med* **18**, 77-88, vi, doi:10.1016/s0749-0690(03)00035-1 (2002).
293 Brem, H. *et al.* Molecular markers in patients with chronic wounds to guide surgical debridement. *Mol Med* **13**, 30-39, doi:10.2119/2006-00054.Brem (2007).
294 Falanga, V. Wound healing and its impairment in the diabetic foot. *Lancet* **366**, 1736-1743, doi:10.1016/s0140-6736(05)67700-8 (2005).

295 Demidova-Rice, T. N., Durham, J. T. & Herman, I. M. Wound Healing Angiogenesis: Innovations and Challenges in Acute and Chronic Wound Healing. *Adv Wound Care (New Rochelle)* **1**, 17-22, doi:10.1089/wound.2011.0308 (2012).
296 Dos Santos, V. P., da Silveira, D. R. & Caffaro, R. A. Risk factors for primary major amputation in diabetic patients. *Sao Paulo Med J* **124**, 66-70, doi:10.1590/s1516-31802006000200004 (2006).
297 Simader, E. *et al.* Tissue-regenerative potential of the secretome of gamma-irradiated peripheral blood mononuclear cells is mediated via TNFRSF1B-induced necroptosis. *Cell Death Dis* **10**, 729, doi:10.1038/s41419-019-1974-6 (2019).
298 Greenhalgh, D. G. The role of apoptosis in wound healing. *Int J Biochem Cell Biol* **30**, 1019-1030, doi:10.1016/s1357-2725(98)00058-2 (1998).
299 Ohta, H., Yatomi, Y., Sweeney, E. A., Hakomori, S. & Igarashi, Y. A possible role of sphingosine in induction of apoptosis by tumor necrosis factor-alpha in human neutrophils. *FEBS Lett* **355**, 267-270, doi:10.1016/0014-5793(94)01218-0 (1994).
300 Appleton, I., Brown, N. J. & Willoughby, D. A. Apoptosis, necrosis, and proliferation: possible implications in the etiology of keloids. *Am J Pathol* **149**, 1441-1447 (1996).
301 Khandelwal, P. *et al.* A surfactant polymer wound dressing protects human keratinocytes from inducible necroptosis. *Sci Rep* **11**, 4357, doi:10.1038/s41598-021-82260-x (2021).
302 Song, J. *et al.* Deciphering The Emerging Role of Programmed Cell Death in Diabetic Wound Healing. *Int J Biol Sci* **19**, 4989-5003, doi:10.7150/ijbs.88461 (2023).
303 Yang, S., Xu, M., Meng, G. & Lu, Y. SIRT3 deficiency delays diabetic skin wound healing via oxidative stress and necroptosis enhancement. *J Cell Mol Med* **24**, 4415-4427, doi:10.1111/jcmm.15100 (2020).
304 Izumov, I. S. *et al.* RIPK3 Expression in Fibroblasts in an in vivo and in vitro Skin Wound Model: A Controversial Result. *Acta Naturae* **15**, 65-74, doi:10.32607/actanaturae.25452 (2023).
305 Injarabian, L. *et al.* FADD- and RIPK3-Mediated Cell Death Ensures Clearance of Ly6C(high) Wound Macrophages from Damaged Tissue. *J Invest Dermatol* **144**, 152-164.e157, doi:10.1016/j.jid.2023.06.203 (2024).
306 Luthfiana, D. & Utomo, D. H. Network pharmacology reveals the potential of Dolastatin 16 as a diabetic wound healing agent. *In Silico Pharmacol* **11**, 23, doi:10.1007/s40203-023-00161-5 (2023).
307 Justynski, O. *et al.* Apoptosis recognition receptors regulate skin tissue repair in mice. *Elife* **12**, doi:10.7554/eLife.86269 (2023).
308 Wu, Y. S. & Chen, S. N. Apoptotic cell: linkage of inflammation and wound healing. *Front Pharmacol* **5**, 1, doi:10.3389/fphar.2014.00001 (2014).
309 Medina, C. B. *et al.* Metabolites released from apoptotic cells act as tissue messengers. *Nature* **580**, 130-135, doi:10.1038/s41586-020-2121-3 (2020).
310 Li, F. *et al.* Apoptotic cells activate the "phoenix rising" pathway to promote wound healing and tissue regeneration. *Sci Signal* **3**, ra13, doi:10.1126/scisignal.2000634 (2010).
311 Chen, C. Y. *et al.* Exosomal DMBT1 from human urine-derived stem cells facilitates diabetic wound repair by promoting angiogenesis. *Theranostics* **8**, 1607-1623, doi:10.7150/thno.22958 (2018).
312 Li, J. Y. *et al.* Human amniotic mesenchymal stem cells and their paracrine factors promote wound healing by inhibiting heat stress-induced skin cell apoptosis and enhancing their proliferation through activating PI3K/AKT signaling pathway. *Stem Cell Res Ther* **10**, 247, doi:10.1186/s13287-019-1366-y (2019).
313 Karar, J. & Maity, A. PI3K/AKT/mTOR Pathway in Angiogenesis. *Front Mol Neurosci* **4**, 51, doi:10.3389/fnmol.2011.00051 (2011).

314 Hoeben, A. *et al.* Vascular endothelial growth factor and angiogenesis. *Pharmacol Rev* **56**, 549-580, doi:10.1124/pr.56.4.3 (2004).
315 Gnecchi, M. *et al.* Evidence supporting paracrine hypothesis for Akt-modified mesenchymal stem cell-mediated cardiac protection and functional improvement. *FASEB J* **20**, 661-669, doi:10.1096/fj.05-5211com (2006).
316 Matzinger, P. Tolerance, danger, and the extended family. *Annu Rev Immunol* **12**, 991-1045, doi:10.1146/annurev.iy.12.040194.005015 (1994).
317 Varricchi, G. *et al.* Physiological Roles of Mast Cells: Collegium Internationale Allergologicum Update 2019. *Int Arch Allergy Immunol* **179**, 247-261, doi:10.1159/000500088 (2019).
318 Dong, J. *et al.* Mast Cells in Diabetes and Diabetic Wound Healing. *Adv Ther* **37**, 4519-4537, doi:10.1007/s12325-020-01499-4 (2020).
319 Mukai, K., Tsai, M., Saito, H. & Galli, S. J. Mast cells as sources of cytokines, chemokines, and growth factors. *Immunol Rev* **282**, 121-150, doi:10.1111/imr.12634 (2018).
320 Galli, S. J. & Tsai, M. IgE and mast cells in allergic disease. *Nat Med* **18**, 693-704, doi:10.1038/nm.2755 (2012).
321 Bot, I. *et al.* Local Mast Cell Activation Promotes Neovascularization. *Cells* **9**, doi:10.3390/cells9030701 (2020).
322 Divoux, A. *et al.* Mast cells in human adipose tissue: link with morbid obesity, inflammatory status, and diabetes. *J Clin Endocrinol Metab* **97**, E1677-1685, doi:10.1210/jc.2012-1532 (2012).
323 Egozi, E. I., Ferreira, A. M., Burns, A. L., Gamelli, R. L. & Dipietro, L. A. Mast cells modulate the inflammatory but not the proliferative response in healing wounds. *Wound Repair Regen* **11**, 46-54, doi:10.1046/j.1524-475x.2003.11108.x (2003).
324 Weller, K., Foitzik, K., Paus, R., Syska, W. & Maurer, M. Mast cells are required for normal healing of skin wounds in mice. *Faseb j* **20**, 2366-2368, doi:10.1096/fj.06-5837fje (2006).
325 Dong, X., Chen, J., Zhang, Y. & Cen, Y. Mast cell chymase promotes cell proliferation and expression of certain cytokines in a dose-dependent manner. *Mol Med Rep* **5**, 1487-1490, doi:10.3892/mmr.2012.851 (2012).
326 Miao, M. *et al.* Diabetes-impaired wound healing and altered macrophage activation: a possible pathophysiologic correlation. *Wound Repair Regen* **20**, 203-213, doi:10.1111/j.1524-475X.2012.00772.x (2012).
327 Mirza, R. & Koh, T. J. Dysregulation of monocyte/macrophage phenotype in wounds of diabetic mice. *Cytokine* **56**, 256-264, doi:10.1016/j.cyto.2011.06.016 (2011).
328 Huang, S. M. *et al.* High glucose environment induces M1 macrophage polarization that impairs keratinocyte migration via TNF-α: An important mechanism to delay the diabetic wound healing. *J Dermatol Sci* **96**, 159-167, doi:10.1016/j.jdermsci.2019.11.004 (2019).
329 Morey, M., O'Gaora, P., Pandit, A. & Hélary, C. Hyperglycemia acts in synergy with hypoxia to maintain the pro-inflammatory phenotype of macrophages. *PLoS One* **14**, e0220577, doi:10.1371/journal.pone.0220577 (2019).
330 Lee, J. *et al.* Interleukin-23 regulates interleukin-17 expression in wounds, and its inhibition accelerates diabetic wound healing through the alteration of macrophage polarization. *Faseb j* **32**, 2086-2094, doi:10.1096/fj.201700773R (2018).
331 Chen, S. *et al.* Pseudomonas aeruginosa infection alters the macrophage phenotype switching process during wound healing in diabetic mice. *Cell Biol Int* **42**, 877-889, doi:10.1002/cbin.10955 (2018).

332 Ti, D. *et al.* LPS-preconditioned mesenchymal stromal cells modify macrophage polarization for resolution of chronic inflammation via exosome-shuttled let-7b. *J Transl Med* **13**, 308, doi:10.1186/s12967-015-0642-6 (2015).
333 Simader, E. *et al.* Safety and tolerability of topically administered autologous, apoptotic PBMC secretome (APOSEC) in dermal wounds: a randomized Phase 1 trial (MARSYAS I). *Sci Rep* **7**, 6216, doi:10.1038/s41598-017-06223-x (2017).
334 Wuschko, S. *et al.* Toxicological testing of allogeneic secretome derived from peripheral mononuclear cells (APOSEC): a novel cell-free therapeutic agent in skin disease. *Sci Rep* **9**, 5598, doi:10.1038/s41598-019-42057-5 (2019).
335 Beer, L., Mildner, M., Gyöngyösi, M. & Ankersmit, H. J. Peripheral blood mononuclear cell secretome for tissue repair. *Apoptosis* **21**, 1336-1353, doi:10.1007/s10495-016-1292-8 (2016).
336 Gugerell, A. *et al.* Viral safety of APOSECTM: a novel peripheral blood mononuclear cell derived-biological for regenerative medicine. *Blood Transfus* **18**, 30-39, doi:10.2450/2019.0249-18 (2020).
337 Horowitz, B. *et al.* WHO Expert Committee on Biological Standardization. *World Health Organ Tech Rep Ser* **924**, 1-232, backcover (2004).
338 Brem, H., Sheehan, P., Rosenberg, H. J., Schneider, J. S. & Boulton, A. J. Evidence-based protocol for diabetic foot ulcers. *Plast Reconstr Surg* **117**, 193S-209S; discussion 210S-211S, doi:10.1097/01.prs.0000225459.93750.29 (2006).
339 Chatterjee, S. & Davies, M. J. Current management of diabetes mellitus and future directions in care. *Postgrad Med J*, doi:10.1136/postgradmedj-2014-133200 (2015).
340 Gugerell, A. *et al.* Safety and clinical efficacy of the secretome of stressed peripheral blood mononuclear cells in patients with diabetic foot ulcer-study protocol of the randomized, placebo-controlled, double-blind, multicenter, international phase II clinical trial MARSYAS II. *Trials* **22**, 10, doi:10.1186/s13063-020-04948-1 (2021).
341 Hunt, T. K. & Hopf, H. W. Wound healing and wound infection. What surgeons and anesthesiologists can do. *Surg Clin North Am* **77**, 587-606, doi:10.1016/s0039-6109(05)70570-3 (1997).
342 Howell-Jones, R. S. *et al.* A review of the microbiology, antibiotic usage and resistance in chronic skin wounds. *J Antimicrob Chemother* **55**, 143-149, doi:10.1093/jac/dkh513 (2005).
343 Salisbury, A. M. *et al.* Tolerance of Biofilms to Antimicrobials and Significance to Antibiotic Resistance in Wounds. *Surg Technol Int* **33**, 59-66 (2018).
344 Huemer, M., Mairpady Shambat, S., Brugger, S. D. & Zinkernagel, A. S. Antibiotic resistance and persistence-Implications for human health and treatment perspectives. *EMBO Rep* **21**, e51034, doi:10.15252/embr.202051034 (2020).
345 Hsu, S. M., Raine, L. & Fanger, H. Use of avidin-biotin-peroxidase complex (ABC) in immunoperoxidase techniques: a comparison between ABC and unlabeled antibody (PAP) procedures. *J Histochem Cytochem* **29**, 577-580, doi:10.1177/29.4.6166661 (1981).
346 Brazma, A. *et al.* Minimum information about a microarray experiment (MIAME)-toward standards for microarray data. *Nat Genet* **29**, 365-371, doi:10.1038/ng1201-365 (2001).
347 Wang, J., Duncan, D., Shi, Z. & Zhang, B. WEB-based GEne SeT AnaLysis Toolkit (WebGestalt): update 2013. *Nucleic Acids Res* **41**, W77-83, doi:10.1093/nar/gkt439 (2013).
348 Song, X. *et al.* Autophagy deficient keratinocytes display increased DNA damage, senescence and aberrant lipid composition after oxidative stress in vitro and in vivo. *Redox Biol* **11**, 219-230, doi:10.1016/j.redox.2016.12.015 (2017).

349 Narzt, M. S. *et al.* A novel role for NUPR1 in the keratinocyte stress response to UV oxidized phospholipids. *Redox Biol* **20**, 467-482, doi:10.1016/j.redox.2018.11.006 (2019).

Appendix

The publications reprinted in this thesis are open access publications of the Springer Nature Publishing group and licensed under the Creative Commons Attributions 4.0 International License:

http://creativecommons.org/licenses/by/4.0

The published papers can be accessed using this links:

https://www.nature.com/articles/s41419-019-1974-6#rightslink

https://www.nature.com/articles/s41598-017-06223-x

RE: Reprint in Thesis

Von Journalpermissions <journalpermissions@springernature.com>
An Elisabeth Simader <elisabeth.simader@meduniwien.ac.at>
Datum 2024-02-22 15:38

Dear Elisabeth,

Thank you for your recent Springer Nature permissions enquiry.

The work available here: https://www.nature.com/articles/s41419-019-1974-6#rightslink is licensed under the Creative Commons Attribution 4.0 International License, which permits unrestricted use, distribution, modification, and reproduction in any medium, provided you:

1. give appropriate acknowledgment to the original author(s) including the publication source,

2. provide a link to the Creative Commons license, and indicate if changes were made.

Therefore, you do not need a licence to reuse, republish, or adapt this material.

Kind Regards,

Elise

Elise Lagden
Permissions Executive
SpringerNature
The Campus, 4 Crinan Street, London N1 9XW, United Kingdom
T: +442078434596
E elise.lagden@springernature.com
http://www.nature.com
http://www.springernature.com

--
Visitor address: Porters Gate Building, Wharfdale Road, London N1 9FN, UK
--

--

-----Original Message-----
From: Elisabeth Simader <elisabeth.simader@meduniwien.ac.at>
Sent: Thursday, February 22, 2024 1:59 PM
To: Journalpermissions <journalpermissions@springernature.com>
Subject: Reprint in Thesis

To whom it may concern,

I am planning to use the article

Simader, E. et al. Tissue-regenerative potential of the secretome of gamma-irradiated peripheral blood mononuclear cells is mediated via TNFRSF1B-induced necroptosis. Cell Death Dis 10, 729, doi:10.1038/s41419-019-1974-6 (2019).

in my PhD Thesis.
May I have the permission to reprint the paper?

Best regards from Vienna,
Elisabeth Simader

Curriculum Vitae

Elisabeth Maria Simader

PERSONAL BACKGROUND

Nationality: Austria

EDUCATION

1997 – 2001	Elementary School, Vöcklamarkt, Austria
2001 – 2009	Federal Austrian High School with emphasis on modern languages, Austria
2009	Matura (high school graduation)
2009 – 2010	Student in International economics at the University of Business and Administration of Vienna, WU, Austria
2010 – 2016	Medical studies at the Medical University of Vienna, MUW Austria
2013 – 2015	Student Research Fellow at the Christian Doppler Laboratory for Diagnosis and Regeneration of Cardiac and Thoracic Diseases, Medical University of Vienna, Austria
2016 - 2018	Student Research Assistant at the FFG-Project "Aposec", Medical University of Vienna, Austria
2016	Graduation as Medical Doctor; Medical University of Vienna,
2016 – 2024	Austria PhD Student in Vascular Biology at the FFG-Project "Aposec", Medical University of Vienna, Austria

---

CLINICAL TRAINING

2012/07	Clinical Clerkship at the **Department of Surgery**, Empress Elisabeth Hospital, Vienna, Austria (4 weeks)
2012/08	Clinical Clerkship in **Primary Care**, Dr. Maria Gremmel, Vienna, Austria (2 weeks)
2013/07	Clinical Clerkship at the **Department of Emergency Medicine**, State Hospital Vöcklabruck, Austria (2 weeks)
2013/08	Clinical Clerkship at the **Department of Cardiology**, Hospital of Merciful Sisters, Vienna, Austria (4 weeks)
2013/02	Student Surgery Assistant at the University Clinic of **Transplantation**, General Hospital Vienna, Medical University of Vienna, Austria

2014/08	Clinical Clerkship at the **Department of General Surgery**, Prince of Wales Hospital, Chinese University of Hong Kong, Hong Kong (4 weeks)
2015/08-11	Clinical Clerkship in the clinical practical year at the **Department of Thoracic Surgery** Medical University of Vienna, Austria (4 months)
2015/11-2016/03	Clinical Clerkship in the clinical practical year at the **Department of Internal Medicine III, Clinical Division of Endocrinology and Metabolism**, Medical University of Vienna, Austria (4 months)
2016/03-2016/07	Clinical Clerkship in the clinical practical year at the **Department of Emergency Medicine**, Medical University of Vienna, Austria (4 months)
2018/04-Present	Assistant Doctor at the **Department of Internal Medicine III, Division of Rheumatology**, Medical University of Vienna, Austria

CONTINUING EDUCATION

2013/01	Internal intensive medicine-training, Univ.-Prof. Dr.med.univ. Thomas Staudinger, Medical University of Vienna, Austria
2013/07	Summer School/Emergency Simulation Training, General Hospital Linz, Austria
2014/04	Methodenseminar: “Molekularbiologie“- Methods Seminar „Molecular Biology“, Medical University of Vienna, Austria
2014/05	Methodenseminar: “Statistik” – Methods Seminar “Statistics”- Dr.rer.nat. Angelika Geroldinger, Medical University of Vienna, Austria
2014/11	Biometry II: Statistical Testing, PE-Seminar, Medical University of Vienna
2016/12	Certificate of the Federation of European Laboratory Science (FELASA) for experimental biomedical studies in animals.
2018/11	Synovial fluid analysis course; Medical University of Vienna, Austria
2019/02	Musculoskeletal infiltration course, Medical University of Graz, Austria
2019/11	Musculoskeletal ultrasound refresher Course, Medical University of Vienna, Austria

CONGRESSES AND MEETINGS

2014/06	55. Österreichischer Chirurgenkongress, Gesellschaft für Chirurgie, Graz

2014/12	Oral presentation as representative of Dr. Matthias Zimmermann - Bone conditioned medium increases proteoglycan-4 (lubricin) in mesenchymal cells via TGF-betaR1
2015/06	4th EACTS Meeting on Cardiac and Pulmonary Regeneration and Stem Cell Technology, Bern
2016/09	Jahrestagung der ÖKG - Österreichische Kardiologische Gesellschaft, Salzburg Poster presentation in basic science - Difference in MIF production by PBMC in patients with Diabetes mellitus type II
2016/10	47. Jahrestagung der Österreichischen Gesellschaft für Innere Medizin 22.-24. September 2016, Salzburg Poster presentation Heat shock protein 27 urine excretion levels in acute exacerbation of chronic obstructive pulmonary disease
2017/11	40. Jahrestagung der Österreichischen Gesellschaft für Pneumologie 6.-8. Oktober 2016, Wien Poster presentation Heat shock protein 27 urine excretion levels in acute exacerbation of chronic obstructive pulmonary disease
2017/12	EACTS - PACT Joint Symposium"Regenerative Medicine: Taking the Science to the Patient" , Austria, Vienna Poster presentation The Influence of cell-cell communication of peripheral blood mononuclear cells on cell death and cytokine secretion
2018/09	ÖGDV Jahrestagung 2017 am 30.11-02.12. 2017, Salzburg Poster presentation Effect of the secretome of apoptotic peripheral blood mononuclear cells (APOSEC) on tissue regeneration and wound healing
2018/11-12	46. DGRh Congress, Annual Meeting of the German Association of Rheumatology, Mannheim, Germany
2019/06	ÖGR Annual Meeting of the Austrian Association of Rheumatology, Vienna, Austria
2019/11	EULAR European Rheumatology Congress, Madrid, Spain Poster presentation as representative of Dr. Antonia Puchner

	American College of Rheumatology ACR/ARP Annual Meeting 2019, Atlanta, USA Poster presentation Important Role of CD11c+ Dendtritic Cells in Inflammatory
2019/11-12	arthritis
2020/11	ÖGR Annual Meeting of the Austrian Association of Rheumatology, Vienna, Austria
2021/06	ÖGR Annual Meeting of the Austrian Association of Rheumatology, Vienna, Austria
2022/06	EULAR European Rheumatology Congress, Paris, France, Virtual Congress
2022/11	EULAR European Rheumatology Congress, Copenhagen, Denmark Poster presentation Accelerated waning of protective immunity after SARS-CoV-2 mRNA vaccination in patients treated with biological and targeted synthetic disease modifying antirheumatic drugs
2022/11	American College of Rheumatology ACR/ARP Annual Meeting 2022, Philadelphia, USA Ignite Talk Accelerated Waning of Protective Immunity after SARS-CoV-2 mRNA Vaccination in Patients treated with Biological and Targeted Synthetic Disease Modifying Antirheumatic Drugs
2023/06	ÖGR Annual Meeting of the Austrian Association of Rheumatology, Vienna, Austria
	EULAR European Rheumatology Congress, Milano, Italy

AWARDS AND GRANTS

2014/01	Advancement Scholarship – Medical University Vienna, Austria
2014/01	Research Scholarship – Christian Doppler Laboratory for Cardiac and Thoracic Diagnosis and Regeneration, Medical University of Vienna, Austria
2014/07	Research Scholarship – Christian Doppler Laboratory for Cardiac and Thoracic Diagnosis and Regeneration, Medical University of Vienna, Austria
2015/01	Research Scholarship – Christian Doppler Laboratory for Cardiac and Thoracic Diagnosis and Regeneration, Medical University of Vienna, Austria

2015/07	Research Scholarship – Christian Doppler Laboratory for Cardiac and Thoracic Diagnosis and Regeneration, Medical University of Vienna, Austria
2016/12	Academic excellence scholarship – Medical University of Vienna, Austria
2020/06	Medical-Scientific Fund of the Mayor of the Federal Capital Vienna, Austria Project: Dendritic cells and osteoclastic bone destruction in rheumatoid arthritis
2020/11	Theodor Billroth Prize (3rd Place) of the Vienna Medical Association
2022/11	ACR Scholarship of the ÖGR
2022/11	Publication Award ÖGR

TEACHING ACTIVITY

2023/10	SSM1- Methods in Scientific work, Medical University of Vienna
2022/11	Vasculitis, BL 21 Lecture, Medical University of Vienna
2022/10	SSM1- Methods in Scientific work, Medical University of Vienna
2021/11	Vasculitis, BL 21 Lecture, Medical University of Vienna
2021/02	Rheumatology BL 27- Internal Medicine, elective seminar in Rheumatology, Medical University of Vienna
2020/02	Rheumatology BL 27- Internal Medicine, elective seminar in Rheumatology, Medical University of Vienna
2019/10-2020/02	Journal Club - Current Topics in Applied Immunology, Medical University of Vienna
2019/10-2020/02	Thesis Seminar- Applied Immunology and Tissue Regeneration, Medical University of Vienna
2019/02	BL 27- Internal Medicine, elective seminar in Rheumatology, Medical University of Vienna
2019/03	Clinical Physical Examination, Medical University of Vienna
2018/10-2019/02	Basic Life Support Course, Medical University of Vienna
2016/10 – 2019/06	Junior supervisor of the Diploma thesis of Cand. med. Dragan Copic

	Cytokine secretion level of peripheral blood mononuclear cells (PBMCs) after exposure to irradiated PBMC secretome
2016/02 – 2016/07	Tutor at the Medical University of Vienna, University Clinic of medical Education and Training OSCE exam preparation assistant for Surgical skills
2016/02 – 2016/07	Tutor at the Medical University of Vienna, University Clinic of Anaesthesia for Dyspnoea
2015/10 – 2016/02	Tutor at the Medical University of Vienna, University Clinic of Anaesthesia for Surgical skills, Blood serology, Performance diagnostics
2015/09 – 2015/09	Tutor at the Medical University of Vienna, University Clinic of medical Education and Training Return Week exam assistant
2015/07 – 2015/07	Tutor at the Medical University of Vienna, University Clinic of medical Education and Training Return Week exam assistant
2015/02 – 2015/07	Tutor at the Medical University of Vienna, University Clinic of medical Education and Training OSCE exam preparation assistant for Surgical skills
2014/10 – 2015/02	Tutor at the Medical University of Vienna, University Clinic of Anaesthesia ,for Surgical skills, Blood serology, ECG, Spirometry
2013/10 – 2014/02	Tutor at the Medical University of Vienna, University Clinic of Anaesthesia, for Surgical skills, Blood serology

Review activity

Since 2020	Reviewer for Scientific Reports
Since 2022	Reviewer for Wiener Klinische Wochenschrift-Rheumatology
Since 2023	Reviewer for Frontiers in Medicine

PUBLICATIONS

Co-Authorships

1. Analysis of the Secretome of Apoptotic Peripheral Blood Mononuclear Cells: Impact of Released Proteins and Exosomes for Tissue Regeneration.

Beer L, Zimmermann M, Mitterbauer A, Ellinger A, Gruber F, Narzt MS, Zellner M, Gyöngyösi M, Madlener S, Simader E, Gabriel C, Mildner M, Ankersmit HJ. Sci Rep. 2015 Nov 16;5:16662. PMID: 26567861

2. In vitro Stability of Heat Shock Protein 27 in Serum and Plasma Under Different Pre-analytical Conditions: Implications for Large-Scale Clinical Studies.
Zimmermann M, Traxler D, Simader E, Bekos C, Dieplinger B, Lainscak M, Ankersmit HJ, Mueller T. Ann Lab Med. 2016 Jul;36(4):353-7. PMID: 27139608

3. Dying blood mononuclear cell secretome exerts antimicrobial activity.
Kasiri MM, Beer L, Nemec L, Gruber F, Pietkiewicz S, Haider T, Simader EM, Traxler D, Schweiger T, Janik S, Taghavi S, Gabriel C, Mildner M, Ankersmit HJ. Eur J Clin Invest. 2016 Oct;46(10):853-63. PMID: 27513763

4. Heat shock protein 27 acts as a predictor of prognosis in chronic heart failure patients.
Traxler D, Lainscak M, Simader E, Ankersmit HJ, Jug B. Clin Chim Acta. 2017 Oct;473:127-132 Epub 2017 Aug 24. PMID: 28844461

5. Analysis of region specific gene expression patterns in the heart and systemic responses after experimental myocardial ischemia.
Zimmermann M, Beer L, Ullrich R, Lukovic D, Simader E, Traxler D, Wagner T, Nemec L, Altenburger L, Zuckermann A, Gyöngyösi M, Ankersmit HJ, Mildner M. Oncotarget. 2017 May 17;8(37):60809-60825. eCollection 2017 Sep 22. PMID: 28977827

6. Increased serum concentrations of soluble ST2 are associated with pulmonary complications and mortality in polytraumatized patients.
Haider T, Simader E, Hacker P, Ankersmit HJ, Heinz T, Hajdu S, Negrin LL. Clin Chem Lab Med. 2018 Apr 25;56(5):810-817. PMID: 29341938

7. Non-classical monocytes as mediators of tissue destruction in arthritis.
Puchner A, Saferding V, Bonelli M, Mikami Y, Hofmann M, Brunner JS, Caldera M, Goncalves-Alves E, Binder NB, Fischer A, Simader E, Steiner CW, Leiss H, Hayer S, Niederreiter B, Karonitsch T, Koenders MI, Podesser BK, O'Shea JJ, Menche J, Smolen JS, Redlich K, Blüml S. Ann Rheum Dis. 2018 Oct;77(10):1490-1497. Epub 2018 Jun 29. PMID: 29959183

8. Different pro-angiogenic potential of γ-irradiated PBMC-derived secretome and its subfractions.
Wagner T, Traxler D, Simader E, Beer L, Narzt MS, Gruber F, Madlener S, Laggner M, Erb M, Vorstandlechner V, Gugerell A, Radtke C, Gnecchi M, Peterbauer A, Gschwandtner M, Tschachler E, Keibl C, Slezak P, Ankersmit HJ, Mildner M. Sci Rep. 2018 Dec 20;8(1):18016. PMID: 30573762

9. Systemic release of heat-shock protein 27 and 70 following severe trauma.
Haider T, Simader E, Glück O, Ankersmit HJ, Heinz T, Hajdu S, Negrin LL. Sci Rep. 2019 Jul 3;9(1):9595. PMID: 31270381

10. Heat shock protein 27 as a predictor of prognosis in patients admitted to hospital with acute COPD exacerbation.

Zimmermann M, Traxler D, Bekos C, Simader E, Mueller T, Graf A, Lainscak M, Marčun R, Košnik M, Fležar M, Rozman A, Korošec P, Klepetko W, Moser B, Ankersmit HJ. Cell Stress Chaperones. 2020 Jan;25(1):141-149. Epub 2019 Dec 9. PMID: 31820266

11. The inflammatory markers sST2, HSP27 and hsCRP as a prognostic biomarker panel in chronic heart failure patients.
Traxler D, Zimmermann M, Simader E, Veraar CM, Moser B, Mueller T, Mildner M, Dannenberg V, Lainscak M, Jug B, Ankersmit HJ. Clin Chim Acta. 2020 Nov;510:507-514. Epub 2020 Jul 29. PMID: 32735982

12. Early sST2 Liberation after Implantation of a Left Ventricular Assist Device in Patients with Advanced Heart Failure.
Opfermann P, Simader E, Felli A, Bevilacqua M, Holaubek C, Dworschak M, Mouhieddine M, Zimpfer D, Ankersmit JH, Steinlechner B. J Immunol Res. 2020 Dec 26;2020:5826176. eCollection 2020. PMID: 36301686

13. Fractional heat shock protein 27 urine excretion as a short-term predictor in acute exacerbation of chronic obstructive pulmonary disease.
Traxler D, Zimmermann M, Simader E, Einwallner E, Copic D, Graf A, Mueller T, Veraar C, Lainscak M, Marčun R, Košnik M, Fležar M, Rozman A, Korošec P, Klepetko W, Moser B, Ankersmit HJ. Ann Transl Med. 2021 Jan;9(2):117. PMID: 33569419

14. Additional heterologous versus homologous booster vaccination in immunosuppressed patients without SARS-CoV-2 antibody seroconversion after primary mRNA vaccination: a randomised controlled trial.
Bonelli M, Mrak D, Tobudic S, Sieghart D, Koblischke M, Mandl P, Kornek B, Simader E, Radner H, Perkmann T, Haslacher H, Mayer M, Hofer P, Redlich K, Husar-Memmer E, Fritsch-Stork R, Thalhammer R, Stiasny K, Winkler S, Smolen JS, Aberle JH, Zeitlinger M, Heinz LX, Aletaha D. Ann Rheum Dis. 2022 May;81(5):687-694 Epub 2022 Jan 13. PMID: 35027397

15. Response to SARS-CoV-2 vaccination in systemic autoimmune rheumatic disease depends on immunosuppressive regimen: a matched, prospective cohort study.
Mandl P, Tobudic S, Haslacher H, Karonitsch T, Mrak D, Nothnagl T, Perkmann T, Radner H, Sautner J, Simader E, Winkler F, Burgmann H, Aletaha D, Winkler S, Blüml S. Ann Rheum Dis. 2022 Jul;81(7):1017-1022. Epub 2022 Mar 18. PMID: 35304407

16. Immunogenicity and safety of a fourth COVID-19 vaccination in rituximab-treated patients: an open-label extension study.
Mrak D, Simader E, Sieghart D, Mandl P, Radner H, Perkmann T, Haslacher H, Mayer M, Koblischke M, Hofer P, Göschl L, Kartnig F, Deimel T, Kerschbaumer A, Hummel T, Kornek B, Thalhammer R, Stiasny K, Winkler S, Smolen JS, Aberle JH, Aletaha D, Heinz LX, Bonelli M. Ann Rheum Dis. 2022 Dec;81(12):1750-1756. Epub 2022 Aug 17. PMID: 35977809

17. Heterologous vector versus homologous mRNA COVID-19 booster vaccination in non-seroconverted immunosuppressed patients: a randomized controlled trial.
Mrak D, Sieghart D, Simader E, Tobudic S, Radner H, Mandl P, Göschl L, Koblischke M, Hommer N, Wagner A, Mayer M, Schubert L, Hartl L, Kozbial K, Hofer P, Kartnig F, Hummel T, Kerschbaumer A, Deimel T, Puchner A, Gudipati V, Thalhammer R, Munda P, Uyanik-Ünal K, Zuckermann A, Novacek G, Reiberger T, Garner-Spitzer E, Reindl-Schwaighofer R, Kain R, Winkler S, Smolen JS, Stiasny K, Fischer GF, Perkmann T, Haslacher H, Zeitlinger M,

Wiedermann U, Aberle JH, Aletaha D, Heinz LX, Bonelli M. Nat Commun. 2022 Sep 12;13(1):5362. PMID: 36097029

18. Safety and immunogenicity of a third COVID-19 vaccination in patients with immune-mediated inflammatory diseases compared with healthy controls.
Kartnig F, Mrak D, Simader E, Tobudic S, Radner H, Mandl P, Göschl L, Hommer N, Mayer M, Hofer P, Hummel T, Deimel T, Geßl I, Puchner A, Kerschbaumer A, Thalhammer R, Handisurya A, Kain R, Winkler S, Smolen JS, Stiasny K, Perkmann T, Haslacher H, Aberle JH, Aletaha D, Heinz LX, Sieghart D, Bonelli M. Ann Rheum Dis. 2023 Feb;82(2):292-300. Epub 2022 Sep 15. PMID: 36109141

19. Accelerated waning of immune responses to a third COVID-19 vaccination in patients with immune-mediated inflammatory diseases.
Mrak D, Kartnig F, Sieghart D, Simader E, Radner H, Mandl P, Göschl L, Hofer P, Deimel T, Gessl I, Kain R, Winkler S, Smolen JS, Perkmann T, Haslacher H, Aletaha D, Heinz LX, Bonelli M. J Autoimmun. 2023 Feb;135:102981. Epub 2022 Dec 22. PMID: 36706534

20. Cytokine-directed cellular cross-talk imprints synovial pathotypes in rheumatoid arthritis.
Kugler M, Dellinger M, Kartnig F, Müller L, Preglej T, Heinz LX, Simader E, Göschl L, Puchner SE, Weiss S, Shaw LE, Farlik M, Weninger W, Superti-Furga G, Smolen JS, Steiner G, Aletaha D, Kiener HP, Lewis MJ, Pitzalis C, Tosevska A, Karonitsch T, Bonelli M. Ann Rheum Dis. 2023 Sep;82(9):1142-1152. Epub 2023 Jun 21. PMID: 37344156

First authorships

1. Safety and tolerability of topically administered autologous, apoptotic PBMC secretome (APOSEC) in dermal wounds: a randomized Phase 1 trial (MARSYAS I).
Simader E, Traxler D, Kasiri MM, Hofbauer H, Wolzt M, Glogner C, Storka A, Mildner M, Gouya G, Geusau A, Fuchs C, Eder C, Graf A, Schaden M, Golabi B, Aretin MB, Suessner S, Gabriel C, Klepetko W, Tschachler E, Ankersmit HJ. Sci Rep. 2017 Jul 24;7(1):6216 PMID: 28740204

2. Subarachnoid hemorrhage in rats - Visualizing blood distribution in vivo using gadolinium-enhanced magnetic resonance imaging: Technical note.
Simader E, Budinsky L, Helbich TH, Sherif C, Höftberger R, Kasprian G, Raunegger T, Hacker P, Ankersmit HJ, Beer L, Haider T. J Neurosci Methods. 2019 Sep 1;325:108370. Epub 2019 Jul 19. PMID: 31326605

3. Tissue-regenerative potential of the secretome of γ-irradiated peripheral blood mononuclear cells is mediated via TNFRSF1B-induced necroptosis.
Simader E, Beer L, Laggner M, Vorstandlechner V, Gugerell A, Erb M, Kalinina P, Copic D, Moser D, Spittler A, Tschachler E, Jan Ankersmit H, Mildner M. Cell Death Dis. 2019 Sep 30;10(10):729. PMID: 31570701

4. Importance of the second SARS-CoV-2 vaccination dose for achieving serological response in patients with rheumatoid arthritis and seronegative spondyloarthritis.
Simader E, Tobudic S, Mandl P, Haslacher H, Perkmann T, Nothnagl T, Sautner J, Radner H, Winkler F, Burgmann H, Mrak D, Aletaha D, Winkler S, Blüml S. Ann Rheum Dis. 2022 Mar;81(3):416-421. Epub 2021 Nov 29. PMID: 34844927

5. Immunogenicity and safety of a fourth COVID-19 vaccination in rituximab-treated patients: an open-label extension study.
Mrak D, Simader E, Sieghart D, Mandl P, Radner H, Perkmann T, Haslacher H, Mayer M, Koblischke M, Hofer P, Göschl L, Kartnig F, Deimel T, Kerschbaumer A, Hummel T, Kornek B, Thalhammer R, Stiasny K, Winkler S, Smolen JS, Aberle JH, Aletaha D, Heinz LX, Bonelli M. Ann Rheum Dis. 2022 Dec;81(12):1750-1756. doi: 10.1136/ard-2022-222579. Epub 2022 Aug 17. PMID: 35977809

6. The accelerated waning of immunity and reduced effect of booster in patients treated with bDMARD and tsDMARD after SARS-CoV-2 mRNA vaccination.
Tobudic S, Simader E, Deimel T, Straub J, Kartnig F, Heinz LX, Mandl P, Haslacher H, Perkmann T, Schneider L, Nothnagl T, Radner H, Winkler F, Burgmann H, Stiasny K, Novacek G, Reinisch W, Aletaha D, Winkler S, Blüml S. Front Med (Lausanne). 2023 Feb 9;10:1049157. doi: 10.3389/fmed.2023.1049157. eCollection 2023. PMID: 36844197